STOCHASTIC POWER SYSTEM OPTIMISATION ALGORITHM WITH APPLICATIONS TO DISTRIBUTED GENERATION INTEGRATION

Idris Musa

B.Eng., M.Eng.

A thesis submitted for the degree of

Doctor of Philosophy

December 2014

School of Electrical and Electronic Engineering

Newcastle University

United Kingdom

Acknowledgments

Praise is to Allah (God) the omnipotent, for guiding me to this work: Never could I found guidance had it not been for the appeasement and consent of Allah.

The research work in this thesis was funded by the Petroleum Technology Development Fund (PTDF) Overseas Scholarship Scheme of my home country, Nigeria. I wish to thank them for their generous financial support during the entire period of my study. I would also like to thank my employer, Kaduna Polytechnic, Kaduna – Nigeria for giving me the time and financial support towards the successful completion of this research work.

I acknowledge wholeheartedly with gratitude the valuable guidance and unvarying support provided by my supervisors, Dr. Bashar Zahawi and Dr. Shady Gadoue. The successful completion of this research work would not have been possible without their excellent support. And to Dr Mohammed Elgendy, I say thank you for your morale and financial support you are a friend indeed.

I extend my gratitude to the school of Electrical and Electronic Engineering in particular, the staff at the Power Electronics, Drives and Machines group for giving me the enabling environment for my research work. I want to thank the students at the Power Electronics, Drives and Machines group, for their support and occasional active discussions during the course of my program. My thanks go to Mr. James Richardson and other technical support staff for their valuable assistance during the course of this research work. My particular thanks go Postgraduate Research Coordinator, Mrs. Gillian Webber and other administrative staff for their untiring support and for facilitating all the administrative work.

Special thanks go to the Power Holding Company of Nigeria (PHCN) staff at the Doka and the Kawo Distribution Business Units, in my home country Kaduna, Nigeria, in particular to Engr Tukur Bilya Bakori for his valuable help and support during my fieldwork study in Nigeria.

Finally, I am infinitely grateful to my parent, sisters and brothers for their words of encouragement, prayer and endless morale support. I would like to appreciate the great support I received from my family, my wife Maryam Idris, and my sons Abdulbasit Idris, Muntasir Idris and Nabil Idris.

They have been behind me throughout my extended academic career. Their guidance and enthusiasm have given me strength to complete my thesis. Their understanding and unconditional love are long to be forgotten.

Abstract

The ever increasing level of penetration of Distributed Generation (DG) in power distribution networks is not without its challenges for network planners and operators. Some of these challenges are in the areas of voltage regulation, increase of network fault levels and the disturbance to the network protection settings. Distributed generation can be beneficial to both electricity consumers and if the integration is properly engineered the energy utility. Thus, the need for tools considering these challenges for the optimal placement and sizing of DG units cannot be over emphasized.

This dissertation focuses on the application of a soft computing technique based on a stochastic optimisation algorithm (Particle Swarm Optimisation or PSO) for the integration of DG in a power distribution network. The proposed algorithm takes into consideration the inherent nature of the control variables that comprise the search space in the optimal DG sizing/location optimisation problem, without compromising the network operational constraints.

The developments of the proposed Multi-Search PSO algorithm (MSPSO) is described, and the algorithm is tested using a standard, benchmarking 69-bus radial distribution network. MSPSO results and performance are compared with that of a conventional PSO algorithm (and other analytical and stochastic methods). Both single-objective (minimising network power loss) and multi-objective (considering nodal voltages as part of the cost function) optimisation studies were conducted.

When compared with previously published studies, the proposed MSPSO algorithm produces more realistic results since it accounts for the discrete sizes of commercially available DG units. The new MSPSO algorithm was also found to be the most computationally efficient, substantially reducing the search space and hence the computational cost of the algorithm compared with other methods, without loss of quality in the obtained solutions. As well as the size and location of DG units, these studies considered the operation of the generators to provide ancillary voltage support to the network (i.e. with the generators operating over a realistic range of lagging power factors, injecting reactive power into the network).

The algorithm was also employed to optimise the integration of induction generation based DG into the network, considering network short-circuit current ratings and line loading constraints. A new method for computing the reactive power requirement of the

induction generator (based on the machine equivalent circuit) was developed and interfaced with the MSPSO to solve the optimization problem, including the generator shunt compensation capacitors. Finally, the MSPSO was implemented to carry out a DG integration problem for a real distribution network and the results validated using a commercial power system analysis tool (ERACS).

Table of Contents

List of Figures

List of Tables

List of Abbreviations

μGA	Micro-Genetic Algorithm
ABC	Artificial Bee Colony
ACO	Ant Colony Optimisation
AI	Artificial Intelligence
AVR	Voltage Regulator
°C	Degree Centigrade
CHP	Combined Heat and Power
DE	Differential Evolution
DERs	Distributed Energy Resources
DG	Distributed Generation
DGU	Distributed Generation Unit
DPSO	Discrete Particle Swarm Optimisation
DSA	Differential Search Algorithm
DisCos	Distribution Companies
DNO	Distribution Network Operators
DOE	Department of Energy
DP	Dynamic Programming
EPSRA	Electric Power Sector Reform Act
EG	Embedded Generation
EP	Evolutionary Programming
GA	Genetic Algorithm
GenCos	Generation Companies
GMR_i	Geometric Mean Radius of conductor *i*
GMDs	Geometric Mean Distances
HV	High Voltage

IG	Induction Generator
IPPs	Independent Power Producers
IEEE	Institution of Electronic and Electrical Engineers
IEC	International Electrotechnical Commission
Kvar	Reactive Kilo-Volt-ampere
kWh	kilowatt hour
LV	Low voltage
LP	Linear Programming
MINLPs	Mixed Integer Non-Linear Problems
MO	Multi Objective
MOF	Multi Objective Function
MV	Medium Voltage
MSPSO	Multi Search Particle Swarm Optimisation
Mvar	Reactive Mega-Volt-ampere
MW	Mega Watt
NERC	Nigerian Electricity Regulatory Commission
NESI	Nigeria Electricity Supply Industry
O&M	Operation and Maintenance
OPF	Optimal Power Flow
OLTC	On-Line Tap Change
PCC	Point of Common Coupling
PF	Power Factor
PSO	Particle Swarm Optimisation
PSO-W	PSO with inertia weight
PV	Photovoltaic
PV bus	Constant Active Power and Voltage Magnitude bus Model

PQ bus	Constant Active and Reactive Power bus model
RDN	Radial Distribution Network
SCMVA	Short Circuit Mega-Volt –Ampere
Isc	Short Circuit Current
SPPSO	Small Population Particle Swarm Optimisation
SSEV	Sum of Squared Error Voltages
Std. Dev	Standard Deviation
SO	Single Objective
T & D	Transmission and Distribution
TranSysCos	Transmission System Companies
V_n	Nominal System Voltage
USA	United States of America
UK	United Kingdom
var	Volt-amperes reactive
WPP	Wind Power Plant

CHAPTER 1

Introduction

1.1 Background

Climate scientists and policy makers in developed countries consider that an 80% reduction in greenhouse gas emissions by 2050 is necessary if average global temperature rises of more than 2°C are to be avoided [1]. The electrical power sector is seen as offering easier and more immediate opportunity to reduce greenhouse gas emission than, for example, road or air transport and so likely to bear a large share of any emission reductions [1].

These problems have led to a new trend of generating power locally at the distribution voltage level by using non-conventional/renewable energy sources. These sources include natural gas, biogas, wind power, solar photovoltaic cells, fuel cells, combined heat and power (CHP) systems, microturbines, and Stirling engines and their integration into the utility distribution network. This type of power generation is termed Distributed Generation (DG) and ranges from few kWs to 50MW for medium size DG units and the energy sources are termed as 'distributed energy resources (DERs). The term ‘Distributed Generation’ has been devised to distinguish this concept of generation from centralised conventional generation [2].

There is no accepted definition of distributed generation both in the literature and in practice. Several country-specific strict definitions are available for DG all over the world, depending upon plant rating, generation voltage level, etc. In broad terms “*Distributed generation is an electric power source connected directly to the distribution network or on the customer site of the meter”* [3]. A classification of DG units based on their power rating as summarised in [4] is presented in Table 1.1. However, irrespective of these differences in definitions, the impact of DG on the power system is the same.

Table 1.1 DISTRIBUTED GENERATION UNIT CLASSIFICATION [4]

S/N	Type of DGU	Power Rating range
1	Micro DGUs	1 watt < 5kW
2	Small DGUs	5kW < 5MW
3	Medium DGUs	5MW < 50 MW
4	Large DGUs	50MW < 300MW

DG offers a long list of benefits that are highly dependent on the characteristics of each installation and the characteristics of the local power system. These benefits can be primarily classified into three broad categories [5] namely; economical, technical and environmental advantages.

Economical advantages can be realized when utilities deploy DG to defer investments in transmission or distribution infrastructure. These are related to fuel savings as a result of reduced over-reliance on fossil fuel, saving transmission and distribution cost and in some instances reducing wholesale electricity price. Since DG is typically located closer to the load centre in contrast with central generating stations, it can reduce congestion and system losses in some instances. On the other hand, environmental advantages include low noise and low emission and can be realized by renewable generators such as solar photovoltaics (PV), which have no marginal emissions or CHP systems whose use of waste heat can result in higher efficiencies than central generation units. The magnitudes of emissions benefits associated with DG depend on both the characteristics of individual DG units and the characteristics of power system to which they are connected. Potential technical advantages cover a wide variety of issues such as peak load saving, good voltage profile, reduced system losses, improved continuity and reliability, removal of some power quality problems and associated thermal constraints of Transmission and Distribution (T&D) feeders. Furthermore, many benefits accrue to particular stakeholders and may not benefit the distribution system operator or the other customers of the system [6].

The proliferation DG in the last decade has brought a tremendous alteration to the structure of a typical distribution network, making it an active network. Thus, presenting new challenges for distribution system planning and operations, as these circuits were designed to supply loads with power flows from the higher to lower voltage circuits [1]. Some of these challenges are in the area of voltage regulation, power quality, increase of network fault levels and the possible disruption to the network protection settings.

The integration of DG alters the flows of power in the network and consequently, will alter network losses. The location and the size of the distributed generator to the load have effect on the network losses; for a small distributed generator located at the vicinity of a large load, will reduce network losses and conversely, a large distributed generator located far away from network loads is likely to increase distribution system losses. Therefore, proper allocation of DG units into an existing distribution system will play a crucial role in the improvement of the power system's performance and meeting the world target of reducing greenhouse gas emissions.

The optimal allocation of DG is one of the most-important aspects of DG planning; Distribution Network Operators (DNOs) will require an effective solution optimisation tool for network planning and integration. This thesis focuses on developing and implementing an optimisation tool that can be valuable to utilities and DNOs for integrating distributed generation into the power system network. The problem of DG integration can be considered as a combinatorial, discrete and continuous nonlinear problem that involves the determination of the optimal or near optimal overall combination of locations and capacities in a network of n buses. Determining the best solution is a non-trivial effort beyond the feasibility of manual searches not even for a small distribution power network. Artificial intelligence techniques (AI) offer a practical alternative for solving such problems.

In this current research work, a stochastic optimisation technique based on particle swarm optimisation has been used to reach technical conclusions without violating distribution system operating constraints. Distribution systems operational constraints such as power balance, bus voltage and line loading limits are effectively handled by the cost function computation algorithm. Additional constraints such as constraints on the discrete size of DG unit and short circuit current level constraints were included are handled by the stochastic algorithm preceding the optimisation. The constraints were considered either as imperative (hard) or indicative (soft).

1.2 Statement of the Problem

A number of Distributed Energy Resources (DERs) technologies are now commercially available in different discrete sizes, the most-notable being micro-turbines, combustion turbines, reciprocating engines, wind power, photovoltaic, solar thermal systems, biomass, and various forms of hydraulic power. DGs are known to inject a constant amount of real and reactive power. For a grid-connected synchronous generator, this

corresponds to the operation at its continuous power output rating at a range of possible lagging power factors up to a maximum reactive power output limited by the current rating of the stator or rotor windings. Thus, in optimal DG studies, the variable defining DG size can be considered as discrete variable.

Therefore, in optimal DG studies, while some control variables are inherently integer and discrete some are continuous variables. This result in a problem with a mix of control variables, referred to in this thesis as multi search space problem. Multi search space problem is best solved by an optimisation algorithm that is capable of operating integer, discrete and continuous variables (i.e. mixed search spaces). The use of continuous optimisation algorithms in such problems can substantially increase the search space and hence the computational cost of the algorithm.

Distributed generation plants with rotating machines will contribute to the network fault levels. For instance, both induction and synchronous generators will increase the fault level of the distribution system when connected to it. In most existing utility distribution networks in the urban areas, where the fault level approaches the ratings of the switchgear, the increase in fault level can be a serious bottleneck in the development of distributed generation schemes. Increasing the short-circuit rating of the distribution network switchgear and cables as an option to overcome such problem can be extremely expensive and difficult particularly in congested city substations and cable routes. Also, the option of reducing the fault level contribution of distributed generator by introducing impedance between the generator and the network, with a transformer or reactor will be at the expense of increased losses and wider network voltage variations. Therefore, there is the need to appropriately incorporate this effect into the problem of DG integration.

Induction generators are becoming common as a source of distributed generation on distribution system. However, DG of type based on induction generator behaves differently from synchronous generator based DG. Induction generator requires reactive power support for its operation thus, the need to incorporate this requirement into the optimisation process. A simultaneous capacitor and induction generator placement problem will require an optimisation algorithm capable of handling the discrete size nature of both capacitor and induction generator. In addition, induction generator based DG is required to remain connected to the grid during low-voltage supply faults [7]. This will require that the reactive power requirement of such plant be met fully and locally supplied from compensating devices.

This research work, intends to explore decision making techniques to determine the optimum siting and sizing of distributed generation in an existing distribution utility power network. The decision making technique is based on stochastic optimisation technique employing particle swarm optimisation (PSO).

In this work, the major objective of the placement technique is to reduce active power loss in the network while ensuring that the operational and security constraints of the network are respected. This implies that the study considered both a single and multi-objective formulation. Minimizing system power losses has a positive impact on relieving the feeders, reducing the voltage drop and improving the voltage profile and has other environmental and economical benefits.

In the current methods of formulating DG optimisation problem available in the literature, variables representing the sizes of DG units are usually continuous. Their solution needs to be rounded to the nearest available commercial generator size, which can affect the accuracy of the optimized results. The physical aspects of distribution system such as busbar location numbers are normally rounded to their nearest integer variables. Rounding-off issues with respect to the DG-unit's size are overcome by considering DG sizes with a fixed step size increment within a practical range of generator sizes. Thus, the solution attained may not be the best available choice since some sizes are left out of the search space. In addition, previous optimisation studies on IG based DG have calculated the reactive power requirement of IG based on approximate empirical formula as discussed in [8]. And shunt compensation capacitors are not considered as part of the optimisation process neither is the effect of short circuit current considered as part of the optimisation process.

Optimisation problems in distribution system involve integer, discrete and continuous variables. The problem formulation of distributed generation integration leads to nonlinear, stochastic equation as objective function or constraints with a mix of these variables. Thus, the need for an effective algorithm that operates well on these variables. An optimisation tool with such capabilities is considered in this research work. The reactive power requirement of IG is computed based on per phase equivalent circuit parameters of the induction machine, with both shunt capacitor and effect of short circuit current included in the optimisation process. DG short circuit current level consideration is to ensure that the interruptible capability of the protective equipment is not compromised.

The model of IG considered in this study, facilitates the computation of real and reactive power output for a specified generator rating (power output) and operating terminal voltage. The slip is varied from zero at certain step intervals and the corresponding output power is computed. The process is continued until the difference between the computed output power and the specified output power is within a specified error tolerance.

A power system optimisation tool based on stochastic (random search) technique (PSO) that operates integer, discrete and continuous variables for the nonlinear optimisation problem is developed. A multi-valued discrete PSO (DPSO) is proposed, to effectively handle the integer nature of the bus number location. The discrete nature of the size of DG and the capacitor is handled by an algorithm capable of searching discrete space variables (referred in this thesis as a dichotomy search algorithm), developed mainly for this purpose.

In this study, the algorithm proposed for computing the reactive power requirement of the IG based DG is interfaced with the stochastic power system optimisation tool. The reactive power of the IG calculated, forms the basis for selecting the required value of the shunt compensating device that will provide entirely the reactive power required by the generator. Thus, the network voltage profile is enhanced with the integration of IG compared to when the reactive power requirement of the generator is to be met by the grid. The constraint on fault level considered in the optimisation process is handled by a three phase symmetrical fault algorithm interfaced with the developed stochastic optimisation tool. The fault algorithm is executed prior to the optimisation process using a simple and practical method that is based on the bus impedance matrix by the building algorithm. The technique fully accounts for the impact of DG on short circuit current rating of the switchgear, allowing the integration of DG within the available switchgear rating.

The proposed algorithm is tested on a standard 69 bus benchmarking network used by other researchers [9-13] for power system optimisation problems, including. In addition to this network, the algorithm is also implemented on a 47 bus practical Nigerian medium voltage distribution network.

1.3 Motivation and Objectives of the Study

Utility deregulation and the growing challenge of system reliability are some of the primary reasons for the high level of interest in distributed energy resources in addition to economic and environmental pressures. Nigeria like many other developing countries has its electricity generating stations centrally located (Centralized Generation) based on the bulk power planning methodology. In the recent past, the government has taken a bold step to decentralize the power sector into Generation Companies (GenCos), Transmission System Companies (TranSysCo) and Distribution Companies (DisCos). This was in line with global trends of encouraging the participation of Independent Power Producers (IPPs) in the electricity Industry. A deregulated electricity market will introduce competition in generation, transmission and distribution, thus, giving DG applications a very favourable market. This in no small measure will release the government from the burden of investment in the generation sector and could result in a reduction in electricity prices and an improvement in the quality of supply. An optimisation algorithm of this type can be valuable to the IPPs for finding the best location and size of their distributed resources for efficient power loss reduction. Optimal allocation of DG units into an existing distribution system will improve the power system's performance and will benefit both the IPPs and the end customers with their power supply reliability and adequacy greatly enhanced.

The major aim of this research work is to develop a power system optimisation tool based on the PSO algorithm with applications to integration of distributed generation in the power network. The purpose of which is a power loss reduction while ensuring that the operational and security constraints of the distribution system are respected. PSO algorithm offers many advantages that include; simple implementations, speed of convergence, very few algorithm parameters, very efficient global search compared to other stochastic methods such as GA.

The main objectives of the study can be summarised as follows;

- To develop a Particle Swarm Optimisation procedure for evaluating the best locations and injection levels of distributed generation in an existing electric power utilities network. In addition to the power flow equality and non equality constraints (power balance, bus voltage drop and line capacity limits); constraints such as discrete size of DG units and the short circuit current level are to be considered.

- To extend the developed PSO procedure for solving optimisation problems of simultaneous placement of shunt capacitor and distributed generation in a power distribution network considering both synchronous and induction generators based distributed generation. Constraints that can impede the development of both DGs are to be considered.
- To collate necessary and available practical data from an existing utilities' network in addition to the available standard benchmark networks, for modelling and optimisation study using the proposed optimisation tool.

1.4 Contributions

The main contributions of this research are in the development of a novel decision making optimisation procedure, based on a stochastic technique using particle swarm optimisation (referred to as Multi Search PSO "MSPSO" in this thesis), and its applications to power system optimisation problems. First is the development of MSPSO which is an ensemble of a multi-valued discrete particle swarm optimisation (DPSO) that handles integer variable, a dichotomy search algorithm (an algorithm capable of searching through discrete space variables) that handles the discrete constraint on the capacitor and DG units and the continuous PSO that handles the continuous variable. The dichotomy search algorithm is first proposed and reported by this research work for optimal DG integration problems.

The second is the application of the proposed technique to solve the conventional problem of optimum sizes and location of capacitor and distributed generation (that include synchronous and induction generators) in a power distribution network.

The third contribution is in the modelling of the practical network and the application of the proposed optimisation technique to solve the optimal location and sizes problem for the practical network considering fault current level constraints. And the validation of the results with an actual simulation using commercial power system analysis software tool 'ERACS'.

The research work carried out in this thesis has resulted in the following publications:

[1] **I. Musa,** S. M. Gadoue, B. Zahawi, "Integration of Induction Generator Based Distributed Generation in Power Networks Using Discrete Particle Swarm Optimisation Algorithm", submitted to *Electric Power Components and Systems,* accepted and re-submitted after minor corrections on 3rd December 2014.

[2] I. Musa, S. M. Gadoue, B. Zahawi, "Integration of Distributed Generation in Power Networks Considering Constraints on Discrete Size of DG units", *Electric Power Components and Systems,* vol. 42: 9, pp. 984-994, 2014.

[3] I. Musa, B. Zahawi, S. M. Gadoue, "Integration of Induction Generator Based Distributed Generation and Shunt Compensation Capacitors in Power Distribution Networks", presented at the *4th International Conference on Power Engineering, Energy and Electric Drives (POWERENG), 2013*, Istanbul, Turkey, 13th -17th of May 2013 doi: 10.1109/PowerEng.2013.6635765

[4] I. Musa, B. Zahawi, S. M. Gadoue, D. Giaouris, "Integration of Distributed Generation for network loss minimization and voltage support using Particle Swarm Optimisation", presented at the *6th IET International Conference on Power Electronics, Machines and Drives (PEMD 2012),* , Bristol, UK, 27-29 March 2012 doi: 10.1049/cp.2012.0150

1.5 Organization of thesis

Chapter 1 presents the background of the study with highlights focused on the benefits of DG, the problem statement for the research work, motivation and objective of the study. Finally the contributions of the research work are presented.

Chapter 2 provides a basic review of the literature with respect to operational and other problems that can critically impact the operation of distribution network with the integration of distributed generation. The possible challenges posed to planning and operation engineers are briefly discussed. A brief introduction of the conventional and stochastic evolutionary computation algorithms techniques (analytical, genetic algorithm, PSO and artificial bee colony algorithm) used in power system optimisation studies is presented. A State-of-the-art review of the conventional and stochastic power system optimisation algorithms is also discussed. The available solution approaches and how they have been applied to power distribution systems are summarized.

Chapter 3 explores the Particle Swarm Optimisation technique. An overview of the trend from the original PSO to PSO with inertia weight (PSO-W) is discussed. The trend in adopting the PSO, which operates on continuous problems to solve discrete optimisation problems, is discussed. The proposed Multi Search Particle Swarm Optimisation (MSPSO) procedure specifically meant for DG and shunt capacitors integration into distribution network is presented. Features of the MSPSO such as the multi-valued DPSO, dichotomy algorithm and few informants PSO implementations are

presented. An overview of variant PSO 'Small Population Particle Swarm Optimisation (SPPSO)' for the optimal DG problem is likewise introduced. The purpose of discussing the SPPSO algorithm is that its results will be utilised to compare with that of the proposed MSPSO.

Chapter 4 presents simulation study of distributed generation integration in a compensated distribution network to provide voltage support for the network. The optimisation process is based on the traditional PSO-W algorithm. The study considered various scenarios with different test cases and operating power factors. The ancillary services of voltage support by DG and the effect of power factor on such services are presented considering both single and multi-objective cases. The results of this study are used as a benchmark to assess the improvement obtained with the proposed algorithm.

Chapter 5 presents the application of the proposed algorithm 'MSPSO' for distributed generation integration in a compensated distribution network to provide ancillary of voltage support for the network. The study considered various scenarios with different cases and operating power factors. The ancillary services of voltage support by DG and the effect of power factor on such services are also presented considering both single and multi-objective cases. Finally a comparison of results from previous studies on DG integration, the studies in chapter 4 and chapter 5 are presented to demonstrate the significance of the proposed algorithm used in the current study.

Chapter 6 presents the application of MSPSO to the simultaneous integration of induction generator based distributed generation and shunt compensation capacitor for single and multi-objective cases. The short circuit current and line loading constraints are considered in both a single and multi-objective cases. A derivation of the power flow procedure based on per phase equivalent circuit parameters of a 3-phase Induction Generator (IG) is presented. The developed MSPSO algorithm is combined with an IG algorithm procedure and AC power flow to solve the optimisation problem of IGs.

Chapter 7 presents the application of multi search particle swarm optimisation for integration of distributed generation onto the practical distribution network. An overview of the Nigeria distribution power system network is presented, highlighting the potential for distributed generation integration. In addition, modelling equations for computing the line series and shunt elements relating to the practical network are discussed. The ERACS power system software is used to validate the results of the MSPSO. The chapters end with a summary of the simulation results, findings and some conclusions. The final chapter discusses the conclusions drawn from this research work,

outlines a summary of the contributions made, and some suggestions for possible areas of future research to extend the work.

CHAPTER 2

Review of Distributed Generation Integration studies

In this chapter, a general overview of Distributed Generation (DG) is presented. The review includes the discussion of the benefits from the application of DG for utility and customer, the technical challenges that may impede their development onto the utility network. Later in the chapter, some few selected conventional and stochastic evolutionary methods employed in power system optimisation problems that are considered particularly relevant to the current study are briefly introduced. Moreover, a literature review of optimisation techniques used in DG integration studies is presented.

2.1 Introduction

Conventional power systems provide several advantages that include [1]:

1. Large generating units can be made efficient and operated with only relatively small staff
2. The interconnected high voltage transmission network allows the most efficient generating plant to be dispatched at any time, bulk power to be transported large distances with limited electrical losses and generation reserved to be minimised.
3. The distribution networks can be designed simply for unidirectional flows of power and sized to accommodate custom loads only.

The structure of the centralized large electric power system that exists today is borne out of these advantages. The structure is a hierarchical system of voltage levels used to transport the electrical power, sometimes over considerable distances from a bulk generating station with a limited number of large central generating sources to the consumers. The process involves generating and stepping up of voltages at the central generation station to high voltages, and stepping down gradually as the power get closer to the consumer. These differences in voltage levels lead to the classification of different parts of the power system as depicted in Figure. 2.1. The voltage levels depicted are the voltage level used on the Nigerian electrical power system.

All major generating stations are interconnected to load centres via the high voltage transmission network. The distribution systems are assigned three voltage levels, with 33kV referred to as high voltage level (HV) distribution, 11kV as medium voltage (MV) distribution and 0.240-0.415kV as low voltage (LV) distribution. The transfer of power down to the individual customer is via the distribution network. Power transfer between the various transmission and distribution circuits is achieved through electrical substations with chains of distribution transformers. The distribution circuits are radially operated, with a number of feeders emanating from each substation in common with many distribution systems around the world.

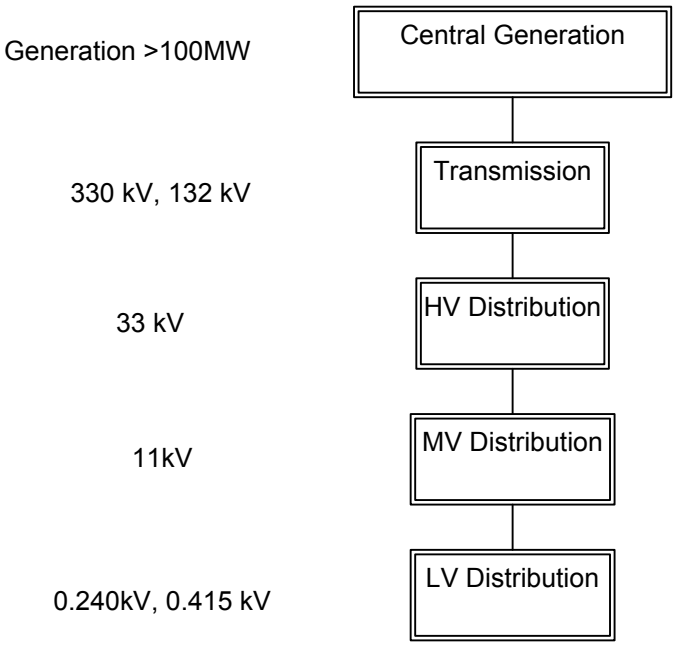

Figure 2.1: Transmission & Distribution (T&D) Levels in Nigeria

Radial feeders have the advantages of being simple and less expensive, both to construct and in terms of their protection system. Their major disadvantage lies with the difficulty of maintaining supply in the event of a fault occurring in the feeder. A fault could result in the isolation of a large number of customers until it is located and cleared.

In spite of the advantages of centralized generation, technical, economic and environmental benefits have been the three key drivers behind increasing levels of DG. Connection of a generation to a distribution network leads to a number of challenges as existing distribution networks are passive, in that they were designed and built purely for the delivery of electricity to the customer. The introduction of DG is changing the characteristics of the distribution network. It has led to increased and bidirectional

active and reactive power flows, along with wider variation in voltage levels, both of which affect the operation of equipment on the network and the level of losses [14]. These technical challenges are impacted by the number of DG connected to distribution system network and need to be taken into account in DG problem planning and operation.

2.2 DG Types and Applications

Distributed generation can come from a variety of sources and technology. DG from renewable sources, such as wind, solar, hydro and biomass are often referred to as 'Green Energy'. In addition to these, DG from non renewable sources includes fuel cells, micro turbine, internal combustion engine, and combined cycles. Some renewable and non-renewable energy sources will require a power conversion system in the form of converter for interconnection to the grid, e.g. solar, fuel cell, micro-turbine and some wind turbines. Others like rotating synchronous and induction AC machines based DG such as a fixed speed induction generator, internal combustion engine directly interconnect to the grid (without the need for power converters).

The applications of DGs are customer related. Some of the major customer applications of distributed or dispersed generation include [5]:

1. Own electricity generation with or without grid backup.
2. Generating a portion of electricity to save peak period to reduce the cost of electricity purchased during the peak hours.
3. Sell excess generation back into the grid, when there is a surplus of power.
4. Standby or emergency power.
5. Improving the quality of supply and increase reliability.
6. Serving niche applications, such as "Green Power" or "remote Power"
7. Meeting continuous power, premium power or cogeneration needs of the residential market.

2.3 DG Benefits

DG provides several potential opportunities, benefits and services to both utility and the consumer depending on whether it is used as grid connected DG, dispersed DG (stand-by generating systems) or both. For instance using dispersed DG, the consumer will

have consumption choices; they can reduce their energy expenditures by incorporating DGs that are powered by cheaper fuel sources. As for the utility, it can use the DG power to enforce its distribution network voltage stability, as well as to increase its peaking capacity without suffering financial costs[15].

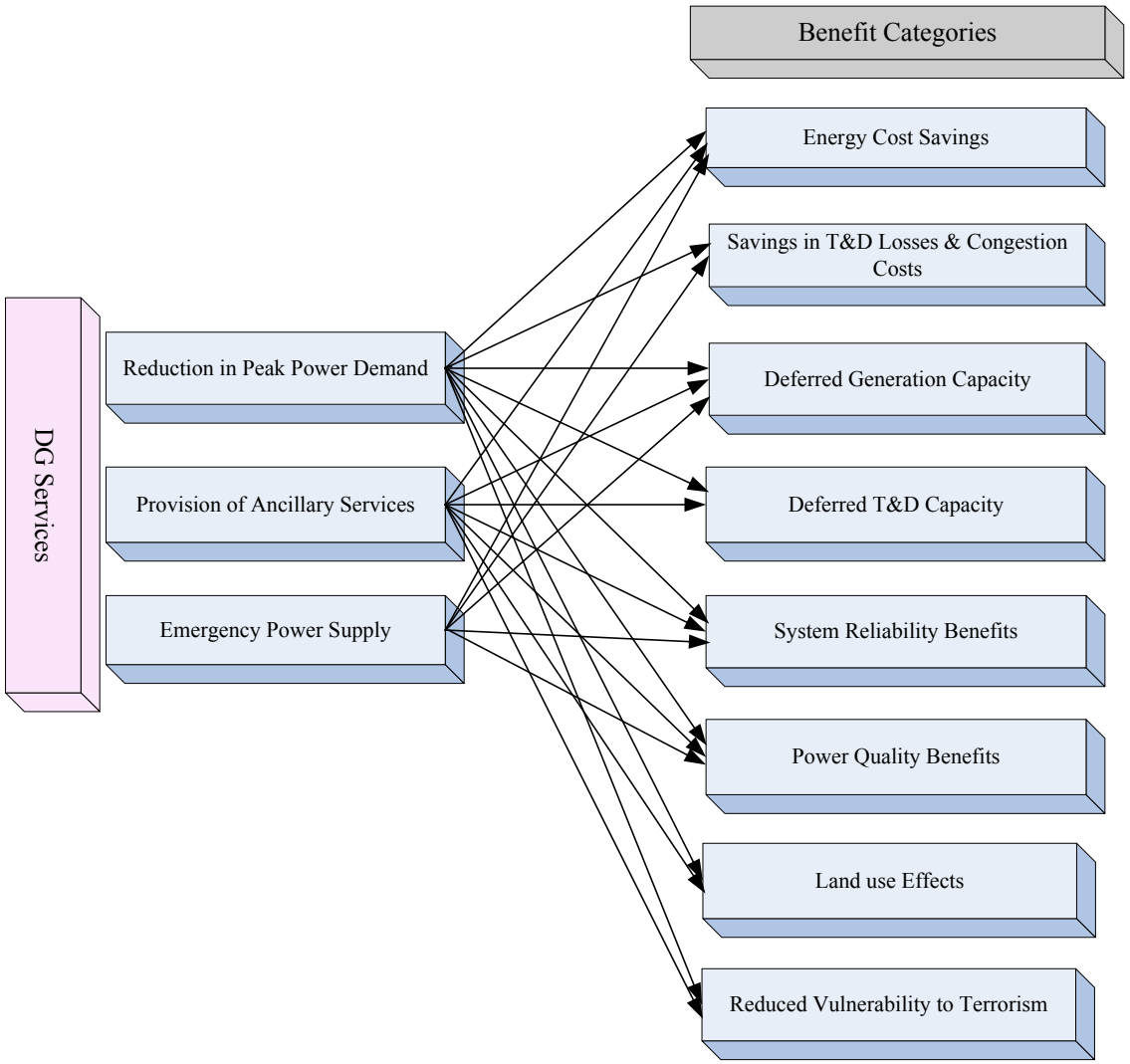

Figure 2.2: Charts of Distributed Generation Benefits and Services

However, grid connected DG has the potential to provide some services that may results in specific benefits to the grid and to other customers within the area that is been served by the grid. Figure 2.2 show some of these specific services and the potential benefits that can be derived from those services. The first lists to the left of the chart are specific services DG is capable of providing. The potential benefits derived from those services are categorized and listed to right-hand of the chart. For example, new capacity investments may be deferred by reducing peak power requirements on the grid, or by the provision of ancillary services. Distributed generation available as an emergency supply of power can also be used in demand response programs to reduce congestion, or

increase system reliability via peak-shaving [16]. The ancillary services include some of the following; operating reserves, regulation, black start and reactive power provision.

2.4 Technical challenges of DG

The integration of DG presents new challenges for distribution system planning and operations, principally because the configuration of power lines and protective relaying in most existing distribution systems assume a unidirectional power flow and are designed and operated on that assumption. In recognition of the potential adverse impacts of DG on distribution systems and the need for uniform criteria and requirements for the interconnection of DG, standard interconnection guide are developed.

In UK, the standard guiding the interconnection of DG is the Engineering Recommendation (ER) G59/2-1 which is now G59/3 and G83/1-2 which is now G83/2. The G59 documents set out standards and guidance on technical requirement for the connection of generating plant to the distribution systems of licensed Distribution Network Operators (DNOs). These requirements must be met before the local DNO will allow generating plant to be connected to its network. On the other hand, G83 documents set out standards and guidance on technical requirement for the connection of Small-Scale Embedded Generators (SSEG) in parallel with low-voltage distribution systems [17]. In the US, it is the IEEE Standard 1547, first released in 2003 and later incorporated into the Energy Policy Act of 2005 [6]. The standard applies to the interconnection of all generations with aggregate capacity of 10 megavolt amperes (10 MVA, approximately 10 MW) or less to the distribution system. The primary aim of these standards is to ensure that the negative impacts of DG units on other customers or equipment connected to the grid are controlled.

These technical challenges include some of the followings:

- Network voltage rise
- Losses
- Short circuit fault level
- Protection

2.4.1 Network voltage rise

Supplying customers within a specified voltage limits is an obligation which every distribution network operator must fulfil. This voltage limits is typically around ±5% of nominal. This requirement often determines the design and capital cost of the distribution circuits and so, over the years, techniques have been developed to make the maximum use of distribution circuits to supply customers within the required voltages [1]. The connection of DG to the circuit, changes the flows of power and reactive power and hence the voltage profile of the network. The most familiar case is when the customer load on the network is at a minimum, resulting in the output of the DG flowing back to the source.

This voltage rise can be limited by reversing the flow of reactive power, achieved using an induction generator, under exciting a synchronous machine or operating an inverter so as to absorb reactive power. A very laborious method is carrying out successive power solutions, repeated for different load levels. A technique for evaluating the required penetration of DG level that will not increase the steady state voltage rise of the network has been shown in recent work [18]. The technique is based on analytical solution using Jacobian sensitivities to direct estimation of the amount of active and reactive power that DG can inject into each system bus without causing voltage limit violation.

2.4.2 Short circuit level

Connecting any form of DG to a distribution network can increase the level of fault current in the network. This could result in fault levels exceeding the design limit of the network, particularly if it is already being operated close to its design limit. The fault level contribution from DG is determined by a number of factors [19], including: the size, types of DG and the distance of the DG from the fault, whether a transformer is present between the fault location and the contributing DG, the configuration of the network between the DG and the fault and the method of coupling the DG to the network.

Fault levels are normally calculated at the network planning stage and for operational reasons, to ensure that they remain within the design limits of the power network. The solutions for mitigating the impact of DG on fault level are discussed in [19] they include; uprating the capability of existing equipment such as Circuit Breaker (CB), introducing higher impedances in the network to limit the fault level etc. The

significance of considering restriction imposed by switchgear fault rating with the connection of DG has been shown in previous work [20], ignoring such constraint the capacity of the network to absorb new generation can be overestimated.

2.4.3 Losses

Line losses are a critical consideration when designing and planning electrical power network systems. The losses are the results of current flowing through the lines of distribution and transmission systems, and they are inevitable on any network. The magnitude of the losses depends on the quantity of the current flow and the line impedance. Consequently, line losses can be decreased by reducing either line current or network impedance or both. Therefore total current flow in a power network is the sum of the current flows associated with the real and reactive power components.

If DG is used to provide energy locally to the load, line losses can be reduced because of the decrease in current flow in some part of the network. DG can deliver a portion of real and/or reactive power so that the feeder current is reduced and voltage profile can be improved with reduction in losses. Line losses occur not only in lines, but also in transformers and other transmission and distribution system devices [16]. Previous studies have indicated that poor selection of the location and size of DG for serving load locally would lead to higher network losses than the losses without DGs [10, 21, 22].

2.4.4 Protection

Distributed generation units can reduce current at the unit protection for the period before the DG senses the fault and disconnects, making it harder to detect a fault and complicating the coordination among protection devices. In addition, fault currents at points of system protection will depend on which DG units are connected and operating at the given time. Changing fault currents with the introduction of DG could lead to unreliable operation of protective equipment and result in faults propagating beyond the first level of protection reducing system reliability and safety.

It has been suggested that utilities could use real-time information about the operation of the network and the nature of connected resources to dynamically change protective relay settings [2].

2.5 Optimisation Techniques

In optimisation problems, the task is in choosing the alternative that either maximises or minimises an evaluation function which is defined on the selected evaluation criteria.

Hence, possible goals of optimisation process are either to find an optimal solution for the problem or to find a solution that is better than some predefined threshold (for example the current solution) [23]. There is no single method available for solving all optimisation problems efficiently. Hence a number of optimisation methods have been developed for solving different types of optimisation problems. Optimisation techniques such as analytical, genetic algorithms, artificial bee colony, etc., have been used for tracking optimal location of DGs in power distribution networks.

Analytical techniques represent the system by a mathematical model and evaluate it using direct numerical solution [24]. Analytical techniques offer the advantage of short computing time. However, when the problem becomes complex, the assumptions used in order to simplify the problem may override the accuracy of the solution.

The genetic algorithms (GA) are computerized search and optimisation algorithms based on the mechanics of natural genetics and natural selection. John Holland in 1975 [25], originally proposed the genetic algorithms. The most basic concept of the GA is that the strong tend to adapt and survive while the weak tend to die out. Thus implying that, optimisation is based on evolution, and the "Survival of the fittest" concept. The basic elements of natural genetics used in the genetic search procedure are reproduction, crossover, and mutation.

PSO is a cooperative population-based global stochastic optimisation technique inspired by the behaviour of swarms such as fish schooling and birds flocking proposed by Kennedy and Eberhart in 1995 [26, 27]. PSO differs from other evolutionary algorithms in that better solutions are evolved through the social interactions of individual particles within the group or swarm. The particles move through the problem space, and over time converge upon the optimal solution. Unlike in genetic algorithms, where the weakest individuals are discarded and replaced by each subsequent generation, with PSO individuals is not eliminated, and the best solutions are evolved through cooperation and position updates.

The artificial bee colony (ABC) algorithm is a new meta-heuristic optimisation approach inspired by the intelligent foraging behaviour of the honey bee, introduced in 2005 by Karaboga [28]. It was proposed, initially for unconstrained optimisation problems and later extended to handle constrained optimisation problems [29]. The ABC algorithm has only two parameters (colony size and max. iteration number) to be tuned in comparison with other meta-heuristic algorithms such as PSO and GA with

many parameters to tune. The colony of artificial bees consists of three groups of bees: employed onlookers and scout bees and are responsible for the exploration and exploitation processes of the search space.

In the next section, a detailed overview of the optimisation techniques employed in optimal DG studies is discussed.

2.5.1 Literature Review of Optimisation Techniques used in DG Integration studies

The proliferation of the DG in the last decade has brought a tremendous alteration to the structure of a typical distribution network. DGs are available in modular units, characterized by ease of finding sites for smaller generators, shorter construction times, and lower capital costs [30]. However, their integration into a distribution system requires in-depth analysis and planning that usually include technical, economical and regulatory aspects [31]. These factors can affect the final optimal attained solution. A number of Distributed Generation (DG) technologies are now commercially available in different discrete sizes. The most notable being micro-turbines, combustion turbines, reciprocating engines, wind power, photovoltaic, solar thermal systems, biomass, and various forms of hydraulic power. DG can be rotating devices (synchronous or asynchronous machines) directly coupled to the network, or they can be rotating or static devices interfaced via power electronics devices. The impact of DG technology on power system operation, control and stability affect the size and optimal placement of DG [30]. A large amount of research has been carried out on DG sizing and placement problem. A selection of some of the relevant publications is reviewed here.

A numerical method based on exhaustive search technique is employed in [32, 33] to find DG location (as viewed from an electric utility technical perspective) that optimizes a multi-objective performance index for a given DG size. The index estimates the benefits of DG insertion by evaluating indices for various technical impacts related to power loss, voltage profile, line capacity and short circuit level. The various technical impacts were weighted in accordance with their relevance to form a single objective function.

A numerical method based on gradient search is proposed for optimal sizing of multiple DG in a meshed network considering fault level constraints [34]. An iterative process is used to allocate new capacity using optimal power flow mechanisms and re-adjusts capacity to bring fault currents within the specifications of switchgear. Other numerical

methods based DG integration are linear programming [14, 35], sequential quadratic programming [36], non linear programming [37, 38], dynamic programming[39] and ordinal optimisation[40]. The nonlinear programming, the sequential quadratic programming and the ordinal optimisation methods have been described to be the most efficient of the available numerical methods for problem of optimal DG placement [30].

Several analytical techniques have also been implemented for optimal DG sizing and placement problems. In[10] an analytical method, based on the exact loss formula, is proposed to optimally site and size a single DG with the objective of network power loss reduction. An analytical method that is applicable to radial feeder with uniformly distributed load is suggested in [22] to install a DG of 2/3 capacity of the incoming generation at 2/3 of the length of the line. Analytical expressions for finding optimal size and power factor of different types of DGs are proposed in [11] with the objective of power loss reduction. An analytical method suggested in [9] determines the optimal location and size of multiple DGs, considering different types of DGs with the aim of power loss reduction. Analytical methods are characterized by ease of implementation and fast execution. The major setbacks of these methods is that their results are only indicative, since they make simplified assumptions including the consideration of only one power system loading snapshot [30]. In addition the capacities of the optimal DG sizes calculated using these methods are continuous values that do not always represent the practical available DG size units. Their solution need to be rounded to the nearest available commercial generator size to fulfil the discrete size of DG units constraints which can affect the accuracy of the results.

Several techniques based on stochastic computing algorithms have been proposed to solve the problem of optimal DG sizing and location. The use of evolutionary programming to maximise the reduction of load supply costs is presented in [41]. An Ant Colony Optimisation (ACO) technique for optimal placement and sizing of DG is proposed in [42]. The objective was to minimise the investment and the total operational cost of the system. In attempt to address practical concerns in terms of available DG-unit sizes, the proposer considered DG sizes in multiples of 1MVA up to a maximum of 4MW at unity power factor, based on a fixed step size increment.
Genetic Algorithm (GA) for optimal DG capacity and location to maximise system loading margins and the distribution company's profit is suggested in [43]. A multi-objective performance index-based size and location determination of DG with different

load model based on GA is presented in [44]. In this study, DG sizes are considered with a fixed step size increment within a practical range of generator sizes.

In [45], an Artificial Bee Colony (ABC) algorithm is presented for determination of optimal DG size, location and power factor to minimise the total system power loss. This study considered discrete size of DG units with 100 step interval between sizes. A hybrid genetic algorithm and Optimal Power Flow (OFP) technique is suggested in [46] to efficiently site and size a predefined number of DGs. However, the pre-selection of DG sizes using a fixed step size increment [42, 44, 45] implies that there is a likelihood of the optimal commercially available DG size being left out of the search space. Thus, the solution attained may not be the best choice.

Particle Swarm Optimisation (PSO) has been previously used in a wide range of power system applications [47-51]. It was shown to be an effective tool for solving large-scale nonlinear optimisation problems. A stochastic dynamic multi-objective model based on Binary PSO is proposed in [52] find the optimal location and size to minimise a multi-objective cost function. Recent literatures have presented techniques to extend the application of PSO to solve discrete problem of DG integration. A multi-objective index-based approach using PSO is presented in [53] to optimally determine the size and location of multiple DG units. In [54] a hybrid method employing discrete PSO and optimal power flow is proposed to find the optimal size and location of a predefined number of DG units within a distribution network. This hybrid discrete PSO technique determines the location of the DG units and the OPF computes the optimal capacity of each DG and the objective function (production cost of generation and cost of network power loss). The results of the optimisation process are continuous capacity DG units.

In [55] a new problem formulation for connecting a predefined number of biomass fuelled gas micro-turbines to a distribution network using the algorithm employed in [54] is presented. In [56, 57], discrete PSO is proposed for optimal DG placement. However, the search for discrete sizes of DG is in step size of 50kW and 100kW. This implies that DG sizes not within the range of selected step size would be left out of the discrete search space.

The PSO algorithms used in previous studies have been designed and intended to handle continuous optimisation problems. The real value solutions are usually rounded to the nearest integer. In optimal DG studies however, the inherent integer nature of some control variables implies that the problem of DG sizing and placement is by its' very nature a mixed search space (of integer, discrete and continuous) combinatorial

problem. This implies that the problem is best solved using a mixed search space optimisation algorithm that can independently handle each of the variables involved. The use of continuous optimisation algorithms in such problems can substantially increase the search space and hence the computational cost of the algorithm.

Induction generators have long been used for wind energy applications [58] and are currently the standard technology for network connected wind turbines. Several studies have been conducted on the integration of induction generator based DG in electrical power networks. In [12] an analytical technique for optimal placement of wind turbine based DG is presented. A PSO-based technique for optimal placement of wind generation in distribution networks is presented in [59]. An optimal multiple DG placement study using adaptive weight PSO is presented in [60]. However, in all these studies, the reactive power requirement of the induction machine is calculated by an approximate empirical formula and no shunt compensation capacitors were considered as part of the network optimisation problem. Uncompensated reactive power can cause stress on the hosting utility grid with added expenses, which can create in difficulties for power purchasing agreements from independent wind energy producers. Providing compensation can increase the penetration level of wind power into existing distribution networks [61].

In [62], a multi-objective methodology for finding the optimal location and size of DG is presented. The optimal location is found using voltage stability index and the optimal sizing of the DG and the optimisation is carried out employing genetic algorithm. The reactive power compensation for the network was also considered but there are no details on how it was achieved. And the use of sensitivity index approach for location selection may not lead to the best choice. Consequently, the result obtained may not give the optimum result for the optimisation problem considered [10].

Wind Power Plant (WPP) can contribute to initial short circuit current fault if fully compensated locally such that the air gap flux does not collapse in the event of disturbances. The UK national grid codes specify that the generator must exhibit a fault ride through capability to remain connected and contributing to network stability during a fault [63]. Investigations on the dynamic performance of wind power plants during low voltage fault-ride-through are presented in [64, 65]. A dynamic analysis of short circuit current contributions of different types of WTGs is presented in [66, 67]. The fixed speed induction generator was found to be among the types with the largest three-phase Short Circuit (SC) current fault [66]. A dynamic performance of wind

asynchronous generators using different types and locations of fault is presented in [68], the short circuit current contribution considering different types of faults and locations were obtained via transient analysis using squirrel cage generator model. Thus, the need to include the effect of short circuit current in the optimisation process involving IG based DG cannot be overemphasized.

The Current regulatory interconnection standards for DGs 'IEEE Standard 1547', does not encourage DG to regulate voltage at their PCC [69], and therefore, they have been modelled in power flow studies as a PQ node (i.e., a negative load). However, a recent study [6], has recommended that the main standard governing DG interconnection (IEEE Standard 1547) be revised to permit voltage regulation by DG units. The advantage of which is a reduced voltage variation under high penetrations of DG in distribution network. DG units with reactive power control capability provide better network voltage profile and lower losses.

Some studies have also considered the integration of both DG and shunt capacitor to provide network voltage support. A numerical method associated with PSO is proposed in [70] for strategic placement of DG units and shunt capacitors in a distribution network. The target voltage support zones are identified numerically and the PSO algorithm solves the overall objective function to minimise the cost of DG units and shunt capacitors. In this case, the only source of reactive power is the shunt capacitors as the DG units were assumed to be operating at unity power factor. A numerical method to determine the optimal DG placement with the objective of maximizing voltage support is proposed in [71]. In this case, the DG is modelled to inject real and reactive power into the network. The location of the generator is determined using a line sensitivity index where the most vulnerable voltage bus is selected as the generator location. The generator size is then calculated such that the voltage at the DG bus is 1p.u. However, this technique results in a generator with a non-optimal output capacity connected at a non-optimal location.

Nevertheless, if DG reactive power capability and control is considered, the node where DG is connected should be modelled as a PV node. This represents the DG generator capability to keep a voltage reference value while the supplied reactive power is within its maximum and minimum limits [72].

To address these issues presented in this review and in line with the defined problems of this study and to achieve the major objectives of this research work, this thesis proposed

a PSO based stochastic optimisation algorithm for DG optimum sizing and location study. The proposed algorithm is specifically suited for the solution of mixed search spaced optimisation problems. Unlike other approaches, the proposed algorithm is an ensemble of techniques to handle variables of mixed search space of integer, discrete and continuous variables. This significantly reduces the execution time of the algorithm and accelerates convergence due to the much reduced search space of the optimisation problem.

The study takes into consideration network operational and security constraints of power, voltage, line loading and short circuit current fault level by incorporating them in the optimisation process. The study considered that DG can operate to inject constant real and reactive (PQ model) or inject constant real power at a specified voltage magnitude (PV model). The current study is carried out on standard 69-bus benchmarking network and as well as a 47-bus Nigeria practical medium voltage distribution network.

The effectiveness of the algorithm in solving the two well know optimisation problems that are inherently integer, discrete and continuous in nature (optimal DG and shunt capacitor sizing and placement problem) are demonstrated. The capability of the algorithm to handle optimal integration of induction generator based DG is also demonstrated. The results of study on the 47-bus is validated with a commercial power system analysis tool ERACS. The results show the proposed algorithm to be an efficient, fast and reliable tool capable of solving complex nonlinear optimisation problems.

Inappropriate DG placement may increase power system losses and the capital cost of operating the network. Conversely, optimal DG placement can improve the performance of the host network in terms of voltage profile, reduce line loading and system losses, and improve power quality and reliability of supply for both network operators and the customers. So an optimisation technique must be used in order to come up with the highest power loss reduction within the best combination of feasible DG size and location, without violation of the network constraints.

In the chapter that follows, the development of the proposed PSO multi search optimisation algorithm will be presented.

CHAPTER 3

Particle Swarm Optimisation

In this chapter, a general overview of Particle Swarm Optimisation is presented. The review includes the variants PSO that forms the basis for the current proposer. The proposed Multi-Search Particle Swarm Optimisation (MSPSO) procedure that specifically suit DG and shunt capacitors integration onto distribution network is developed and discussed. Features of the proposed MSPSO such as the multi-valued discrete PSO, dichotomy algorithm and few informants PSO implementations are presented.

3.1 Background

Natural creatures sometimes behave as a swarm. One of the main streams of artificial life research is to examine how natural creatures behave as a swarm and reconfigure the swarm models inside a computer [73]. Craig Reynolds in 1986 developed an artificial life program, simulating the flocking behaviour of birds called Boids [74]. Reynolds employed a set of three vectors as simple rules in his researches on Boid as follows,

Separation: steer to avoid crowding local flockmates (i.e. step away from the nearest agent)

Alignment: steer to towards the average heading of local flockmates (i.e. go towards the destination)

Cohesion: steer to move toward the average position of local flockmates (i.e. go to the centre of the swarm).

The Boids framework is often used in computer graphics, providing realistic-looking representations of flocks of birds and other creatures, such as schools of fish or herds of animals. The decision process of human beings was examined by Boyd and Richerson they then developed the *concept of individual learning and cultural transmission* [74]. According to their examination, human beings make decisions using their own experiences and other persons' experiences. These research efforts were the basis for the emergence of new optimisation techniques in the 1990s utilizing an analogy of the swarm behaviour of natural creatures. Eberhart and Kennedy developed a PSO as a

technique for the optimisation of continuous nonlinear functions based on the analogy of swarms of birds and fish schooling [26].

3.2 Basic Particle Swarm Optimisation with Inertia Weight (PSO-W)

PSO is a cooperative population-based global stochastic optimisation technique inspired by the behaviour of swarms such as fish schooling and birds flocking proposed by Kennedy and Eberhart in 1995 [26, 27]. PSO has been found to be very robust in solving non- linear problems where multiple optima and high dimensionality exists [75]. PSO differs from other evolutionary algorithms in that better solutions are evolved through the social interactions of individual particles within the group or swarm. The particles move through the problem space, and over time converge upon the optimal solution. Unlike in genetic algorithms, where the weakest individuals are discarded and replaced by each subsequent generation, with PSO individuals is not eliminated, and the best solutions are evolved through cooperation and position updates.

In order to improve the performance of PSO, Shi and Eberhart[76] introduced a new parameter '*w*' called the inertia weight into the first part of original PSO equation as given in Equation (3.1), so as to improve the exploration and exploitation ability of the swarm optimiser. This parameter plays the role of balancing the global search and local search of the swarm [76]. Each individual in a PSO swarm moves in the search space with a velocity that is dynamically adjusted according to its own previous experience and the experience of other members of the swarm. Each particle keeps track of its coordinates in the search space associated with the best fitness it has achieved so far (pbest) and the overall best value (and its location) obtained so far by any particle in the population (gbest). The particle then calculates its next displacement vector in the search space (or velocity if each step in an iterative process is regarded as representing a time unit of 1) as a combination of three factors: the particle's own velocity, moving towards the particle's own best position so far and moving towards the best position of its best informer, giving the following equations of motion for each particle:

$$V_{id}^{k+1} = w^{k} \times v_{id}^{k} + c_1 \times rand_{1} \times (pbest_{id} - x_{id}^{k}) + c_2 \times rand_{2} \times (gbest - x_{id}^{k}) \quad (3.1)$$

$$x_{id}^{k+1} = x_{id}^{k} + v_{id}^{k+1} \quad (3.2)$$

Where:

v_{id}^{k} : current velocity of individual *i* in dimension *d* at iteration *k*

x_{id}^{k} : current position of individual *i* in dimension *d* at iteration *k*

V_{id}^{k+1} : new velocity of individual *i* in dimension *d* at iteration *k+1*

x_{id}^{k+1} : new position of individual *i* in dimension *d* at iteration *k+1*

$rand_1$, $rand_2$: are random numbers between 0 and 1

p_{besti}: is the best position to-date of particle *i*,

g_{best}: is the global best position of the group to-date

c_1, c_2: are constants (weighting functions) determining the relative influences of p_{besti} and g_{best} also called the cognitive and social acceleration constant respectively

d: is the number of dimensions in the search space

w: is an inertia constant (or weighting function) determining the relative influence of the particle's own velocity. For the k^{th} iteration, it is computed as;

$$w_k = w_{\max} - \frac{w_{\max} - w_{\min}}{k_{\max}} \cdot k \tag{3.3}$$

where, w_{min} and w_{max} : are the minimum and maximum inertia weights, respectively, and k_{max} is the maximum allowable number of iterations before the search is aborted.

This factor allows the particles to move freely within the search space at the beginning of the search process (exploration) while giving greater significance to p_{best} and g_{best} during the later stages of the search (exploitation).

If the search space is not infinite, it is necessary to confine the search space to prevent a particle leaving the search space altogether. A simple mechanism for such confinement is described by the following operations [77]:

$$x_{id}^{k} \notin [x_{\min}, x_{\max}] \Rightarrow \begin{cases} v_{id}^{k} = 0 \\ x_{id}^{k} < x_{\min} \Rightarrow x_{id}^{k} = x_{\min} \\ x_{id}^{k} > x_{\max} \Rightarrow x_{id}^{k} = x_{\max} \end{cases} \tag{3.4}$$

The particle velocity is limited by the maximum value v_{max}. Thus, the resolution and fitness of the search depend on v_{max}. If v_{max} is too high, then the particles will move in larger steps and the solution reached may not be optimal. If v_{max} is too low, then the

particles will take a long time to reach the desired solution or even get captured in a local minimum. The basic flow chart of PSO is shown in Figure 3.1.

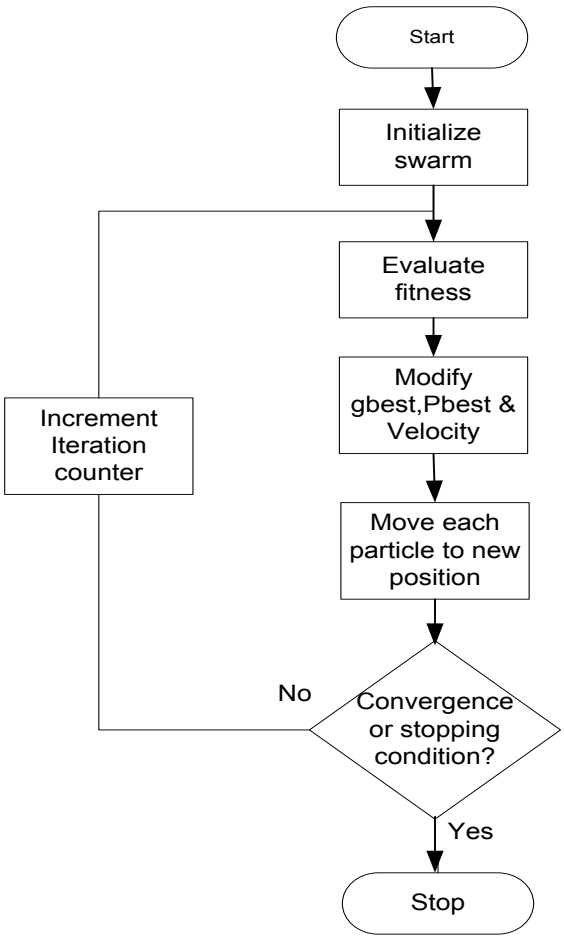

Figure 3.1: Basic Flow chart of PSO

In the past several years, PSO has been successfully applied in many areas of research and application related to electrical power systems [47, 73]. Some of the characteristics features that make PSO attractive to researchers are related to their high search speed with better results in a simple and efficient way when compared with other methods. They have few parameters to adjust and are more flexible and works well in a wide variety of applications[78]. Particle swarm optimisation can be used for optimisation problem that is non-differentiable, non-convex, and highly nonlinear with many local optima.

Different variants of PSO algorithm have been proposed in the literature. Some of these variants incorporate the capabilities of other evolutionary computation techniques while others adapt the algorithm parameters for enhanced performance [47, 79-81]. In this study, two variants PSO algorithms: discrete binary PSO and PSO for Mixed Integer

Nonlinear Problems form the basis for which MSPSO algorithms proposed in this thesis is developed and are discussed below;

3.3 Discrete Binary Particle Swarm Optimisation Algorithm

The basic PSO described in section 3.2 apply to nonlinear optimisation problems with continuous variables. However, practical engineering problems are often formulated as combinatorial and mixed variables optimisation problem [73]. The first PSO algorithm for discrete problems was developed by Kennedy and Eberhart in 1997 [82] where particles were encoded as binary sequences. Particle trajectories and velocities were defined as probabilities of a bit change from 0 to 1 (no or yes). This binary value can be a representation of the real- value (continuous value) in binary search space.

In the binary PSO, the particle's personal best and global best is updated as in the basic continuous version. The major difference between binary PSO and the basic PSO is that the velocities of the particles are rather defined in terms of probabilities that a bit will change to one. By this definition, the velocity '*v*' must be restricted within the range [0, 1]. If *v* is higher, the particle is more likely to choose 1, and lower values favour 0 choices. One of the functions, accomplishing this feature is the sigmoid function defined in Equation (3.5)

$$Sig\ (v_{id}^{k}) = \frac{1}{1 + \exp(-v_{id}^{k})} \tag{3.5}$$

Like the basic continuous version, the velocity update formula for the binary version of PSO can be described as follows:

$$V_{id}^{k+1} = v_{id}^{k} + c_1 \times rand_1 \times (pbest_{id} - x_{id}^{k}) + c_2 \times rand_2 \times (gbest - x_{id}^{k}) \tag{3.6}$$

$$\rho_{id}^{k+1} < sig\ (v_{id}^{k+1}) \quad \text{then} \quad x_{id}^{k+1} = 1\ ; \tag{3.7}$$

$$\text{Else} \quad x_{id}^{k+1} = 0$$

where; rand is a positive random number drawn from a uniform distribution with a predefined upper limit, and ρ_{id}^{k+1} is a vector of random numbers of [0, 1]. Unlike in continuous-valued version of PSO where high maximum velocity (*Vmax*) increase the range explored by particle, the opposite occurs in the binary version; smaller *Vmax* allows higher exploration.

3.4 PSO for Mixed Integer Non-Linear Problems

In general, design variables of the object function in optimisation problems are normally assumed to be continuous. However, practical engineering problems have design variables that are integer, discrete, binary (zero-one) and continuous, with non-linear objective functions. Binary variables are usually required in the formulation of design problems with a decision options such as yes or no and in switch selection problems (On or off). Problems which contain integer, discrete or zero-one and continuous variables are called mixed-variable optimisation problems [83].

For mixed-variable optimisation problems, however, not so many PSO-based approaches have been proposed as for continuous ones, because it is difficult to find an appropriate constraint-handling mechanism and a proper non-continuous variables handling method simultaneously [83]. The integration of binary and continuous versions of PSO is discussed in [84]. The study in [85] demonstrates the application of MINLP to power system problem. A continuous version of the PSO was modified to handle MINLPs, and used to solve reactive power and voltage control problem in electric power systems. The continuous and discrete control variables related to automatic voltage regulator (AVR) operating values of generators, tap positions of on-load tap changer (OLTC) of transformers, and the number of reactive power compensation equipment.

3.5 Proposed Multi-Search PSO (MSPSO) for DG Integration

A number of Distributed Generation (DG) technologies are now commercially available in different discrete sizes. DG is often limited to a set of standard available sizes depending on the manufacturers. The problem of DG integration can be considered as a combinatorial nonlinear problem that involves the determination of the optimal or near optimal overall combination of locations and capacities in a power network [46]. To solve the optimisation problem, the search space consists of mixed-variables that are of continuous, integer and discrete in nature. Integer values are commonly used to represent the bus number locations for the DG; discrete values are used to represent the DG capacities (MVA) or DG rated output power (MW) while the reactive power output from the generator is related to continuous variables. This implies that, the DG optimisation problem can be classified into the category of mixed integer-discrete-continuous non-linear optimisation problems.

A mixed integer-discrete-continuous, non-linear optimisation problem can be mathematically expressed as follows [86];

Find

$$X = \{x_1, x_2, x_3 \cdots x_n\} = \left[X^{(i)}, X^{(d)}, X^{(c)} \right]^T = \left[X_1^{(i)}, X_2^{(i)}, \cdots X_{ni}^{(i)}, X_1^{(d)}, X_2^{(d)}, \cdots X_{nd}^{(d)}, X_1^{(c)}, X_2^{(c)}, \cdots X_{nc}^{(c)} \right]^T \quad (3.8)$$

To minimise

$f(\mathbf{X})$ Subject to equality and inequality constraint $h_j(X) = 0 \quad j = 1, \ldots l$

$g_i(X) \le 0 \quad i = 1, \ldots m$

and subject to boundary constraints

$x_i^{(L)} \le x_i \le x_i^{(U)} \quad i = 1, \ldots n$

$X^{(i)} \in \Re^i, \quad X^{(d)} \in \Re^d, \quad X^{(c)} \in \Re^c$

where, *f(X)* is the objective function, $\mathbf{x} = \left[X^{(i)}, X^{(d)}, X^{(c)} \right]^T$ is the vector of solution comprising of *ni* integer, *nd* discrete and *nc* continuous variables. Since $X^{(i)}$, $X^{(d)}$ and $X^{(c)}$ denotes feasible subsets of integers, discrete and continuous variables respectively. In DG optimisation problem, the subsets are related to cases of multiple DG locations and sizes. The total number of variables $n = ni + nd + nc$ and represents the dimension of the optimisation problem.

The problem also accounts for *l* equality functions $h(X)$ and *m* inequality functions *g(X)*. The variables are also subject to lower '*L'* and upper '*U* 'boundary constraints. In DG optimisation, the equality constraint is related to the network real and reactive power balanced constraint. This is normally handled by the power flow algorithm that computes the objective function. The inequality constraints are related to nodal voltages, line flow limits, reactive power limits of the generators, short circuit current level constraints, etc. If the voltage and line flow constraints are violated, the absolute violated value of the maximum and minimum boundaries is largely weighted and added to the objective function.

The formulation in Equation (3.8) is general and basically the same for all types of variables. The only distinguishing feature of one problem from another is the structure of the design domain. It is also worth mentioning that the major differences between the integer and the discrete variables are; while integer and discrete variables both have a discrete nature, only discrete variables can assume floating point values. In practice the discrete value of the feasible set are often unevenly spaced [86] thus, integer and discrete variables will require different handling. The techniques employed in this current study to handle the various control variables that constitute the mixed search space are discussed in the following section.

3.5.1 Handling Mechanism of Mixed Variables for DG Optimisation Problem

In this section, the handling mechanism for integer and discrete variables of the optimal DG problem is presented. The PSO algorithms used in previous studies have been designed and intended to handle nonlinear continuous optimisation problems. Generally, values for non-continuous variables are obtained by rounding-off to their closest values. Despite the simplicity of the rounding-off principle, the optimal mixed-variable solutions obtained by this method are probably not the best solution. Considering the nature of some control variables in optimal DG problem, implies that the problem will be best solved using a multi search optimisation algorithm. The consequence of which is a substantial reduction in the search space and hence the computational cost of the algorithm.

Consider a solution vector **X** in D dimensional space for an individual *i* as $\mathbf{X_i} = (x_{i1}, x_{i2}, \ldots. x_{iD})$. In the case of single distributed generator placement problem with three dimension, $\mathbf{X_i} = (x_{i1}, x_{i2}, x_{i3})$. The variables, x_{i1}, x_{i2}, x_{i3} represent the generator location, generator output power and VArs, respectively. A multi-valued discrete PSO and a dichotomy algorithm are proposed to handle the integer and the discrete variables respectively.

3.5.1.1 Multi- Valued Discrete PSO

The discrete PSO algorithm proposed in this study to handle the integer variables is an extension of the original discrete binary PSO [82]. Similar to the binary PSO, the proposed discrete PSO uses probabilistic transition rules to move from one discrete value to another in search for the optimum solution. However, it neither requires encoding of particles into binary sequences nor the decoding process. This makes it

simple to implement and suitable to handle optimal DG and capacitor location and sizing problems that are by their very nature integer and discrete optimisation problems.

For discrete multi valued optimisation problems the range of the discrete variable lies between 0 and *M-1*, where '*M*' is an integer [87]. The algorithm uses the same velocity update equation as that described in Equation (3.6). However, the position update equation is modified as described below.

First, the velocity is transformed into a number between [0, *M*] using the transformation:

$$S_{id} = \frac{M}{1 + e^{-V_{id}}} \tag{3.9}$$

A random number is then generated using a normal distribution with a mean of S_{id} and a standard deviation of $\alpha(M-1)$ i.e. $N(S_{id}, \alpha(M-1))$ and the result rounded to the nearest discrete value to give the position update:

$$x_{id} = round\left\{S_{id} + (M-1) \times \alpha \times randn(1)\right\} \tag{3.10}$$

where α is a constant, *randn*(1) is a random number drawn from the standard normal distribution and:

$$x_{id} = \begin{cases} M-1, & x_{id} > M-1 \\ 0, & x_{id} < 0 \end{cases} \tag{3.11}$$

x_{id} is then a discrete value between [0, *M-1*]. Thus, for any given S_{id}, there is an associated probability of choosing any number between [0, *M-1*] with the probability of randomly selecting a number decreasing as its distance from S_{id} increases as depicted in Figure 3.2. The selection of the value of the constant α is very important to the algorithm performance as detailed in [87]. In this current optimisation study, a value of 0.4 is used [87]. Controlling the α controls the standard deviation of the Gaussian distribution and, hence, the probabilities of different discrete variables.

The expressions in (3.9)-(3.11) are used in this study to handle the integer variables of the DG bus number locations.

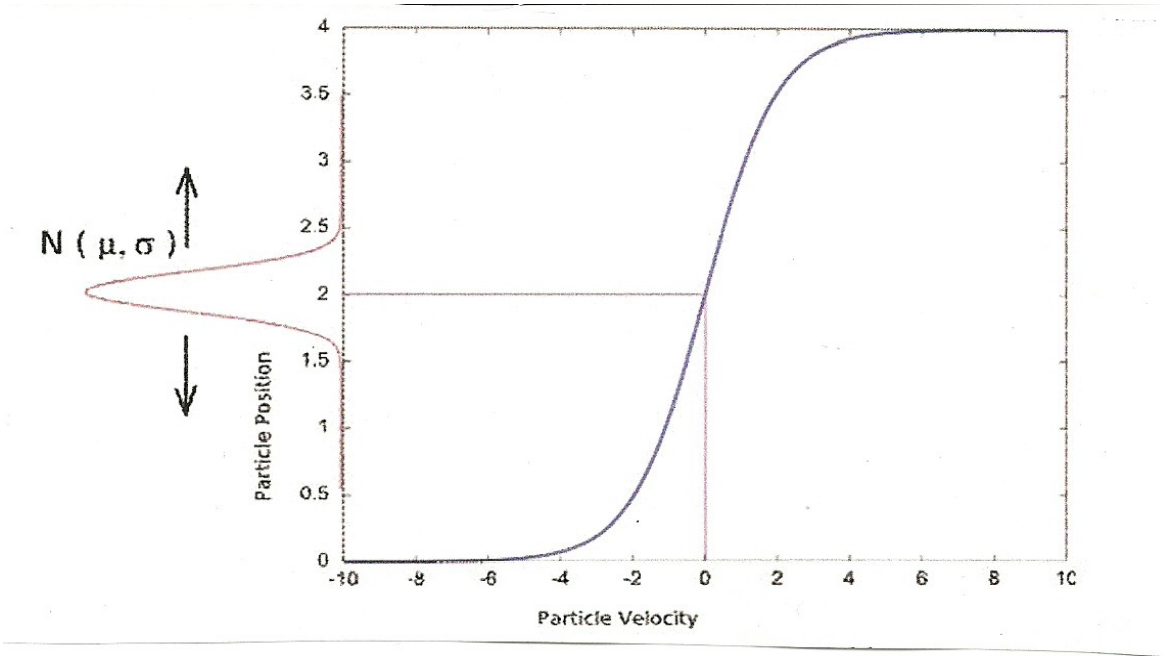

Figure 3.2: Transformation of the Particle Velocity to a Discrete Variable [87]

3.5.1.2 Dichotomy Search Algorithm for Discrete Variables

In practice, the discrete values of the feasible set representing DG units are often unevenly spaced. The dichotomy algorithm [77] is used to restrict the continuous variables representing DG sizes to be within a feasible and acceptable predefined search list of standard size of DG units. Variables representing DG output power are initially treated as continuous variables using Equations (3.1) and (3.2) to update the corresponding position vectors.

To launch this iterative algorithm, it is necessary to have one acceptable position defined as *X_ admissible* (discrete variable). Very generally, it is approximately the preceding position of the particle to be tested. *X_current* is the particle position to be tested (continuous variable). The technique involves traversing the search list by ascending values and stopping as soon as the found value exceeds or equals the one that is tested. This, easily give the closest value as the one that is found or the one that is found after.

In essence, the dichotomy algorithm is used to constraint the continuous variable (the active power output of the generator or generator capacity) into a discrete variable chosen from unevenly spaced entries in a pre-defined finite search list representing practical DG sizes in megawatts.

The operational flowchart of dichotomy algorithm shown in Figure 3.3

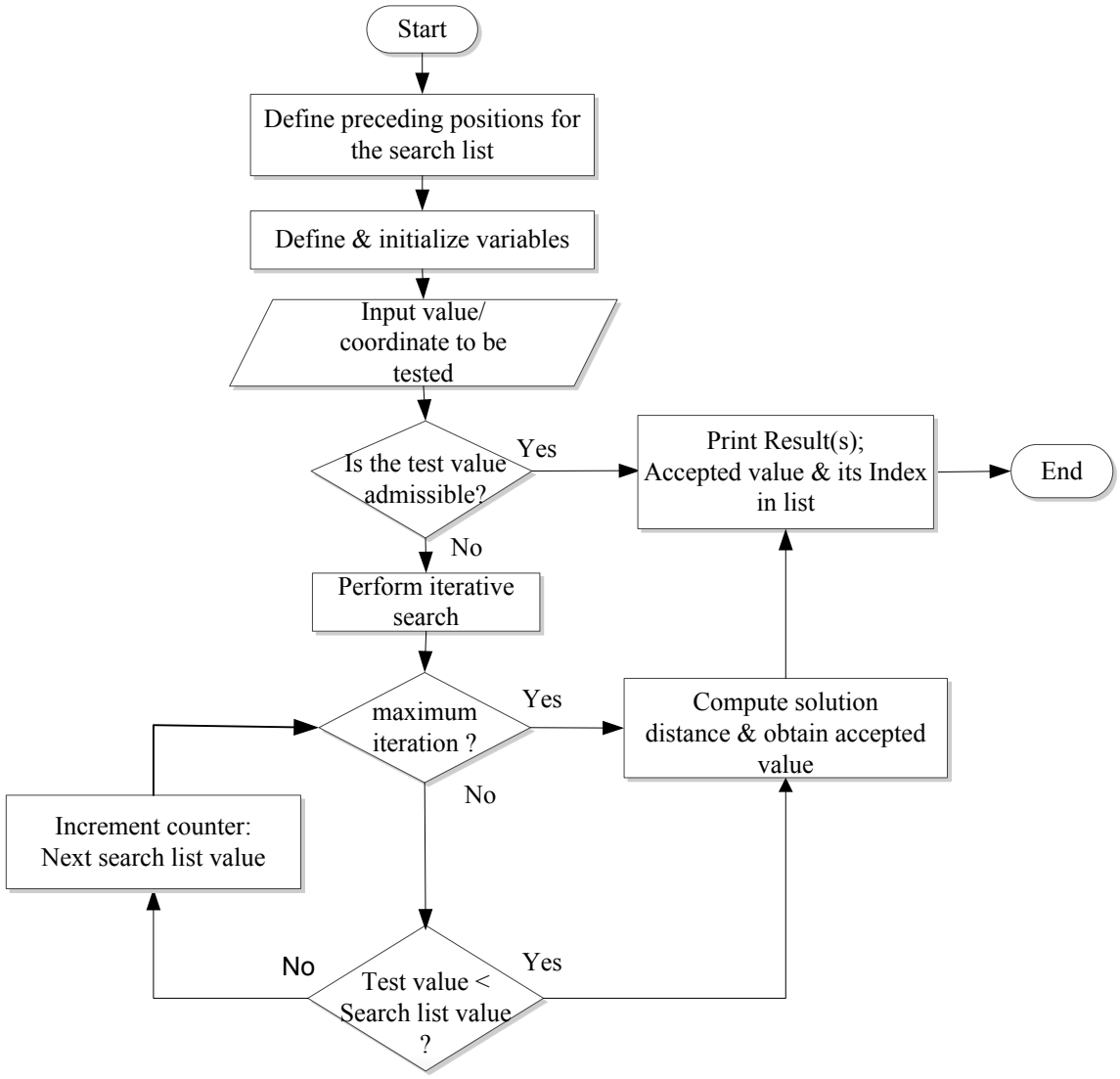

Figure 3.3: Flowchart of dichotomic search in a list; for handling the constraints on discrete size of DG units

The procedural steps for realizing dichotomic search in a list is discussed below with the

Step 1: Define the preceding positions (X_ admissible /acceptable values of the position / set of acceptable *a priori* position) in the search list in ascending order as follows:

$$X_{admissible} = X_{adm} = [X_{adm1}, X_{adm2}, X_{adm(j)}, \cdots\cdots X_{adm(N)}]^T \quad (3.12)$$

where: $j = 1:N$ represents the index of the values in the search list (X_{adm}).

Step 2: Define and initialize variables for search algorithm; *iteration counter, length of list, j_min,* and *j_max* with *j_min* & *j_max* the minimum and the maximum respectively of acceptable value's index of the found of solution

Step 3: Input the value of coordinate to be tested $X = X^k_i$ (the i^{th} particle at k iteration whose value is to be tested)

Note: X^k_i is admissible *if* $X^k_i \in X_{adm}$ therefore, we can generally define X^k_i as follows:

Step 4: *If* X^k_i is admissible (i.e is contained in the search list) stop, print its value and index

In other words,

$$if\ X^k_i == X_{adm}\ \text{then}\ X^k_i = X_{adm}(j) \tag{3.13}$$

Step 5: Else perform iterative search to compute X^k_i as follows

$$X^k_i = \begin{cases} X_{adm}(index): \quad if \quad X^k_i < X_{adm}(j),\ j\_\max = j \\ \qquad if\ X^k_i - X_{adm}(j\_\min) < X_{adm}(j\_\max) - X^k_i, \\ \qquad index = j\_\min \quad else \quad index = j\_\max \end{cases} \tag{3.14}$$

End subroutine if a solution is found in step 5 and return the accepted value and its index.

Else

$$X^k_i = \begin{cases} X_{adm}(index): \quad if \quad X^k_i > X_{adm}(j),\ j\_\min = j \\ \qquad if\ X^k_i - X_{adm}(j\_\min) < X_{adm}(j\_\max) - X^k_i, \\ \qquad index = j\_\min \quad else \quad index = j\_\max \end{cases} \tag{3.15}$$

Step 6: At maximum iteration, from the computed solution distance return accepted value and its index

Note: the above procedure can be repeated for *nd* discrete variables.

The proposed multi-valued DPSO algorithm that handles the integer variable use real integer numbers other than 0 and 1. This avoids any increase in the particle dimensions and does not require any encoding and decoding of particle position as required in the binary version of PSO. The MSPSO algorithm can search evenly and unevenly discrete spaces. This avoids loss of accuracy in the results of the optimisation process obtained. The final attained optimal solution is a commercially available DG-unit. The mix of

different variable types to form one single particle is possible because the PSO algorithm operates independently on each dimension.

3.5.2 Particle Swarm Optimiser with Few Informants

In the majority of real time problems, the number of times that the function to be minimised need to be evaluated is a very relevant criterion. This evaluation requires a considerable computational time. To reduce the total number of evaluations needed to find a solution, the size of the swarm can be reduced. But if the swarm is too small, the swarm is likely to take a longer time to find a solution if at all. A Large swarm size will increase the average probability of success. Empirically, researchers proposed sizes of 20 to 30 particles, which, have proved entirely sufficient to solve almost all classic test problems [77].

The interaction between particles in the swarm is based on a defined common set of links. The set of links is referred to as the swarm topology [88] and is responsible for controlling the exchange of information between particles. The traditional topologies [89, 90] for classical PSO include;

The Global best (star) topology: in this topology, the source of social influence on each particle is the best performing individual in the entire population. This is equivalent to a sociogram or social network where every individual is connected to every other. The *gbest* topology (i.e., the biggest neighbourhood possible) has often been shown to converge on optima more quickly than the local best (*lbest)*, but it is also more susceptible to the attraction of local optima, as the population rushes unanimously toward the first good solution found.

The Local best (circular) topology: This topology was proposed as a way to deal with more difficult problems. In the *lbest* sociometric structure, each individual is connected to (i.e. Influences and is influenced by) its immediate neighbours in the population array. The *lbest* topology offers the advantage that sub populations could search diverse regions of the problem space.

The Von Neumann (square) topology: This topology results in better performance in the basic particle swarm than any of the three previous traditional topologies. It is formed by arranging the population in a grid and connecting neighbours above, below, and to right and left.

And a recently proposed topology is The *adaptive random topology* [77, 88]: where each particle randomly informs *K* other particles and itself (the same particle may be chosen several times), with *K* usually set to 3 [77]. In this topology the connections between particles randomly change when the global optimum shows no improvement.

In the local best topology, the number of informants (*K*) is always less than the swarm size. And, the smaller the swarm size, the lower the average number of informants of a given particle in respect of *K*. This is relevant when it is required to reduce the swarm size with the goal of reducing the total evaluations required to find a solution based on the *lbest* topology.

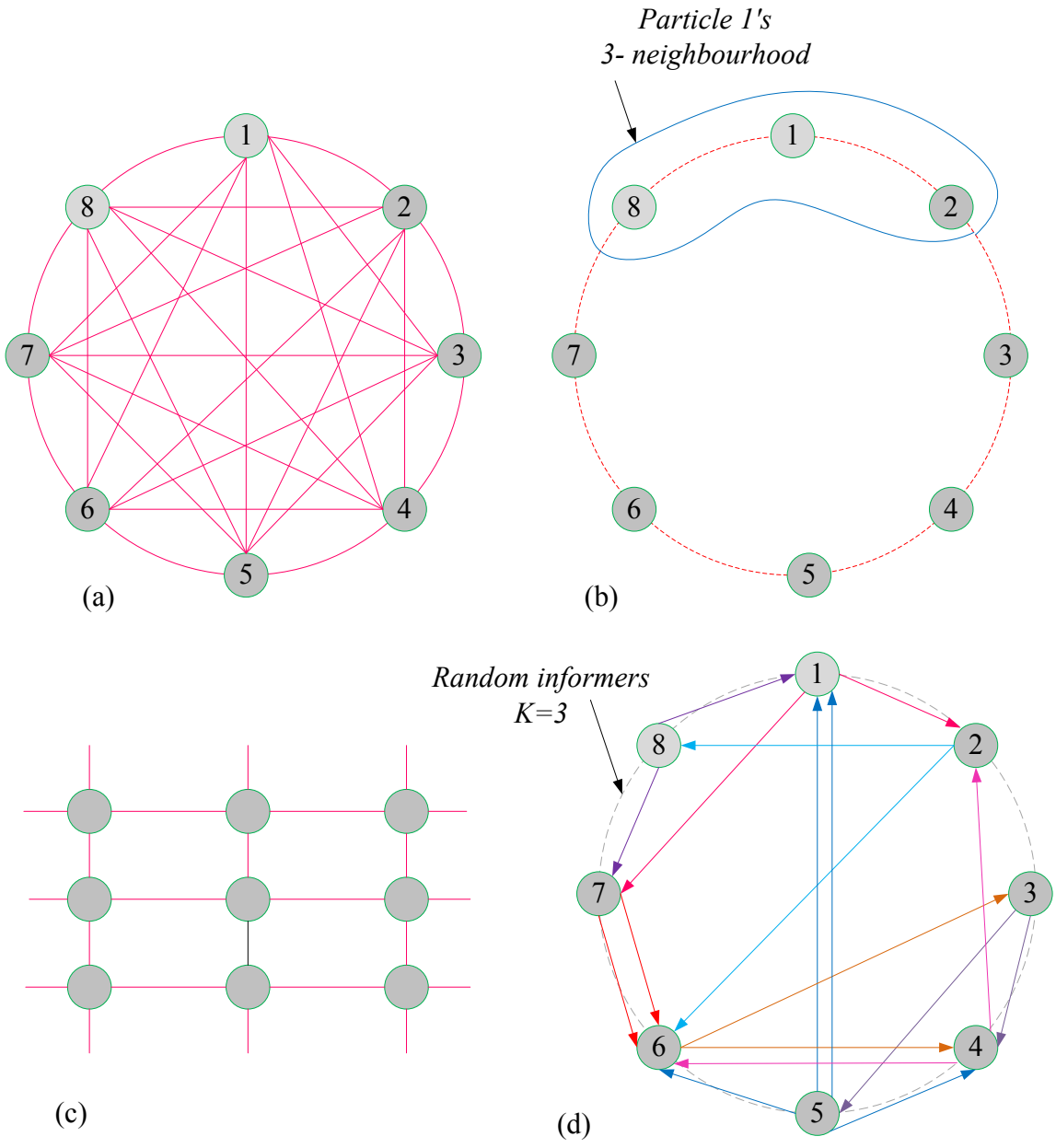

Figure 3.4: PSO topologies: (a) the global best or star (b) the local best or circular (c) the von Neumann or square and (d) random informers.

The reduction in the average size of the groups of informants encourages exploration with increasing diversity.

The problem of DG integration performs well with the global best PSO topology based information links. Where each particle informs all others and the number of informants is taking to equal the swarm size. A topology based on an entirely connected swarm of particles is more effective if there are no local minima.

The current research work is based on *gbest* topology. However, to reduce the total evaluations required to find a solution to the optimisation problem, a PSO concept with few informants is proposed. In this technique, few informants are randomly selected from the main swarm to form a sub-swarm with successive iterations. The source of social influence on each particle of the sub-swarm is the best performing individual in the entire sub-swarm population. This implies that a social network where every individual of the sub-swarm is connected to every other is created. This information is then used to update the entire swarm population. The proposed topology is shown in Figure 3.5 and is referred to as sub-warm *gbest* topology. This technique maintains the swarm size, but at successive iterations few evaluations are performed using the randomly selected informants. Thus, the swarm is able to retain its diversity. The tuning of the inertial weight 'w' to allow balance in the exploration and exploitation of the search space is very important to the success of this technique.

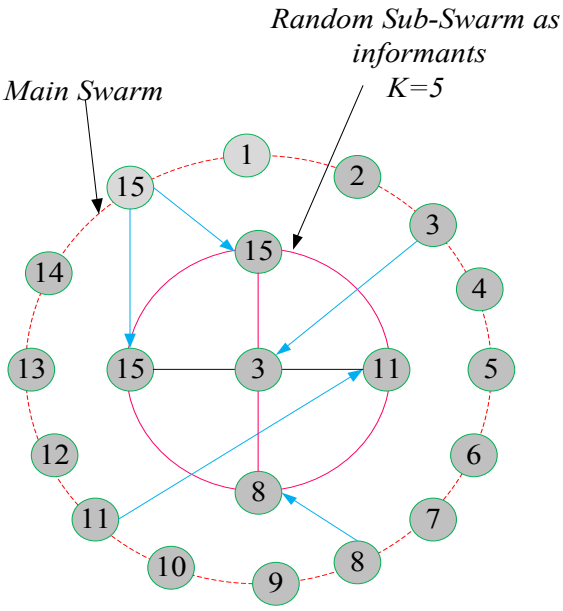

(d) *Sub-Swarm global best (gbest)*

Figure 3.5: PSO sub-swarm global best (*gbest*)

To implement this concept, a sub-routine algorithm based on selecting few informants was combined with the proposed stochastic optimisation and used to reduce the computational burden of the proposed stochastic optimisation algorithm. Some PSO versions have a topology that allows the entire swarm to share information and where every particle compares its position with the global best, the algorithm implemented here select a certain number of particles from the total swarm to use as informants for the entire swarm.

This study uses only five randomly selected informants at each step (though depending on the complexity of the problem, the number informants can be increased or decreased). This reduction in the size of the swarm used in fitness computation and substantially reduces the total number of evaluations needed to achieve convergence. This actually encourages exploration by increasing diversity [77] and speeds up the process of execution of the algorithm.

3.5.3 Procedural Steps and Implementation flow chart of MSPSO

The capability of the particle swarm optimisation algorithms operator to work independently on each dimension makes it possible for mixing different variable types into a single particle. The implementation flow chart is as shown in Figure 3.6 and the procedural steps involves;

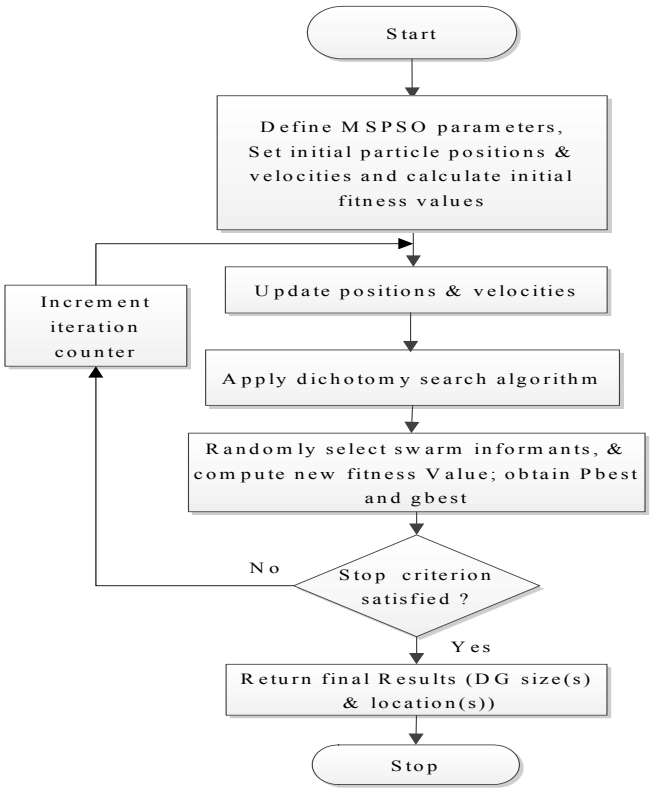

Figure 3.6: Multi-Search PSO (MSPSO) Algorithm flow chart

Step1: Read relevant MSPSO parameters. Also relevant power system data required for the computational process are actualized from the data files.

Step 2: Initialize swarm of particles with random positions and velocities. Each candidate solution should be within the feasible decision variable space

Step3: with the swarm size and problem dimension, commence the iteration process

Step4: Apply velocity update equation (3.6) and limits its magnitude if outside the defined range

Step5: Update position of swarm; if integer, discrete variable use equation (3.9) - (3.11), if continuous variable use equation (3.2)

Step 6: Apply dichotomy search algorithm for continuous variable for transformation into unevenly discrete search space

Step 7: Apply feasibility constraints if applicable (check discrete variables for short circuit current constraints)

Step 9: Randomly select swarm informants

Step 10: compute the objective function by running power flow analysis for the swarm informants

Step 11: Apply relevant constraints if applicable (Busbar voltage and line flow limit violations). If the voltage and line flow constraints are violated, the absolute violated value of the maximum and minimum boundaries should be largely weighted and added to the objective function

Step 12: Evaluate the fitness of sub-swarm particles, obtain their personal best and the global best.

Step 13: If necessary update historical information regarding personal and global best particles for the entire swarm.

Step 14: Repeat from step 4 above until preset convergence criteria: maximum number of generations. The parameters of the *gbest* at the end of the run are returned as the desired optimum discrete DG size and location.

3.6 Small Population Particle Swarm Optimisation (SPPSO)

The SPPSO is a classical PSO algorithm using a small population of particles few as five for a solution to an optimisation problem [91, 92]. This concept is synonymous to

the micro-genetic algorithm (μGA) [93] and is now been adapted in PSO approaches. The algorithm is based on the concept of regeneration of new particles randomly, after a certain number of iterations count *N* to replace all but the *gbest* particle in the swarm. In the addition to keeping the gbest's particle parameters, the population *best* attributes are also transitioning from one set of population to the next every *N*-iteration. In other words, the particles are regenerated after every *N* iterations retaining their previous global best (*gbest*) and personal best (*Pbest*) fitness values and positions.

This concept of particle regeneration was aimed at giving the particles the ability to keep carrying out the search despite a small population. The regeneration concept is to also ensure that faster convergence is achieved as it would be with a large population of PSO. The selection of the value of *N* is crucial in the realizing an efficient SPPSO algorithm. If the value of *N* is low, the new particles may be regenerated too quickly and in turn disturb the search process. Thus the particles will move erratically in the search space. On the other hand, if the particles are regenerated at a higher value of *N* the search process will be delayed. Randomizing the positions and velocities of the particles every *N* iterations aid the particles in avoiding local minima and finding the global minimum. The regeneration concept drastically reduces the number of evaluations required to find the best solution and each evaluation is less computationally intensive compared to the classical PSO algorithm. The SPPSO algorithm implementation flow chart is shown in Figure 3.7.

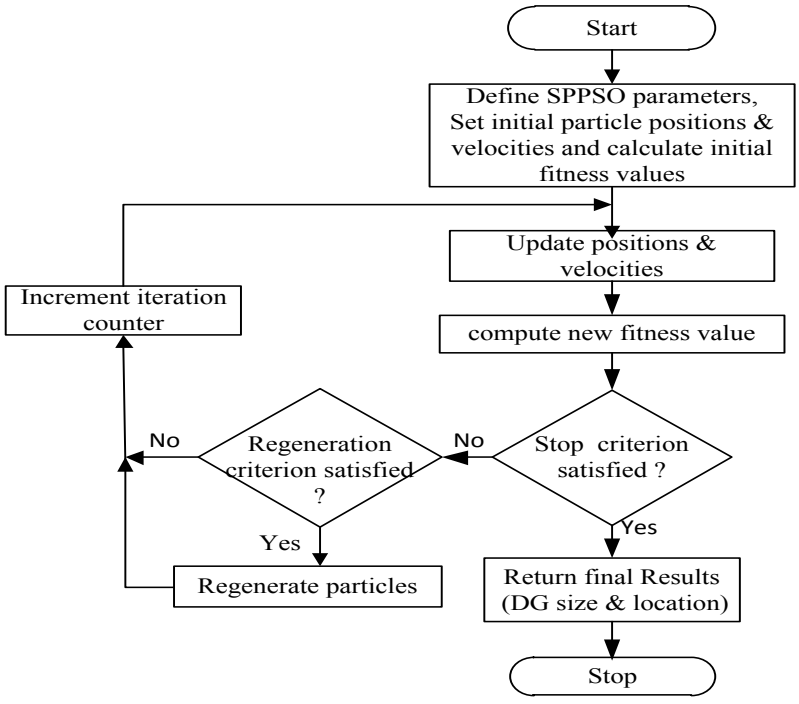

Figure 3.7: SPPSO Algorithm flow chart

The procedural steps for implementing SPPSO is briefly summarised below;

Step 1: If the current iteration number is equal to the set regeneration count number *N*, execute proceeding Step 2; else, jump out of this regeneration strategy and keep updating the position and velocity of particles.

Step2: Discard the current particles except the *gbest* particle parameters and *Pbest* attributes and randomly generate new particles into the searching space.

Step3: Update the position and velocity of particles if required. If better solution is found, the saved global and personal best position and fitness will be replaced. Otherwise, continue searching the solution space

The SPPSO have been used in some power system applications that include optimal design of power system stabilizers [91, 92] and recently for short-term hydrothermal scheduling [94] and reconfiguration of shipboard power system [95]. The SPPSO algorithm results will be utilised to compare with that of the proposed MSPSO.

3.7 Summary

In this chapter, a basic overview of PSO and its variants are discussed. The problem of DG integration is considered as a mixed integer nonlinear problems, with the search space consisting of mixed-variables that are of integer, discrete and continuous in nature. The general formulation of the mixed integer nonlinear problems (MINLPs) is presented. The relationship between the MINLP and the control variables of the optimal DG problem is discussed. The mechanism for handling the mixed search space control variables associated with optimal DG problems are presented. Features of the proposed MSPSO: the multi-valued discrete PSO, dichotomy algorithm and few informants PSO implementations are discussed. A variant PSO called SPPSO that has been used in some power system applications is discussed. Its computational burden with application to the DG integration will be evaluated for the purpose of comparison with the MSPSO.

It is this proposed multi-search particle swarm optimisation presented in this chapter with the power flow algorithms that evolved into the stochastic power system optimisation algorithm that forms the topic of this current research work. To demonstrate the significance of this current study, in the chapters that follow the applications of PSO-W and the proposed MSPSO to the power system in the area of DG (both synchronous and induction machine based) and shunt compensation capacitor integrations are presented.

CHAPTER 4

Distributed Generation Sizing and Location for Power Loss Minimisation and Voltage Support in a Compensated Network Using PSO-W

Efficient operation of transmission and distribution networks requires losses minimisation and the provision of network voltage support. Reactive power compensation is probably the most effective way to provide these services. Among various var compensators, shunt capacitors, are the most attractive because they are simple and inexpensive when compared to dynamic reactive power sources such as generators. The increasing penetration of distributed generation provides an opportunity for effective loss reduction and ancillary services such as network voltage support.

In this chapter, an optimisation technique based on particle swarm optimisation with inertia weight "PSO-W" is employed to optimally locate and size DG in a network that is initially compensated with shunt capacitors. The study considered both single and multi-objective problems at different operating power factors. The results obtained will be used as a benchmark to assess the improvement obtained with the proposed multi-search PSO (MSPSO).

4.1 Problem Formulation

A major advantage of the connection of DG into a distribution network is the reduction in the total real power loss in the network since power is now being generated close to the point of consumption thus avoiding or reducing transmission losses.

The first objective of the integration exercise is to minimise network power loss and improved the voltage profile. The objective of both real and reactive power loss minimisation is derived as follows;

Considering a general electrical network with N_b nodes, the complex power injected at bus i is given by:

$$\mathbf{S}_i^* = \mathbf{V}_i^* \sum_{k=1}^{N_b} \mathbf{Y}_{ik} \mathbf{V}_k \tag{4.1}$$

where $\mathbf{S}_i$ is the complex power injected at node i, $\mathbf{V}_i$ & $\mathbf{V}_k$ are the voltages at nodes i and k, respectively, $\mathbf{Y}_{ik}$ is the admittance between nodes i and k and $\mathbf{s}_i^*$, $\mathbf{v}_i^*$ are the complex conjugates of $\mathbf{S}_i$ and $\mathbf{V}_i$, respectively. The unknown variables are the nodal voltage magnitudes V_i and load angles δ_i.

Consider a line l with an admittance $\mathbf{Y}_{ij}$ connecting nodes i and j. The complex power injected into the line from node i is given by:

$$\mathbf{S}_{i\to j}^{l} = \mathbf{V}_i \mathbf{I}_{ij}^{*} = \mathbf{V}_i \left[(\mathbf{V}_i - \mathbf{V}_j)\mathbf{Y}_{ij} + \mathbf{V}_i \mathbf{Y}_{io}\right]^{*} \tag{4.2}$$

Similarly, the complex power injected from bus j is:

$$\mathbf{S}_{j\to i}^{l} = \mathbf{V}_j \mathbf{I}_{ji}^{*} = \mathbf{V}_j \left[(\mathbf{V}_j - \mathbf{V}_i)\mathbf{Y}_{ij} + \mathbf{V}_j \mathbf{Y}_{jo}\right]^{*} \tag{4.3}$$

The total line loss S_l is the sum of complex power injected over the entire line section given as:

$$\mathbf{S}_l = \sum_{i \in l} (\mathbf{S}_{i\to j}^{l} + \mathbf{S}_{j\to i}^{l}) \tag{4.4}$$

and the objective function (f_{obj}) to be optimized can be written as:

Minimise $\mathrm{Re}(\mathbf{S}_l) = P_L$ (4.5)

Mathematically, the objective is given as in Equation (4.6)

Minimise $$P_L = \sum_{k=1}^{L} Loss_k = \sum_{l \varepsilon L} (P_{i\to j}^{l} + P_{j\to i}^{l}) \tag{4.6}$$

where, L is the total number of branches, P_L is the total real power loss in the network, $Loss_k$ is the power loss at branch k, $P_{i\to j}^{l}$ is the active power flow injected into line l from the bus i and $P_{j\to i}^{l}$ is the active power flow injected into line l from bus j. Equation (4.6) is computed using MATPOWER AC power flow [96].

A second major benefit of the connection of DG is the resulting improvement in network voltage profiles, obtained because the generator unit will normally inject controlled reactive power as well as real power into the network. The improvement in the voltage profile of the network can therefore be used in addition to the reduction in network losses when considering multi-objective optimisation problems.

Additionally, by allowing the DG units to provide power at lower power factors, can support the voltage across the network and alleviate voltage problems at the end users.

Some practical power factors (PF) values usually used are 0.85, 0.9, 0.95 and unity [45]. Power factors of 0.85, 0.95 and unity are used in this study to demonstrate the effect of different power factor values on the ancillary of voltage support with the penetration DG.

Even though, PSO is commonly used for single-objective optimisation studies, but its application can be extended to finding solution of multi-objective optimisation problems by applying weighted aggregate method [97]. The advantage of multi-objective optimisation over single objective optimisation is that multi-objective optimisation can provide a set of promising trade-offs rather than a crisp solution in single objective. The selection of optimised design among the derived solutions can be effectively determined as per the planner's preference without losing generality [98].

The main strength of this aggregate method is its efficiency (Computationally speaking), and its suitability to generate a strongly non-dominated solution that can be used as an initial solution for other techniques. Its main weakness is the difficulty to determine the appropriate weights that can appropriately scale the objectives when there is no enough information about the problem, particularly if it is consider that any optimal point obtained will be a function of such weights [97].

For the multi-objective optimisation problem, the objective function (f_{obj}) can then be written as:

$$f_{obj} = k_1 \cdot \sum_{l \varepsilon L} (P^{l}_{i \to j} + P^{l}_{j \to i}) + k_2 \cdot \sum_{i=1}^{N_b} (V_i - V_{n,i})^2 \qquad (4.7)$$

The first part of Equation (4.7) describes the objective of power loss reduction while the second part represents the objective of voltage optimisation [99]. The values k_1 and k_2 are weighting functions whose values must sum to unity. These weights are indicated to give the corresponding importance to each objective for the penetration of DG. However, these values may vary according to engineer's concerns [33]. For the study presented in this chapter, both objectives are given equal weighting (values of $k_1 = k_2 =$ 0.5 are used). Thus, different settings for k_1 and k_2 may result in a different results. V_n is the nominal voltage of the circuit, and the value of 1.0 pu is used [99].

Equations (4.8), (4.9) and (4.10) show power, voltage and line current constraints, respectively. The Generator's output reactive power limits [100] are given in (4.11).

$$\sum_{i=1}^{N_b} P_{Gi} = \sum_{i=1}^{N_b} P_{Di} + P_L \tag{4.8}$$

$$\left|V_i\right|^{\min} \le \left|V_i\right| \le \left|V_i\right|^{\max} \tag{4.9}$$

$$\left|I_{ij}\right| \le \left|I_{ij}\right|^{\max} \tag{4.10}$$

$$Q_{\lim it}^{lw} < Q_{generated} < Q_{\lim it}^{u} \tag{4.11}$$

where P_{Gi} is the real power generation at bus i and P_{Di} is the real power demand at bus i. $V^{\min}$, $V^{\max}$ are the lower and upper bounds on the voltage magnitude at bus i. I_{ij} (S_{ij}) is the current (or apparent power) flow between buses i and j and $I_{ij}^{\max}$ ($S_{ij}^{\max}$) is the maximum allowable line current (apparent power) flow in branch ij. In practice real generator does not have unlimited capacity to supply reactive power and the constraint on generator must be respected. $Q_{\lim it}^{lw}$, $Q_{\lim it}^{u}$ are the lower and upper limits of the reactive power output of the generator at bus i and $Q_{generated}$ is the reactive power output of the generator at bus i.

The minimum absolute value of the bus voltage deviation [99] is evaluated using (4.12).

$$Min \quad f(x) = -\max_i \left|V_i - 1.00\right| \tag{4.12}$$

This measures the deviation of the nodal voltages from the nominal value of 1pu, where, $i = 1,2,...,N_b$ and N_b is the total number of buses in the network under consideration, V_i is the bus voltage in pu and $f(\mathbf{x})$ is the maximal deviation of the bus voltages in the system. The improvement in the voltage profile of the network is obtained by computing the Sum of Squared Error Voltage (SSEV) defined as:

$$SSEV = \sum_{i=1}^{N_b} (V_i - 1.00)^2 \tag{4.13}$$

The SSEV as an index for the voltage profile enhancement is estimated for the network before and after the installation of the DG. The benefit of DG in terms of line power loss reduction is evaluated using the 'per-unit line loss reduction' (*PULR*) defined as the ratio of loss reduction (*LR*) to the line loss without DG (LL_{woDG}) and is given by Equation (4.14) [21]. The *LR* is the difference in the line loss reduction with and without DG. This presents the benefit of DG in a normalized form. Consequently, the percentage of line loss reduction is then given by Equation (4.15) [21].

$$PULR = \frac{LR}{LL_{woDG}} \tag{4.14}$$

$$\%LR = PULR * 100 \tag{4.15}$$

MATPOWER allows for the representation of both PQ load bus and PV generator bus for power flow analysis. It solve AC power flow by assuming a balanced and transposed three phase system, it can be used for power flow analysis of distribution system when a balanced system is assumed. In [101] it was shown that a simplified balanced three phase system can be used for the determination of equipment sizing, location and their control parameters. By default, the AC power flow solvers in MATPOWER simply solve the power flow analysis problem by ignoring any generator limits, branch flow limits, voltage magnitude limits, etc. Notwithstanding, the generator reactive power limits can be respected on the expense of the voltage set point using, the available option provided by MATPOWER.

In this study, MATPOWER AC power flow is used to analyse DG reactive power control capability under a balanced steady state condition, with the DG node model as a generator (PV) node. PSO-W Equations (4.6) – (4.9) is then employed to optimize DG and the location to minimise the network power losses and provide voltage support. DG achieved this by regulating the voltage at the node to which it is connected.

4.2 The Test System- 69-bus Radial Distribution Network

The test system is a 69-bus 12.66kV radial distribution network [102] and the one-line diagram is shown in Figure 4.1. The system is assumed to be operating under voltage limits of ±6% of nominal. The total network load is 3.802MW and 2.69Mvar. The network is compensated with four capacitor banks located on buses 15, 61, 63 and 65 with ratings of 0.3Mvar each. The base case real, and reactive power loss in the system are obtained as 0.1531MW and 0.0713Mvar, respectively. The real and the reactive power loss for the same network without shunt var compensation are 0.2249MW and 0.102Mvar respectively. A minimum voltage deviation of –0.073 is calculated at node 64 for the network with a shunt capacitor while a minimum voltage deviation of -0.0908 is calculated at node 65 for the network without shunt capacitor compensation. The Network data are provided in appendix A Table A.1 and a system base MVA of 10MVA is used for the study.

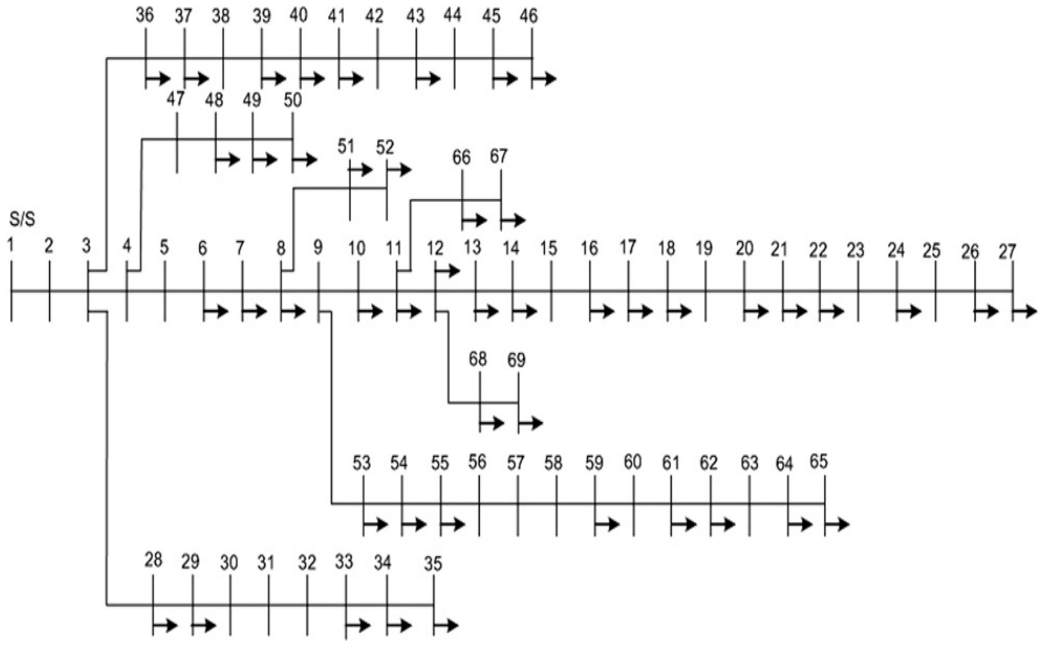

Figure 4.1: 69-bus radial distribution network [102]

4.3 Loss Minimisation and Voltage Support Using Basic PSO-W; Single Objective Optimisation

In this campaign, two network cases each with four scenarios are considered. Case I, is the network with shunt compensation capacitors already installed. Case II, is the same network, but without shunt compensation capacitors. The first scenario is for the base case network with no generation (network without DG), the second involved the integration of one generator of optimal size and location, the third involves the integration of a single generator of optimal size connected at the minimum voltage bus whereas the fourth involved the integration of two generators of optimal size and location. In each scenario different values of power factors (0.85, 0.95 and unity) are considered. In all scenarios the reactive power output of the generator is restricted to a maximum value corresponding to a maximum operating lagging power factor (PF) considered.

The PSO-W results were recorded after 10 independent runs of the algorithm using a swarm population of 20 particles and stop criteria of 50 iterations where the objective function value remains within a margin of 10^{-9} or a maximum number of 1000 iterations. The social and the cognitive constants c1and c2 respectively, are set to equal with both being assigned a value of 1.47 [77]. The maximum and minimum inertia

weight is set to w_{max}=0.9 and w_{min} =0.4 respectively [87]. The objective function is computed using Equation (4.6).

4.3.1 Scenario I: base network with no generation

Table 4.1 shows a summary of the results for the base network with no generation. Case I is the network with shunt compensation capacitors, while case II is the network without shunt compensation capacitors. The voltage profiles of the original test network are shown in Figure 4.2. Clearly, nodal voltages are an issue in both cases even under normal loading conditions and even with shunt capacitor compensation (Case I).

Table 4.1: SUMMARY OF RESULTS; SCENARIO I WITH NO GENERATION (BASE NETWORK)

Test Cases	Σ Load (MW)	Σ Load (Mvar)	Σ MW Loss	Maximum bus voltage (pu)	Minimum bus voltage (pu)	SSEV Index
Case I	3.802	2.690	0.1531	1.0	0.927	0.0665
Case II	3.802	2.690	0.2249	1.0	0.909	0.0993

The mean voltage value and the standard deviation for Case I are 0.9781pu and 0.02220, respectively. For case II, the mean voltage and the standard deviation values are 0.9734pu and 0.02724, respectively.

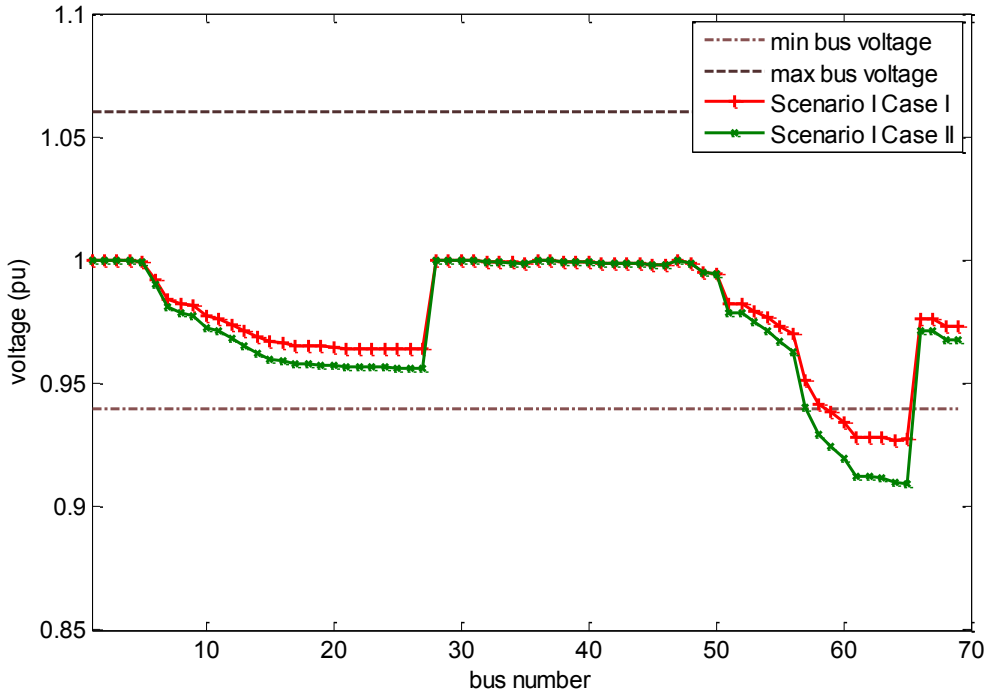

Figure 4.2: Voltage profile of 69-bus radial distribution network Scenario I (no generation); Case I (with shunt compensation) and Case II (no compensation)

Not surprisingly, Case I shows a better voltage profile, better mean voltage with lower value of standard deviation and a better value of the SSEV index when compared with Case II, because the network for Case I already has shunt compensation capacitors installed.

4.3.2 Scenario II: single generator

PSO-W is employed in this scenario to obtain the optimum size/location of a single distributed generator integrated into the network. The results of the PSO-W optimisation process for this scenario (considering Cases I and II) are presented in Table 4.2 for different values of generator operating PF. The resulting network voltage profiles are presented in Figure 4.3 (Case I) and Figure 4.4 (Case II). The required numbers of function evaluations averaged over 10 consecutive runs of the algorithm are presented in Table 4.3.

The best loss reduction (computed using Equation 4.15) and enhanced voltage support for Case I is obtained with one optimally sized (1.8308MW) and located generator injecting 0.35Mvars at bus number 61 where a 0.3Mvar shunt capacitor is already installed. The generator is able to maintain a 1pu voltage at the node operating at a power factor greater than the minimum possible lagging PF of 0.85. The results obtained for operating with a minimum lagging power factor of 0.85 or 0.95 are the same in this case due to the fact that the network is already compensated and therefore, the generator needs to inject less reactive power than its maximum capability to maintain the bus voltage at 1pu.

A 91.69% power loss reduction is achieved for Case I compared with the base case network, with a minimum voltage deviation of -0.0235 at bus number 27. An 89.82% power loss reduction is obtained with one optimally sized (1.8281MW) and located generator at bus number 61 for operating with a unity power factor (Case I). As expected, this power loss reduction is lower than that obtained for the generator operating with 0.85 PF or 0.95 PF. The voltage of the generator bus (0.9949 Pu) is less than 1pu as the generator is operating without injecting var to regulate its terminal voltage.

Table 4.2: DG SIZE AND LOCATION FOR SCENARIO II (SINGLE GENERATOR)

	Case I			**Case II**		
Minimum possible PF	0.85	0.95	1.0	0.85	0.95	1.0
Optimal bus	61	61	61	61	61	61
DG output MW/Mvar	1.8308/0.35	1.8308/0.35	1.8281/0.0	1.8909/1.17	2.048/0.67	1.8722/0.0
Actual operating PF	0.98	0.98	1.0	0.85	0.95	1.0
Max. Voltage	1.0000 pu	1.0000 pu	1.0000 pu	1.0000 pu	1.0000pu	1.0000 pu
Min. Voltage	0.9765 pu	0.9765 pu	0.9753 pu	0.9725 pu	0.9718 pu	0.9683 pu
Mean (pu)	0.9927	0.9927	0.9916	0.9915 pu	0.9910 pu	0.9874 pu
Std. Dev	0.008595	0.008595	0.008727	0.01008	0.01022	0.01151
Total power loss [MW]	0.0187	0.0187	0.0229	0.0238	0.0383	0.0831
Percent loss reduction	91.69%	91.69%	89.82%	89.41%	82.95%	63.03%
SSEV index	0.00868	0.00868	0.01008	0.011849	0.01275	0.02001

Table 4.2 also presents the results of the optimisation process when the shunt compensation capacitors are removed (Case II). The best loss reduction for Case II shows that the generator injects 1.8909 MW and 1.17Mvars at bus 61 giving an 89.41% power loss reduction. A minimum voltage deviation of -0.0275 is obtained at bus number 26. The voltage (0.9981pu) at the generator bus for operating with a minimum PF of 0.95 lagging deviates from 1pu as a result of the constraints placed on the generator's ability to produce reactive power. When operating with a minimum lagging PF of 0.85, the generator is able to maintain a 1pu voltage at its optimal bus location. In both situations, it is evident that the generator needs to inject more reactive power to maintain a pre specified voltage of 1pu at the generator bus following the removal of the shunt capacitors. The percentage reductions in power losses are lower than the corresponding figure for Case I.

The overall best reduction in power loss for this scenario (91.69% loss reduction) is obtained from Case I with the generator operating at a lagging operating power factor of

0.85 PF. The least power loss reduction (63% loss reduction) is found with Case II with the generator not injecting any reactive power into the network (unity PF operation).

It is evident from the results presented above that percentage power loss reduction is dependent on the operating power factor of the DG. Lower values of operating lagging power factor produced better loss reduction figures.

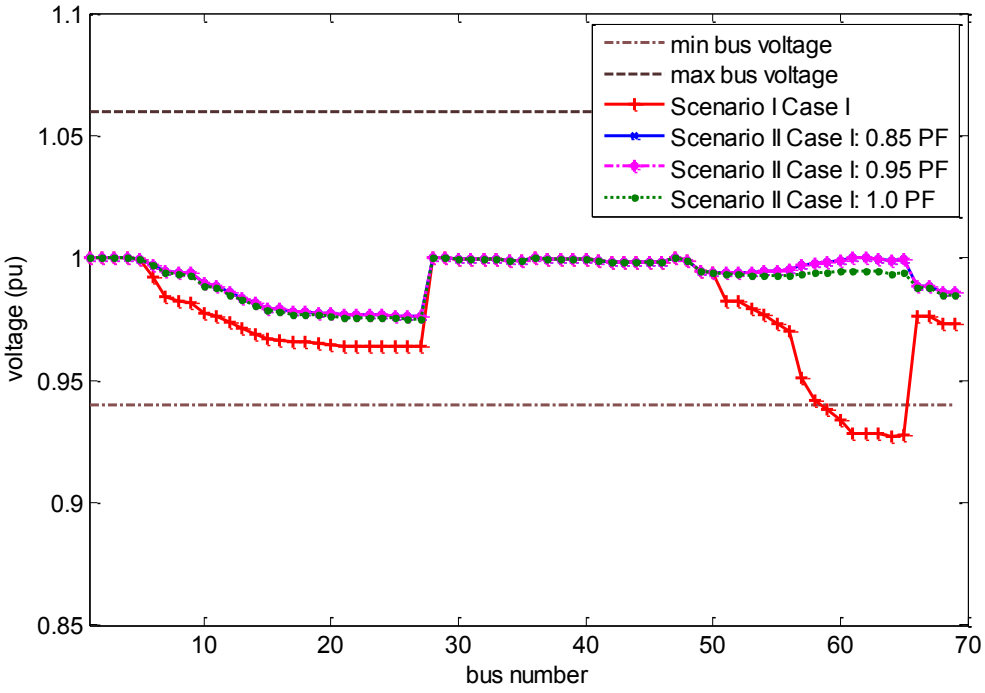

Figure 4.3: Voltage profile Scenario II (single generator); Case I (with shunt compensation)

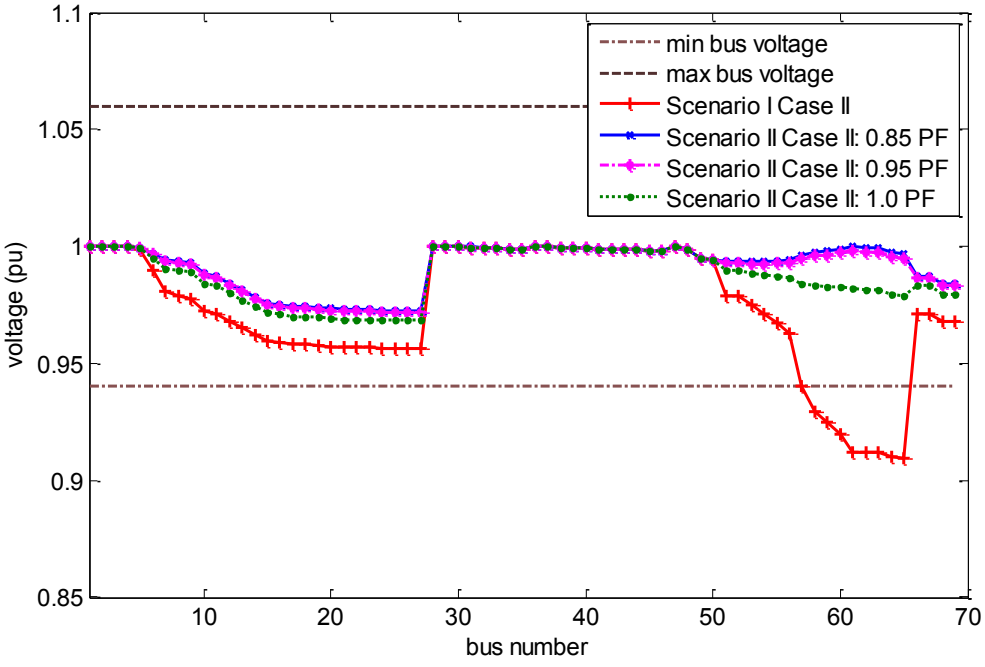

Figure 4.4: Voltage profile Scenario II (single generator); Case II (without shunt compensation)

Thus, allowing generators to provide reactive power locally can relieve the network of unnecessary reactive flow resulting in a drastic reduction in overall power loss. The resulting network voltage profiles are presented in Figures 4.3 and 4.4. It is evident that, the operation of the generator at lower lagging power factors also enhances the network voltage profile compared to unity PF operation, as a result of the injection of reactive power into the network.

The improvement in the network voltage profile can be quantified by calculating the SSEV defined by equation (4.13) and the results verified by computing the mean voltage and standard deviation of the bus voltages. The best voltage profile with a calculated SSEV of 0.00868 is obtained for Case I. The removal of the compensation capacitors (Case II) results in higher values of SSEV at 0.011849 (best SSEV value computed at different power factors). These values are significantly better than the SSEV calculated for the base network (0.0665 and 0.0993 for Case I and Case II, respectively).

The convergence of the objective function to the optimal solution is shown in Figures 4.5 and 4.6. The best (smallest) value of the objective function is obtained with the generator operating at a minimum power factor of 0.85 lagging. In Figure 4.5 it is evident that the algorithm reaches the same final solution for the generator operation at minimum PF of 0.95 or 0.85 lagging. This is due to the facts that the network already has shunt compensation devices installed, indicating that the generator only needs to inject small quantities of vars to keep its bus voltage at 1pu. However, this is not the case when the shunt compensation capacitors were removed (Figure 4.6). The final obtained solutions are based on the quantity of reactive power the generator is allowed to contribute to support the bus voltage. In Table 4.2, a figure of 0.98 PF is calculated as the as the actual operating PF of the generator for both 0.85 and 0.95 minimum lagging PF. Thus, when the network is compensated, the actual operating power factor is higher than 0.95, hence it does not make any difference if the minimum possible is 0.95 or 0.95.

Table 4.3 shows that a substantial number of evaluations of the objective function are required to attain a final solution. The number of such iterations is found to increase with different values of minimum power factor, with unity power factor operation of the generator requiring the least number of iterations (because of the reduced search space).

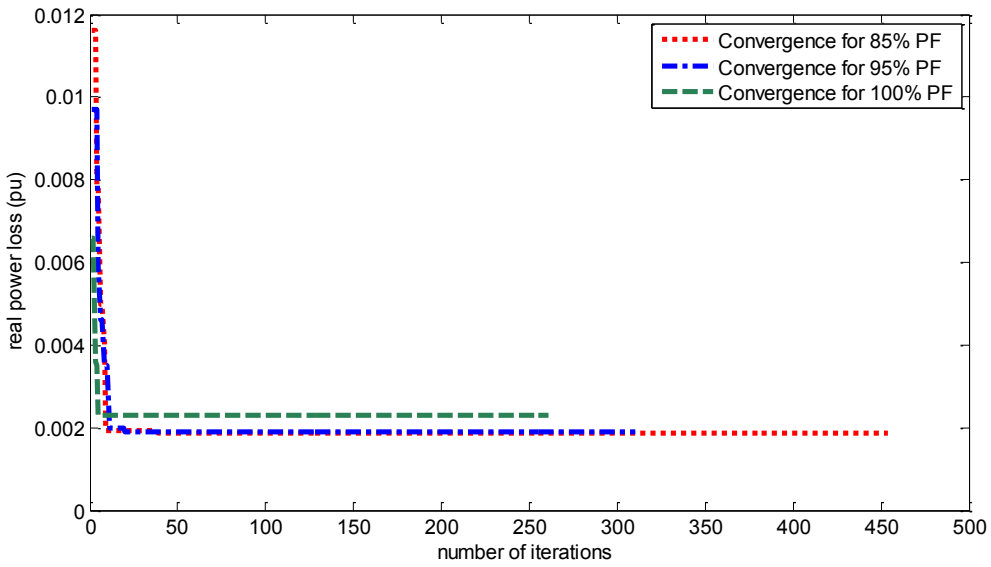

Figure 4.5: Convergence characteristic of PSO-W (Scenario II case I)

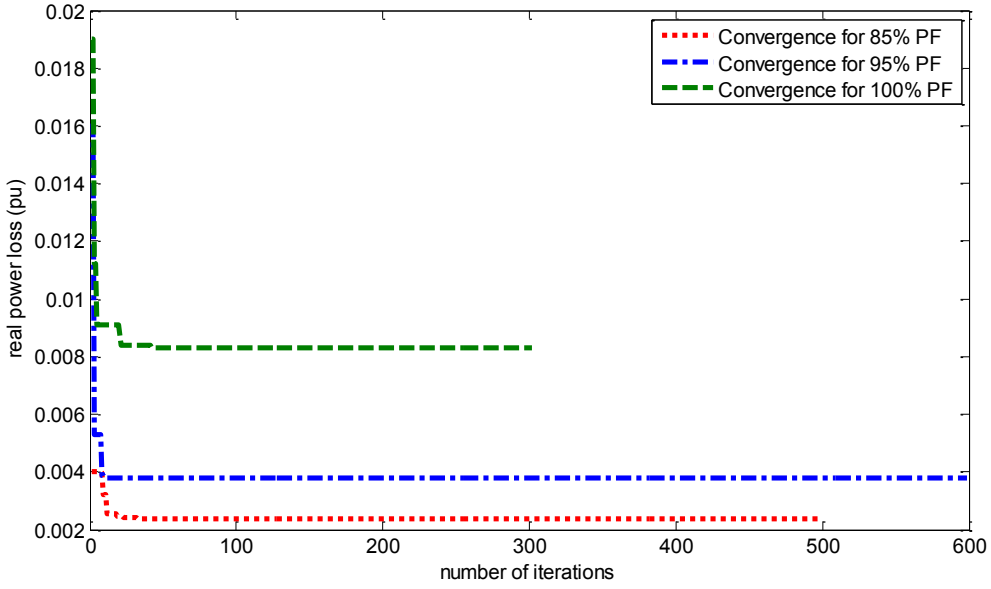

Figure 4.6: Convergence characteristic of PSO-W (Scenario II case II)

Table 4.3: ALGORITHM COMPUTATIONAL BURDEN; SCENARIO II (SINGLE GENERATOR)

	PSO –W Case I			PSO –W Case II		
Minimum power factor	0.85	0.95	0.85	0.95	0.85	0.95
Average no. of steps	483.6	384.2	483.6	384.2	483.6	384.2
No. of function evaluations per step	20	20	20	20	20	20
No of function evaluations	9672	7684	9672	7684	9672	7684

4.3.3 Scenario III: single generator installed at the minimum voltage bus

The results of the PSO-W optimisation process for this scenario are presented in Table 4.4 for different values of minimum generator lagging PF. The improvement in network voltage profile is shown in Figures 4.7 and 4.8. When the generator is connected at bus number 64 (the minimum voltage bus for Case I), the best optimal size of the generator is calculated at 1.6053MW injecting an additional 0.28Mvar into the network. A drastic power loss reduction of 85.99% is achieved in this case (Case I, generator operating with a minimum lagging PF of 0.85) compared with the base network. A minimum voltage deviation of -0.0252 is obtained at bus number 27. The generator operates at a power factor greater than the minimum of 0.85 lagging, due the fact that the network is already compensated.

Table 4.4: DG SIZE AND LOCATION FOR SCENARIO III (ONE GENERATOR INSTALLED AT THE MINIMUM VOLTAGE BUS)

	Case I			**Case II**		
Minimum possible PF	0.85	0.95	1.0	0.85	0.95	1.0
Optimal bus	64	64	64	65	65	65
DG output MW/Mvar	1.6053/0.28	1.6053/0.28	1.6151/0.0	1.4385/0.89	1.5974/0.53	1.4383/0.0
Actual operating PF	0.99	0.99	1.0	0.85	0.95	1.0
Max. voltage	1.0000 pu	1.0000 pu	1.0000 pu	1.0000 pu	1.0000pu	1.0000 pu
Min. voltage	0.9748 pu	0.9748 pu	0.9740 pu	0.9687 pu	0.9684 pu	0.9656 pu
Mean (pu)	0.9912	0.9912	0.9904	0.9878 pu	0.9877 pu	0.9854 pu
Std. Dev	0.009002	0.009002	0.009251	0.01148	0.01157	0.01367
Total power loss [MW]	0.0315	0.0315	0.0348	0.0622	0.0742	0.1120
Percent loss reduction	85.99%	85.99%	84.53%	72.34%	66.99%	50.19%
SSEV index	0.010854	0.010854	0.01242	0.019188	0.019577	0.029807

When the generator is connected at bus number 65 (the minimum voltage bus for Case II), the best optimal size of the generator is calculated at 1.4385MW injecting 0.89Mvar

into the network. The generator operates at its minimum of 0.85 PF to support its bus voltage at 1pu. A power loss reduction of 72.34% is achieved. A minimum voltage deviation of -0.0313 is obtained at bus number 27.

Thus, the location of the generator at the minimum voltage node resulted in a smaller generator at the expense of a lower power loss reduction when compared to scenario II. Again, the optimisation process resulted in the same DG size and location for operation with a minimum lagging PF of 0.85 and 0.95.

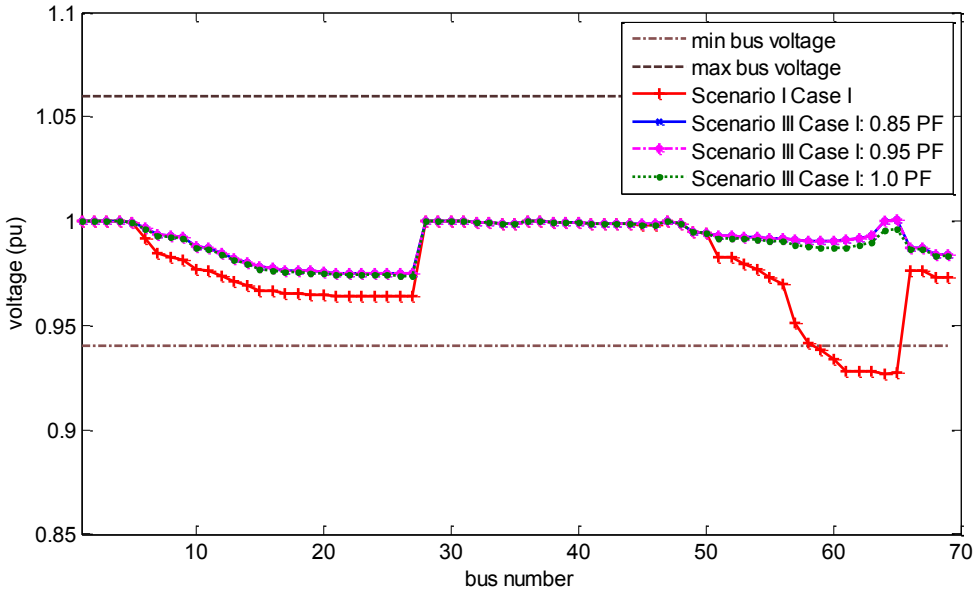

Figure 4.7: Voltage profile Scenario III (single generator at minimum voltage bus); Case I (with shunt compensation)

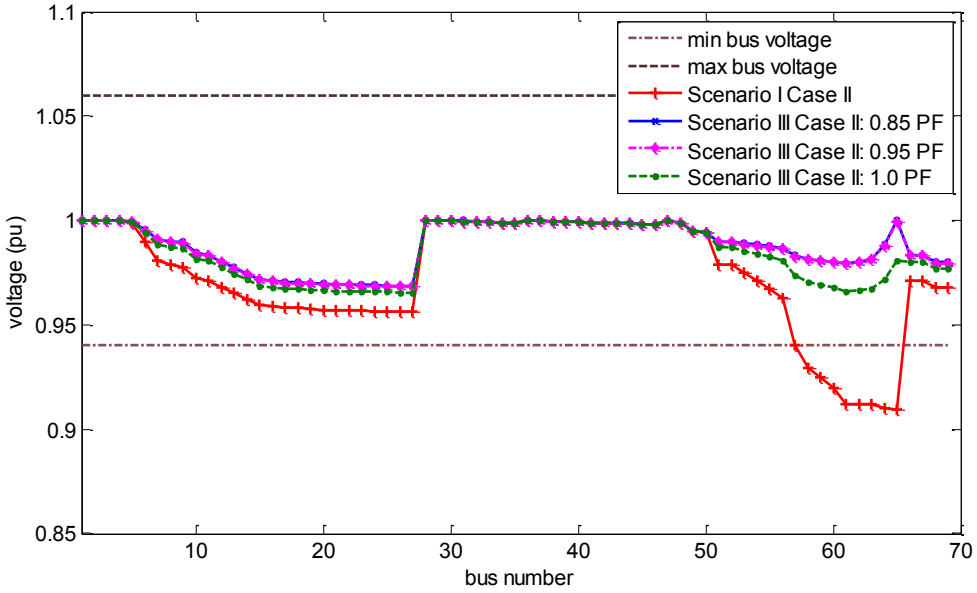

Figure 4.8: Voltage profile Scenario III (single generator at minimum voltage bus); Case II (without shunt compensation)

This is because the network is already installed with shunt compensation capacitors so that the generator needs to inject less reactive power (than its maximum capability) to keep the bus voltage at 1pu. This is evident from the figures of the actual operating PF of the generator presented in Table 4.4. A figureof 0.99 PF is calculated for both 0.85 and 0.95 minimum lagging PF. However, when the generator operates in an uncompensated network (Case II), the operating PF drops to the minimum possible lagging values of 0.85 and 0.95. Thus, resulting in the difference in the results obtained at the different minimum possible lagging PF.

The overall best reduction in power loss for this scenario is obtained for Case I (85.99% loss reduction) when operating with a minimum lagging power factor of 0.85. The lowest power loss reduction is found with Case II (50.19% loss reduction) when the DG is not injecting any reactive power into the network (unity PF operation).

The improvement in the network voltage profile can again be quantified by calculating the SSEV. The best voltage profile was obtained for Case I with a calculated SSEV of 0.010854. The removal of the compensation capacitors (Case II) resulted in a higher best value of SSEV at 0.019188. Even though these SSEV values are higher than those obtained for scenario II, they are still significantly better than the SSEV calculated for the base network.

Table 4.5 shows the number of evaluations of the objective function for the final attained optimal solutions. Similar to scenario II, the numbers of iterations are found to increase at lower values of minimum power factor, with the case of unity power factor operation of the generator requiring the least number of iterations.

Table 4.5: ALGORITHM COMPUTATIONAL BURDEN: SCENARIO III

	PSO –W Case I			PSO –W Case II		
Minimum power factor	0.85	0.95	1.0	0.85	0.95	1.0
Average no. of steps	522.2	342.8	291	522.2	278	250.4
No. of function evaluations per step	20	20	20	20	20	20
No. of function evaluations	6800	6856	5820	10444	5560	5008

4.3.4 Scenario IV: two generators

This scenario involved finding the optimal location and size for two generators operating with different reactive power output capabilities (different minimum operating power factors), first in the presence of shunt compensation capacitors (Case I) and with shunt compensation capacitors removed (Case II).

The results of the PSO-W optimisation process for this scenario are presented in Table 4.6. The best loss reduction with enhanced voltage support is obtained with two optimally sized (1.7384MW and 0.5276MW) and located generators (Case I) injecting additional 0.34Mvars and 0.08Mvars at bus number 61 and 17, respectively.

Table 4.6: DG SIZE AND LOCATION FOR SCENARIO IV (TWO GENERATORS)

	Case I			**Case II**		
Minimum possible PF	0.85	0.95	1.0	0.85	0.95	1.0
Optimal bus 1	17	61	61	61	61	17
DG 1 output MW/Mvar	0.5276/0.08	1.7384/0.34	1.7369/0.0	1.7928/1.11	1.9451/0.64	0.5311/0.0
Actual oper-rating PF 1	0.99	0.98	1.0	0.85	0.95	1.0
Optimal bus 2	61	17	17	17	17	61
DG 2 output MW/Mvar	1.7384/0.34	0.5276/0.08	0.5224/0.0	0.535/0. 33	0.5785/0.19	1.7811/0.0
Actual oper-ating PF 2	0.98	0.99	1.0	0.85	0.95	1.0
Max. Voltage	1.0000 pu	1.0000 pu	1.0000 pu	1.0000 pu	1.0000pu	1.0000 pu
Min. Voltage	0.9943 pu	0.9943 pu	0.9929 pu	0.9943 pu	0.9934 pu	0.9789 pu
Mean (Pu)	0.9983 pu	0.9983 pu	0.9968 pu	0.9982 pu	0.9975 pu	0.9928 pu
Std. Dev	0.001675	0.001675	0.002303	0.001737	0.001973	0.006057
Total power loss [MW]	0.0076	0.0076	0.0120	0.0079	0.0234	0.0716
Percent loss reduction	96.62%	96.62%	94.66%	96.45%	89.58%	68.16%
SSEV index	0.000383	0.000383	0.001051	0.000435	0.000691	0.006095

A dramatic 96.62% power loss reduction is achieved compared with the base case network with a minimum voltage deviation of -0.0057 at bus number 50 and a computed SSEV value of 0.000383. The improvement in network voltage profile is shown in Figures 4.9.

The results of the optimisation process when the compensating shunt capacitors are removed (Case II) are also presented in Table 4.4. The best results for this case shows the generators to inject 1.7928MW/1.11Mvars at bus number 61 and 0.535MW/0.33Mvars at bus number 17, reducing power loss compared with the base network by 96.45%. A minimum voltage deviation of -0.0057 at bus number 50 is calculated with a computed SSEV value of 0.000435. Figure 4.10 shows the resulting network voltage profiles for this case.

The voltages at the generator buses deviated from 1p.u (except for 0.85 PF operations) as a result of the constraints placed on their ability to produce reactive power. Following the removal of the shunt capacitors, it is evident that the generators need to inject more reactive power to maintain a voltage of 1p.u at the generator buses. The percentage reduction in power loss is lower than that for Case I.

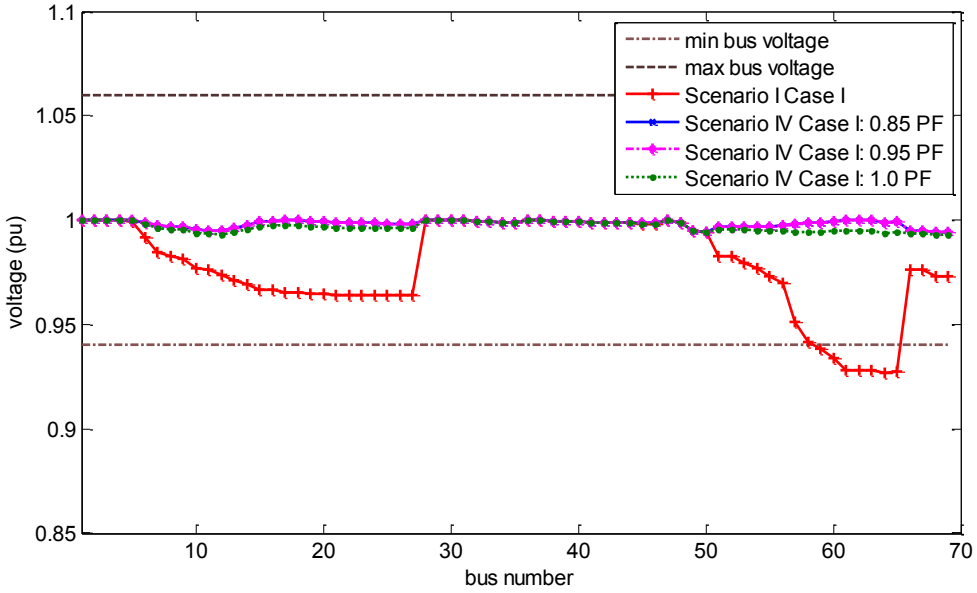

Figure 4.9: Voltage profile Scenario IV (two generators); Case I (with shunt compensation)

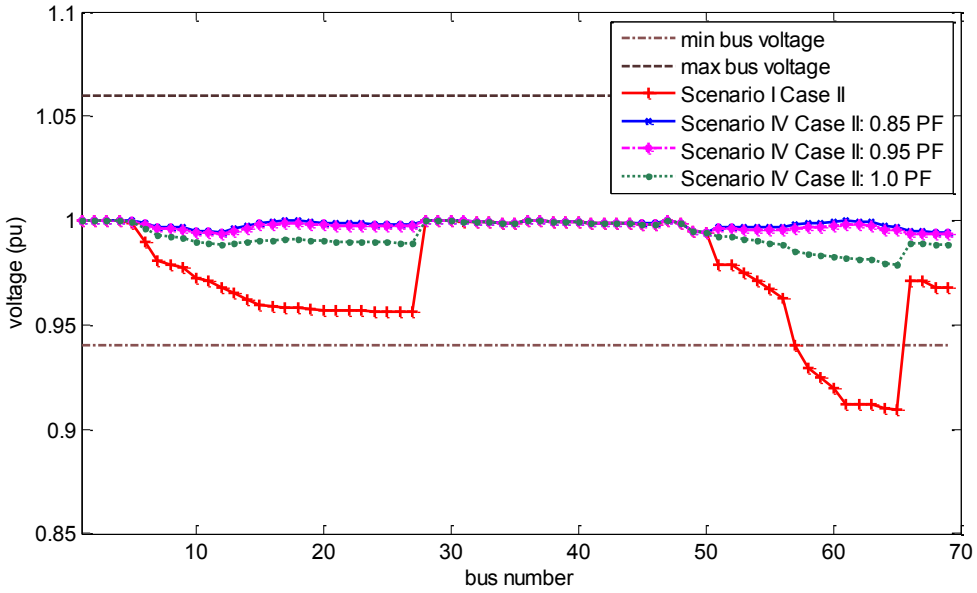

Figure 4.10: Voltage profile Scenario VI (two generators); Case II (without shunt compensation)

Table 4.7 shows the number of evaluations of the objective function for the final attained optimal solutions. Similar to other scenarios, the number of iterations was found to increase at lower values of power factor (because of the wider search space), with the case of unity power factor operation of the generator requiring the least number of iterations.

Table 4.7: ALGORITHM COMPUTATIONAL BURDEN; SCENARIO IV

	PSO –W Case I			PSO –W Case II		
Minimum power factor	0.85	0.95	1.0	0.85	0.95	1.0
Average no. of steps	807.6	806.9	751.2	839.2	753.8	613.2
No. of function evaluations per step	20	20	20	20	20	20
No. of function evaluations	16152	16138	15024	16784	15076	12264

In summary, for all the scenarios the best results are obtained when shunt capacitors are employed as compensation devices with DG to provide reactive power support for the network. This will minimize the reactive power demand from the generators which will nevertheless still be providing ancillary voltage support for the network. The real power loss reduction chart for the best test cases for all the studied scenarios and cases are shown in Figure 4.11. The best loss reduction was obtained with scenario IV/Case I, i.e. two generators operating within a compensated network. Figure 4.12 presents the best SSEV values for all the studied scenarios. Again, the best voltage profile with a calculated SSEV value of 3.830×10^{-4} was obtained with two optimally size and located

generators with the connection of the reactive power compensation capacitors (scenario IV, Case I). The best mean voltage values are presented in Figure 4.13. The best value of mean voltage (0.9983pu) and standard deviation (0.00167) is also obtained with scenario IV, Case I. Thus, the analysis shows that very good results can still be obtained with the generators alone (with the capacitors disconnected) as long as they are allowed to provide network var support.

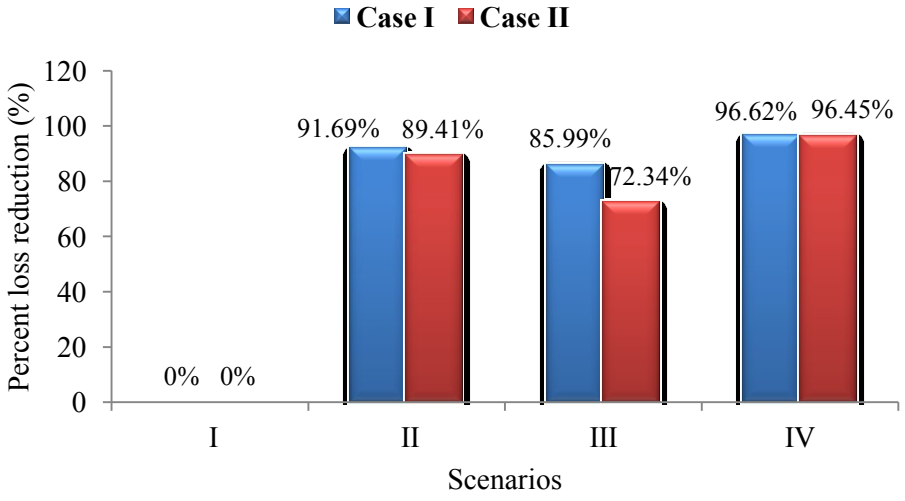

Figure 4.11: Real power loss reduction chart

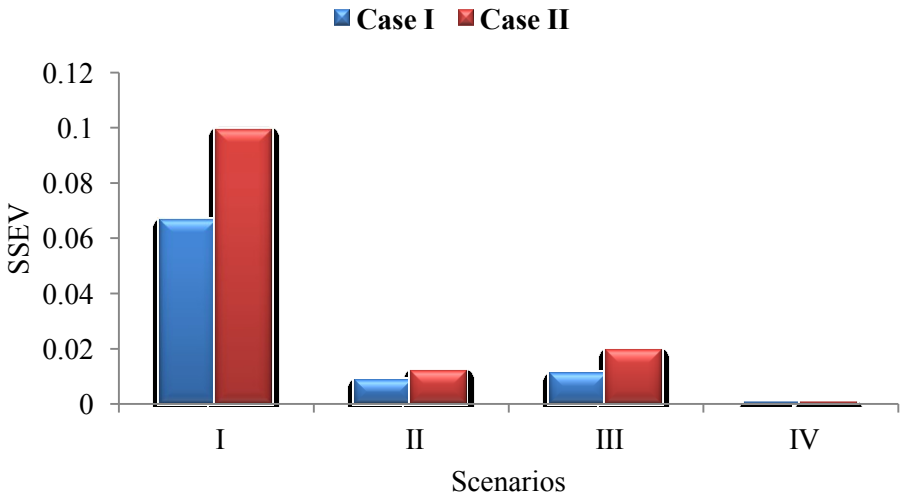

Figure 4.12: SSEV values

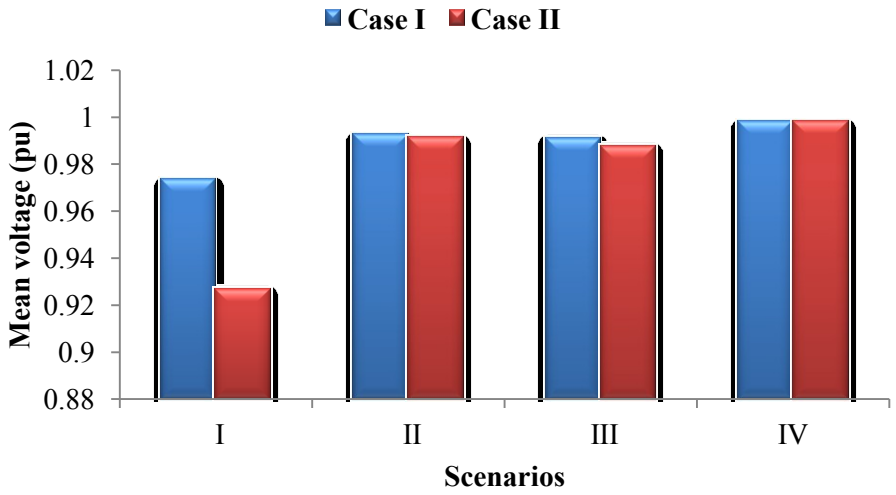

Figure 4.13: Best of mean voltage values

4.4 Loss Minimisation and Voltage Support Using Basic PSO-W; Multi-Objective Optimisation

In this section, the optimisation analysis presented above in section 4.3 is repeated as a multi-objective optimisation exercise considering both the network power loss and the voltage profile in the cost function as expressed in Equation (4.7), all other network scenarios and algorithm parameters being the same.

4.4.1 Scenario I: base network with no generation

This is obviously the same study discussed in section 4.3.1. Results are repeated here in Table 4.8 and Figure 4.14 for convenience.

Table 4.8: SUMMARY OF RESULTS; SCENARIO I WITH NO GENERATION (BASE CASE)

Test Cases	Σ Load (MW)	Σ Load (Mvar)	Σ MW Loss	Maximum bus voltage (pu)	Minimum bus voltage (pu)	SSEV Index
Case I	3.802	2.690	0.1531	1.0	0.927	0.0665
Case II	3.802	2.690	0.2249	1.0	0.909	0.0993

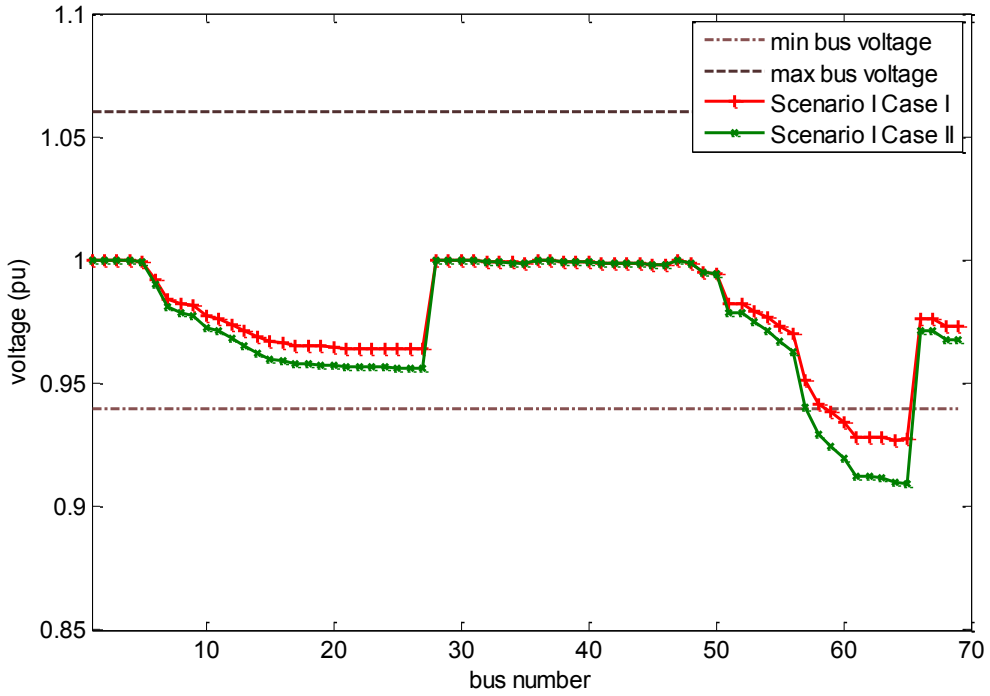

Figure 4.14: Voltage profile of 69-bus radial distribution network; Scenario I (no generation)

4.4.2 Scenario II: single generator; multi-objective optimisation

The results of the PSO-W multi-objective optimisation process for this scenario are presented in Table 4.9. The network voltage profiles for case I and II are presented in Figures 4.10 and 4.11, respectively. The required number of function evaluations computed for 10 consecutive runs are presented in Table 4.10.

The best loss reduction and enhanced voltage profile for Case I is obtained with one optimally sized (1.7977 MW) and located generator injecting 0.43Mvars at bus number 61. The generator is able to maintain a 1pu voltage at the node operating at a power factor greater than the minimum 0.85 lagging. A 91.55% power loss reduction is achieved compared with the base case network, with a minimum voltage deviation of -0.0235 at bus number 27 and a value SSEV of 0.008631.

Table 4.9 also presents the results of the optimisation process when the compensating shunt capacitors are removed (case II). The best loss reduction for this case II is when the generator injects 1.8911 MW and 1.17Mvars at bus 61 producing an 89.41% power loss reduction. A minimum voltage deviation of -0.0275 is obtained at bus number 26 with an SSEV value of 0.011849.

Table 4.9: DG SIZE AND LOCATION FOR SCENARIO II (ONE GENERATOR); MULTI OBJECTIVE OPTIMISATION

	Case I			**Case II**		
Minimum possible PF	0.85	0.95	1.0	0.85	0.95	1.0
Optimal bus	61	61	61	61	61	61
DG output MW/Mvar	1.7977/0.43	1.7977/0.43	2.1762/0.0	1.8911/1.17	2.0975/0.69	2.5681/0.0
Actual operating PF	0.97	0.97	1.0	0.85	0.95	1.0
Max. voltage	1.0000 pu	1.0000 pu	1.0070 pu	1.0000 pu	1.0000pu	1.0050 pu
Min. voltage	0.9765 pu	0.9765 pu	0.9773 pu	0.9725 pu	0.9721 pu	0.9723 pu
Mean (pu)	0.9927 pu	0.9927 pu	0.9939 pu	0.9915 pu	0.9913 pu	0.9920 pu
Std. Dev	0.008575	0.008575	0.009031	0.01008	0.01022	0.01066
Total power loss [MW]	0.019	0.019	0.027	0.0238	0.0384	0.0993
Percent loss reduction	91.55%	91.55%	87.99%	89.41%	82.91%	55.85%
SSEV index	0.008631	0.008631	0.008109	0.011849	0.012283	0.012107

The percentage reductions in power losses are lower than the corresponding figure for Case I due to the removal of shunt capacitors. Without the shunt compensation capacitors, the generator needs to inject more reactive power to maintain a pre specified voltage of 1pu at the generator bus. Again, the percent power loss reduction is dependent on the operating power factor of the DG with lower values of lagging power factor producing better loss reduction results. The lowest case of power loss reduction (55.85%) is obtained when DG is not injecting reactive power into the network (unity PF operation).

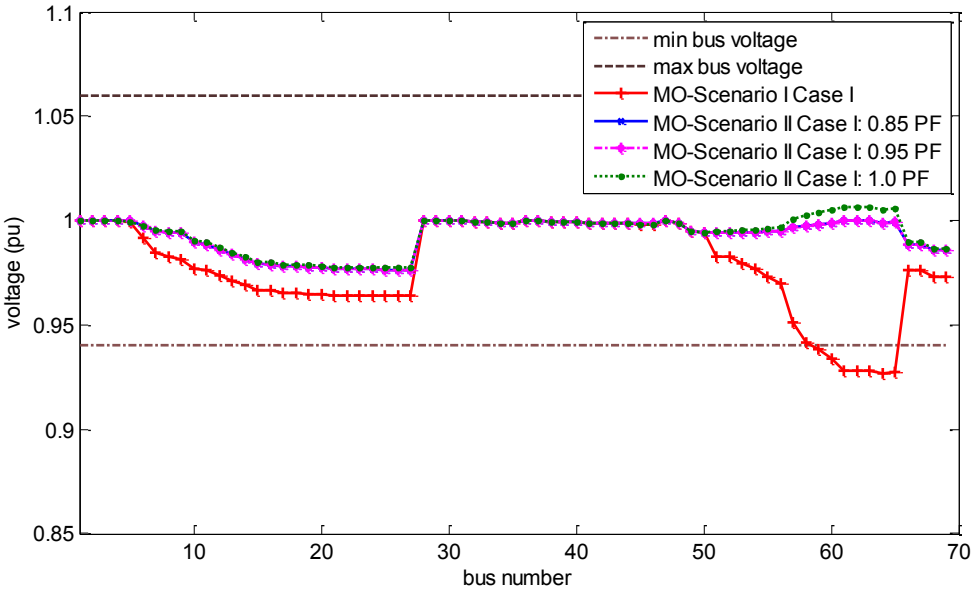

Figure 4.15: Voltage profile Scenario II (single generator); Case I (with shunt compensation), Multi Objective Optimisation

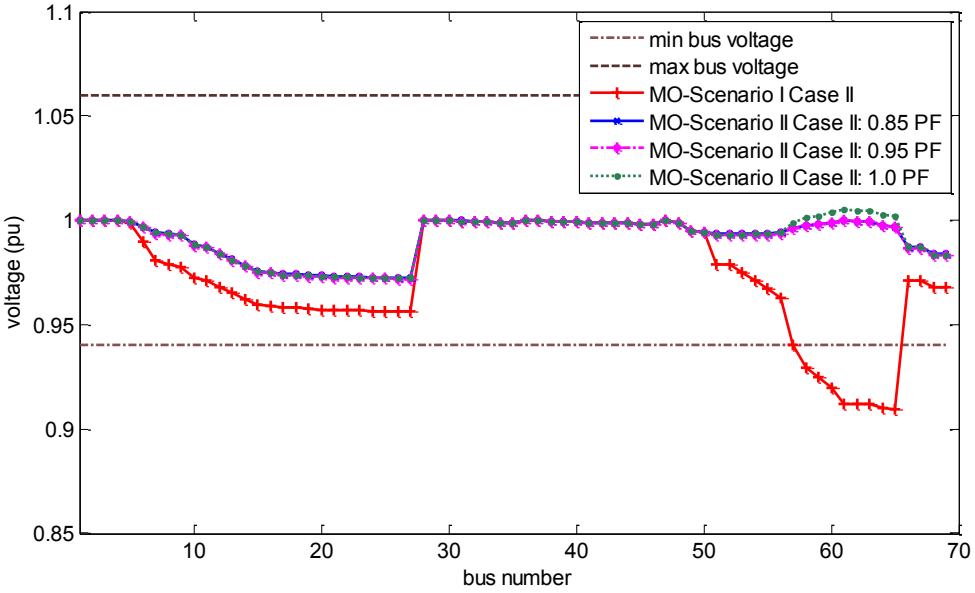

Figure 4.16: Voltage profile Scenario II (single generator); Case II (without shunt compensation), Multi-Objective Optimisation

Comparing the results of the multi-objective optimisation presented in Table 4.9 and Figures 4.15 and 4.16 with those obtained for the single-objective study (Table 4.2, Figures 4.3 and 4.4) it is interesting to note that the two sets of results are very similar. The impact of including the voltage profile in the cost function to be optimized is only significant in the case of DG operation at unity power factor resulting in a better network voltage profile at the expense of a higher DG size and lower power loss reduction figure.

The convergence of the multi-objective cost function is shown in Figures 4.17 and 4.18 for Case I and Case II, respectively. Table 4.10 shows the number of evaluations of the objective function required to attain a final optimal solution. The number of such iterations is again found to increase with lower values of DG operating power factors. These results are also evident from Figure 4.17 and 4.18.

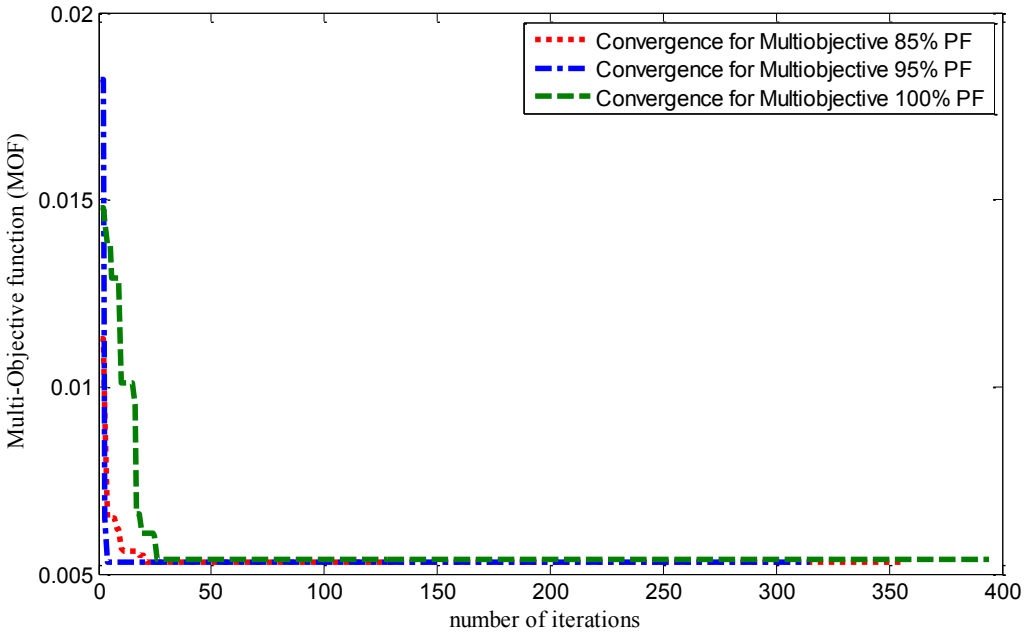

Figure 4.17: Convergence characteristic of PSO-W (Scenario II, Case I); Multi Objective Optimisation

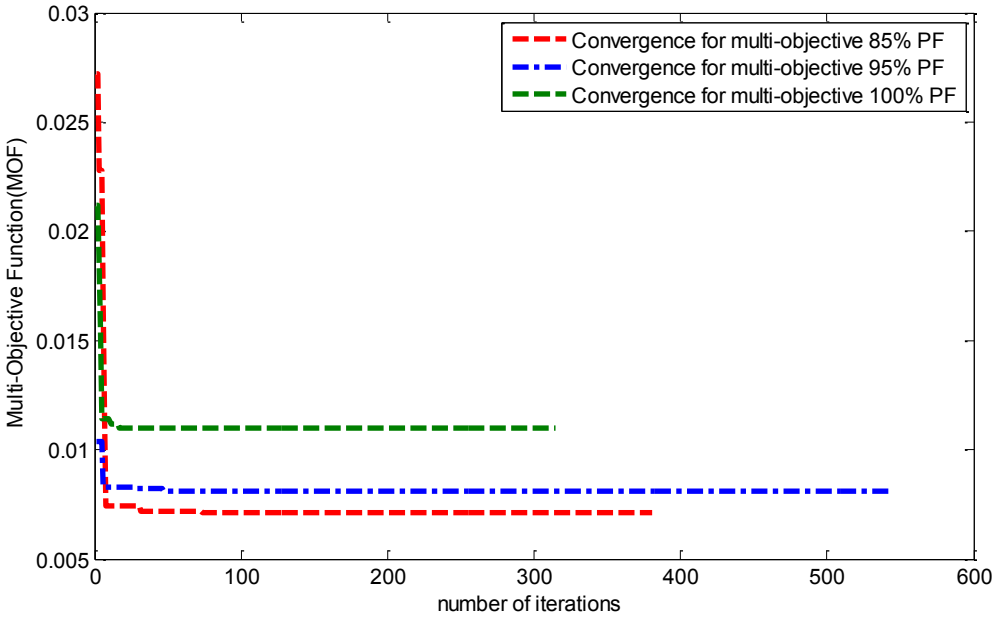

Figure 4.18: Convergence characteristic of PSO-W (Scenario II, Case II); Multi Objective Optimisation

Table 4.10: ALGORITHM COMPUTATIONAL BURDEN: SCENARIO II, MULTI OBJECTIVE OPTIMISATION

	PSO –W Case I			PSO –W Case II		
Minimum power factor	0.85	0.95	1.0	0.85	0.95	1.0
Average no. of steps	327.2	338.4	334.4	512	539	320
No. of function evaluations per step	20	20	20	20	20	20
No. of function evaluations	6544	6768	6688	10240	10780	6400

4.4.3 Scenario III: single generator connected at the minimum voltage bus; multi-objective optimisation

The results of the PSO-W optimisation process for this scenario are presented in Table 4.11. The corresponding improvement in network voltage profile is shown in Figures 4.19 and 4.20. The minimum bus voltages are bus 64 for Case I and bus 65 for Case II. Surprisingly for Case I the best optimal size of the generator (with minimum objective) is calculated at 2.0352 MW injecting an additional 0.0 Mvar (unity PF) into the network. A power loss reduction of 81.55% is achieved compared with the base case network. A minimum voltage deviation of -0.0236 is obtained at bus number 27.

The generator penetration level suddenly increased at the fixed location (bus 64) because the network is already compensated. As expected, this increased in the penetration level at the fixed location resulted in a lower power loss reduction (compared with 0.85 and 0.95 PF operation) but with an improved voltage profile (Figure 4.19) for the network. For Case II, the best optimal size of the generator (with minimum objective) is calculated at 1.4385MW injecting 0.89Mvar. The generator operates at the limit of its reactive power range, i.e. at a power factor of 0.85 lagging to keep its bus voltage at 1pu. A power loss reduction of 72.34% is achieved with a minimum voltage deviation of -0.0313 at bus number 27.

The locating of the generator at the minimum voltage node results in a smaller generator at the expense of a lower power loss reduction when compared to Case I of this scenario and the scenario II.

Table 4.11: DG SIZE AND LOCATION FOR SCENARIO III (ONE GENERATOR AT MINIMUM VOLTAGE BUS); MULTI-OBJECTIVE OPTIMISATION

	Case I			**Case II**		
Minimum possible PF	0.85	0.95	1.0	0.85	0.95	1.0
Optimal bus	64	64	64	65	65	65
DG output MW/Mvar	1.5799/0.34	1.5797/0.34	2.0352/0.0	1.4385/0.89	1.6030/0.53	2.2897/0.0
Actual oper-ating PF	0.98	0.98	1.0	0.85	0.95	1.0
Max. voltage	1.0000 pu	1.0000 pu	1.0000 pu	1.0000 pu	1.0000pu	1.0190 pu
Min. voltage	0.9748 pu	0.9748 pu	0.9764 pu	0.9687 pu	0.9684 pu	0.9703 pu
Mean (pu)	0.9912	0.9912 pu	0.9932pu	0.9878 pu	0.9877 pu	0.9904 pu
Std. Dev	0.008989	0.008991	0.009306	0.01148	0.01156	0.01128
Total power loss [MW]	0.0317	0.0317	0.0415	0.0622	0.0742	0.1437
Percent loss reduction	85.90%	85.90%	81.55%	72.34%	66.99%	36.11%
SSEV index	0.010811	0.010816	0.009051	0.019188	0.019476	0.015006

The best of voltage support with a calculated SSEV of 0.009051 is obtained for Case I (with unity PF operation). The removal of the capacitors (Case II) resulted in a higher value of SSEV at 0.015006 (unity PF operation) as the best of voltage support provided, but still significantly better than the SSEV calculated for the base case network (0.0665 for Case I and 0.0993 for Case II).

Thus, the best voltage profile for both Case I and II is achieved with unity power factor operation (Figures 4.19 and 4.20) when multi-objective is considered. However, this is at the expense of increased DG size and lower power loss reduction obtained as 81.55% and 36.11% respectively for Case I and II. The results also show that savings in the generator size at the expense of less power loss reduction are feasible if an optimal size generator is located at the bus with the minimum voltage.

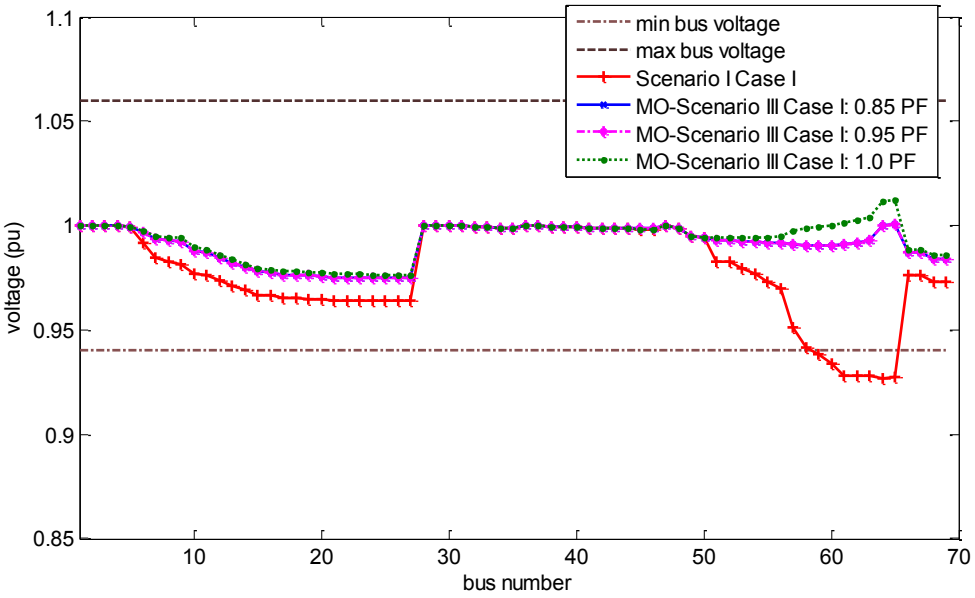

Figure 4.19: Voltage profile Scenario III (single generator connected at minimum voltage bus); Case I (with shunt compensation), Multi-objective optimisation

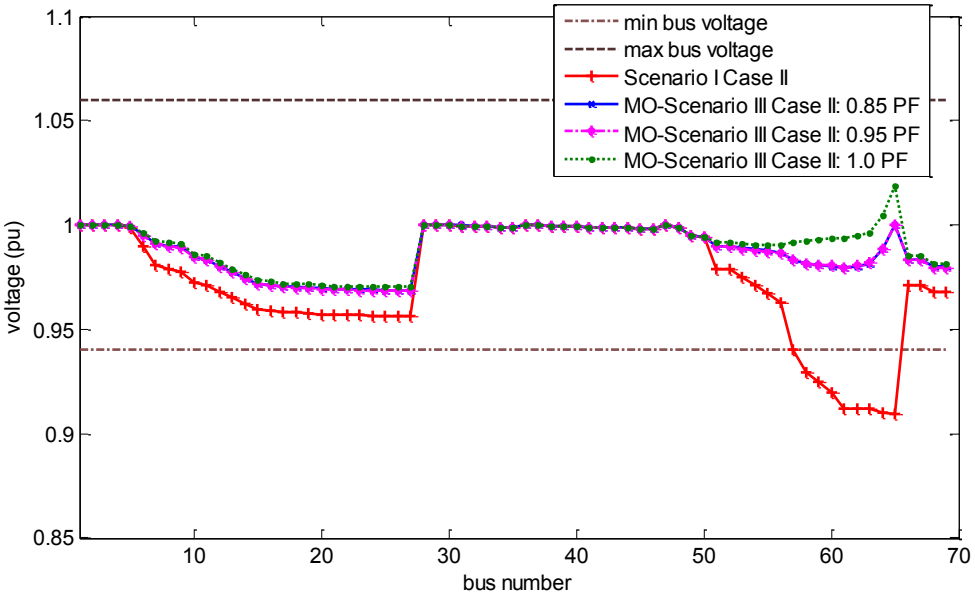

Figure 4.20: Voltage profile Scenario III (single generator connected at minimum voltage bus); Case I (without shunt compensation), Multi-objective optimisation

Table 4.12 shows the number of evaluations of the objective function for the final attained optimal solutions. These values are based on an average of 10 independent executions of the PSO-W algorithm.

Table 4.12: ALGORITHM COMPUTATIONAL BURDEN: SCENARIO III; MULTI- OBJECTIVE OPTIMISATION

	PSO –W Case I			PSO –W Case II		
Minimum power factor	0.85	0.95	1.0	0.85	0.95	1.0
Average no. of steps	331.6	286.2	331.4	540.8	573.6	257.4
No. of function evaluations per step	20	20	20	20	20	20
No. of function evaluations	6632	5724	6268	10816	11472	5148

4.4.4 Scenario IV: two generators, multi-objective optimisation

The results of the PSO-W optimisation process for this scenario are presented in Table 4.13. The best solution (with loss reduction and enhanced voltage support) is obtained with two optimally sized (1.7349MW and 0.5242 MW) and located generators (Case I) injecting additional 0.34Mvars and 0.09Mvars at bus number 61 and 17, respectively.

A 96.62% power loss reduction is achieved compared with the base network with a minimum voltage deviation of -0.0057 at bus number 50. The improvement in network voltage profile is shown in Fig. 4.21. Interestingly, the bus voltages at the optimal bus locations is 1pu for unity power factor operation (Case I) despite the fact that there is no reactive power exchange between the generator and the network. This is obtained at the expense of increased DG capacity (compared with the single objective optimisation study) resulting in a slight decrease in the power loss reduction (94.09% compared with 94.66%).

When the shunt compensation capacitors are removed (Case II) the best result shows the generators injecting 1.7923MW/1.11Mvars at bus number 61 and 0.5381MW/0.33Mvars at bus number 17, reducing power loss compared with the base network by 96.49%. A minimum voltage deviation of -0.0063 at bus number 50 is obtained. Figure 4.22 shows the resulting network voltage profiles.

Table 4.13: DG SIZE AND LOCATION FOR SCENARIO IV (TWO GENERATORS); MULTI-OBJECTIVE OPTIMISATION

	Case I			**Case II**		
Minimum possible PF	0.85	0.95	1.0	0.85	0.95	1.0
Optimal bus 1	61	17	15	61	17	17
DG 1 output MW/Mvar	1.7349/0.34	0.5242/0.09	0.6511/0.0	1.7923/1.11	0.5966/0.2	0.7843/0.0
Actual operating PF 1	0.98	0.99	1.0	0.85	0.95	1.0
Optimal bus 2	17	61	61	17	61	61
DG 2 output MW/Mvar	0.5242/0.09	1.7349/0.34	1.8685/0.0	0.5381/0. 33	1.9905/0.65	2.197/0.0
Actual operating PF 2	0.99	0.98	1.0	0.85	0.95	1.0
Max. voltage	1.0000 pu	1.0000 pu	1.0020 pu	1.0000 pu	1.0000pu	1.0020 pu
Min. voltage	0.9943 pu	0.9943 pu	0.9943 pu	0.9943 pu	0.9941 pu	0.9942 pu
Mean (pu)	0.9983 pu	0.9983 pu	0.9988 pu	0.9982 pu	0.9981 pu	0.9979 pu
Std. Dev	0.001673	0.001673	0.001680	0.00173	0.001852	0.002164
Total power loss [MW]	0.0076	0.0076	0.0133	0.0079	0.0235	0.0808
Percent loss reduction	96.62%	96.62%	94.09%	96.49%	89.54%	64.09%
SSEV index	0.000382	0.000382	0.000299	0.000424	0.000484	0.000627

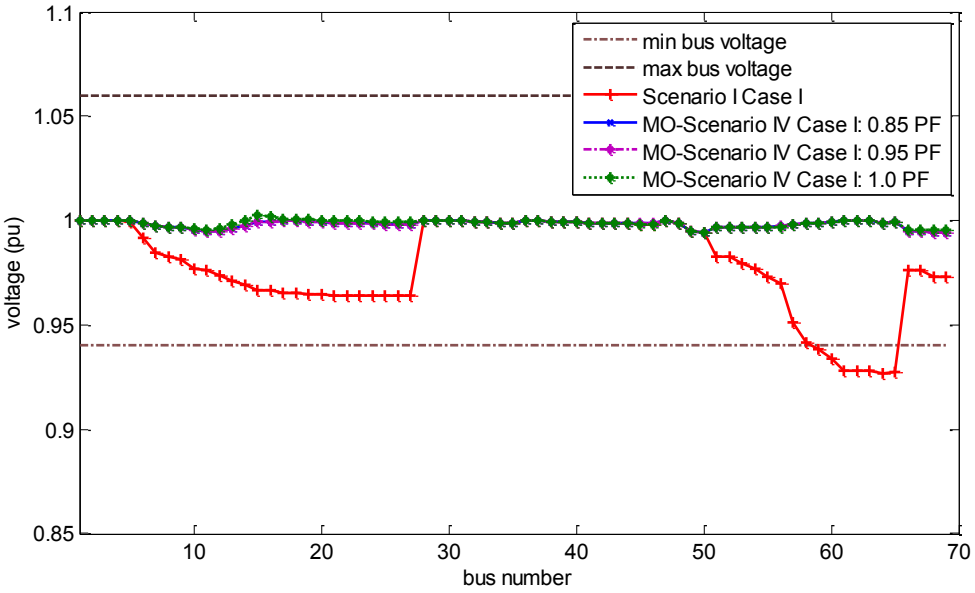

Figure 4.21: Voltage profile Scenario IV (two generators); Case I (with shunt compensation), Multi-Objective Optimisation

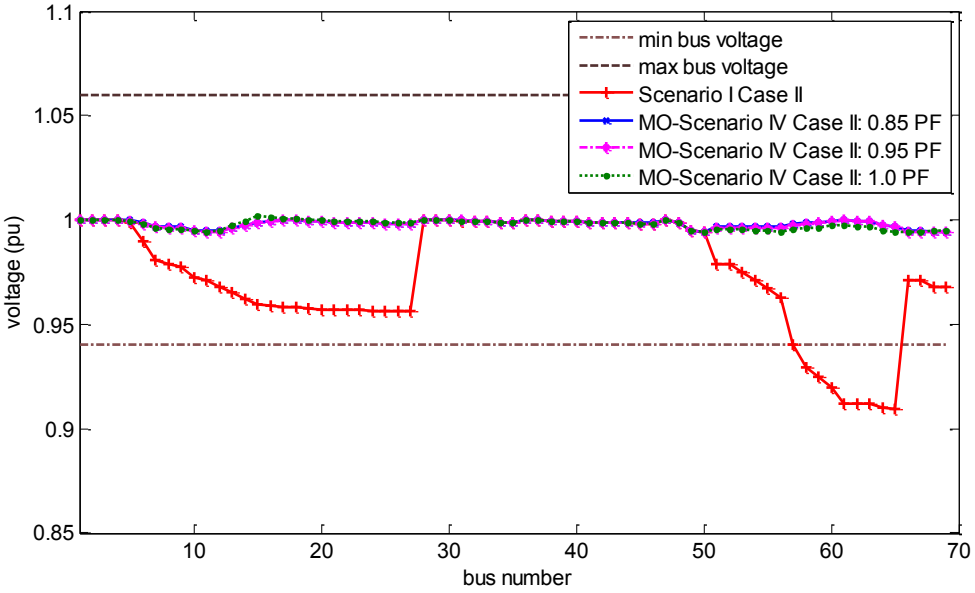

Figure 4.22: Voltage profile Scenario IV (two generators); Case II (without shunt compensation), Multi-Objective Optimisation

For Case II, the generators operate at the limit of their reactive power range. It is evident that the generators need to inject more reactive power to maintain a voltage of 1pu at the generator buses following the removal of the shunt capacitors. As with all the multi-objective optimisation studies presented above, the percentage reduction in power loss is lower than that the corresponding single objective study but with a better voltage profile. When optimising for a number of objectives, the improvement in one always leads to a worsening of another.

Table 4.14 shows the number of evaluations of the objective function for the final attained optimal solutions.

Table 4.14: ALGORITHM COMPUTATIONAL BURDEN; SCENARIO III, MULTI-OBJECTIVE OPTIMISATION

	PSO –W Case I			PSO –W Case II		
Minimum power factor	0.85	0.95	1.0	0.85	0.95	1.0
Average no. of steps	628.2	738.6	673.	635.8	825.8	584.2
No. of function evaluations per step	20	20	20	20	20	20
No. of function evaluations	12564	14772	13460	12716	16516	11684

Similar to the study presented in section 4.3, the best results are obtained when shunt capacitors are employed as compensation devices together with DG to provide reactive power support for the network. This allows the generator sizing and placement to be optimised for the best overall voltage support and loss reduction. The real power loss reduction chart for the best test cases for all the studied scenarios are shown in Figure 4.23. The overall best of loss reduction from the chart also correspond with the best case of voltage support. This is obtained with scenario IV/Case I for the multi-objective optimisation.

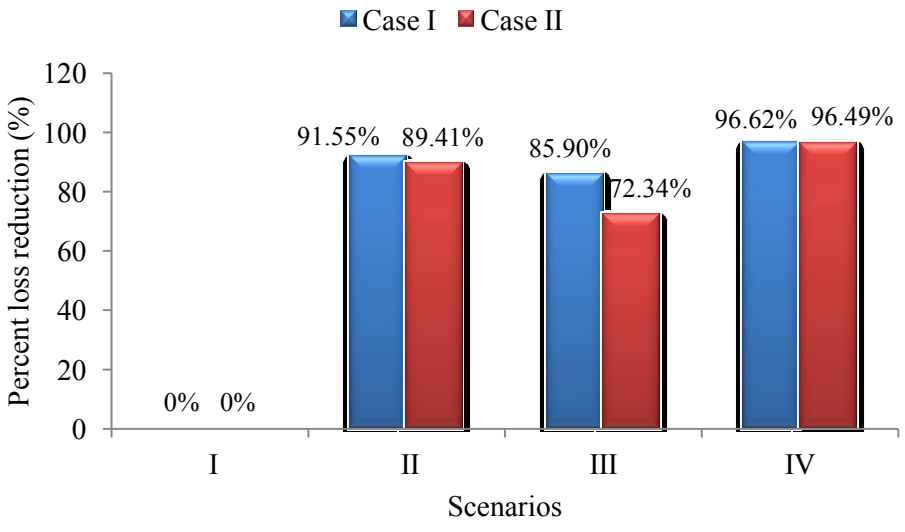

Figure 4.23: Real power loss reduction chart

Figure 4.24 presents the best SSEV values for all the studied scenarios. The best of voltage support with a calculated SSEV value of 2.990×10^{-4} was obtained with two optimally size and located generators in a compensated network (scenario IV/Case I). The best of mean voltage values for all the scenarios are presented in Figure 4.25. Not

surprisingly, the best values of mean voltage (0.9983pu) and standard deviation (0.00167) are also obtained with scenario IV/Case I.

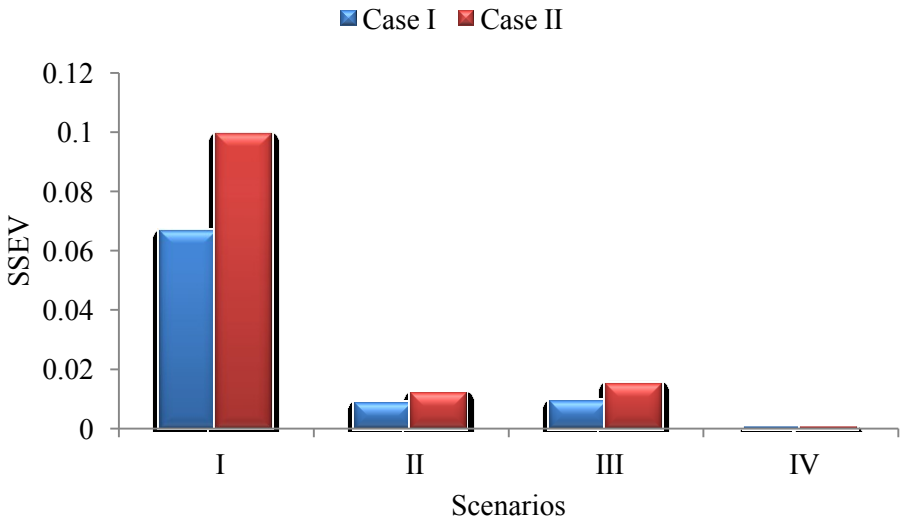

Figure 4.24: SSEV values

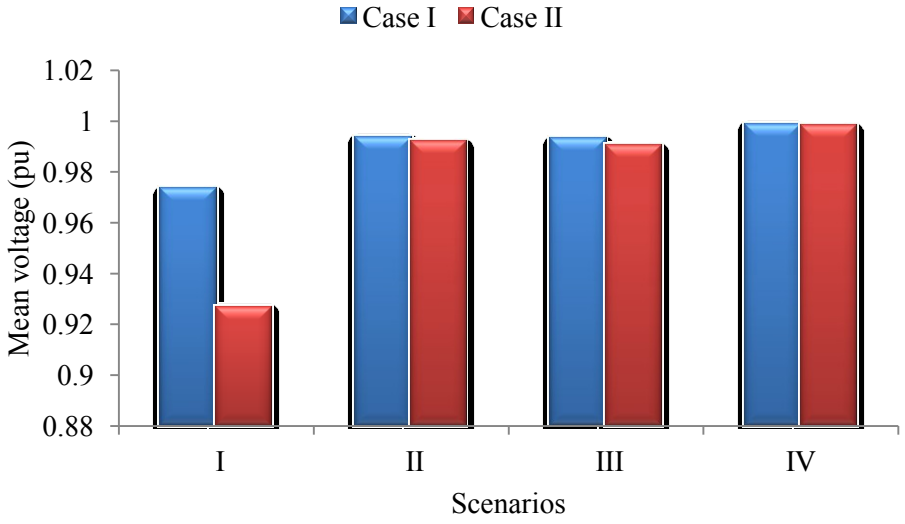

Figure 4.25: Best mean voltage values

4.5 Summary

In this chapter, a PSO-W algorithm was used to optimize the integration of DG into a 69-bus radial distribution network (with and without shunt capacitor compensation). The power loss within the circuit is minimised with the generator modelled as a PV node to inject reactive power into the generator node considering different minimum operating power factors (lagging). The improvement in network voltage profile is assessed by calculating the sum of the squares of the nodal voltage deviations from 1pu.

Four different scenarios were considered: the first was the base network with no DG. The second was to find the optimal size/location of a single DG integrated into the network. The third was also with a single DG connected to the bus number with minimum voltage. The fourth scenario was to find the optimal sizes and locations of two DG connected to the network. In all scenarios, two cases were considered, Case I for operation with reactive power compensating capacitors (compensated network) and Case II with the compensation capacitors removed.

The study was carried out in two phases. The first considered a single objective optimisation study where the sole objective is to minimise the network overall power loss. In the second phase, a multi-objective optimisation study was presented where the voltage profile of the network was considered as part of the optimisation cost function in addition to the network power loss.

The best improvement in network loss reduction and voltage support was obtained with two generators integrated into the compensated network. Nevertheless, good results in terms of overall loss reduction and voltage profile improvement were also obtained with the compensation capacitors disconnected, as long as the generators were allowed to provide network var support. Savings in the generator size at the expense of less power loss reduction were shown to be feasible if an optimal size generator is located at the bus with the minimum voltage. The multi-objective study showed how an improvement in one of the objectives (improved voltage profile) resulted in a worsening of the other (power loss reduction).

In the chapter that follows, the proposed Multi-Search Particle Swarm Optimisation (MSPSO) algorithm is demonstrated. The MSPSO is employed for the solution of optimal location and size of DG, using the same network scenarios to allow for direct comparisons.

CHAPTER 5

Distributed Generation Sizing and Location for Power Loss Minimisation and Voltage Support in a Compensated Network Using Multi-Search PSO

The values of the optimal DG sizes obtained from the simulation study of chapter 4 are continuous values that cannot be obtained in real practical applications. Typically, these will be rounded to the nearest standard sizes DG. In some of the reviewed literatures [42, 44, 45], generator sizes with a fixed step value are used to partially fulfil the discrete constraint imposed by the actual size of DG units. For example, the values can be in multiples of 100; (i.e. 100, 200, 300… etc.), or multiples of 50; (i.e. 100, 150, 200, 250, 300… etc.). The solutions thus attained will not be the best possible choices as some actual generator sizes will be left out of the search space. DG units are commercially available in discrete sizes with varying step sizes that are not fixed. This and the discrete integer nature of some of the parameters in the distribution network (i.e. busbar location numbers) make the DG optimisation problem a mixed search space problem requiring a multi-search optimisation algorithm.

In order to address these issues, this chapter proposes a Multi-Search PSO (MSPSO) algorithm, especially suited for the solution of mixed-spaced DG sizing and location optimisation problems in a shunt compensated distribution network. The proposed algorithm treats the generator sizes as real discrete variables with uneven step sizes that reflect the sizes of commercially available generators. The proposed MSPSO algorithm can handle a multi-search space of integer (generator location); discrete (generator sizes) and continuous (reactive power output) variables while substantially reducing the search space and consequently the computational burden of the optimisation problem.

The validity of the algorithm is tested on the standard 69-bus benchmark distribution network, and the results are compared with those obtained in chapter 4 using the standard PSO-W algorithm. The MSPSO algorithm is shown to be effective in finding the optimal or near-optimal solution to the problem at a fraction of the computational cost associated with other PSO algorithms (PSO-W and SPPSO) and is a reliable tool capable of solving complex multivariable nonlinear optimisation problems.

5.1 Applying the MSPSO algorithm for optimal DG Sizing and Location Problems

In order to check the validity of the results of the MSPSO algorithm and allow comparisons with previously published works and the study in chapter 4, the algorithm is tested on the same standard benchmarking network (69-bus RDN), and the same network scenarios used in Chapter 4. The network data is re-presented and summarized in Table 5.1 for convenience. The network is compensated with shunt capacitors of 0.3 Mvar each at the bus locations 15, 61, 63 and 65. The substation voltage is taken as 1.0pu, and the voltage profile of the network is shown in Figure 5.1.

The implementation flow chart and procedural steps of the MSPSO algorithm were presented in section 3.5.3. Now consider a solution vector **X** in D dimensional space $\mathbf{X}_i = (x_{i1}, x_{i2}, \ldots. x_{iD})$. In general, for a three-dimensional single distributed generator placement problem, x_{i1}, x_{i2}, x_{i3} represent generator location, generator output power and injected vars, respectively. The integration of two generators will involve six dimensions in the candidate or the particle solution expressed as $\mathbf{X}_i = (x_{i1}, x_{i2}, x_{i3}\, x_{i4,}\, x_{i5,}\, x_{i6})$. Where the two generators' locations are defined by x_{i1}, x_{i2}, (integer variables), $x_{i3,}\, x_{i4}$ are the generators' sizes /output power (discrete variables) and $x_{i5,}\, x_{i6}$ are the reactive power outputs *(*vars) related to the two generators (continuous variables). The integration of one generator with one shunt capacitor, will involve five dimensions in the candidate, or the particle solution expressed as $\mathbf{X}_i = (x_{i1}, x_{i2}, x_{i3}\, x_{i4,}\, x_{i5})$. The bus locations for the generator and capacitor are described by x_{i1}, x_{i2} (integer variables), $x_{i3}$is the generator output power (discrete variable), x_{i4} is the vars related to the generator (continuous variable) and x_{i5} is the vars for the shunt capacitor (discrete variable).

The expressions in (3.9) - (3.11) are used to handle the integer nature of the DG bus number locations. The variable representing DG sizes/output power are initially treated as continuous variables using Equations (3.1) and (3.2) to update the corresponding position and velocity vectors. The dichotomy algorithm (Equations (3.12) – (3.15)) is then used to constrain the continuous variable (the active power output of the generator) into a discrete variable chosen from unevenly spaced entries in a pre-defined finite search list.

The predefined finite search list represents practical, commercially available DG sizes in the range 0 MW-5 MW, with a size of zero corresponds to a network with no DG (see Appendix A, Table A.2 for a complete list of generator sizes considered in this

study). This ability of the MSPSO to search unevenly spaced discrete spaces avoids the loss of accuracy in the results of the optimisation process obtained by other methods and algorithms that consider evenly spaced discrete values, missing out on potential optimum or near optimum solutions. The mix of different variable types to form one single particle is possible because the PSO algorithm operates independently in each dimension.

The implementation flowchart of the MSPSO algorithm was presented in section 3.5.3 and is again repeated here for convenience (Figure 5.2).

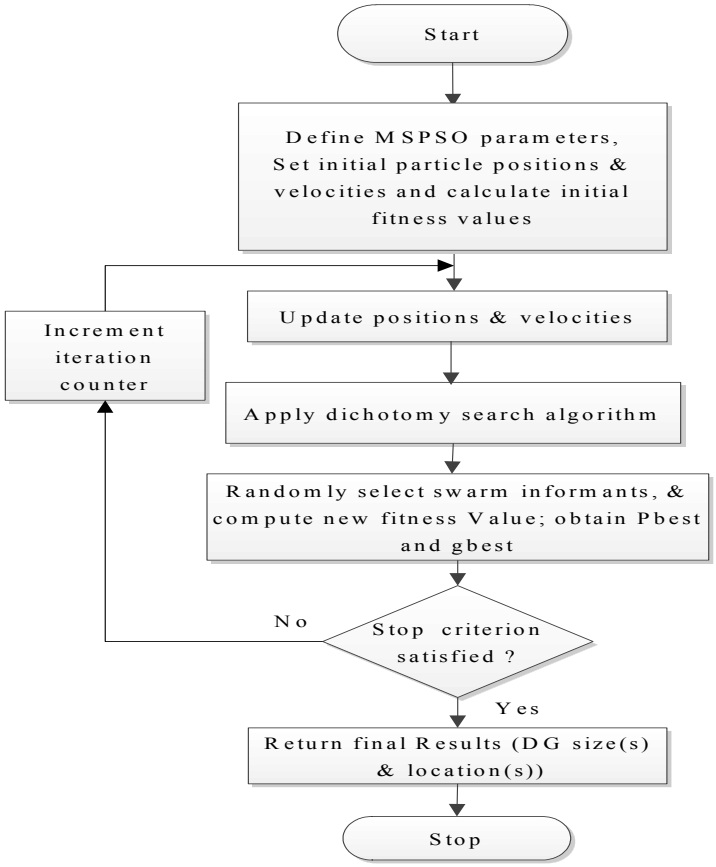

Figure 5.1: Multi-Search PSO (MSPSO) implementation flow chart

MSPSO results are recorded after ten independent runs of the algorithm using a swarm population of 20 particles (with five informants) and a stopping criteria of 50 iterations where the objective function value remains within the margin of 10^{-9} or a maximum number of 1000 iterations. The social and the cognitive constants $c_1$and c_2 are both assigned a value of 1.47 [77]. For the 69-bus network, values of M=70, α=0.4 , w_{max}=0.9 and w_{min} =0.4 [87] are used. The MSPSO has one more parameter (α: a constant that controls the probabilities of generating discrete integer variables) to tune compared with the PSO-W. With the exclusion of this parameter, the other parameters setting used here are the same parameters setting used in chapter 4.

5.2 Loss Minimisation and Voltage Support Using MSPSO; Single Objective Optimisation

In this section, the same scenarios studied previously in section 4.3 are investigated using the proposed MSPSO algorithm.

5.2.1 Scenario I: base network with no generation

The results of this base case network are in common with the results of Table 4.1 and Figure 4.2 of section 4.3.1 and are represented here for conveniences (Table 5.1 and Figure 5.2).

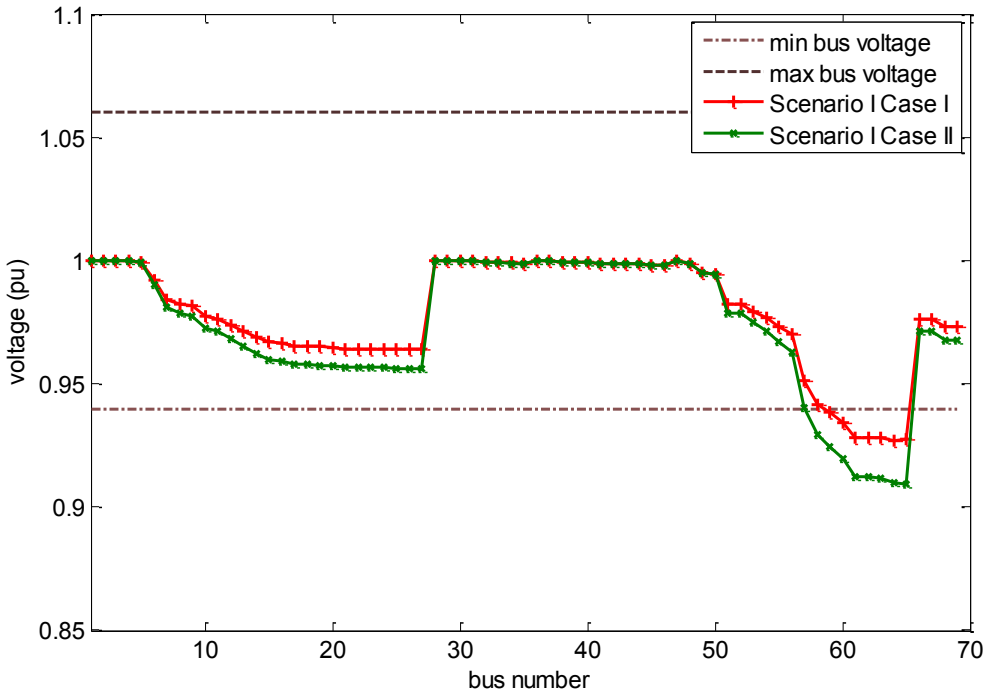

Figure 5.2: Voltage profile of the 69-bus radial distribution network Scenario I (no generation); Case I (with shunt compensation) and Case II (no compensation)

Table 5.1: SUMMARY OF RESULTS; SCENARIO I WITH NO GENERATION (BASE NETWORK)

Test Cases	Σ Load (MW)	Σ Load (Mvar)	Σ MW Loss	Maximum bus voltage (pu)	Minimum bus voltage (pu)	SSEV Index
Case I	3.802	2.690	0.1531	1.0	0.927	0.0665
Case II	3.802	2.690	0.2249	1.0	0.909	0.0993

5.2.2 Scenario II: single generator

The optimum size/location results for a single generator using the MSPSO algorithm are summarized in Table 5.2. The improvement obtained with the network voltage profiles are shown in Figures 5.3 and 5.4. The required number of function evaluations computed for ten independent runs of the MSPSO is shown in Table 5.3.

The best loss reduction and enhanced voltage support for Case I is obtained with one optimally sized (1.84MW) and located generator injecting 0.33Mvars at bus number 61 (generator operating with a minimum lagging power factor of 0.85) where a shunt capacitor of 0.3Mvar is already installed. The generator can maintain a fixed voltage of 1pu at its bus location number 61, operating at a power factor greater than the minimum allowed 0.85 lagging. A 91.69% power loss reduction is achieved compared with the base case network, with a minimum voltage deviation of -0.0236 at bus number 27.

Table 5.2: DG SIZE AND LOCATION FOR SCENARIO II (SINGLE GENERATOR)

	Case I			**Case II**		
Minimum possible PF	0.85	0.95	1.0	0.85	0.95	1.0
Optimal bus	61	61	61	61	61	61
DG output MW/Mvar	1.84/0.33	1.84/0.33	1.84/0.0	1.85/1.15	2.0/0.66	1.85/0.0
Actual operating PF	0.98	0.98	1.0	0.85	0.95	1.0
Max. Voltage	1.0000 pu	1.0000 pu	1.0000 pu	1.0000 pu	1.0000pu	1.0000 pu
Min. Voltage	0.9764 pu	0.9764 pu	0.9754 pu	0.9722 pu	0.9714 pu	0.9682 pu
Mean (pu)	0.9927	0.9927	0.9916	0.9912 pu	0.9906 pu	0.9872 pu
Std. Dev	0.008605	0.008605	0.008714	0.01008	0.01024	0.01161
Total power loss [MW]	0.0187	0.0187	0.0229	0.0238	0.0383	0.0831
Percent loss reduction	91.69%	91.69%	89.82%	89.35%	82.91%	63.02%
SSEV index	0.008698	0.008698	0.009975	0.01007	0.013264	0.020427

The results are similar to but slightly different from those obtained in section 4.3.2 using the PSO-W algorithm where the best loss reduction and enhanced voltage support

in Case I is obtained with one optimally sized (1.8308MW) and located generator injecting 0.35Mvars at bus number 61 (generator operating with a minimum lagging power factor of 0.85). Both algorithms obtain the same optimal locations, however, the optimal DG size obtained with PSO-W is a continuous value that do not necessarily reflect the size of practical commercially available DG units in contrast to the MSPSO algorithm. However, similar to the PSO-W, the optimisation results obtained for operating with a minimum lagging power factor of 0.85 or 0.95 (in Case I) are also the same due to the fact that the network is already compensated and therefore, the generator needs to inject less reactive power than its maximum capability to maintain the bus voltage at 1pu. From Table 5.2, the calculated actual PF of the generator shows that the generator operates above 0.95 lagging hence it does not make any difference whether the minimum PF is 0.85 or 0.95 the results will be identical in both cases.

Table 5.2 also presents the results of the MSPSO optimisation process when the shunt capacitors are removed (Case II). In this case as expected, the operating PF of the generator drop to the minimum lagging value of 0.85 PF or 0.95 PF. Hence the results with 0.85 minmum PF and 0.95 minmum PF are different (as shown in Table 5.2). The best loss reduction for Case II shows that the generator injects 1.85MW and 1.15Mvars at bus 61 giving an 89.35% power loss reduction compared with the base case network. A minimum voltage deviation of -0.0278 is obtained at bus number 26. The voltages at the generator bus deviated from 1pu as a result of the constraint placed on the generator's ability to produce reactive power. The lowest power loss reduction (63.02%) is found with Case II, when the generator is not injecting reactive power into the network (unity PF operation).

The corresponding results obtained with PSO-W (section 4.3.2) show that, the best loss reduction and enhanced voltage support for Case II is also achieved with one optimally sized (1.8909MW) and located generator injecting 1.17Mvars at bus number 61 (generator operating with a minimum lagging power factor of 0.85). An 89.41% power loss reduction was achieved compared with the base case network. Both algorithms obtained the same optimal locations, but the optimal DG sizes and the computed percent loss reductions differ slightly.

The PSO-W shows a higher percentage real power loss reduction (89.41%). However, since the optimal DG size obtained with PSO-W is a continuous value that does not reflect the size of commercially available DG units; this percentage reduction is not realistic and the rounding up process to the next available generator size will naturally

affect the accuracy of the results obtained by the PSO-W algorithm. Thus, the PSO-W algorithm solutions can sometimes result in the overestimation of the percent power loss reduction in the network.

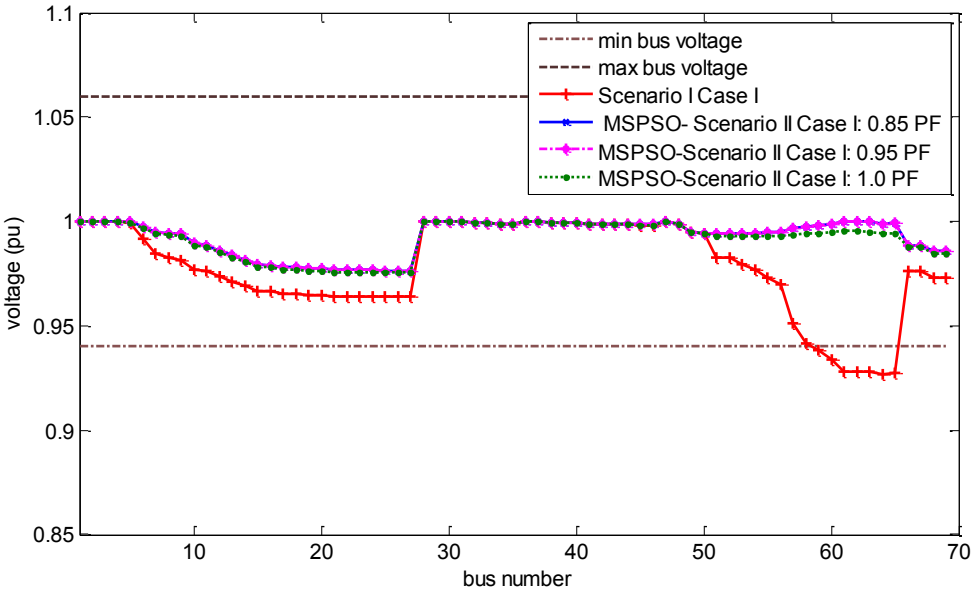

Figure 5.3: Voltage profile Scenario II (single generator); Case I (with shunt compensation)

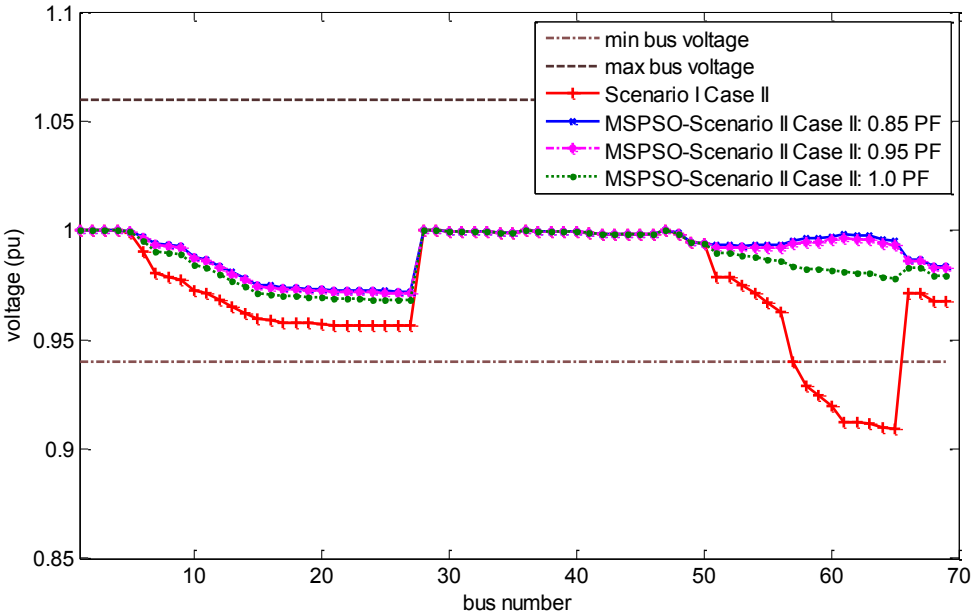

Figure 5.4: Voltage profile Scenario II (single generator); Case II (without shunt compensation)

The improvement in the network voltage profile quantified by the SSEV shows that the best voltage support is obtained from Case I, with a calculated SSEV of 0.008698. The removal of the capacitors (Case II) resulted in a higher value of SSEV at 0.01007. Again, these are slightly different from the corresponding SSEV values presented in section 4.3.2.

The MSPSO convergence to the optimal solution is as shown in Figures 5.5 and 5.6. The best (smallest) objective function is obtained with the generator operating at a minimum power factor of 0.85 lagging (Figures 5.5 and 5.6). Tables 5.3 and 5.4 show that fewer numbers of evaluations of the objective function are required to attain a final solution with MSPSO compared with the PSO-W algorithm. The results are based on average values with ten independent runs of the algorithms. From both Tables, it is evident that the MSPSO algorithm has the advantage of fewer function evaluations compared with the PSO-W algorithm.

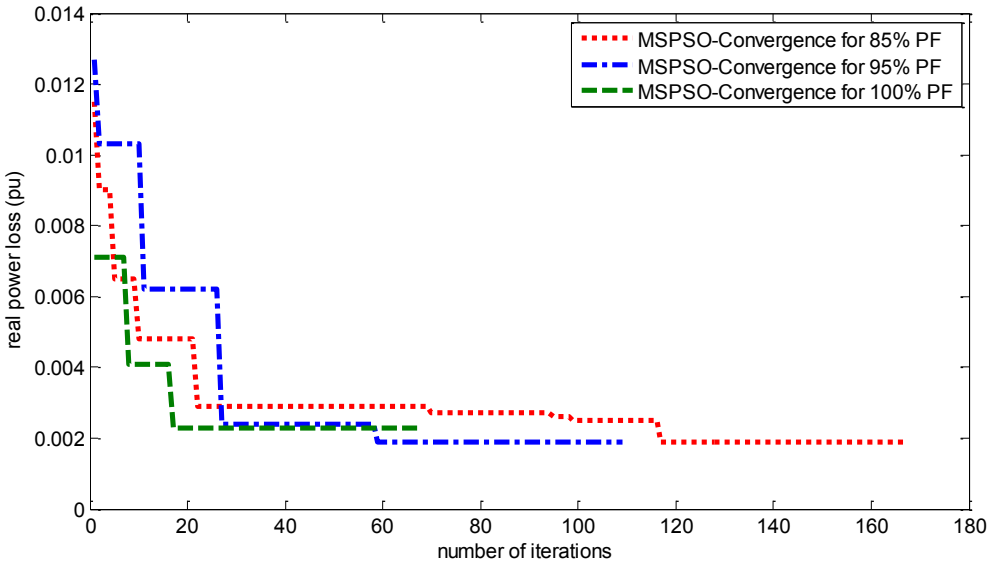

Figure 5.5: Convergence characteristic of MSPSO (Scenario II Case I)

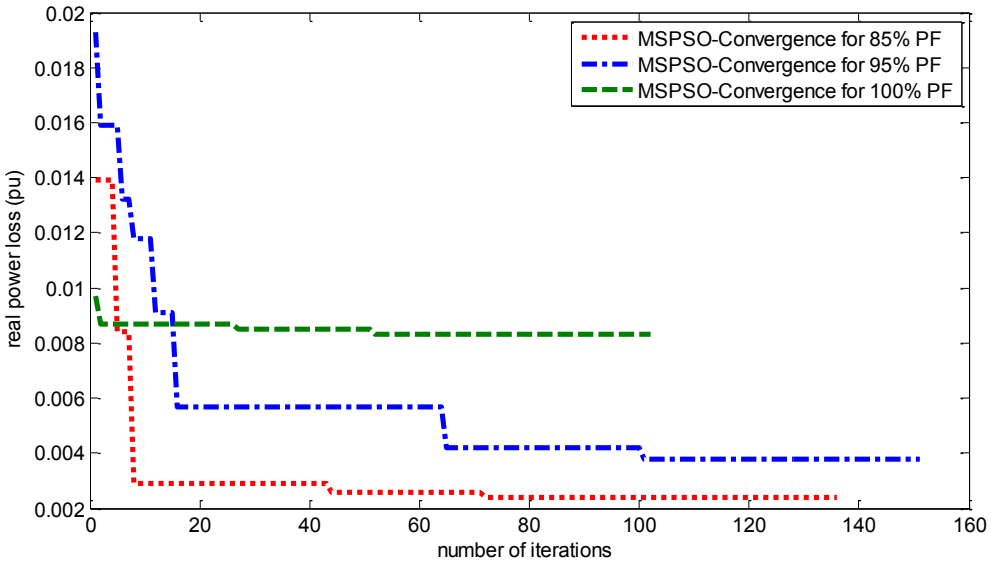

Figure 5.6: Convergence characteristic of MSPSO (Scenario II Case II)

The required number of function evaluations for the smallest objective cost function (at minimum PF of 0.85 lagging) is reduced by 95.34% and 94.76% for Case I and Case II, respectively, compared with the PSO-W algorithm. The discrete nature of the search space means quicker solution with fewer iterations due to the reduced size of the search space without loss of accuracy in the obtained solution.

Table 5.3: COMPARISION OF ALGORITHMS COMPUTATIONAL BURDEN; SCENARIO II, CASE I (SINGLE GENERATOR)

	MSPSO Case I			PSO-W Case I		
Minimum power factor	0.85	0.95	1.0	0.85	0.95	1.0
Average no. of steps	90.2	117.2	102.4	483.6	384.2	327.8
No. of function evaluations per step	5	5	5	20	20	20
No. of function evaluations	451	586	512	9672	7684	6556

Table 5.4: COMPARISION OF ALGORITHMS COMPUTATIONAL BURDEN; SCENARIO II, CASE II (SINGLE GENERATOR)

	MSPSO Case II			PSO-W Case II		
Minimum power factor	0.85	0.95	1.0	0.85	0.95	1.0
Average no. of steps	104	144.2	113.2	496	329.6	283.8
No. of function evaluations per step	5	5	5	20	20	20
No. of function evaluations	520	721	566	9920	6592	5676

5.2.3 Scenario III: single generator installed at the minimum voltage bus

The results of the MSPSO optimisation process for this scenario are summarized in Table 5.5. The improved network voltage profiles shown in Figures 5.7 and 5.8. When the generator is connected with bus number 64 (the minimum voltage bus for Case I), the best optimal size of the generator is calculated at 1.6MW injecting an additional 0.29Mvar into the network. A power loss reduction of 85.99% is achieved compared with the base network.

The corresponding results using PSO-W (section 4.3.3) show that the best loss reduction and enhanced voltage support is obtained with one optimally sized (1.6053MW) and located generator injecting 0.28Mvars at bus number 64.When the generator is connected at bus number 65 (the minimum voltage bus for Case II), the best optimal size of the generator is calculated at 1.42MW injecting 0.88Mvar into the

network. A power loss reduction of 72.28% compared to the base network is achieved. The best of voltage support with a calculated SSEV of 0.010846 is obtained for Case I. The removal of the capacitors (Case II) resulted in higher SSEV values.

Table 5.5: DG SIZE AND LOCATION FOR SCENARIO III (ONE GENERATOR INSTALLED AT THE MINIMUM VOLTAGE BUS)

	Case I			**Case II**		
Minimum possible PF	0.85	0.95	1.0	0.85	0.95	1.0
Optimal bus	64	64	64	65	65	65
DG output MW/Mvar	1.60/0.29	1.60/0.29	1.60/0.0	1.42/0.88	1.60/0.53	1.42/0.0
Actual oper-ating PF	0.98	0.98	1.0	0.85	0.95	1.0
Max. Voltage	1.0000 pu	1.0000 pu	1.0000 pu	1.0000 pu	1.0000pu	1.0000 pu
Min. Voltage	0.9748 pu	0.9748 pu	0.9739 pu	0.9685 pu	0.9684 pu	0.9652pu
Mean	0.9912 pu	0.9912 pu	0.9902 pu	0.9877 pu	0.9877 pu	0.9845 pu
Std. Dev	0.009000	0.009000	0.009284	0.01157	0.01157	0.01379
Total power loss [MW]	0.0315	0.0315	0.0348	0.0623	0.0742	0.1120
Percent loss reduction	85.99%	85.99%	84.53%	72.29%	66.99%	50.18%
SSEV index	0.010846	0.010846	0.012429	0.019604	0.019542	0.029584

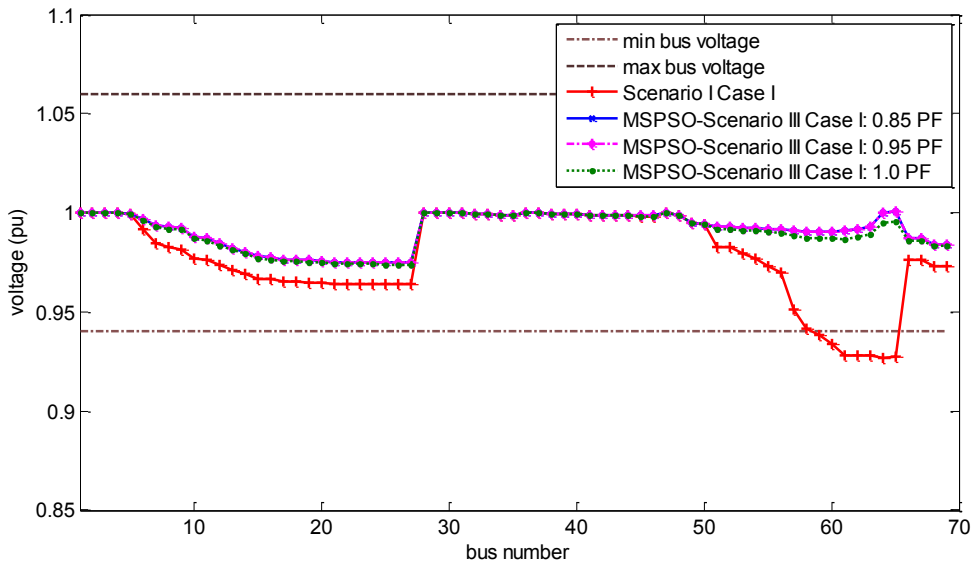

Figure 5.7: Voltage profile Scenario III (single generator at minimum voltage bus); Case I (with shunt compensation)

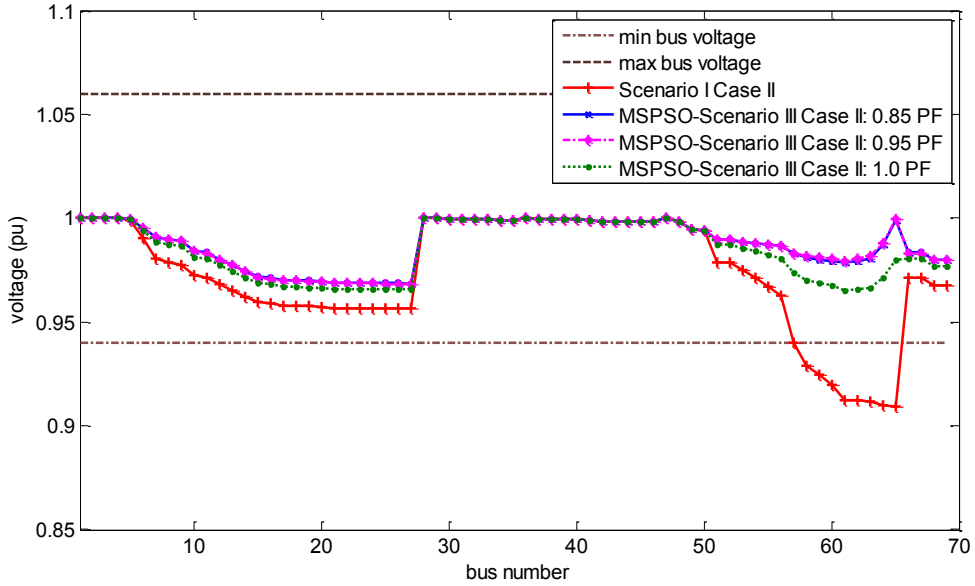

Figure 5.8: Voltage profile Scenario III (single generator at minimum voltage bus); Case II (without shunt compensation)

The results of a similar scenario in section 4.3.3 with PSO-W show that, the best loss reduction and enhanced voltage support for Case II is obtained with one optimally sized (1.4385MW) and located generator injecting 0.89Mvars at bus number 65. The optimum generator size and SSEV values obtained with both algorithms differ very slightly.

Tables 5.6 and 5.7 show that fewer numbers of evaluations of the objective function are required to attain a final solution with MSPSO compared with the PSO-W algorithm.

The results are again based on the average values after ten independent runs of the algorithms. The best optimal solution is obtained with an average value of 295 evaluations of the objective function in Case I. While an average value of 307 evaluations of the objective function is required for the best optimal solution in Case II.

The corresponding PSO-W results presented in section 4.3.3 and repeated here in Tables 5.6 and 5.7 for comparison purposes show that the best optimal solution is obtained with an average value of 6800 evaluations of the objective function in Case I and 10444 evaluations in Case II. This represents a reduction of 95.66% (Case I) and 97.06% (Case II) in the required numbers of function evaluations compared with the PSO-W algorithm.

Table 5.6: COMPARISION OF ALGORITHMS COMPUTATIONAL BURDEN: SCENARIO III, CASE I (SINGLE GENERATOR AT MINIMUM VOLTAGE BUS)

	MSPSO Case I			PSO-W Case I		
Minimum power factor	0.85	0.95	1.0	0.85	0.95	1.0
Average no. of steps	59	56.2	55.5	522.2	342.8	291
No. of function evaluations per step	5	5	5	20	20	20
No. of function evaluations	295	281	276	6800	6856	5820

Table 5.7: COMPARISION OF ALGORITHMS COMPUTATIONAL BURDEN: SCENARIO III, CASE II (SINGLE GENERATOR AT MINIMUM VOLTAGE BUS)

	MSPSO Case II			PSO-W Case II		
Minimum power factor	0.85	0.95	1.0	0.85	0.95	1.0
Average no. of steps	61.4	54.2	52.8	522.2	278	250.4
No. of function evaluations per step	5	5	5	20	20	20
No. of function evaluations	307	271	264	10444	5560	5008

5.2.4 Scenario IV: two generators

This scenario involved finding the optimal location and size for two generators operating with different reactive power output capabilities, first in the presence of shunt compensation capacitors (Case I) and with the shunt compensation capacitors removed (Case II).

The results of the MSPSO optimisation process for this scenario are presented in Table 5.8. The improvement in network voltage profile is shown in Figures 4.9 and 4.10 for

Case I and Case II, respectively. The best loss reduction is obtained with two optimally sized (1.75MW and 0.53MW) generators (Case I) injecting additional 0.31Mvars and 0.08Mvars located at bus number 61 and bus number 17, respectively. A 96.62% power loss reduction is achieved compared with the base case network.

The results presented in section 4.3.2 with PSO-W show that, the best solution was obtained with 1.7384MW injecting 0.34Mvar at bus 61 and 0.5276MW injecting 0.08Mvar at bus 17 for Case I. A 96.62% power loss reduction compared with the base case network was also achieved.

Table 5.8: DG SIZE AND LOCATION FOR SCENARIO IV (TWO GENERATORS)

	Case I			**Case II**		
Minimum possible PF	0.85	0.95	1.0	0.85	0.95	1.0
Optimal bus 1	61	61	61	61	61	61
DG 1 output MW/Mvar	1.75/0.31	1.75/0.31	1.75/0.0	1.8/1.11	1.9/0.64	1.8/0.0
Actual operating PF 1	0.99	0.99	1.0	0.85	0.85	1.0
Optimal bus 2	17	17	17	17	17	17
DG 2 output MW/Mvar	0.53/0.08	0.536/0.08	0.52/0.0	0.5/0. 31	0.576/0.19	0.536/0.0
Actual operating PF 2	0.99	0.99	1.0	0.85	0.95	1.0
Max. voltage	1.0000 pu	1.0000 pu	1.0000 pu	1.0000 pu	1.0000pu	1.0000 pu
Min. voltage	0.9943 pu	0.9943 pu	0.9929 pu	0.9930 pu	0.9943 pu	0.9930 pu
Mean (pu)	0.9983 pu	0.9983 pu	0.9968 pu	0.9969pu	0.9983 pu	0.9969 pu
Std. Dev	0.001684	0.001679	0.002303	0.002238	0.001679	0.002238
Total power loss [MW]	0.0076	0.0076	0.0120	0.0080	0.0235	0.0716
Percent loss reduction	96.62%	96.62%	94.66%	96.45%	89.55%	68.15%
SSEV index	0.000387	0.000387	0.001001	0.000589	0.000895	0.00576

The results for both algorithms are not an exact match, but produced the same percent power loss reduction. This is because the optimal continuous value generator size obtained with PSO-W is very close to the available realistic generator size.

The results of the optimisation process when the compensating shunt capacitors are removed (Case II) are also presented in Table 5.8. The best results for this case show the generators to inject 1.80MW/1.11Mvars at bus number 61 and 0.5MW/0.31Mvars at bus number 17, reducing power loss compared with the base network by 96.45%. The best of voltage support with a calculated SSEV of 0.000387 is obtained by Case I.

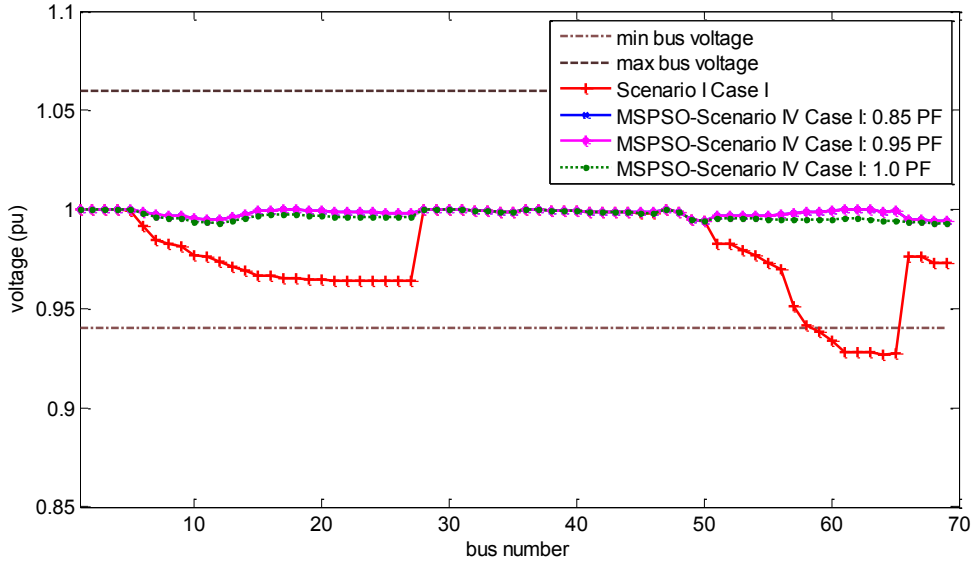

Figure 5.9: Voltage profile Scenario IV (two generators); Case I (with shunt compensation)

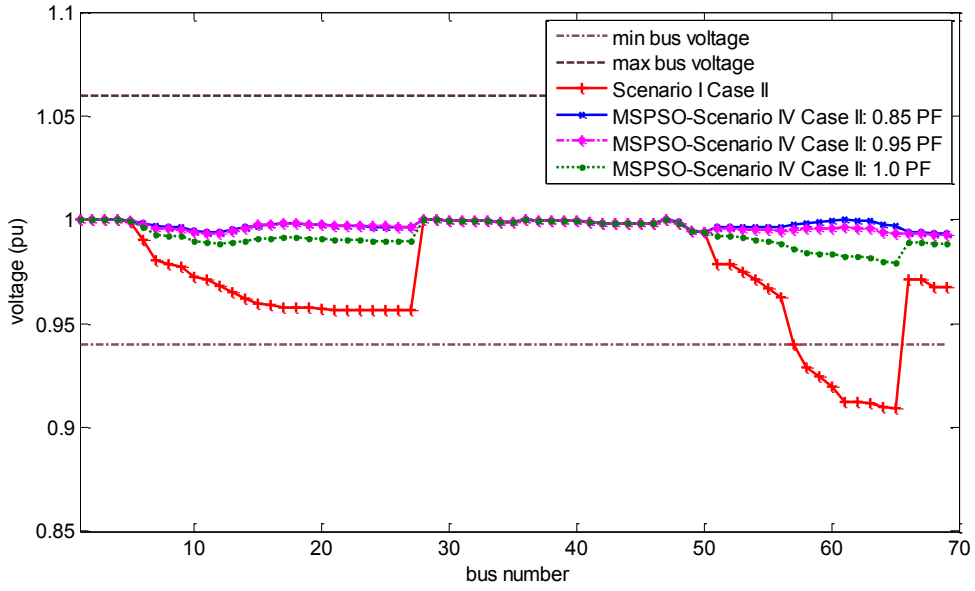

Figure 5.10: Voltage profile Scenario VI (two generators); Case II (without shunt compensation)

The removal of the capacitors (Case II) resulted in higher values of SSEV. The results obtained with PSO-W (section 4.3.4) for Case II show that the best optimal pair of generators was obtained as 1.7928MW injecting 1.11Mvar at bus 61 and 0.535MW injecting 0.33Mvar at bus 17. A 96.45% power loss reduction compared with the base case network was again achieved. Similar to Case I results of both algorithms produced the same percent power loss reduction.

Tables 5.9 and 5.10 shows the numbers of evaluations of the objective function for the final attained optimal solutions with both algorithms. The results are also based on the average values after ten independent executions of the algorithms. It is evident from the Tables 5.9 and 5.10 that the MSPSO algorithm is faster with a smaller computational burden compared with PSO-W algorithm. The required number of function evaluations for the smallest objective cost function (at minimum PF of 0.85 lagging) is reduced by 95.46% and 96.35%, respectively, for Case I and Case II compared with the PSO-W algorithm for this scenario.

Table 5.9: COMPARISON OF ALGORITHMS COMPUTATIONAL BURDEN: SCENARIO IV, CASE I (TWO GENERATORS)

	MSPSO Case I			PSO-W Case I		
Minimum power factor	0.85	0.95	1.0	0.85	0.95	1.0
Average no. of steps	146.8	118.8	108	807.6	806.9	751.2
No. of function evaluations per step	5	5	5	20	20	20
No. of function evaluations	734	594	540	16152	16138	15024

Table 5.10: COMPARISON OF ALGORITHMS COMPUTATIONAL BURDEN: SCENARIO IV, CASE II (TWO GENERATORS)

	MSPSO Case II			PSO-W Case II		
Minimum power factor	0.85	0.95	1.0	0.85	0.95	1.0
Average no. of steps	122.4	100.6	138	839.2	753.8	613.2
No. of function evaluations per step	5	5	5	20	20	20
No. of function evaluations	612	503	690	16784	15076	12264

In conclusion, the best results are obtained when shunt capacitors are employed as compensation devices with DG to provide reactive power support for the network. Increasing the penetration level of DG and permitting voltage regulation at its bus

location resulted in the significant improvements in both loss reduction and voltage profile in contrast to a single DG deployment.

The real power loss reduction chart for the best test cases for all the studied scenarios and cases are shown Figure 5.11. Similar to the investigation in section 4.3, the best loss reduction is obtained with scenario IV/Case I i.e. when two generators are allowed to operate in a compensated network. Figure 5.12 presents the best of SSEV values for all the studied scenarios. Again the best voltage support with a calculated SSEV of 3.870×10^{-4} was obtained with two optimally size and located generators with the connection of the reactive power compensation capacitors (scenario IV, Case I).

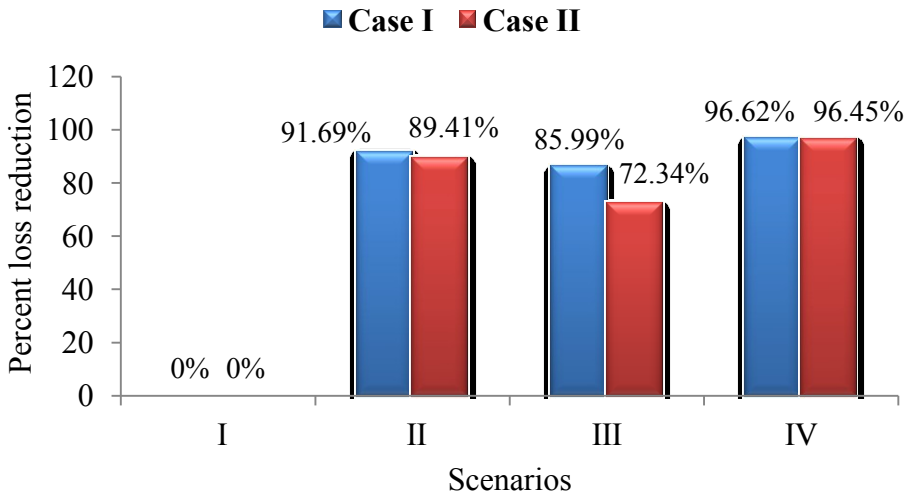

Figure 5.11: Real power loss reduction chart; MSPSO results

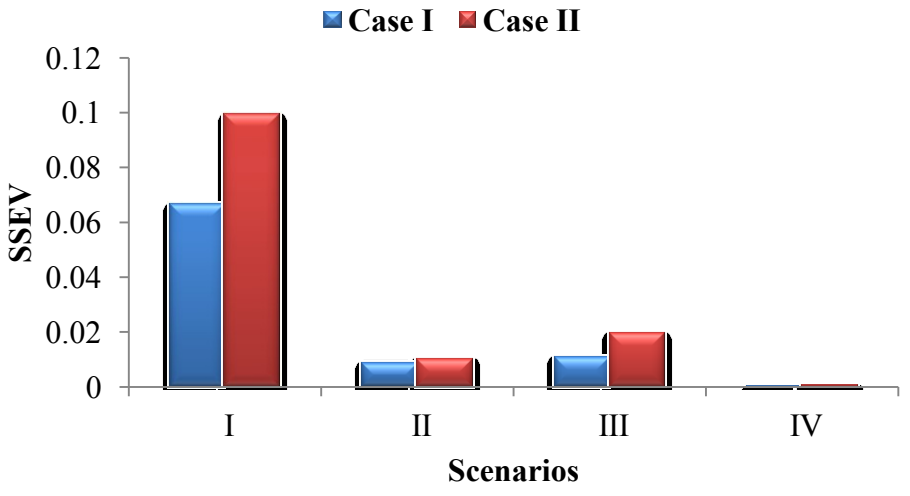

Figure 5.12: SSEV values; MSPSO results

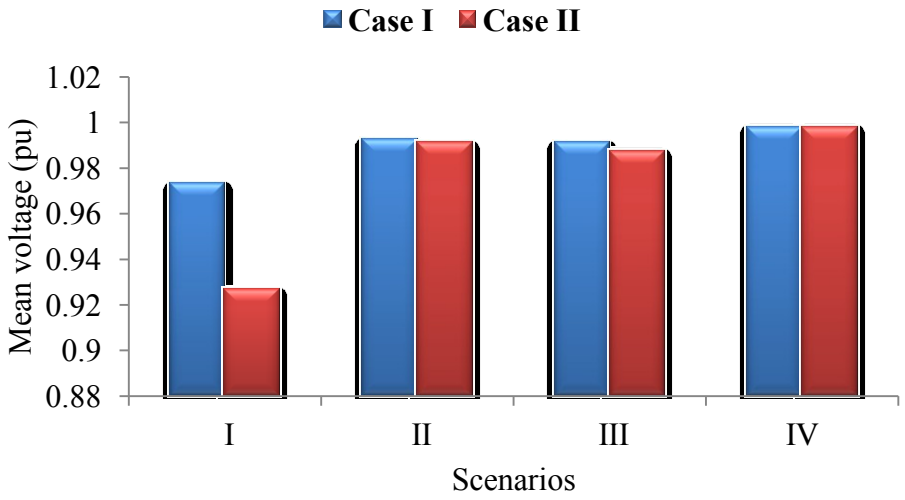

Figure 5.13: Best of mean voltage values; MSPSO results

The best value of the mean voltage (0.9983pu) and the voltage standard deviation (0.00168) are also obtained with scenario IV, Case I (Figure 5.13).

Finally, a summary of comparison of the best of optimal DG size and location results using PSO-W and the MSPSO are presented in Tables 5.11 and 5.12. It is evident that both algorithms obtained the same optimal locations with small variations in the optimal generator sizes. The optimal DG sizes obtained with PSO-W are continuous values that may not reflect the size of practical commercially available DG units. The MSPSO algorithm, on the other hand, uses a pre-defined list of commercially available generator sizes (see appendix A, Table A.2) to define the discrete DG size variable. Thus, its results reflect the practical commercial available DG units. The computed percent loss reductions are found to be practically the same, especially when the continuous optimal DG value obtained with PSO-W is not far from the available realistic generator size. The MSPSO algorithm has the advantage of the lower computational burden due to fewer function evaluations compared with the PSO-W. This accomplishd with the use of fewer particles in the computation of the cost function.

The summary of the MSPSO algorithm computational burden evaluated and compared with the PSO-W algorithm from Tables 5.11 and 5.12 clearly show the advantage of the former. In case I, the required number of function evaluations is reduced by 95.34%, 95.66%, and 95.46% for scenarios II, III and IV, respectively, compared with the PSO-W algorithm.

Table 5.11: SINGLE OBJECTIVE; COMPARISON OF PSO-W AND MSPSO OPTIMAL DG SIZE AND LOCATION RESULTS (CASE I)

			Optimal bus location(s)	Optimum DG size (s) (MW/Mvar)	Power loss reduction (%)	SSEV	No. of function evaluations
PSO-W	Scenarios	I	-	-	-	0.0665	-
		II	61	1.8308/0.35	91.69	0.00868	9672
		III	64	1.6053/0.28	85.99	0.010854	6800
		IV	61/17	1.7384/0.34; 0.5276/0.08	96.62	0.000383	16152
MSPSO	Scenarios	I	-	-	-	0.0665	-
		II	61	1.84/0.33	91.69	0.008698	586
		III	64	1.6/0.29	85.99	0.010846	307
		IV	61/17	1.75/0.31; 0.53/0.08	96.62	0.000387	734

Table 5.12: SINGLE OBJECTIVE; COMPARISON OF PSO-W AND MSPSO OPTIMAL DG SIZE AND LOCATION RESULTS (CASE II)

			Optimal bus location(s)	Optimum DG size (s) (MW/Mvar)	Power loss reduction (%)	SSEV	No. of function evaluations
PSO-W	Scenarios	I	-	-	-	0.0993	-
		II	61	1.8909/1.17	89.41	0.011849	9920
		III	65	1.4385/0.0.89	72.34	0.019188	10444
		IV	61/17	1.7928/1.11; 0.535/0.33	96.49	0.000435	16784
MSPSO	Scenarios	I	-	-	-	0.0993	-
		II	61	1.85/1.15	89.35	0.01007	520
		III	65	1.42/0.88	72.29	0.019542	295
		IV	61/17	1.80/1.11; 0.50/0.31	96.45	0.000576	612

In case II, the required number of function evaluations is reduced by 94.76%, 97.06%, and 96.35% for scenarios II, III and IV respectively, compared with the PSO-W algorithm.

5.3 Loss Minimisation and Voltage Support Using MSPSO; Multi-Objective Optimisation

In this section, the optimisation analysis presented above is repeated as a multi-objective optimisation exercise considering both the network power loss and the voltage profile in the cost function as expressed in Equation (4.7). All other network scenarios and algorithm parameters being the same as in section 5.2. The weighting factors k_1 and k_2 in (4.7) are set equal to 0.5 each. With the exclusion of the constant parameter α, the other parameters setting is the same as parameters setting used for the multi-objective optimization in section 4.4.

5.3.1 Scenario I: base network with no generation

This scenario is obviously the same study discussed in section 5.2.1. Results were presented in Table 5.1 and Figure 5.2.

5.3.2 Scenario II: single generator; multi-objective optimisation

The results of the MSPSO multi-objective optimisation process for this scenario are presented in Table 5.13. The network voltage profile for Case I and Case II are shown in Figures 5.14 and 5.15, respectively. The required number of function evaluations computed after ten independent runs with both algorithms are presented in Tables 5.14 and 5.15.

The best minimum Multi-Objective cost Function (MOF) for Case I is obtained with one optimally sized (1.8 MW) and located generator injecting 0.43Mvars at bus number 61 at 0.85 minimum lagging operating PF. A 91.60% power loss reduction is achieved compared with the base network, and a SSEV index of 0.008635 is computed. The corresponding study in section 4.4.2 with PSO-W, showed that the best minimum objective was obtained with one 1.7977 MW optimally sized and located generator injecting 0.43Mvars at bus number 61, also operating with a minimum PF of 0.85 lagging. A 91.55% power loss reduction was achieved compared with the base case network and a SSEV index of 0.008631was computed.

Thus, both algorithms obtained the same optimal location with variation in the optimal generator size. The power loss reduction with MSPSO is slightly better than that obtained with PSO-W but at the expense of the lower value of SSEV when compared with PSO-W.

Table 5.13: DG SIZE AND LOCATION FOR SCENARIO II (ONE GENERATOR); MULTI OBJECTIVE OPTIMISATION

	Case I			**Case II**		
Minimum possible PF	0.85	0.95	1.0	0.85	0.95	1.0
Optimal bus	61	61	61	61	61	61
DG output MW/Mvar	1.8/0.43	1.8/0.43	2.2/0.0	1.9/1.15	2.1/0.68	2.6/0.0
Actual oper-ating PF	0.97	0.97	1.0	0.85	0.95	1.0
Max. Voltage	1.0000 pu	1.0000 pu	1.0070 pu	1.0000 pu	1.0000pu	1.0060 pu
Min. Voltage	0.9765 pu	0.9765 pu	0.9775 pu	0.9725 pu	0.9721 pu	0.9725 pu
Mean (pu)	0.9927 pu	0.9927 pu	0.9941 pu	0.9915 pu	0.9913 pu	0.9922 pu
Std. Dev	0.008578	0.008578	0.009095	0.01008	0.01023	0.01072
Total power loss [MW]	0.0189	0.0189	0.0275	0.0241	0.0387	0.1008
Percent loss reduction	91.60%	91.60%	87.77%	89.30%	82.78%	55.19%
SSEV index	0.008635	0.008635	0.008053	0.011867	0.01229	0.011971

The results of the MSPSO optimisation process when the shunt compensation capacitors are removed (Case II), show that the best minimum MOF value is obtained with one optimally size and located generator (1.9MW) injecting 1.15Mvars at bus number 61. The power loss was reduced by 89.30% compared with the base network with a computed SSEV of 0.011867. The corresponding Case II PSO-W results (section 4.4.2) show that the best minimum MOF value was obtained with one optimally size generator of 1.8911MW injecting 1.17Mvar at bus 61. An 89.41% power loss reduction compared with the base case network was achieved with an SSEV of 0.011849. Both algorithms achieved same optimal location, but with small differences in optimal generator size, percentage power loss reduction and SSEV value.

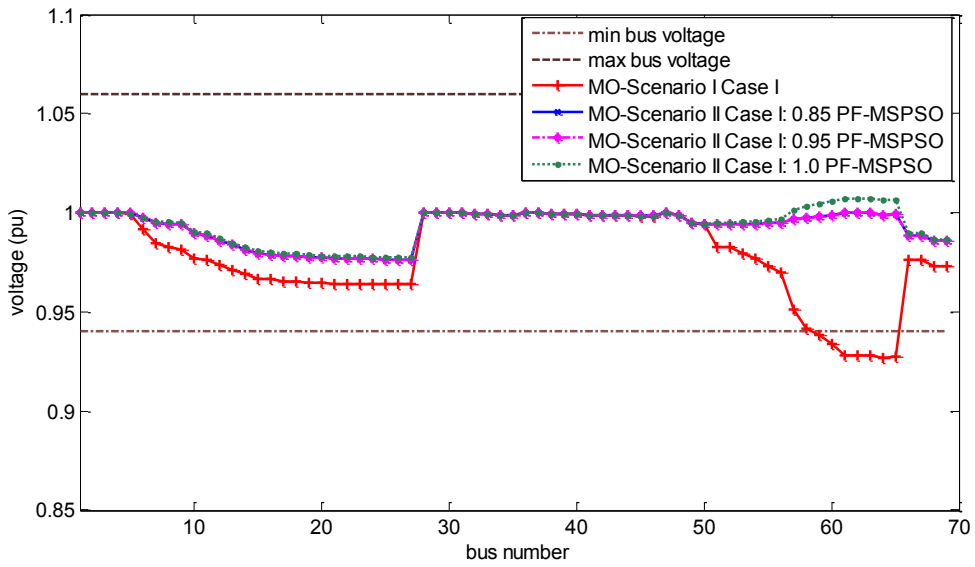

Figure 5.14: Voltage profile Scenario II (single generator); Case I (with shunt compensation), Multi-Objective Optimisation

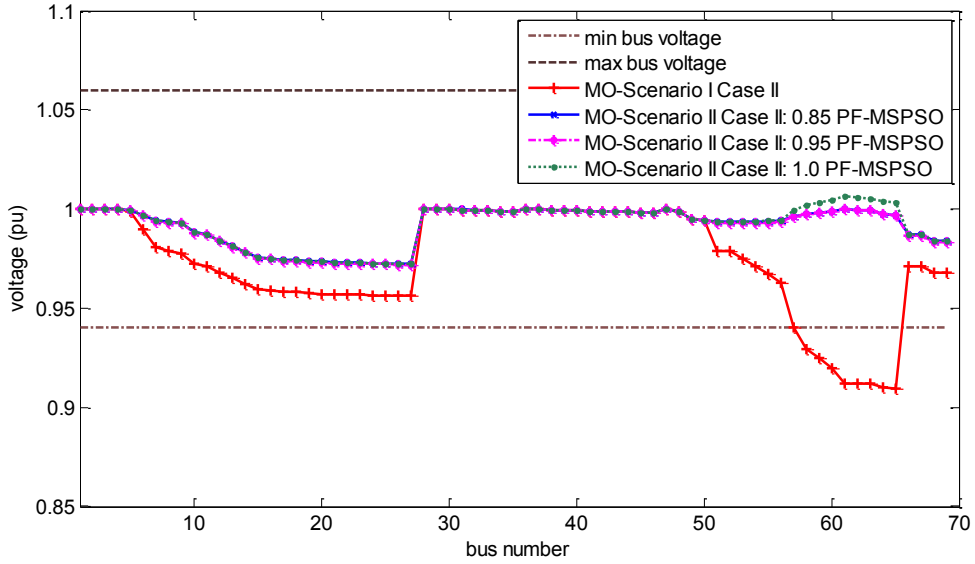

Figure 5.15: Voltage profile Scenario II (single generator); Case II (without shunt compensation), Multi-Objective Optimisation

The convergence of the multi-objective cost function is shown in Figures 5.16 and 5.17 for Case I and Case II, respectively. A comparison with the convergence characteristics of the PSO-W algorithm for the same exercise (section 4.42, Figures 4.17 and 4.18) shows the MSPSO algorithm is quicker and requires much less iteration to attain the optimal solution.Table 5.14 shows the numbers of evaluations of the objective function required to attain a final optimal solution for both MSPSO and PSO-W. The required number of function evaluations for the best MSPSO result is reduced by 92.92% and 95.41%, respectively, for Case I and Case II when compared with PSO-W algorithm.

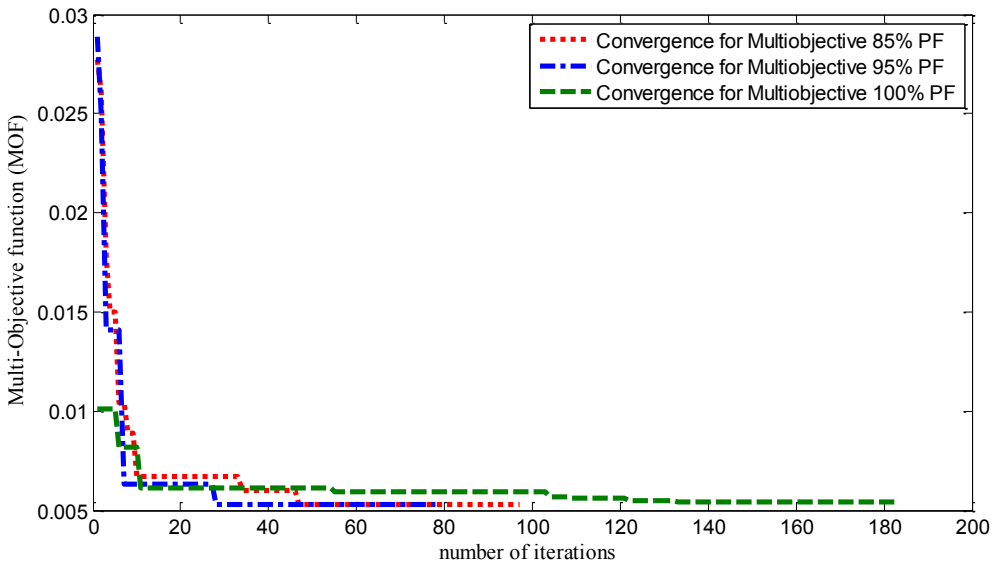

Figure 5.16: Convergence characteristic of MSPSO (Scenario II, Case I); Multi-Objective Optimisation

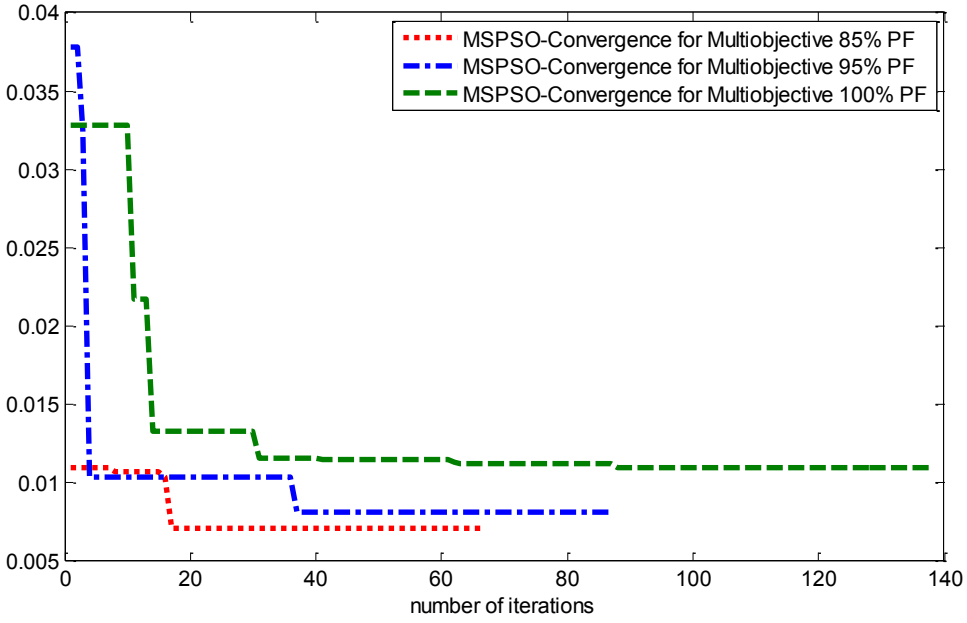

Figure 5.17: Convergence characteristic of MSPSO (Scenario II case II) with Multi-Objective Optimisation

Table 5.14:COMPARISON OF ALGORITHMS COMPUTATIONAL BURDEN: SCENARIO II, CASE I (ONE GENERATOR); MULTI OBJECTIVE OPTIMISATION

	MSPSO Case I			PSO-W Case I		
Minimum power factor	0.85	0.95	1.0	0.85	0.95	1.0
Average no. of steps	92.6	92.8	128	327.2	338.4	334.4
No. of function evaluations per step	5	5	5	20	20	20
No. of function evaluations	463	464	640	6544	6768	6688

Table 5.15:COMPARISON OF ALGORITHMS COMPUTATIONAL BURDEN: SCENARIO II, CASE II (ONE GENERATOR); MULTI OBJECTIVE OPTIMISATION

	MSPSO Case II			PSO-W Case II		
Minimum power factor	0.85	0.95	1.0	0.85	0.95	1.0
Average no. of steps	94	86	97.6	512	539	320
No. of function evaluations per step	5	5	5	20	20	20
No. of function evaluations	470	430	488	10240	10780	6400

5.3.3 Scenario III: single generator connected at the minimum voltage bus; multi-objective optimisation

The results of the MSPSO optimisation process for this scenario are presented in Table 5.16. The corresponding improvement in network voltage profile is shown in Figures 5.18 and 5.19. The minimum bus voltages are bus 64 for Case I and bus 65 for Case II.

Table 5.16: DG SIZE AND LOCATION FOR SCENARIO III (ONE GENERATOR AT MINIMUM VOLTAGE BUS); MULTI-OBJECTIVE OPTIMISATION

	Case I			**Case II**		
Minimum possible PF	0.85	0.95	1.0	0.85	0.95	1.0
Optimal bus	64	64	64	65	65	65
DG output MW/Mvar	1.6/0.29	1.6/0.29	2/0.0	1.50/0.75	1.60/0.53	2.3/0.0
Actual operating PF	0.98	0.98	1.0	0.89	0.95	1.0
Max. voltage	1.0000 pu	1.0000 pu	1.0110 pu	1.0000 pu	1.0000pu	1.0190 pu
Min. voltage	0.9748 pu	0.9748 pu	0.9764 pu	0.9686 pu	0.9684 pu	0.9704 pu
Mean (pu)	0.9912	0.9912	0.9930pu	0.9878 pu	0.9877 pu	0.9905 pu
Std. Dev	0.0090	0.0090	0.009229	0.01150	0.01157	0.01129
Total power loss [MW]	0.0315	0.0315	0.0404	0.0649	0.0742	0.1444
Percent loss reduction	85.99%	85.99%	82.04%	71.13%	66.99%	35.77%
SSEV index	0.010846	0.010846	0.009178	0.019273	0.019542	0.014927

For Case I the best MOF (i.e. Minimum objective function value) is obtained with one optimally size generator calculated at 2.0 MW injecting an additional 0.0 Mvar into the network. A power loss reduction of 82.04% is achieved compared with the base case network and a SSEV 0.009178 is computed. The results of the optimisation process when the compensating shunt capacitors are removed (Case II) show that the best minimum MOF value is obtained with one optimally size generator (1.5MW) injecting 0.75Mvars.

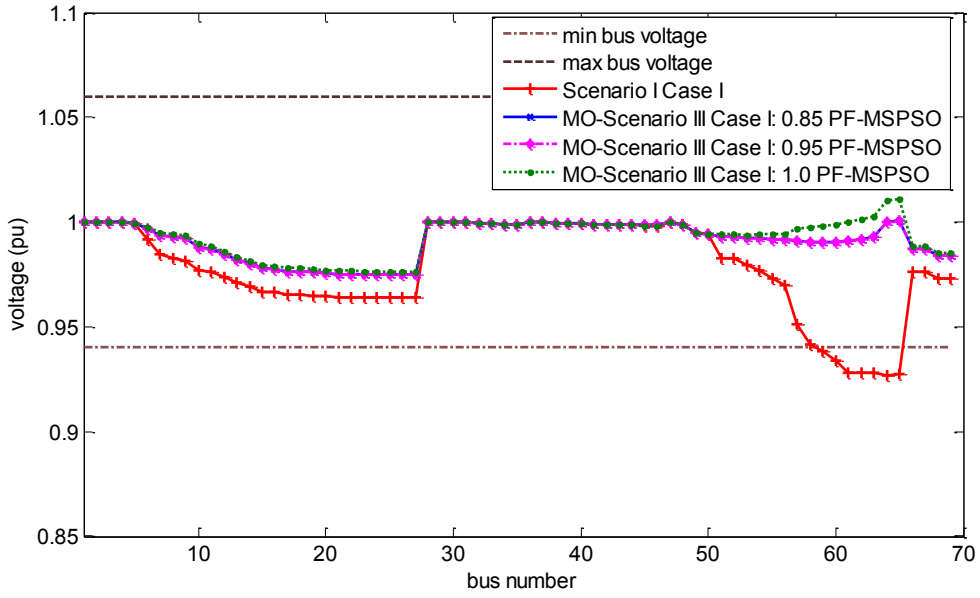

Figure 5.18: Voltage profile Scenario III (single generator connected at minimum voltage bus); Case I (with shunt compensation), Multi-objective optimisation

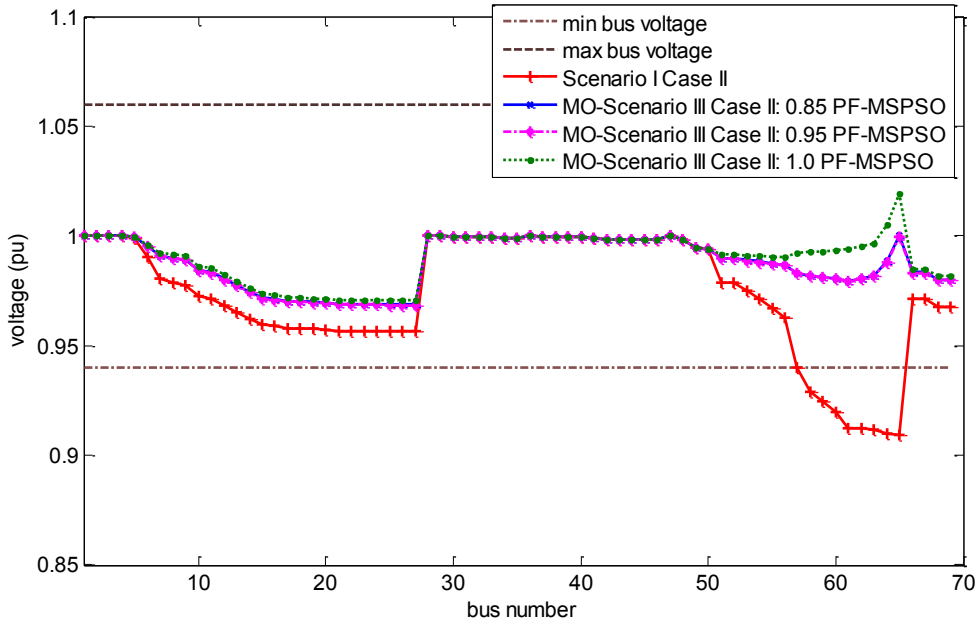

Figure 5.19: Voltage profile Scenario III (single generator connected at minimum voltage bus); Case I (without shunt compensation), Multi-objective optimisation

The power loss is reduced by 71.13% compared with the base network with a computed SSEV of 0.019273. Comparing these results with those presented in section 4.4.3 (Case I, PSO-W) shows that the calculated optimal generator sizes are at variance. The MSPSO results produced a better power loss reduction at the expense of higher value of SSEV. The results of MSPSO are obtained for realistic generator sizes, while the PSO-W use continuous generator sizes and thus the results are not necessarily realistic.

Tables 5.17 and 5.18 show the number of evaluations of the objective cost function required to attain a final optimal solution with both algorithms for Case I and II, respectively. The number of evaluations of MSPSO for the best optimal solution when compared with those obtained with the PSO-W algorithm in section 4.4.3 shows a reduction of 95.77% for Case I and 97.32% for Case II.

Table 5.17: COMPARISON OF ALGORITHMS COMPUTATIONAL BURDEN: SCENARIO III, CASE I (ONE GENERATOR AT MINIMUM VOLTAGE BUS); MULTI OBJECTIVE OPTIMISATION

	MSPSO Case I			PSO-W Case I		
Minimum power factor	0.85	0.95	1.0	0.85	0.95	1.0
Average no. of steps	55.8	64.4	53	331.6	286.2	331.4
No. of function evaluations per step	5	5	5	20	20	20
No. of function evaluations	279	322	265	6632	5724	6268

Table 5.18: COMPARISON OF ALGORITHMS COMPUTATIONAL BURDEN: SCENARIO III, CASE II (ONE GENERATOR AT MINIMUM VOLTAGE BUS); MULTI OBJECTIVE OPTIMISATION

	MSPSO Case II			PSO-W Case II		
Minimum power factor	0.85	0.95	1.0	0.85	0.95	1.0
Average no. of steps	58	60.2	58.4	540.8	573.6	257.4
No. of function evaluations per step	5	5	5	20	20	20
No. of function evaluations	290	301	292	10816	11472	5148

5.3.4 Scenario IV: two generators; multi-objective optimisation

This scenario involved finding the optimal location and size for two generators operating with different minimum operating power factors, first in the presence of shunt compensation capacitors (Case I) and with shunt compensation capacitors removed (Case II).

The results of the MSPSO optimisation process for this scenario are presented in Table 5.19. The MOF values are shown in Figure 5.20. The improvement in network voltage profile is shown in Figures 5.21 and 5.22 for Case I and Case II, respectively.

Table 5.19: DG SIZE AND LOCATION FOR SCENARIO IV (TWO GENERATORS); MULTI-OBJECTIVE OPTIMISATION

	Case I			**Case II**		
Minimum possible PF	0.85	0.95	1.0	0.85	0.95	1.0
Optimal bus 1	61	61	61	61	61	61
DG 1 output MW/Mvar	1.75/0.31	1.75/0.31	1.9/0.0	1.8/1.09	2/0.63	2.2/0.0
Actual operating PF 1	0.98	0.98	1.0	0.85	0.95	1.0
Optimal bus 2	17	17	15	17	17	17
DG 2 output MW/Mvar	0.536/0.06	0.53/0.08	0.625/0.0	0.536/0. 33	0.6/0. 19	0.8/0. 0
Actual operating PF 2	0.99	0.99	1.0	0.85	0.95	1.0
Max. voltage	1.0000 pu	1.0000 pu	1.0020 pu	1.0000 pu	1.0000pu	1.0020 pu
Min. voltage	0.9943 pu	0.9943 pu	0.9943 pu	0.9943 pu	0.9941 pu	0.9942pu
Mean (pu)	0.9983 pu	0.9983 pu	0.9987 pu	0.9982 pu	0.9981 pu	0.9981 pu
Std. Dev	0.001679	0.001679	0.0016680	0.001736	0.001864	0.002211
Total power loss [MW]	0.0076	0.0076	0.0135	0.0081	0.0248	0.0812
Percent loss reduction	96.62%	96.62%	94.0%	96.40%	88.97%	63.90%
SSEV index	0.000385	0.000385	0.000208	0.000433	0.00049	0.000589

The best loss reduction with enhanced voltage support is obtained with two optimally sized (1.75MW and 0.536MW) and located generators (Case I) injecting additional 0.31Mvars and 0.06Mvars at bus number 61 and 17, respectively. A 96.62% power loss reduction is achieved compared with the base case network with a SSEV value of 0.000385.

The results of the optimisation process when the compensating shunt capacitors are removed (Case II) are also presented in Table 5.19. The best results for this case show the generators to inject 1.80MW/1.09Mvars at bus number 61 and 0.536MW/0.33Mvars at bus number 17. A power loss reduction of 96.40% compared with the base network and a SSEV of 0.000208 are computed. As with previous scenarios, these results differ slightly from those obtained using the PSO-W algorithm for the reasons outlined above.

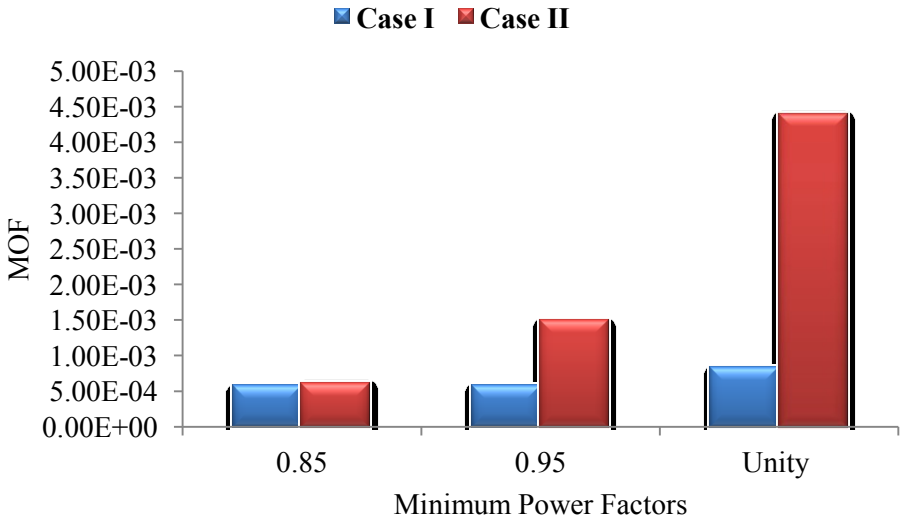

Figure 5.20: Scenario IV: minimum objective cost function values

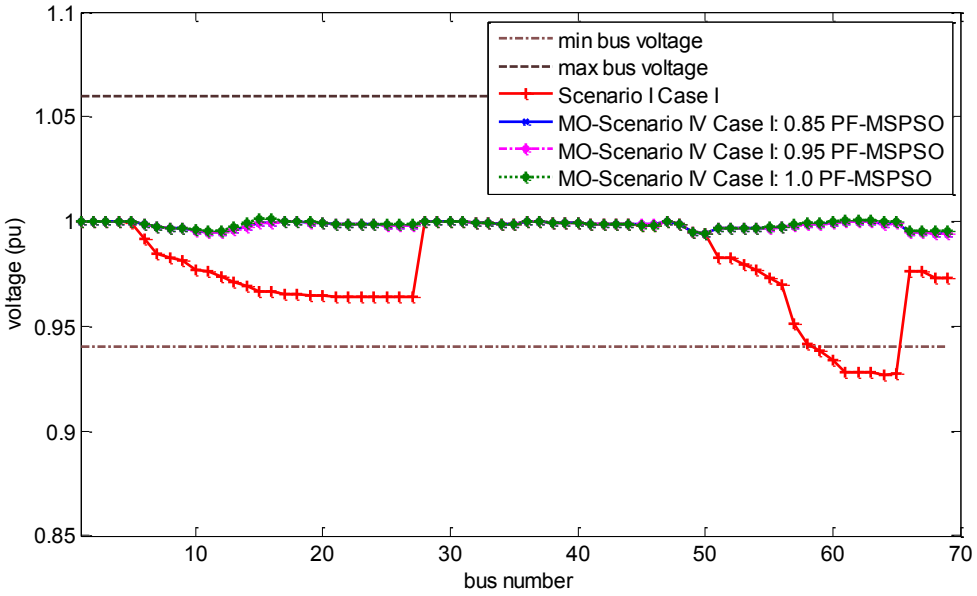

Figure 5.21: Voltage profile Scenario IV (two generators); Case I (with shunt compensation), Multi-Objective Optimisation

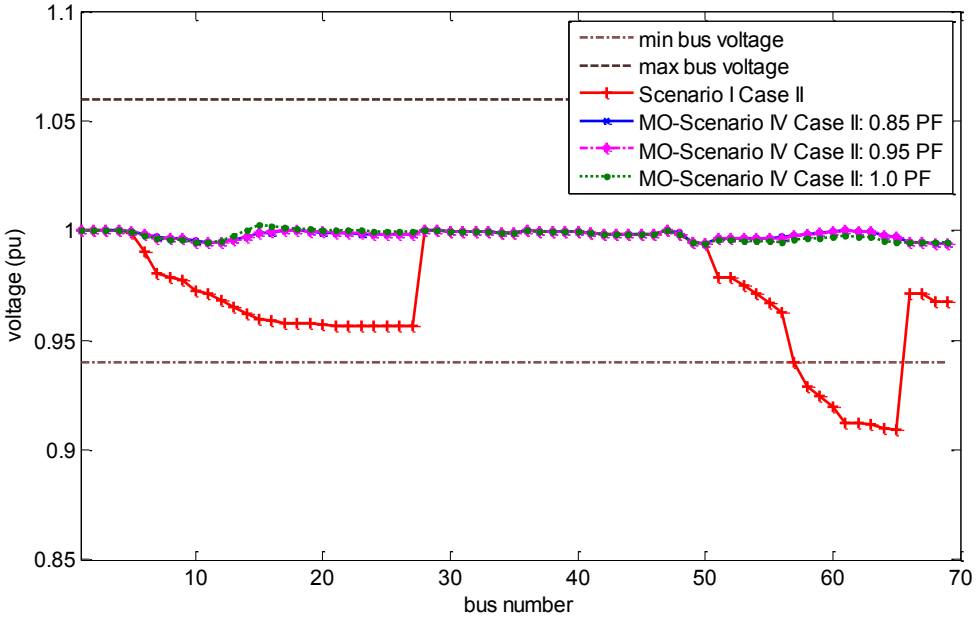

Figure 5.22: Voltage profile Scenario IV (two generators); Case II (without shunt compensation), Multi-Objective Optimisation

Tables 5.20 and 5.21 shows the number of evaluations of the objective function required for the final optimal solution to be attained for both algorithms. Similar to other scenarios, the number of evaluations is substantially reduced with MSPSO when compared with the PSO-W results (Table 4.14) summarised and represented in Tables 5.20 and 5.21.

Table 5.20: COMPARISON OF ALGORITHMS COMPUTATIONAL BURDEN; SCENARIO IV, CASE I (TWO GENERATORS); MULTI-OBJECTIVE OPTIMISATION

	MSPSO Case I			PSO-W Case I		
Minimum power factor	0.85	0.95	1.0	0.85	0.95	1.0
Average no. of steps	116.8	96	93.8	628.2	738.6	673.
No. of function evaluations per step	5	5	5	20	20	20
No. of function evaluations	584	480	469	12564	14772	13460

Table 5.21: COMPARISON OF ALGORITHMS COMPUTATIONAL BURDEN; SCENARIO IV, CASE I (TWO GENERATORS); MULTI-OBJECTIVE OPTIMISATION

	MSPSO Case II			PSO Case II		
Minimum power factor	0.85	0.95	1.0	0.85	0.95	1.0
Average no. of steps	106.2	94.4	102.8	635.8	825.8	584.2
No. of function evaluations per step	5	5	5	20	20	20
No. of function evaluations	531	472	514	12716	16516	11684

The real power loss reduction chart for the best test cases for all the studied scenarios and cases are shown Figure 5.23. Similar to the investigation in section 4.4, the best loss reduction with improved voltage profile is obtained with scenario IV/Case I (i.e. when two generators are allowed to operate in a compensated network). This is evident from the loss reduction and the SSEV charts of Figures 5.24 and 5.25.

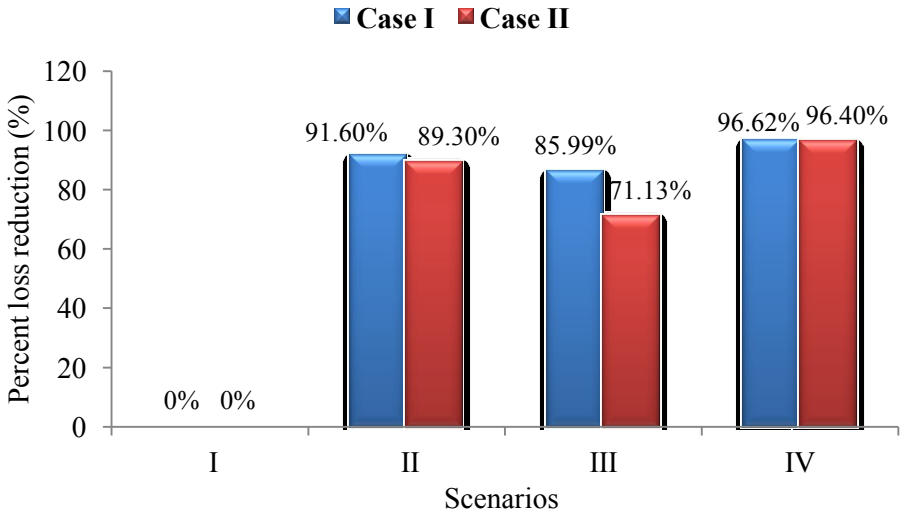

Figure 5.23: Real power loss reduction chart

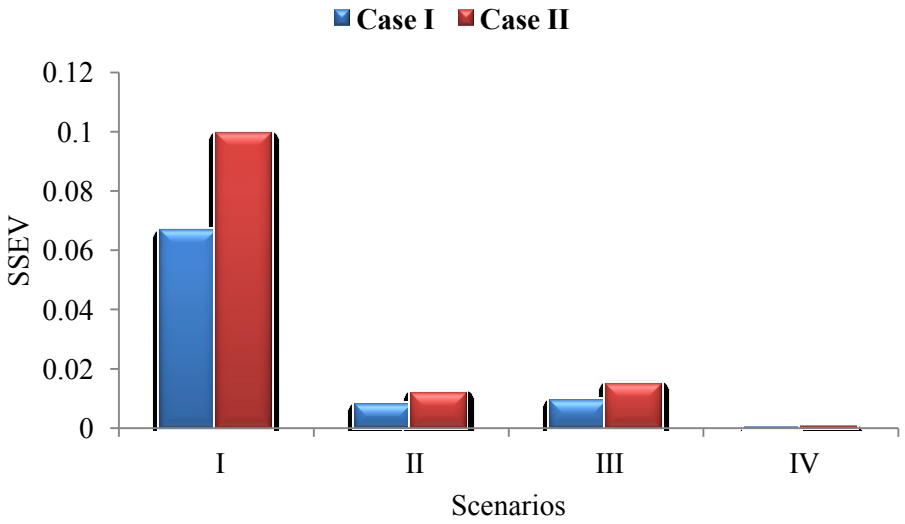

Figure 5.24: SSEV values

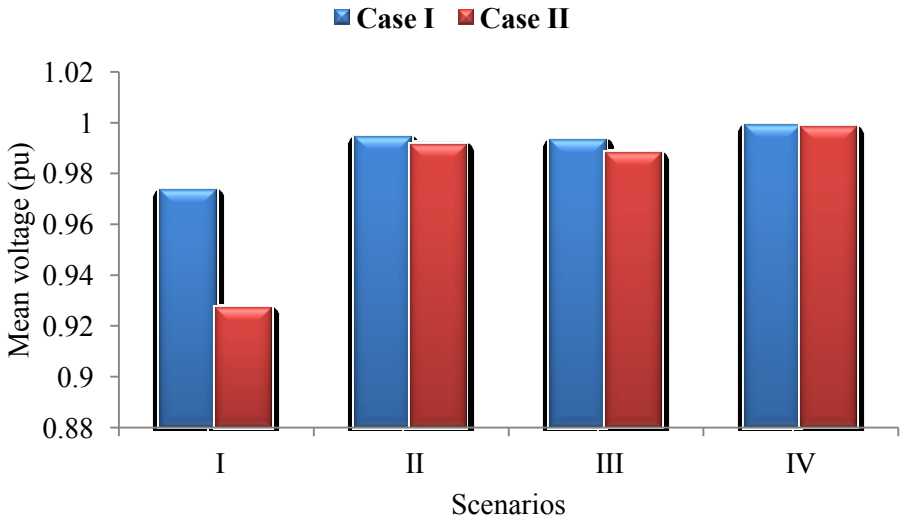

Figure 5.25: Best of mean voltage values

Finally, a summary of the results using PSO-W and the MSPSO for the multi-objective optimisation investigation are presented in Tables 5.22 and 5.23. It is evident that the both algorithms obtained the same optimal location with small variations in the optimal generator sizes and the percent power loss reduction figure. This is because the optimal DG sizes obtained with PSO-W are continuous values that may not represent actual generator sizes. The MSPSO algorithm, on the other hand, employs a pre-defined list of commercial generator sizes (see appendix A, Table A.2). The MSPSO algorithm, however, has clear advantages in terms of the speed of convergence, lower computational burden due to fewer function evaluations and the capability to explore discrete search space composed of realistic generator sizes.

Table 5.22: COMPARISON OF PSO-W AND MSPSO OPTIMAL DG SIZE AND LOCATION RESULTS CASE I (MULTI OBJECTIVE)

			Optimal bus location(s)	Optimum DG size (s) (MW/Mvar)	Power loss reduction (%)	SSEV	No. of function evaluations
PSO-W	Scenarios	I	-	-	-	0.0665	-
		II	61	1.7977/0.43	91.55	0.00868	6544
		III	64	1.5797/0.34	85.90	0.010854	6800
		IV	61/17	1.7349/0.34; 0.5242/0.09	96.62	0.000383	16152
MSPSO	Scenarios	I	-	-	-	0.0665	-
		II	61	1.8/0.43	91.60	0.008053	463
		III	64	1.6/0.29	85.99	0.009178	279
		IV	61/17	1.75/0.31; 0.536/0.08	96.62	0.000208	584

Table 5.23: COMPARISON OF PSO-W AND MSPSO OPTIMAL DG SIZE AND LOCATION RESULTS CASE II (MULTI OBJECTIVE)

			Optimal bus location(s)	Optimum DG size (s) (MW/Mvar)	Power loss reduction (%)	SSEV	No. of function evaluations
PSO-W	Scenarios	I	-	-	-	0.0993	-
		II	61	1.8911/1.17	89.41	0.011849	10240
		III	65	1.4385/0.69	72.34	0.015006	10816
		IV	61/17	1.7923/1.11; 0.5381/0.33	96.49	0.000424	12716
MSPSO	Scenarios	I	-	-	-	0.0993	-
		II	61	1.9/1.15	89.35	0.011867	470
		III	65	1.5/0.75	71.13	0.014927	295
		IV	61/17	1.80/1.09; 0.536/0.33	96.40	0.000433	531

From Tables 5.22 and 5.23, for case I, the required number of function evaluations for best minimum MOF is reduced by 92.92%, 95.77%, and 95.35% for scenarios II, III and IV, respectively, compared with the PSO-W algorithm. While for case II, the required number of function evaluations for best minimum MOF is reduced by 95.41%, 97.32%, and 95.82% for scenarios II, III and IV respectively, compared with the PSO-W algorithm.

5.4 Comparative Study: Scenario II Case II: Single generator at unity PF

In addition to the above studies, this test scenario is considered to allow direct comparisons of the results obtained from the MSPSO algorithm with previously published solutions obtained using analytical techniques [10], genetic algorithms [103], the Artificial Bee Colony (ABC) algorithm [45] and SPPSO as well as the PSO-W algorithm. The optimisation studies in [10], [45] and [103] were limited to the single-objective function of minimizing network losses. These studies are similar to that presented in section 5.2 (scenario II, case II). Table 5.24 shows the optimal solutions (in terms of network loss reduction) achieved by all six optimisation methods.

Table 5.24: COMPARISON OF OPTIMAL DG SIZE AND LOCATION RESULTS (SCENARIO II CASE II: MINIMUM NETWORK LOSSES)

	69-bus network					
	Analytical Method [10]	GA [103]	ABC Algorithm[45]	Proposed MSPSO Algorithm	Implemented PSO-W	Implemented SPPSO
Optimum bus location	61	61	61	61	61	61
Optimum DG size (MW)	1.810	1.827	1.900	1.850	1.8722	1.8726
% MW loss reduction	62.86%	62.91%	62.97%	63.02%	63.03%	63.0%

The results obtained from the six methods are identical in terms of the optimal location of the DG unit. However, an improvement in loss reduction is achieved by the proposed MSPSO algorithm and other variants PSO (PSO-W and SPPSO) when compared with Analytical, GA and ABC methods. The result of ABC algorithm like the proposed MSPSO considered constraints on the discrete size of DG units. A slight improvement is achieved with MSPSO when compared with the ABC method which misses out the 1850kW generator size because it only considers generator sizes in even steps of 100kW. The proposed MSPSO avoids the rounding up errors inherent in analytical and GA methods. For the results of analytical and GA methods to reflect the realistic generator sizes), the solutions will need to be rounded to the nearest available size. Thus, it is evident from Table 5.24 that such approximation will affect the accuracy of the obtained optimal solution.

In Table 5.25, the performance of the proposed MSPSO algorithm is compared with the two other variants PSO algorithms for scenario II case II in terms of the computational

burden of the optimisation process. All the three algorithms produce the same final solution, but the MSPSO algorithm has the advantage of fewer function evaluations compared with the other versions. The results shown in Table 5.25 are average values based on ten independent runs of the algorithm. The advantage of the proposed MSPSO algorithm is clearly demonstrated. The required number of function evaluations is reduced by 90% compared with the standard PSO-W algorithm and by 69.73% compared with a small population PSO algorithm [91, 92].

Table 5.25: ADDITIONAL ALGORITHM COMPARISON; SCENARIO II CASE II (MINIMUM NETWORK LOSSES AT UNITY PF)

	Proposed MSPSO algorithm	PSO-W algorithm	SPPSO algorithm
Average no. of steps	113.2	283.8	374
No. of function evaluations per step	5	20	5
No. of function evaluations	566	5676	1870

5.5 Summary

In this chapter, the MSPSO optimisation algorithm proposed in this research work has been applied to optimise the integration of DG into a 69-bus radial distribution network (with and without shunt compensation capacitors). The proposed algorithm is a multi-search PSO in which the swarm particles are allowed to move in a mixed search space composed of integer variables (bus location numbers); continuous variables constrained to discrete unevenly spaced variables (generator active power output) and continuous variables (generator reactive power output). The MSPSO study was standardised to the study in chapter 4 (based on PSO-W) for validation purpose. In addition, the significance of the proposed scheme is demonstrated by comparing its results with the results of previously published works (where such studies exist).

It has shown that the MSPSO and the PSO-W algorithms obtained the same optimal locations with small variations in the optimal generator sizes and the percent power loss reduction figure at some instances. The divergence between the two algorithms is due to the ability of MSPSO to operate on mixed search variables of integer, discrete and continuous variable. MSPSO results are thus obtained for realistic, commercially available generator sizes (see appendix A, Table A.2) with no loss of accuracy. Quicker results due to fewer iterations, lower computational burden due to fewer function

evaluations using few informants and the capability to explore discrete search space composed of realistic generator sizes using a dichotomic search algorithm are the many advantages of MSPSO in contrast with the PSO-W algorithm.

Additionally, it is shown that an improvement in the network power loss reduction is achieved by the proposed MSPSO algorithm compared with other optimisation algorithms (analytical, GA and ABC) used previously in the literature. The MSPSO avoids the rounding up errors inherent in analytical and GA methods and is found to be robust and efficient method for solving the DG optimisation problem.

In the chapter that follows, the application of the proposed MSPSO to the problem of integrating induction machine based DG is introduced.

CHAPTER 6

Induction Generator Based DG and Shunt Compensation Capacitors Integration Using MSPSO Algorithm

Wind driven Induction Generators (IGs) are becoming common sources of Distributed Generation (DG) in distribution systems. This IG-based DG supplies real power and in turn absorbs reactive power from the system. It is, therefore, necessary to account for this reactive power requirement in any network integration exercise involving induction generators. Moreover, just like an induction motor, re-magnetization of an induction generator following a fault consumes a large amount of reactive power. If the grid to which the wind power plant (WPP) is connected is not strong, reactive demands of induction wind turbine generators (WTGs) can suppress voltage recovery and potentially cause voltage collapse. Hence, it is often necessary to provide some means of dynamic or static reactive compensation, such as STATCOMs or SVCs to meet low-voltage ride-through requirements with induction generators of type fixed speed [7].

In this chapter, a technique is proposed and formulated for induction generator integration to determine the reactive power required for its operation. The technique that is based on per phase equivalent circuit of the induction machine is employed to compute machine steady state output characteristics. General formulations to handle the impact of DG on the rating of the protective switchgear and the network line capacity limits are presented. These formulations are incorporated with the MSPSO algorithm to allow the enforcement of these constraints.

Induction generator based DG units like its synchronous counterparts (discussed in chapters 4 and 5) are also commercially available in a non-fixed discrete step sizes. Additionally, the shunt capacitors are known to be available in a fixed discrete step size. Thus, the problem of IG DG integration, also involved mixed search space variables that require a multi-search space optimisation algorithm. The capability of the MSPSO algorithm to solve this optimization problem is demonstrated in this study.

6.1 Modelling of IG for Distribution Network Integration

The modelling of the induction generator for network integration and power flow analysis based on conventional per phase equivalent circuit of induction machine is presented in this section. The model developed here applies to a fixed speed induction generator that is directly connected to the grid. Usually in this induction generator, a fixed shunt capacitor is required to provide reactive power compensation. Given the generator's characteristics, rated output power and operating voltage an iterative procedure is used to find the reactive power required by the generator.

6.1.1 Induction Machine Model

A conventional line-to-neutral equivalent circuit of a three-phase induction machine is shown in Figure 6.1

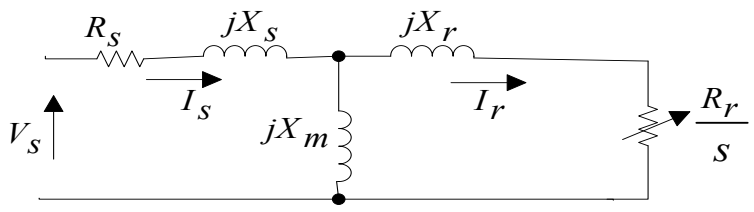

Figure 6.1: a per-phase induction machine equivalent circuit

Where R_s, X_s are stator resistance and reactance, respectively, X_m is the magnetizing reactance; R_r and X_r is the referred rotor resistance and reactance, respectively. The operating slip of the machine s is given by:

$$s = \frac{n_s - n_r}{n_s} \tag{6.1}$$

Where n_s is the synchronous speed of the generator and n_r is the actual rotor speed.

If the operating slip of the generator is known, the complex power drawn from the supply network can be readily obtained as:

The input impedance for the network is determined from Figure 6.1 as

$$ZM = Rs + jXs + \frac{(jXm)(Rr/s + jXr)}{Rr/s + j(Xm + Xr)} \tag{6.2}$$

The input admittance is given by

$$YM = \frac{1}{ZM} \tag{6.3}$$

$$YM_{LN} = YM \cdot t^{*} \tag{6.4}$$

Where, t is the phase to neutral transformation from Line to Line [104] and is given by

$$t = \frac{1}{\sqrt{3}} \cdot \angle 30 \tag{6.5}$$

The machine terminal line-to-neutral voltage

$$V_{LN} = V_{s} \cdot t \tag{6.6}$$

The per phase motor current from the equivalent machine is

$$I_{s1\phi} = YM_{LN} \cdot V_{s} \cdot t \tag{6.7}$$

With Equations (6.6) and (6.7); machine terminal line-to-neutral voltage and current, known, the input phase complex power and total three-phase input complex power can be computed:

$$S_{1-\phi} = V_{LN} \cdot (YM_{LN} \cdot V_{s} \cdot t)^{*} \tag{6.8}$$

$$S_{Total} = 3 \times V_{LN} \cdot (YM_{LN} \cdot V_{s} \cdot t)^{*} \tag{6.9}$$

The above machine model is used for the induction generator with the value of slip been negative. This means the generator will be driven at speed in excess of synchronous speed. The generator is modelled with the equivalent admittance matrix Equation (6.3). The IG reactive power requirement calculation procedure is implemented in MATLAB and interfaced with MSPSO and MATPOWER AC power flow algorithm for the IG DG optimization problem.

6.1.2 Computation of slip

In distributed generation placement problem, the discrete variables representing the DG sizes, are the specified output power of the induction generators. The slip values for the induction generators are not known. The goal is to find iteratively the value of slip that will force the real part of the complex output power to be computed for the generator using Equations (6.1) – (6.9) to be within some small tolerance of the specified output power. In this study, a tolerance value of 0.001 is used. The procedure starts with the assumption of initial values of the slip (S_{old}) and change in slip (d_s) as [104]:

$$S_{old} = 0.0 \tag{6.10}$$

$$d_s = 0.01$$

The value of the slip used in the first iteration is then

$$S_{new} = S_{old} + d_s \tag{6.11}$$

where, S_{new} is the new value of positive sequence slip.

When the new value of the slip is known, the input shunt admittance matrix (*YM*) in Equation (6.3) is computed. The given line-to-line voltage is transformed into Line-to-neutral and used to compute the stator currents Equation (6.6). The per-phase and the total three-phase input complex power are computed using Equations (6.8) - (6.9). The computed three-phase input power is compared to the specified three-phase output power and error is computed as

$$Error = P_{specified} - P_{computed} \tag{6.12}$$

If the error is negative, the slip needs to be increased so that the computed power will increase. This is done using Equations (6.11) & (6.13)

$$S_{old} = S_{new} \tag{6.13}$$

The new value of slip is used to repeat the calculations for the output power to the generator. If the error is positive, that means that a bracket has been established. The required value of slip lies between the S_{old} and S_{new}. In order to zero in on the required slip, the old value of the slip will be used, and the change in slip will be reduced by a factor of 10 Equation (6.14):

$$d_s = d_s / 10 \tag{6.14}$$

The new slip is recomputed using Equation (6.11) when the slip has produced the specified output power, then the reactive power required can be obtained. The imaginary of the computed complex power obtained at this value of slip represent the reactive power required by induction generator. That need to be compensated for locally at the PCC to avoid unnecessary reactive power flows and hence losses in the network. The above procedure for the computation of the reactive power requirement of the induction generator is summarized in the flowchart in Figure 6.2.

To sum up, the IG power flow algorithm procedure that determines the IG steady state analysis, operate iteratively to find the required slip that will force the real value of the

computed complex output power of the generator to be within a small tolerance band of the specified output power. MSPSO is then employed as a global optimization tool to find the globally optimal solution, allowing for the use of shunt compensation to provide the reactive power required by the induction generator locally at the point of connection to the hosting utility grid.

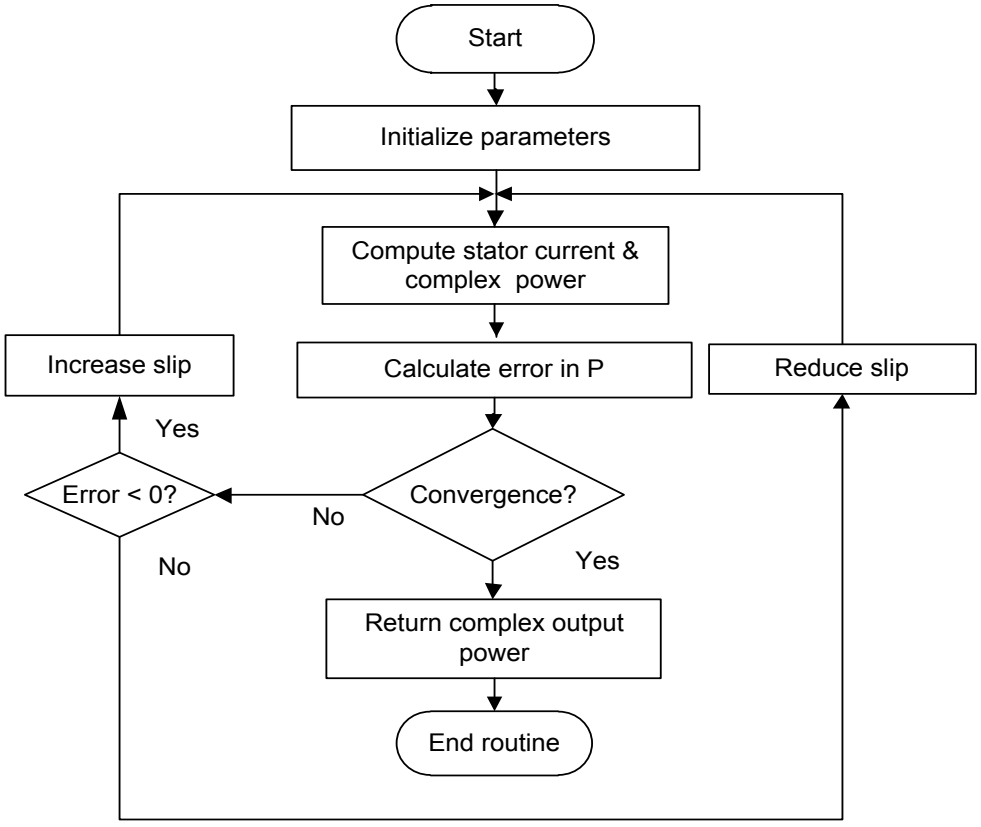

Figure 6.2:Flowchart for induction generator output power & reactive power calculation

6.2 Fault Level / Short Circuit Current and Line Loading Capacity Constraints

The fault level constraint refers to the operational limitations of protection equipment (e.g. switchgear) during a fault. If the specification of the protection equipment is not adequate to clear or isolate a fault, then not only the equipment itself will possibly be damaged, but the operation of the broader part of the power system will become insecure [14]. The magnitude of the fault current is, usually, used to select the rating (breaking capacity) of the protective device. In this study, bus impedance matrix by the building algorithm [105] is formulated and used to compute the fault current. This method is based on the classical impedance method [106] and is undemanding and practical.

Figure 6.3(a) shows a typical bus of a *n* bus power system network. The system is assumed to be operating under a balanced condition, and per phase circuit model is used. Each machine is represented by a constant voltage source behind subtransient reactance *(X_d")*.Branches/ lines are represented by their equivalent pi model with all impedances expressed on a common MVA base.

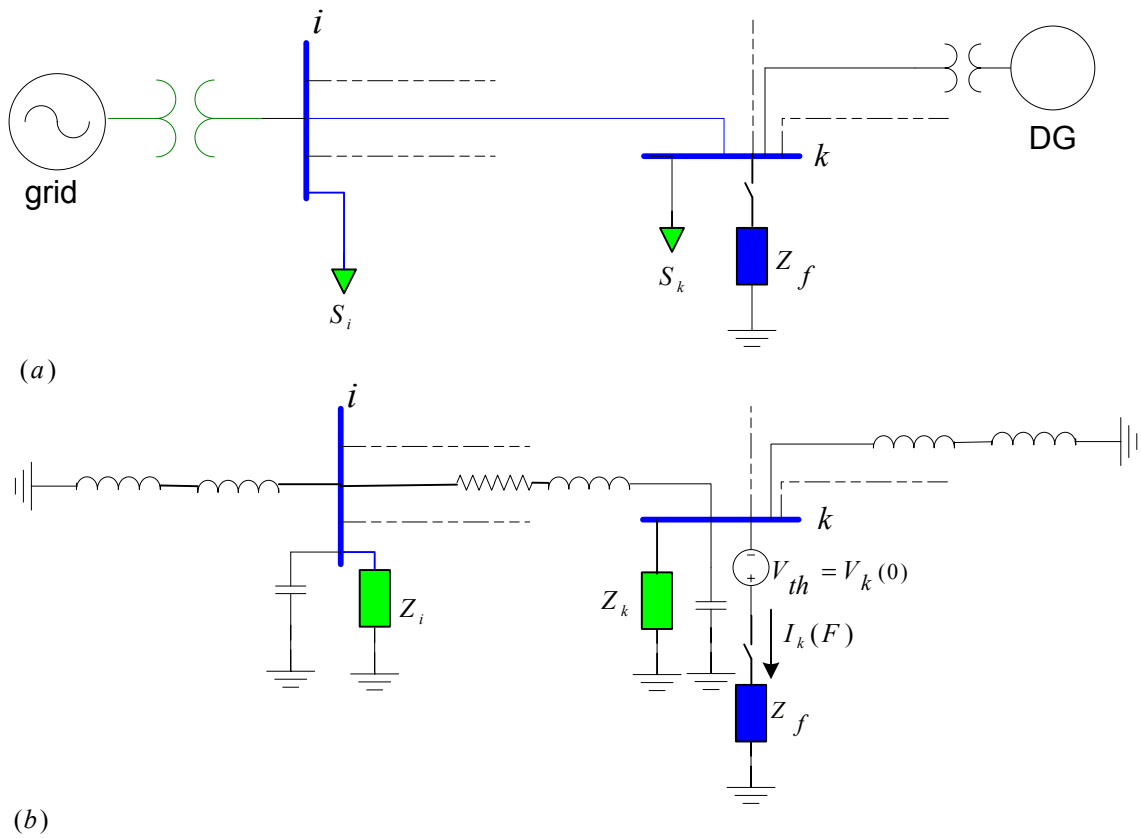

Figure 6.3: Typical Bus of a Power System [105]: (a) per phase model of a balanced power system, (b) Thevenin's equivalent circuit of (a)

The balanced three-phase current at fault bus *k* is given by

$$I_k(F) = \frac{V_k(0)}{Z_{k,k} + Z_f} \tag{6.15}$$

$V_k(0)$ is the pre-fault bus voltage at the fault bus *k*, Z_{kk} is the element of the bus impedance matrix and is the element of the Thevenin's impedance as viewed from the faulted bus. Z_f is the fault impedance to earth and for bolted fault as considered in this study, its value is zero.

The constraint on fault level imposed by the breaking capacity of the switchgear is given as

$$\left|I_k(F)\right| < \left|I_{spec}\right| \tag{6.16}$$

Equation (6.17) gives the coordination of the protective switchgear due to the connection of DG

$$\left|I_k(F)\right| < \left|I_{fDG}\right| < \left|I_{spec}\right| \tag{6.17}$$

$I_k(F)$ is the current at the faulted bus and the current that flows in the line *ij* following the occurrence of a fault. While I_{fDG} is the fault current due to the impact of the new generation and I_{spec} is the maximum allowed by the specifications of the switchgear at the terminal bus *i* and *j*.

This method for computing the short circuit current involves adding the various resistances and reactance of the fault loop separately and then calculating the corresponding impedance. These include network feeders as well as the synchronous and asynchronous machines that are replaced by their respective impedances, from (and including) the source to a given point.

Equations (6.16) & (6.17) are checked by PSO algorithm and handled as constraints on the swarm. Each particle of the swarm is checked against the constraints (6.16) & (6.17) ensuring only those particles that respect the constraints are used in the evaluation of the objective function. Particles that violate the constraints are rejected and never forms part of the solution. This approach means that the constraint on short circuit current is applied prior to the optimisation process. This will make it easier for the effect of the constraint on DG integration to be assessed.

6.2.1 Short-circuit current constraint with induction generator DG

In the real situation, the number of DG connected to the distribution system network can impact adversely on the distribution system operation. One of the technical impacts of DG is that it can adversely affect the protection setting and the rating of the switchgear that could destabilize the hosting network system's operation. The fault of interest to this study is a balanced three-phase fault. It is the most severe type of fault encountered in power system.

The initial current contribution to a three-phase fault is defined by the sum of the generator sub transient reactance and the system impedance from the machine terminals to the fault. For IG, this initial fault current decreases as the flux in the machine

collapses and will eventually reach zero unless there is sufficient reactive compensation to maintain the generator excitation during the fault [7]. Even though, this type of fault is known to be the least likely to occur, but power system planners usually, used this fault to calculate the circuit breakers duty and other switchgear devices.

In this research work, the short circuit current is evaluated at the busbar of the infeeding substation. In radial distribution network (with or without DG), the maximum value of short circuit current/ fault level, usually, occurs at the infeeding substation busbars. This is as a result of substantial contributions from the upstream grid and it rapidly decreases downstream the network. In a network with DG, the overall fault is the sum of the maximum fault currents due to the upstream grid through the network line and transformer, DGs and large motors connected to the radial distribution network if present.

In this study, to simplify the computation of short circuit calculations, the following assumptions are made;

1. A 3-phase balanced bolted fault is considered, with the network system assumed to be operating under a balanced condition, and per phase circuit model is used.
2. Each machine is represented by a constant voltage source behind proper reactance given as $X_d"$ (sub transient reactance).
3. The various correction factors recommended in the IEC60909 standard are neglected (voltage and impedance factor)
4. Loads current are assumed to be negligible compared to short–circuit current thus, neglected.
5. Arc resistances are not taken into account and all line capacitances are neglected
6. For the entire duration of the short-circuit, the voltages responsible for the flow of the current and the short-circuit impedance do not change significantly

These assumptions above impose limits for which the calculations are valid, but, usually, will provide good approximations [105], for the goal of this study.

6.2.1.1 Calculation of network feeders (upstream) impedance

The procedure algorithm for determining the maximum short-circuit current of the breaker commence with the computation of upstream grid impedance. This impedance

is made up everything upstream of the substation Busbar including the series connected network cable/conductor and transformers. The approximate fault level of the upstream grid at the connection point is used to calculate the impedance (resistance and reactance) of the network feeder as follows [107]:

$$Z_{up} = \frac{U^2}{SCMVA} \tag{6.18}$$

$$R_{up} = 0.0995 \times Z_{up} \tag{6.19}$$

$$X_{up} = 0.995 \times Z_{up} \tag{6.20}$$

$$Z_{grd} = (R_{up} + j \times X_{up}) \tag{6.21}$$

Where, Z_{up} , R_{up}, and X_{up} are respectively the upstream impedance, resistance and reactance. With Z_{grd} and U are the complex value of the upstream grid impedance and the nominal voltage of the system at the feeder connection point respectively. A value of 10 is used for the ratio X/R [107] and a three phase fault level of 250MVA is assumed for the study.

6.2.1.2 Relationship between generator size and fault currents

Fault currents are computed using the pre-fault voltage at the fault location, and the network impedances: distribution lines, transformer serial impedances, and the generator reactance where applicable, using Equation (6.15). Switchgear, usually, operates during the sub-transient period of generator's response after a fault. This reactance represents the output impedance of the generator within the first few cycles after a short- circuit occurs at the generator's terminal. In this study, generators' reactance is set equal to their sub-transient values. The sub-transient reactance of induction generators is assumed to be about 15%–25% on the generator reactance base with an average value of 16.7% [108]. The average value (16.7%) is used for this study.

$$X''_d = x''_d \times \frac{1}{S_g} \tag{6.22}$$

$$R_g = \frac{X''_d}{\frac{X}{R}} \tag{6.23}$$

$$Z_g = R_g + j \times X''_d \tag{6.24}$$

The sub-transient reactance of new generators x''_{dnew} is estimated as a function of their capacity S_g using the following expression

$$X''_{dnew} = X''_d \times \frac{S_b}{S_g} \tag{6.25}$$

where

X''_d is the per-unit sub-transient reactance of the generator (pu)

R_g is the resistance of the generator (pu)

x''_d is the average per-unit sub-transient reactance of the generator (pu)

S_g is the rated generator capacity (MVA)

S_b is the system MVA base

The $\frac{X}{R}$ is the X/R ratio, typically 10 for medium voltage [109]. The smaller the generator's capacity, the higher will be the sub-transient reactance and the lower the fault current.

6.2.1.3 Procedural steps and implementation flow chart of short-circuit constraint

The short circuit current constraint incorporated with the MSPSO is implemented prior to the optimisation process. After the application of dichotomy algorithm, the sub-routine algorithm on symmetrical fault is executed to compute the short circuit current for each DG at their specified locations. The implementation flow chart is as shown in Figure 6.4 and the procedural steps to compute the short-circuit current are discussed below:

Step1: load the discretized DGs and their corresponding bus number locations

Step2: Define relevant feeder network (upstream grid) parameters and compute upstream impedance.

Step3: Determine sub-transient reactance for the DGs, and set k=1 to start the computation process

Step4: Compute the generator impedance, the resistance and the reactance

Step5: Load relevant power system network impedance data and locate DG at its specified bus location number

Step6: Run three-phase symmetrical fault algorithm to obtain the short circuit current at the substation Busbar

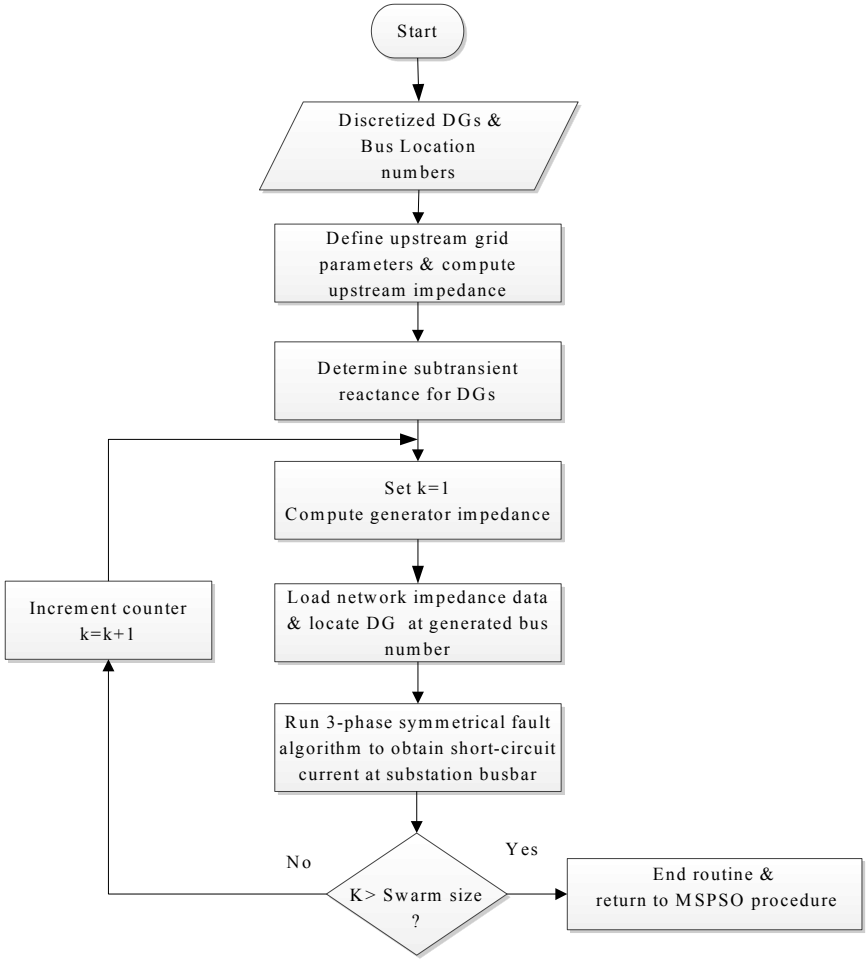

Figure 6.4: Flowchart for short-circuit current calculation

Step7: If k< Swarm size repeats step 4 -6

Step8: Else stop the routine and return to the MSPSO procedure algorithm

At the end of the subroutine, the computed short circuit current resulting from the location of DG (I_{fDG}) in the network is compared with the rated short circuit current of the switchgear (I_{spec}) as expressed by Equations (6.16) through (6.17).

The DGs that violate the constraint at their generated locations are rejected and will not form part of the optimal solution. If $I_k\ (F)$ is considered as the current at the fault bus without DG and this represents the designed fault current (base network short-circuit current). Since the switchgear short circuit current rating capacity is standardized, a standard value for the designed fault current is normally specified. The difference between the designed fault current and the specified switchgear rating represent the available headroom for short-circuit current at the substation feeder.

6.2.2 Line loading capacity constraint

One of the consequences of supplying power near to loads is that MVA flows may diminish in some sections of the network, thus realising more capacity. However, in other sections the may also increase to levels beyond distribution line limits thus the need to consider line limits constraint [53]. The line loading constraint expressed in Equation (4.10) can be enforced by evaluating a quadratic index *f(IC)* given by Equation (6.26).

$$f(IC) = \sum_{l \varepsilon L} (S_l - S_l^{\max})^2 \tag{6.26}$$

Where, S_l (S_{ij}) and S_l^{max} ($S_{ij}^{\max}$) defines the apparent power (*MVAflowmax*) in a line section *l* and the maximum allowable apparent power flow (*MVAflowrated*) in section *l* respectively. In order to enforce the constraint of Equation (4.10), the index in (6.26) is computed, weighted and added to the objective function. The line overloads are computed as:

$$Overloads = \max [MVAflow_{\max} - MVAflowrated] \tag{6.27}$$

Where,

$$MVAflow_{\max} = \max_{l}^{L} \left[\left| \bar{S}_{ij} \right|, \left| \bar{S}_{ji} \right| \right] \tag{6.28}$$

MVAflowmax and *MVAflowrated* denote the $n_l \times 1$ vector of apparent power flow related to all sections (branches) of the network, n_l the total number of sections of the distribution system under consideration. Implementation of the line loading constraint ensures that the location of DG is such that the MVA flows in network sections are within the maximum allowable rating of the sections/branches.

6.3 The Test System- 69-bus Radial Distribution Network

The capability of the MSPSO algorithm to solve this optimization problem of IG integration is demonstrated on the standard 69-bus benchmarking network used in the previous two chapters. This is the same network of Figure 4.1, but with the shunt compensation capacitors removed. The data of this base network are repeated here in Table 6.1 for convenience. The substation voltage is taken as 1.0pu, and the voltage profile of the network is shown in Figure 6.1. The electrical parameters of the induction generators used in this study are taken from [110-113] and are presented in Appendix B, Table B.1.

Two studies: a single-objective optimisation and a multi-objective optimization are carried out, each involving five different network scenarios. In all scenarios (except the base case scenario I), two different cases are considered: Case I entail the integration of one DG and Case II involves the integration of two DGs. The second scenario considers the simultaneous connection of generator units with shunt compensation capacitors, neglecting the constraints on short circuit current and line loading. In the third scenario, only the constraint on short circuit current is enforced while the fourth scenario considers the constraint on line loading only. Both short circuit current and line loading constraints are considered in scenario five.

The single Objective (SO) optimisation study is focused on the determination of the optimum size and location of the generator unit with shunt capacitors in order to minimize the total real power loss in the network. While the second investigation considers a Multi-Objective (MO) function formulation in which the network voltages are taken into account in the optimization process alongside the total real power loss. In these investigations, unlike synchronous generator studies presented in chapters 4 and 5, the generator unit injects real power into the network while consuming reactive power from the network. It is assumed that there will be sufficient reactive power compensation to maintain the generator excitation during a network fault. Thus, the shunt capacitor is required to provide the entire reactive power demand of the generator locally. The shunt capacitor size is set to vary between 150kvar and 4050kvar with a step size increment of 100kvar.

6.4 Optimal Size/Location of IG with Shunt Capacitors Compensation; Single Objective Optimisation

Induction Generator based Distributed generators are known to inject real power into the grid and consume reactive power from the grid. The goal of this optimization problem is to minimize the network power loss by simultaneously integrating an optimally sized induction generator and shunt capacitors at optimal locations in the network. The Connection of an IG DG unit to the bus is modelled as a negative P and positive Q load. The objective function (minimisation of power loss) was presented in Equation (5.1) and repeated here in Equation (6.29) for convenience.

Minimize $$P_L = \sum_{k=1}^{L} Loss_k = \sum_{l \varepsilon L} (P^l_{i \to j} + P^l_{j \to i}) \quad (6.29)$$

Equations (6.16) - (6.17) and (6.26) are employed to enforce the constraints on short-circuit current and line loading, respectively. The power flow algorithm procedure for computing the reactive power required by the IG is based on Equations (6.1) – (6.14).

In this MSPSO optimisation study of IG, Equations (3.9) - (3.11) of section 3.5.3 are used to handle the integer nature of the DG bus number locations. Similar to the study in chapter 5, the variable representing DG size/output power is initially treated as a continuous variable using Equations (3.1) and (3.2) to update the corresponding position and velocity vectors. The dichotomy algorithm (Equations (3.12) – (3.15)) is then used to constrain the continuous variable (the active power output of the IG) into a discrete variable chosen from unevenly spaced entries in a pre-defined finite search list representing practical IG sizes in megawatts (Appendix B, Table B.1). The IG power flow algorithm is then applied to determine the reactive power required by the IG. For the shunt capacitor, the sizes are generated in a fixed step interval of 100. The implementation flowchart for IG DG integration is as shown in Figure 6.5.

The MSPSO results are recorded after ten independent runs of the algorithm using a swarm population of 20 particles (with five informants), and a stopping criteria of 50 iterations where the objective function value remains within the margin of 10^{-9} or a maximum number of 1000 iterations. The social and the cognitive constants c1and c2 are set equals with both being assigned a value of 1.47 [77]. For the 69-bus network M=70, maximum particle velocity (mv)=1, α=0.4 , w_{max}=0.9 and w_{min} =0.4 [87] are used.

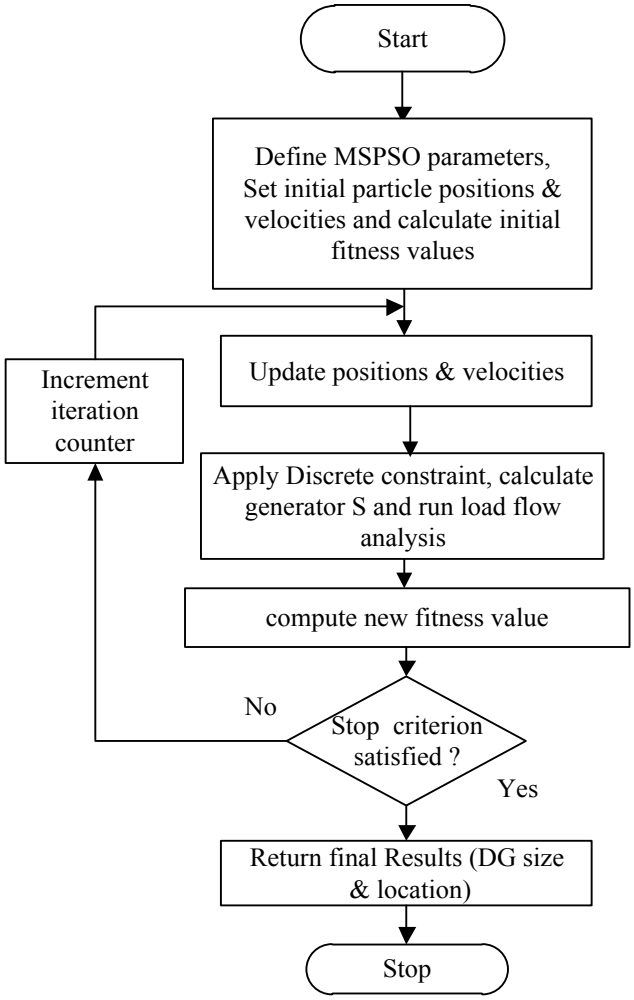

Figure 6.5: MSPSO implementation flowchart for IG DG integration

6.4.1 Scenario I: base network with no generation

Table 6.1 shows a summary of the results for the base test network with no generation. The voltage profile of the original test network (Figure 6.6) clearly shows that nodal voltages are an issue under normal loading condition with an SSEV index 0.0992. The short-circuit current for the base test network is computed as 11.4073kA. In order to demonstrate the importance of short-circuit current constraint in this study, the short-circuit current with the integration of IG DG is set to the assumed value of 11.9kA.

Table 6.1: SUMMARY OF RESULTS; SCENARIO I WITH NO GENERATION (BASE CASE)

Σ Load (MW)	Σ Load (Mvar)	Σ MW Loss	ΣMvar Loss	Max bus voltage (pu)	Min bus voltage (pu)	Mean voltage	Std. Dev	SSEV	Short circuit-current (kA)
3.802	2.690	0.2249	0.1020	1.0000	0.9092	0.9734	0.02724	0.0992	11.4073

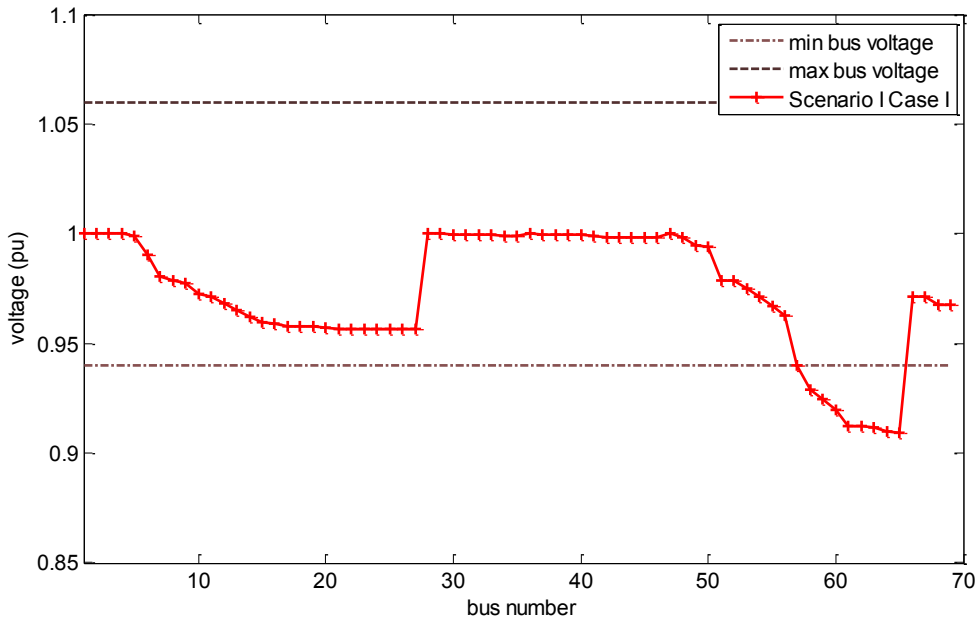

Figure 6.6: Voltage profile of the 69-bus radial distribution network; Scenario I (base case network)

6.4.2 Scenario II: ignoring constraints on short-circuit current and line loading

The results of the MSPSO optimization process for this scenario considering Case I (one generator) and Case II (two generators) are presented in Table 6.2. In Case I, the optimal generator size/location is obtained as 1.85MW (consuming 0.9071Mvar) located at bus number 61. A 63.32% power loss reduction is achieved compared with the base network with the shunt capacitor (0.950Mvar) providing the reactive power demand of the generator entirely locally at the optimal location. For case II, the optimal size/location pair is obtained with two generators sized at 1.85 MW and 0.33MW (consuming 0.9071Mvar and 0.2155 Mvar) located at bus number 61 and 22, respectively. A 68.43% power loss reduction is achieved compared with the base network with the shunt capacitors injecting 0.950Mvar and 0.250Mvar respectively at the optimal bus locations 61 and 22. The entire reactive power demands of the generators are locally provided thus, avoiding unnecessary reactive power flow from the grid.

Table 6.2: MSPSO RESULTS; 69-BUS NETWORK SCENARIO II, CASE I (SINGLE GENERATOR) AND CASE II (TWO GENERATORS)

	Single DG Without constraints; Case I	**Two DG Without constraints; Case II**
Optimal bus location 1	61	61
DG 1 MWs generated	1.85 MW	1.85 MW
DG 1 Mvars consumed	0.9071 Mvar	0.9071 Mvar
Shunt capacitor var 1	0.950 Mvar	0.950 Mvar
Optimal bus location 2	-	22
DG 2 MWs generated	-	0.33 MW
DG 2 Mvars consumed	-	0.2155 Mvar
Shunt capacitor var 2	-	0.250 Mvar
Σ MW loss	0.0825 MW	0.071MW
Σ Mvar loss	0.0402 Mvar	0.0356 Mvar
Min bus voltage	0.9682pu	0.9804pu
Max bus voltage	1.0000 pu	1.0000pu
Mean voltage	0.9873pu	0.9914pu
Standard deviation	0.01159	0.006932
SSEV	0.020344	0.008387
Σ MW loss reduction	63.32%	68.43%
Σ Mvar loss reduction	60.59%	65.10%
Designed Isc (I_k)	11.4073kA	11.4073kA
Specified Isc (I_{spec})	**11.9kA**	
Isc with DGs (I_{fDG})	**11.9664kA**	**11.9913kA**

The improvement in the network voltage profiles for this scenario is presented in Figure 6.7. The minimum bus voltage is improved from 0.9092pu in the base case to 0.9682pu (Case I) and 0.9804pu (Case II). The best improvement in voltage profile is obtained by Case II (with the connection of two generators and shunt capacitors) resulting in a better value of a SSEV (0.008387) compared with the value computed for Case I (0.020344) and the base case (0.0992).

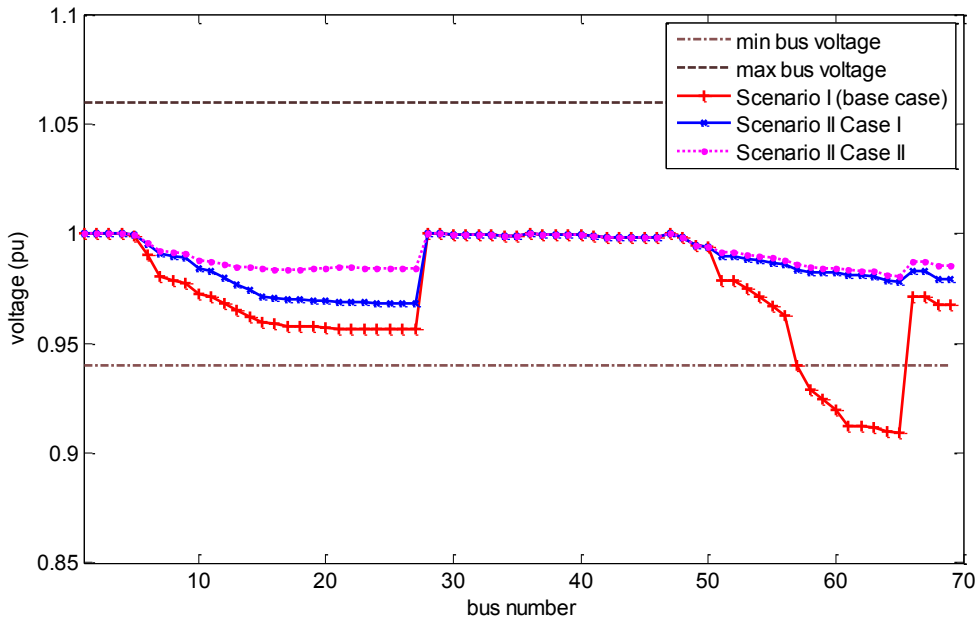

Figure 6.7: Voltage profile of the 69-bus radial distribution network Scenario II (no constraints); Case I (single DG) and Case II (two- DG)

The results in Table 6.2 also show that the final values of short-circuit current (Isc) of 11.9664kA and 11.9913kA (Case I and II, respectively) following the connection of the induction generators, are greater than the computed or design value of the short-circuit current (11.4073kA) for the base case network (without DG). Moreover, these values are equally higher than the presumed allowable short-circuit current (11.9kA). Thus, the connection of the generators resulted in an unacceptable increase in the value of short-circuit current, something that would have to be addressed in practice.

Figures 6.8 and 6.9 show the apparent power (MVA) flow for all branches of the network for Case I and Case II, respectively. It is evident that the connection of DG drastically reduced the apparent power flow in some branches of the network. Moreover, some branches are operating close to their maximum limits with one overloaded branch in the network (Case II, branch 21). There is also a drastic reduction in the apparent power injected from the grid due to the connection of distributed generation as shown in Figures 6.8 and 6.9. Case II resulted in a higher reduction in apparent power flow (due to the connection of two DGs instead of one) when compared with Case I.

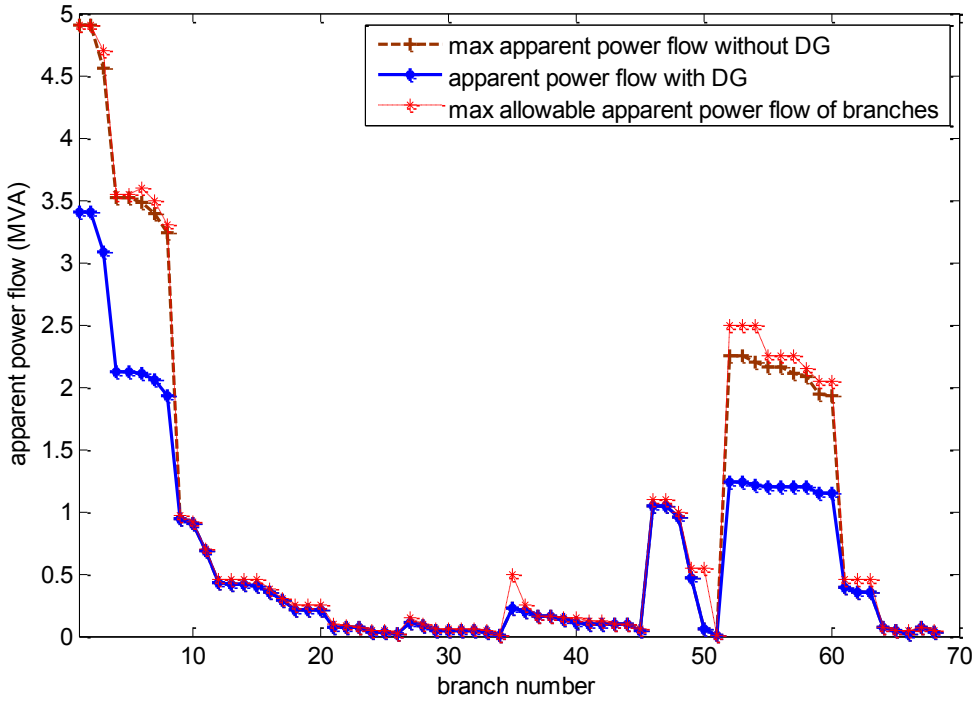

Figure 6.8: Branch apparent power flow/line loading; Scenario II (no constraints), Case I (single DG)

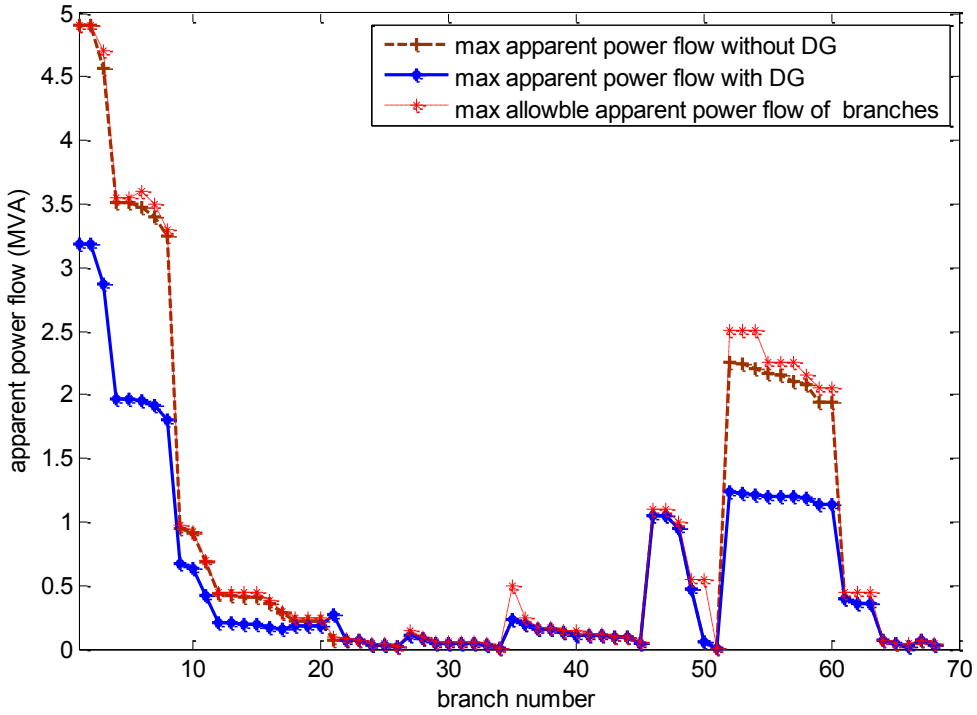

Figure 6.9: Branch apparent power flow/line loading; Scenario II (no constraints), Case II (two-DG)

6.4.3 Scenario III: considering the short-circuit current constraint only

The results of the MSPSO optimization process for this scenario are presented in Table 6.3. In Case I, the optimal size/location is obtained with one optimally sized 1.65MW generator (consuming 0.7635Mvar) located at bus number 63. A 62.96% power loss

reduction is achieved compared with the base case with the shunt capacitor (0.850Mvar) providing the entire of the reactive power requirement of the generator locally. For Case II, the optimal size/location pair is obtained with two optimally sized 0.843 MW generators (each consuming 0.4001Mvar) located at bus number 60 and bus number 64. A 63.36% power loss reduction is achieved compared with the base case. The shunt capacitors (0.450Mvar each) provide the entire reactive power requirement of the generators locally at the optimal locations 60 and 64. A comparison of scenarios II and III show that the percent loss reduction obtained in scenario II (63.32% and 68.43% Case I and II, respectively), is higher than the corresponding figures in scenario III (with a short-circuit constraint). The enforcement of the short-circuit constraint resulted in a

Table 6.3: MSPSO RESULTS; 69-BUS NETWORK SCENARIO III, CASE I (SINGLE GENERATOR) AND CASE II (TWO GENERATORS)

	Single DG With short-circuit constraint Only; Case I	**Two DG With short-circuit constraint only; Case II**
Optimal bus location 1	63	64
DG 1 MWs generated	1.65 MW	0.843MW
DG 1 Mvars consumed	0.7635 Mvar	0.4001 Mvar
Shunt capacitor var 1	0.850 Mvar	0.450 Mvar
Optimal bus location 2	-	60
DG 2 MWs generated	-	0.843 MW
DG 2 Mvars consumed	-	0.4001 Mvar
Shunt capacitor var 2	-	0.450 Mvar
Σ MW loss	0.0833 MW	0.0824MW
Σ Mvar loss	0.0411 Mvar	0.0407 Mvar
Min bus voltage	0.9672pu	0.9674pu
Max bus voltage	1.0000pu	1.0000pu
Mean voltage	0.9861pu	0.9863pu
Standard deviation	0.01237	0.01229
SSEV	0.023701	0.023318
Σ MW loss reduction	62.96%	63.36%
Σ Mvar loss reduction	59.70%	60.10%
Designed Isc (I_k)	11.4073kA	11.4073kA
Specified Isc (I_{spec})	**11.90kA**	
Isc with DGs (I_{fDG})	**11.894kA**	**11.7285kA**

reduction in the optimal size of the IG and a new optimal location compared with scenario II, to satisfy the limitation imposed on switchgear rating.

The improvement in the network voltage profiles with both cases is presented in Figure 6.10. The minimum bus voltage is improved from 0.9092pu in the base case to 0.9672pu (Case I) and 0.9674pu (Case II). Case II resulted in a slightly better voltage profile compared with Case I due to the slight difference in the DG penetration level in both cases (43.40% and 44.35% for Case I and Case II, respectively). However, both these minimum bus voltage values are lower than those obtained in scenario II for the above outlined reasons. Similar to scenario II, the best loss reduction and voltage profile improvement are obtained with the connection of two optimally sized and located generators (Case II).

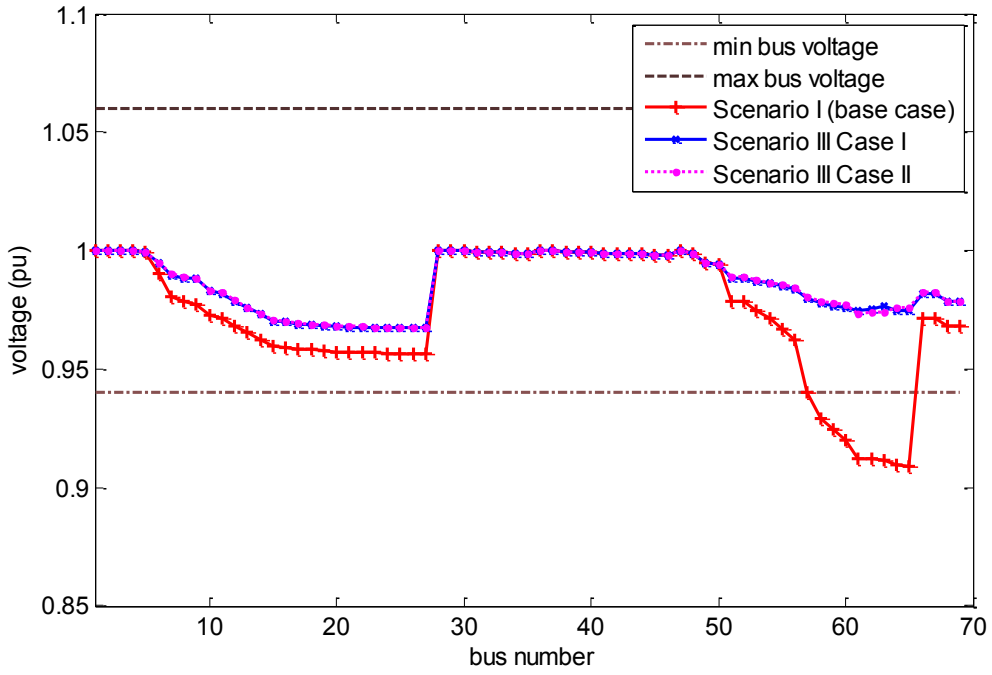

Figure 6.10: Voltage profile of the 69-bus radial distribution network Scenario III (with short-circuit constraint); Case I (single DG) and Case II (two- DG)

The results in Table 6.3 also show that the final values of short-circuit current (Isc) of 11.894kA and 11.7285kA (Case I and Case II, respectively) following the connection of DG are lower than the specified value of the short-circuit current (11.90kA) limit for the network. This is because of the enforcement of short-circuit constraint to ensure that the limitation imposed by the switchgear rating is respected (Equations 6.16 and 6.17). However, the enforcement of the short-circuit current constraint resulted in the violations of the line loading constraint as shown Figure 6.11 and 6.12. The connection

of DG drastically altered the apparent power flows of the network with some branches now operating close to their maximum limits, and some branches (62 and 63 in Case I and 62, 63 and 64 in Case II) exceeding these limits.

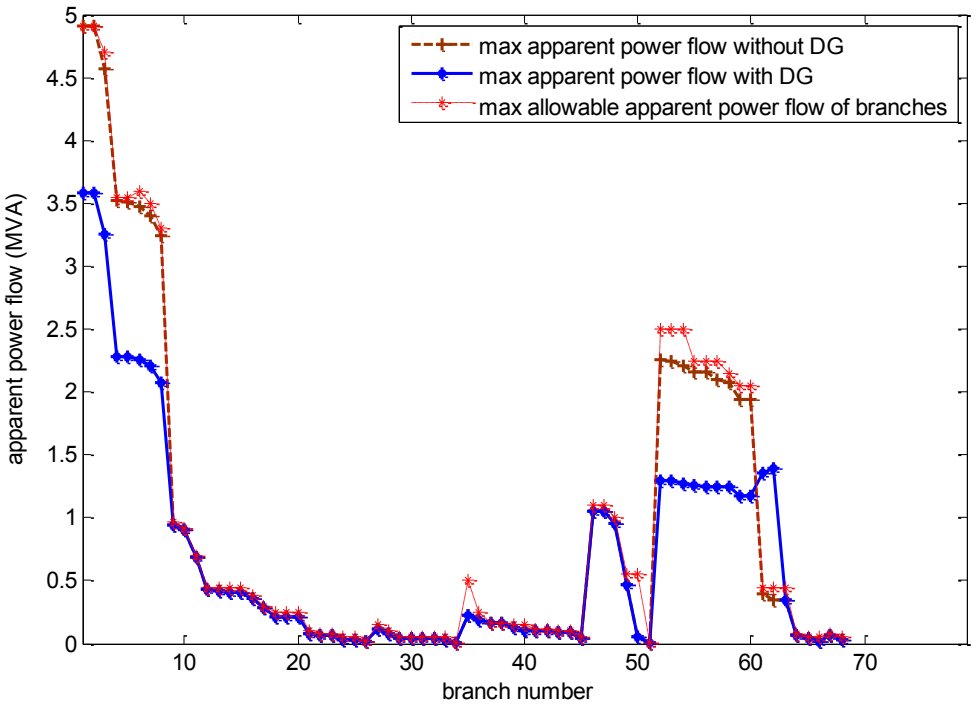

Figure 6.11: 69-bus branch apparent power flow/ line loading Scenario III (with short-circuit constraint), Case I (single DG)

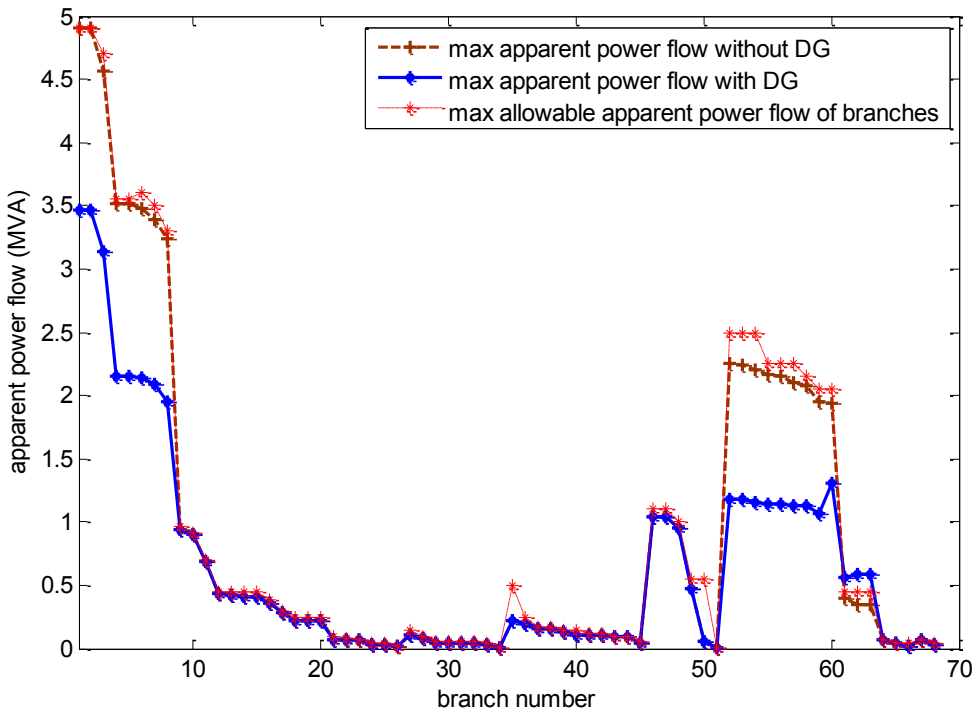

Figure 6.12: 69-bus branch apparent power flow/ line loading Scenario III (with short-circuit constraint), Case I (two- DG)

6.4.4 Scenario IV: considering line loading constraint only

The results of the MSPSO optimization process for this scenario are presented in Table 6.4. In Case I, the optimal size/location is obtained with one 1.85MW generator consuming 0.9071Mvar located at bus number 61. A 63.32% power loss reduction is achieved compared with the base network. The shunt capacitor (0.950Mvar) again provides the entire reactive power demand of the generator locally at the optimal location. Scenario IV (Case I) resulted in the same results as those obtained in scenario II, Case I when both short-circuit current and line loading constraints were neglected.

Table 6.4: MSPSO RESULTS; 69-BUS NETWORK SCENARIO IV, CASE I (SINGLE GENERATOR) AND CASE II (TWO GENERATORS)

	Single DG With line loading constraint Only; Case I	**Two DG With line loading constraint only; Case II**
Optimal bus location 1	61	61
DG 1 MWs generated	1.85 MW	1.85MW
DG 1 Mvars consumed	0.9071 Mvar	0.9071 Mvar
Shunt capacitor var 1	0.950 Mvar	0.950 Mvar
Optimal bus location 2	-	9
DG 2 MWs generated	-	1.50 MW
DG 2 Mvars consumed	-	0.6589 Mvar
Shunt capacitor var 2	-	0.750 Mvar
Σ MW loss	0.0825 MW	0.0756MW
Σ Mvar loss	0.0402 Mvar	0.0368Mvar
Min bus voltage	0.9682pu	0.9774pu
Max bus voltage	1.0000 pu	1.0000pu
Mean voltage	0.9873pu	0.9926pu
Standard deviation	0.01159	0.007986
SSEV	0.020344	0.008151
Σ MW loss reduction	63.32%	66.39%
Σ Mvar loss reduction	60.59%	63.92%
Designed Isc (I_k)	11.4073kA	11.4073kA
Specified Isc (I_{spec})	-	
Isc with DGs (I_{fDG})	**11.9664kA**	**12.461kA**

In Case II, the optimal size/location pair is obtained with two optimally sized 1.85 MW and 1.5 MW generators consuming 0.9071Mvar and 0.6589Mvar located at bus number

61 and 9, respectively. A 66.39% power loss reduction is achieved compared with the base case. The shunt capacitors 0.950Mvar (located at bus 61) and 0.750Mvar (located at bus 9) provide all the reactive power demands of the generators locally.

The enforcement of line loading constraint ensured that the limitation imposed by the line capacity rating is respected. The constraint on line loading Equation (4.10) is implemented by giving an appropriate weighting coefficient to the line loading index of Equation (6.26). In this case, the real power loss is given a higher weighting of 0.9 and the line loading index is given 0.1 thus, the power loss reduction has been given a higher preference. The enforcement of the line loading constraint resulted in the removal of the overload conditions noticed in the branches of the network (Figures 6.11 and 6.12). However, this also resulted in an increase in the values of short-circuit current for both cases. The final values of short-circuit current (11.9664kA and 12.461kA for Case I and Case II, respectively) following the connection of IG are higher than the specified value of the short-circuit current (11.90kA) limit for the network.

The network voltage profiles are presented in Figure 6.13. An improvement in the network voltage profiles is obtained by the simultaneous integration of IG and shunt compensation capacitors in both Cases (the minimum bus voltage is improved from 0.9092pu in the base case to 0.9682pu in Case I and 0.9771pu in Case II). Case II resulted in a better voltage profile compared with Case I due the increased in the penetration level of DG (88.11%). The best loss reduction and voltage profile improvement are obtained with the connection of two optimal DG size and fixed shunt compensation capacitors at the optimal locations (Case II).

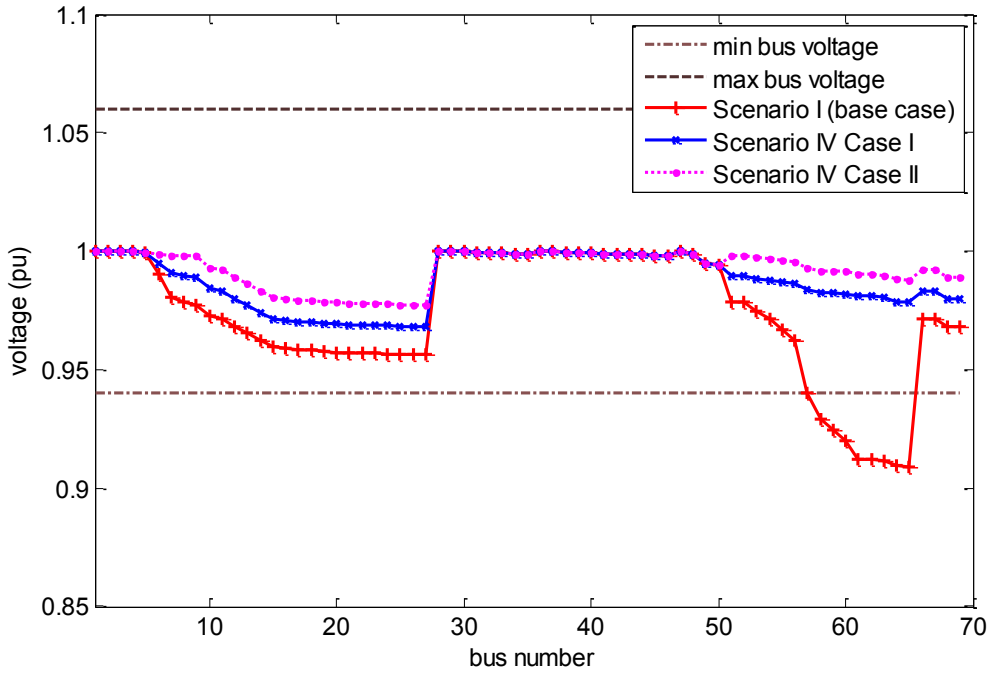

Figure 6.13: Voltage profile of the 69-bus radial distribution network Scenario IV (with line loading constraint), Case I (single DG) and Case II (two-DG)

The results in Table 6.4 also show that the final values of short-circuit current (11.9664kA and 12.461kA for Case I and Case II, respectively) following the connection of IG are higher than the specified value of the short-circuit current (11.90kA) limit for the network.

The apparent power (MVA) flow for all branches of the network is presented in Figures 6.14 and 6.15. Clearly, the overloading of lines that occurs in the branches has been removed with the enforcement of constraints on line loading. There is also a drastic reduction in the apparent power injected from the grid due to the connection of distributed generation as shown in Figures 6.14 and 6.15. Case II resulted in a higher reduction in the apparent power flow (from the connection of two DG) compared to Case I.

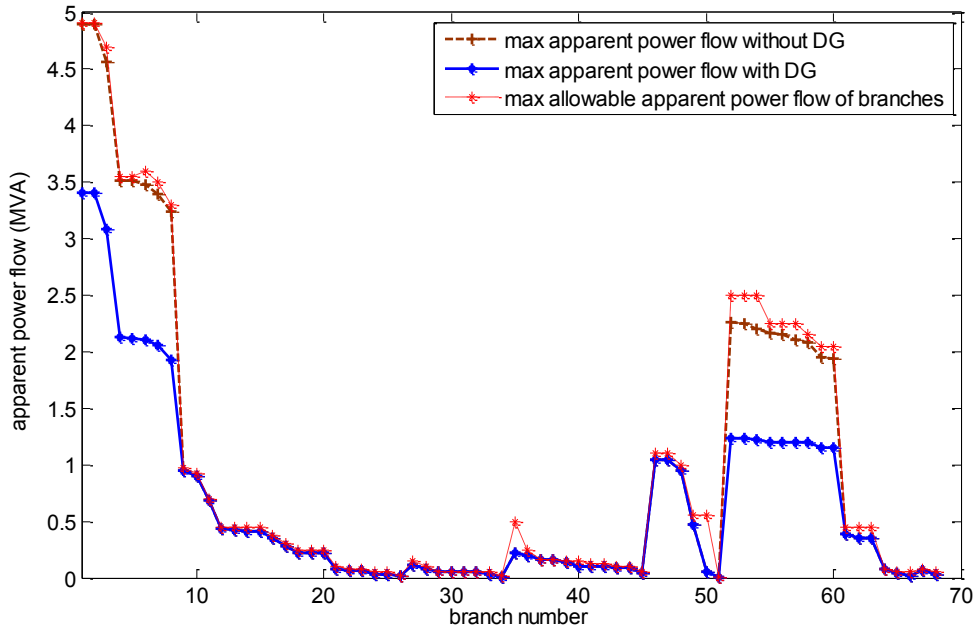

Figure 6.14: 69-bus branch apparent power flow/ line loading Scenario IV (with line loading constraint), Case I (single DG)

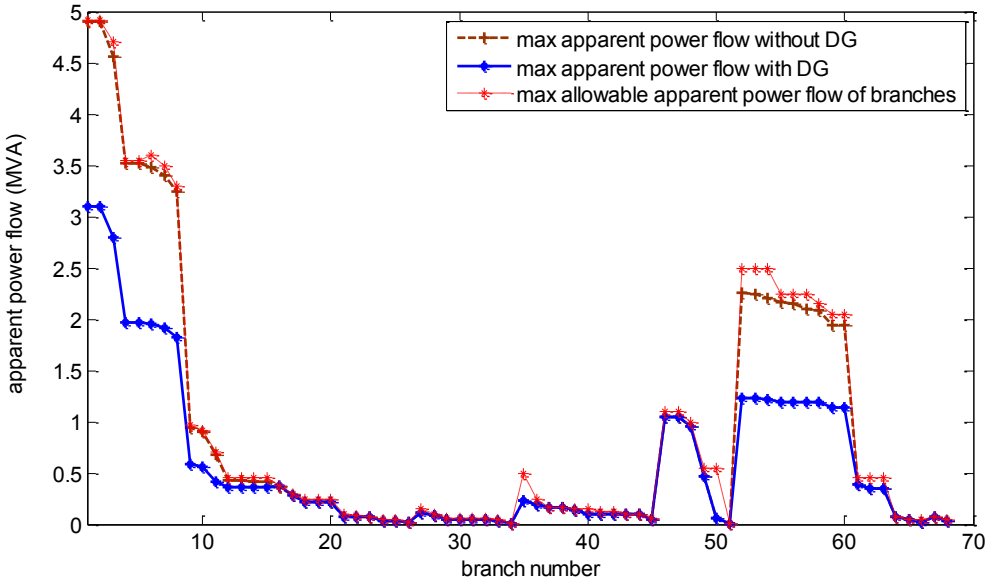

Figure 6.15: 69-bus branch apparent power flow/ line loading Scenario IV (with line loading constraint), Case II (two- DG)

6.4.5 Scenario V: considering both constraints on short-circuit current and line loading

The results of the MSPSO optimization process for this scenario involving Case I and II are presented in Table 6.5. In Case I, the optimal size/location is obtained with one 1.45MW generator consuming 0.9217 Mvar located at bus number 61. A 58.69% power loss reduction is achieved compared to the base case. The shunt capacitor (0.950Mvar) provides above 100% reactive power of the generators locally at the optimal location. In

Case II, the optimal size/location pair is obtained with two 1.0 MW generators, each consuming 0.6389 Mvar located at bus number 61 and bus 60. A 61.85% power loss reduction is achieved compared to the base case. The shunt capacitors (0.650Mvar each) provide above 100% reactive power demands of the generators locally at the optimal locations. A comparison of scenarios II and V shows that the percent loss reduction (63.33%) obtained in scenario II, Case I is higher than the corresponding scenario V, Case I (58.69%). Similarly, for scenario II, case II the percent loss reduction (68.43%) is higher than that of scenario V, case II (61.85%). The lower figures of percent loss reductions obtained with scenario V are due to the enforcement of both short-circuit current (specified as 11.90kA) and line loading constraints.

Table 6.5: MSPSO RESULTS; 69-BUS NETWORK SCENARIO V, CASE I (SINGLE GENERATOR) AND CASE II (TWO GENERATORS)

	Single DG With both short-circuit and line loading constraints; Case I	**Two DG With both short-circuit and line loading constraints; Case II**
Optimal bus location 1	61	61
DG 1 MWs generated	1.45 MW	1.0MW
DG 1 Mvars consumed	0.9217 Mvar	0.6389 Mvar
Shunt capacitor var 1	0.950 Mvar	0.650 Mvar
Optimal bus location 2	-	60
DG 2 MWs generated	-	1.0 MW
DG 2 Mvars consumed	-	0.6389 Mvar
Shunt capacitor var 2	-	0.650 Mvar
Σ MW loss	0.0929 MW	0.0858MW
Σ Mvar loss	0.0452 Mvar	0.0414 Mvar
Min bus voltage	0.9636pu	0.9690pu
Max bus voltage	1.0000pu	1.0000pu
Mean voltage	0.9843pu	0.9879pu
Standard deviation	0.01399	0.01118
SSEV	0.030308	0.018524
Σ MW loss reduction	58.69%	61.85%
Σ Mvar loss reduction	55.68%	59.41%
Designed Isc (I_k)	11.4073kA	11.4073kA
Specified Isc (I_{spec})	**11.90kA**	
Isc with DGs (I_{fDG})	**11.8312kA**	**11.8273kA**

The enforcement is to satisfy the limitations imposed by switchgear rating and the line loading capacity. An improvement in the network voltage profiles are obtained by the simultaneous integration of IG DG and shunt compensation capacitors with both cases as shown in Figure 6.16. The minimum bus voltage is improved from 0.9092pu in the base case to 0.9636pu and 0.9690pu for Case I and II, respectively. Case II resulted in a better voltage profile compared to Case I with an SSEV value of 0.018524. This result is in agreement with the best mean voltage and standard deviation values (0.9879pu and 0.01118, respectively) obtained again by Case II. The best loss reduction and voltage profile improvement are obtained with the connection of two optimal DG size and fixed shunt capacitor compensation at the optimal locations (Case II).

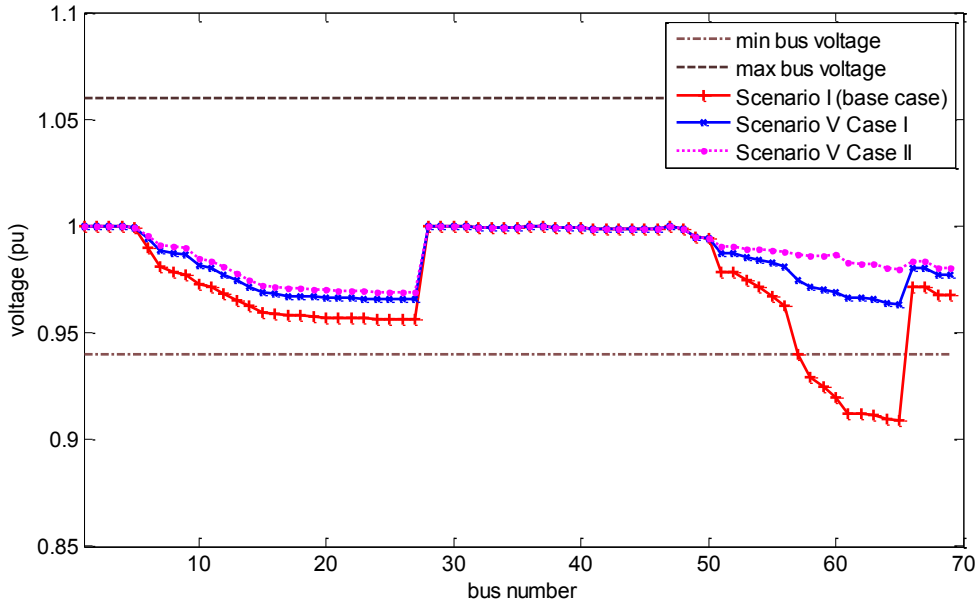

Figure 6.16: Voltage profile of the 69-bus radial distribution network Scenario V (with both constraints) Case I (single DG) and Case II (two- DG)

Table 6.3 also shows that the final values of short-circuit current (11.8312kA and 11.8273kA for Case I and II, respectively) following the connection of IG are lower than the specified value of the short-circuit current (11.90kA) limit for the network. The enforcement of short-circuit constraint ensured that the limitation imposed by the switchgear rating is respected (Equations 6.16 and 6.17). In addition, the enforcement of the constraints of line loading ensured that the apparent power flow in the branches remains within their allowable limits as shown Figure 6.17 and 6.18.

It is evident that the connection of DG resulted in a drastic reduction in the apparent power injected from the grid and the apparent power flow in some branches of the network. Some branches operate close to their maximum limits, but with no branch of

the network overloaded. Case II resulted in a higher reduction in the apparent power injected from the grid compared to the Case I (due to the connection of two DG).

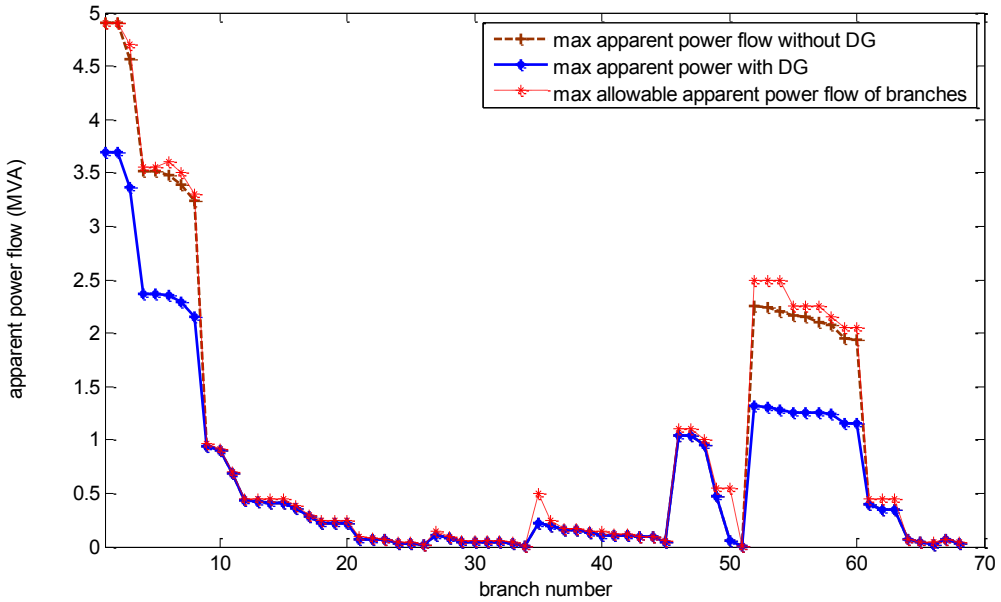

Figure 6.17: 69-bus branch apparent power flow/ line loading Scenario V (with both constraints) Case I (single DG)

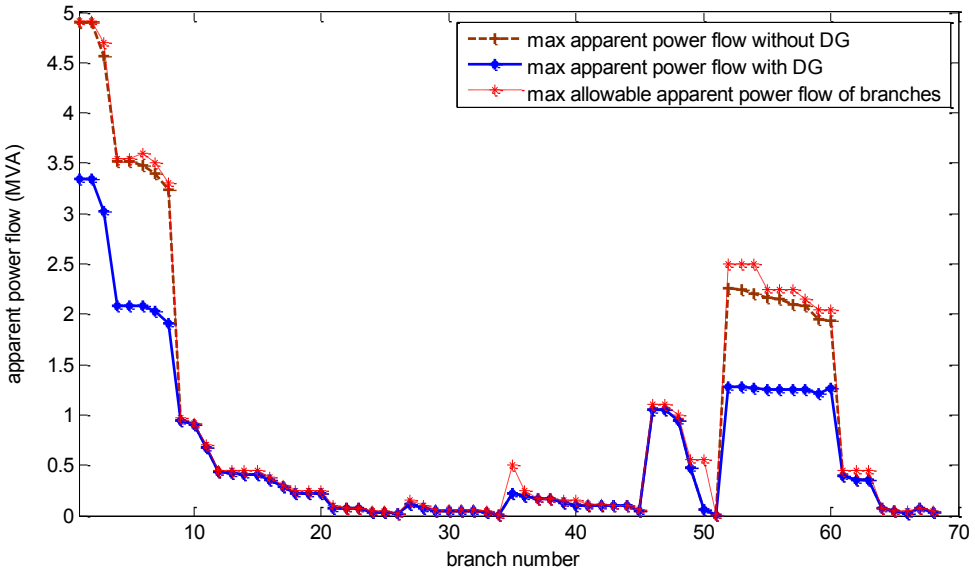

Figure 6.18: 69-bus branch apparent power flow/ line loading Scenario V (with both constraints) Case I (single DG)

A summary of MSPSO results for the single optimization process is presented in Table 6.6 for all the studied scenarios. It is evident from the Table 6.6 that neglecting the constraint imposed by switchgear rating and the line loading limits, the capacity of the network to absorb new generations and thus the technical benefits of the connection of DG is overestimated.

Table 6.6: MSPSO SUMMARY RESULTS; 69-BUS NETWORK SINGLE OBJECTIVE

			Optimal bus location(s)	Optimum DG size (s) (MW/Mvar)	Power loss reduction (%)	SSEV	Short-circuit current
Case I	Scenarios	I	-	-	-	0.0993	11.4073
		II	61	1.85/0.9071	63.32	0.020344	11.9664
		III	63	1.65/0.7635	62.96	0.023701	11.894
		IV	61	1.85/0.9071	63.32	0.020344	11.9664
		V	61	1.45/0.9217	58.69	0.03038	11.8312
Case II	Scenarios	I	-	-	-	0.0993	11.4073
		II	61/22	1.85/0.9071;0.33/0.2155	68.43	0.008387	11.9913
		III	64/60	0.843/0.4001;0.843/0.4001	63.36	0.023318	11.7285
		IV	61/9	1.85/0.9071;1.5/0.6589	66.39	0.008151	12.461
		V	60/61	1/0.6389;1/0.6389	61.85	0.018524	11.8273

6.5 Optimal Size/Location of IG with Shunt Capacitors Compensation; Multi-Objective Optimisation

Renewable DG of the type with electronic converter interfaced to the electric grid can provide voltage support and regulate the voltage at the PCC in a similar way to that of synchronous generator based DG (studies in chapters 4 and 5). However, this is not possible with a fixed speed induction generator DG that is directly interfaced with the grid. Asynchronous induction machines rely on reactive power support from the network to which they are connected. Thus, a fixed speed IG cannot be modelled as PV generator to contribute to network voltage support since it does not have enough reactive power capability to hold its terminal voltage at a specified value. A multi-objective (MO) implementation (considering the improvement in the voltage profile as one of the objectives) can help improve the network voltage profile when IG based distributed generation is employed in the network. Multi-objective problems are likely to be associated with conflicting objectives requiring a trade-off solution.

In this multi-objective formulation, the MSPSO algorithm minimizes the real power loss and network voltage deviations while enforcing the constraints of short circuit-current rating of switchgear and line loading capacity.

The objective function (f_{obj}) to be optimized can be written as:

Minimise $f_{obj} = k_1 \cdot P_L + k_2 \cdot f(v) + k_3 \cdot f(IC)$ (6.30)

where: P_L is the objective of real power loss reduction given in Equation (6.29), *f(v)* and *f(IC)* are the objective of voltage optimisation and the quadratic index that transformed the inequality constraint of line loading into an objective as defined in Equations (5.2) and (6.29) respectively. These objectives are repeated here in Equations (6.31) - (6.34) for convenience.

$$P_L = \sum_{k=1}^{L} Loss_k = \sum_{l \varepsilon L} abs\,(P^l_{i \to j} + P^l_{j \to i}) \tag{6.31}$$

$$f(v) = \sum_{i=1}^{N_b} (V_i - V_{n,i})^2 \tag{6.32}$$

$$f(IC) = \sum_{l \varepsilon L} (S_l - S_l^{\max})^2 \tag{6.33}$$

Thus, minimise

$$f_{obj} = k_1 \cdot \sum_{l \varepsilon L} abs\,(P^l_{i \to j} + P^l_{j \to i}) + k_2 \cdot \sum_{i=1}^{N_b} (V_i - V_{n,i})^2 + k_3 \cdot \sum_{l=1}^{L} (S_l - S_l^{\max})^2 \tag{6.34}$$

Where k_1, k_2 and k_3 are weighting factors selected such that their values must sum to unity. These are used to assign a certain importance to each of the objectives considered in the study and their values may vary according to engineering judgment [33]. In this section, when the objectives of loss reduction and voltage optimization only are considered, they are given equal weighting (values of $k_1 = k_2 = 0.5$ are used) similar to the studies in chapters 4 and 5. The voltages at the buses are bound by the constraints in Equation (4.9) related to upper and lower voltage limit violations. The constraint on short-current rating of the switchgear and line loading capacity are also enforced where applicable. When it is required to enforce the line loading constraint, the weighting factors are adjusted accordingly to accommodate such additional constraint such that their values must sum to unity (values of $k_1 = k_2 = 0.45$ and $k_3 = 0.10$ are used).

This investigation involves the same five scenarios (and Cases) considered previously in the single objective study of section 6.4. The optimization results are recorded after ten independent runs of the MSPSO algorithm using the same parameters setting of section 6.4.

6.5.1 Scenario I: base network with no generation

This scenario is common to both single and multi-objective studies. The results for the base test network are as presented in Table 6.1 (section 6.4).

6.5.2 Scenario II: ignoring constraints on short-circuit current and line loading; multi-objective optimisation

The results of MSPSO for this scenario are presented in Table 6.7. In Case I (one generator), the optimal size/location is obtained with one 3.0MW generator consuming 1.509 Mvar located at bus number 59. A 46.42% power loss reduction is achieved compared to the base case and the shunt capacitor (1.550 Mvar) provides all the reactive power demand of the generator locally at the optimal location.

Table 6.7: MSPSO RESULTS; 69-BUS NETWORK SCENARIO II, CASE I (SINGLE GENERATOR) AND CASE II (TWO GENERATORS); MULTI-OBJECTIVE OPTIMISATION

	Single DG Without constraints; Case I	**Two DG Without constraints; Case II**
Optimal bus location 1	59	63
DG 1 MWs generated	3.0 MW	2.0 MW
DG 1 Mvars consumed	1.509 Mvar	0.9955 Mvar
Shunt capacitor var 1	1.550 Mvar	1.050 Mvar
Optimal bus location 2	-	18
DG 2 MWs generated	-	0.843 MW
DG 2 Mvars consumed	-	0.4001 Mvar
Shunt capacitor var 2	-	0.450 Mvar
Σ MW loss	0.1205 MW	0.0762MW
Σ Mvar loss	0.0542 Mvar	0.0375 Mvar
Min bus voltage	0.9750pu	0.9918pu
Max bus voltage	1.0150 pu	1.0060pu
Mean voltage	0.9938pu	0.9996pu
Standard deviation	0.01031	0.0040
SSEV	0.009904	0.001316
Σ MW loss reduction	46.42%	66.12%
Σ Mvar loss reduction	46.86%	63.24%
Designed Isc (I_k)	11.4073kA	11.4073kA
Specified Isc (I_{spec})	-	
Isc with DGs (I_{fDG})	**12.2539kA**	**12.1348kA**

In Case II (two generators), the optimal size/location pair is obtained with two 2.0 MW and 0.843 MW generators consuming 0.9955Mvar and 0.4001 Mvar located at bus number 63 and 18, respectively. A 66.12% power loss reduction is achieved in this case compared with the base case. Moreover, the shunt capacitors (1.550 Mvar and 0.450Mvar) provide the entire reactive power demand of the generators locally at the optimal locations 63 and 18 respectively.

The improvement in the network voltage profiles is presented in Figure 6.19. The minimum bus voltage is improved from 0.9092pu in the base case to 0.9938pu and 0.9996pu in Case I and II, respectively. The best improvement in the voltage profiles is obtained by Case II with a calculated SSEV value of 0.001316. This result is consistent with the best mean voltage and standard deviation (0.9996pu and 0.0040, respectively) achieved in Case II with the voltages virtually improved to 1pu.

The voltage profile improvement is greater than that obtained in the corresponding scenario in a single objective study (section 6.4.2). The loss reduction figures, however, are lower, reflecting the fact that, in multi-objective optimization study, the improvement in one objective (voltage minimisation) would usually result in the worsening of another objective (power loss reduction).

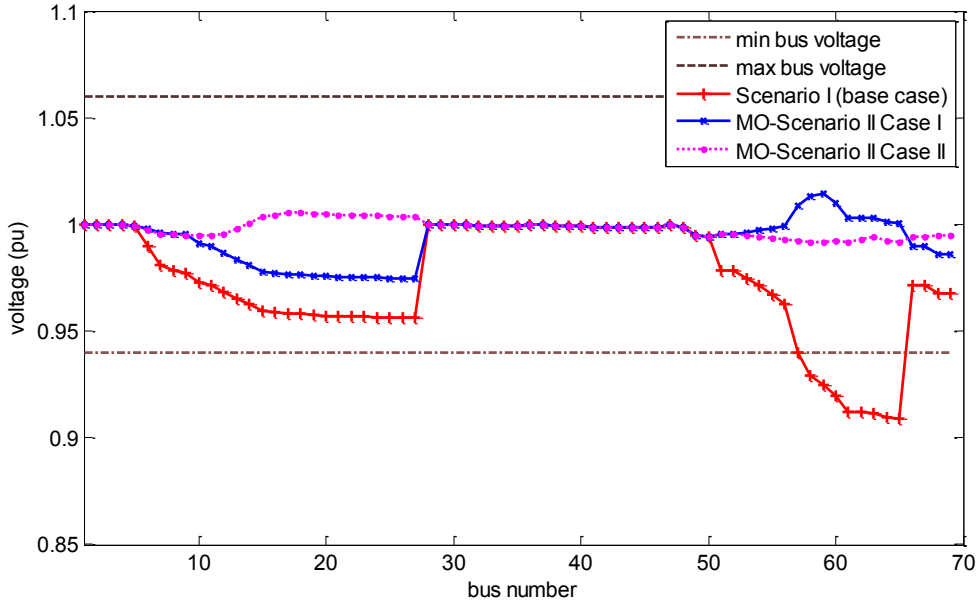

Figure 6.19: Voltage profile of the 69-bus radial distribution network Scenario II (no constraints), Case I (single DG) and Case II (two-DG); multi-objective optimisation

The results in Table 6.7 also show that the final values of short-circuit current (12.2539kA and 12.1348kA for Case I and II, respectively) following the connection of IG are greater than the computed value of the short-circuit current (11.4073kA) for the base case network. Thus, the connections of IG DG results in an increase in the value of short-circuit current.

Figures 6.20 and 6.21 show the apparent power (MVA) flow for all branches of the network for Case I and Case II, respectively. The connection of DG drastically alters the apparent power flow in the network and with some branches operating close to their maximum limits. In Figure 6.24, it is evident that the inclusion of voltage optimization in the objective function results in the overloading of some branches of the network (branches 61 and 62). There is also a drastic reduction in the apparent power injected from the grid due to the connection of DG.

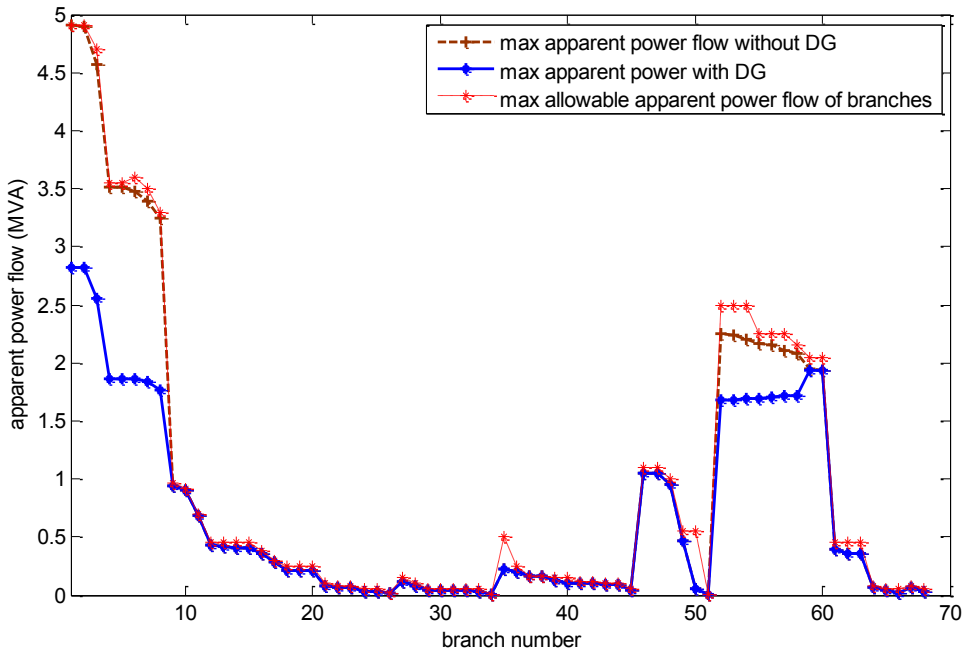

Figure 6.20: 69-bus branch apparent power flow/ line loading Scenario II (no constraints), Case I(single DG); multi-objective optimisation

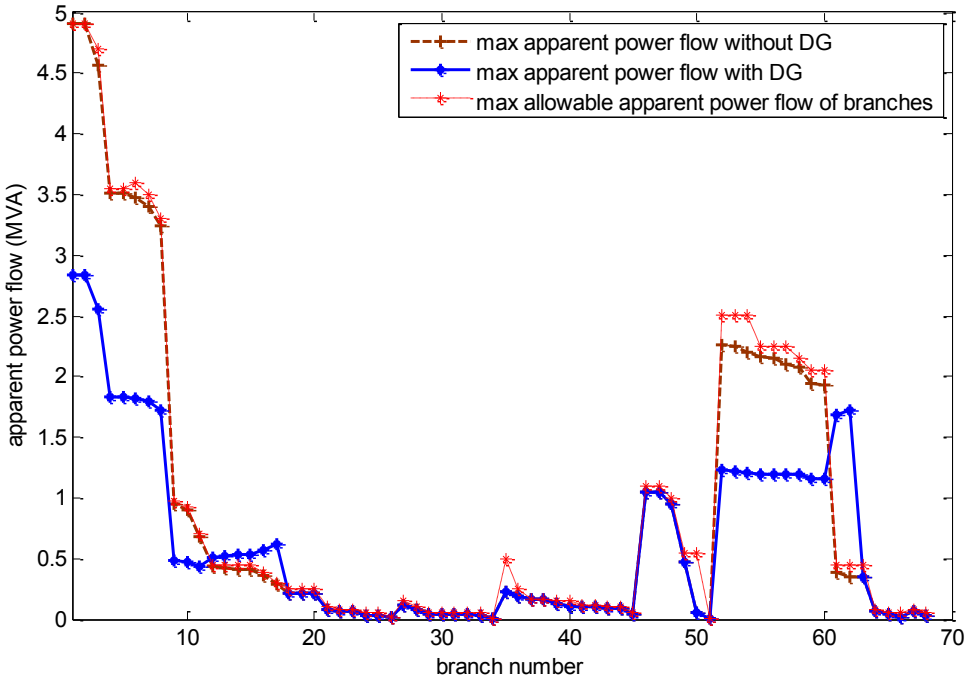

Figure 6.21: 69-bus branch apparent power flow/ line loading Scenario II (no constraints), Case II (two-DG); multi-objective optimisation

6.5.3 Scenario III: considering the short-circuit current constraint only; multi-objective optimisation

The optimal size/location results for this scenario using MSPSO are presented in Table 6.8. In Case I, the optimal size/location is obtained with one 2.0MW generator consuming 0.9955Mvar located at bus number 65. A 46.95% power loss reduction is achieved compared to the base case, with a shunt capacitor (1.05Mvar) providing slightly above 100% reactive power of the generator locally at the optimal bus location. In Case II, the optimal size/location pair is obtained with two 1.0 MW generators, each consuming 0.6389Mvar connected at bus number 61 and bus number 64. A 61.23% power loss reduction is achieved compared to the base case. Two shunt capacitors (0.650Mvars each) provide all the reactive power demands of the generators at the optimal locations.

The network voltage profiles are presented in Figure 6.23. The minimum bus voltage is improved from 0.9092pu in the base case to 0.9690pu (Case I and Case II). The best SSEV value (0.017415) is obtained by Case I. This is in agreement with the best mean voltage and a standard deviation (0.9903pu and 0.0113, respectively) also obtained in Case I.

Table 6.8: MSPSO RESULTS; 69-BUS NETWORK SCENARIO III, CASE I (SINGLE GENERATOR) AND CASE II (TWO GENERATORS); MULTI-OBJECTIVE OPTIMISATION

	1DG With short-circuit constraint Only **Case I**	**2DG With short-circuit constraint only** **Case II**
Optimal bus location 1	65	64
DG 1 MWs generated	2.0 MW	1.0MW
DG 1 Mvars consumed	0.9955 Mvar	0.6389 Mvar
Shunt capacitor var 1	1.050 Mvar	0.650 Mvar
Optimal bus location 2	-	61
DG 2 MWs generated	-	1.0 MW
DG 2 Mvars consumed	-	0.6389 Mvar
Shunt capacitor var 2	-	0.650 Mvar
Σ MW loss	0.1193 MW	0.0872MW
Σ Mvar loss	0.0591 Mvar	0.0422 Mvar
Min bus voltage	0.9690pu	0.9690pu
Max bus voltage	1.008pu	1.0000pu
Mean voltage	0.9903pu	0.9884pu
Standard deviation	0.0113	0.01103
SSEV	0.017415	0.017537
Σ MW loss reduction	46.95%	61.23%
Σ Mvar loss reduction	42.06%	58.63%
Designed Isc (I_k)	11.4073kA	11.4073kA
Specified Isc (I_{spec})	**11.90kA**	
Isc with DGs (I_{fDG})	**11.8875kA**	**11.8111kA**

From the results in Table 6.8 it is obvious that the final values of short-circuit current (11.8875kA and 11.8111kA for Case I and Case II, respectively) with the connection of the generators are lower than the specified value of the short-circuit current (11.90kA) limit for the network. The enforcement of short-circuit constraints ensured that the limitation imposed by the switchgear rating is respected.

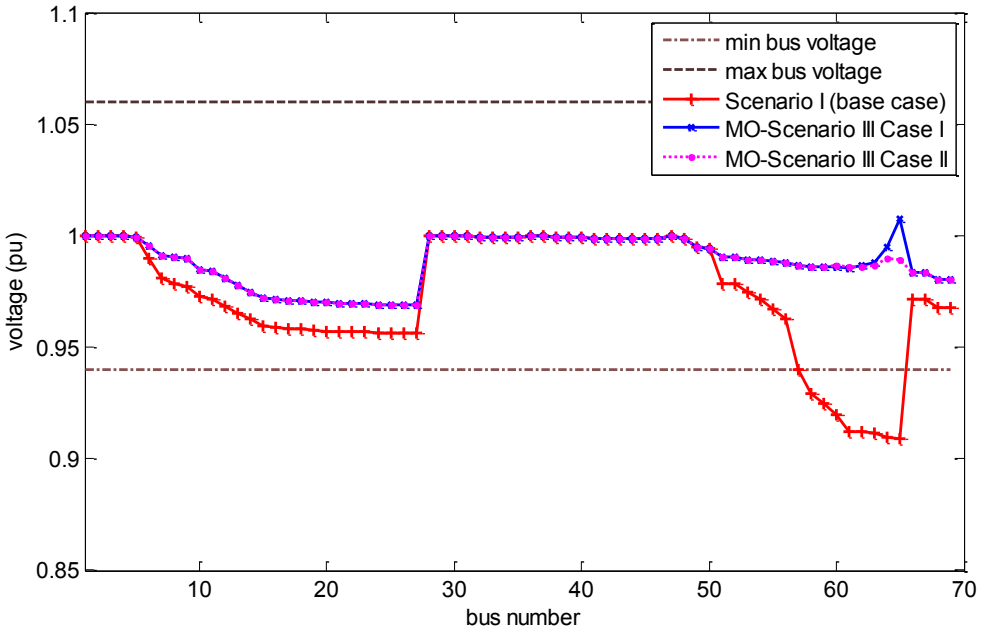

Figure 6.22: Voltage profile of the 69-bus radial distribution network Scenario III (with short-circuit constraints), Case I (single DG) and Case II (two-DG); multi-objective optimisation

This, however, results in violations of the line loading constraint as shown Figure 6.26 (branches 61 and 62, 63 and 64 for case I) and 6.27 (branches 61, 62 and 63 for case II). It is also evident that the connection of DG drastically alters the apparent power flow in some branches of the network with some branches operating close to their maximum limits.

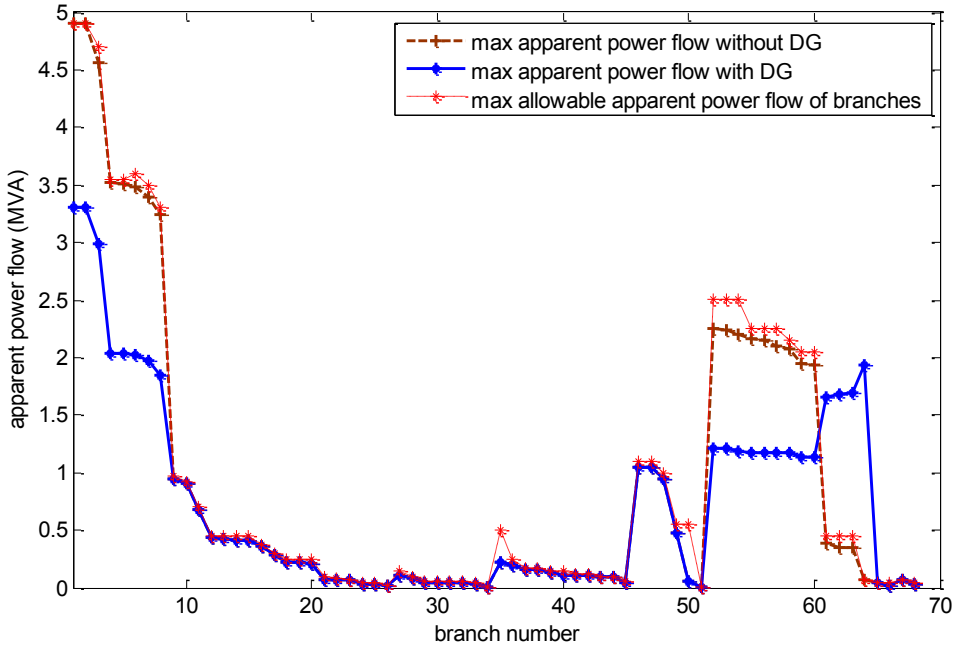

Figure 6.23: 69-bus branch apparent power flow/ line loading Scenario III(with short-circuit constraint), Case I (single DG); multi-objective optimisation

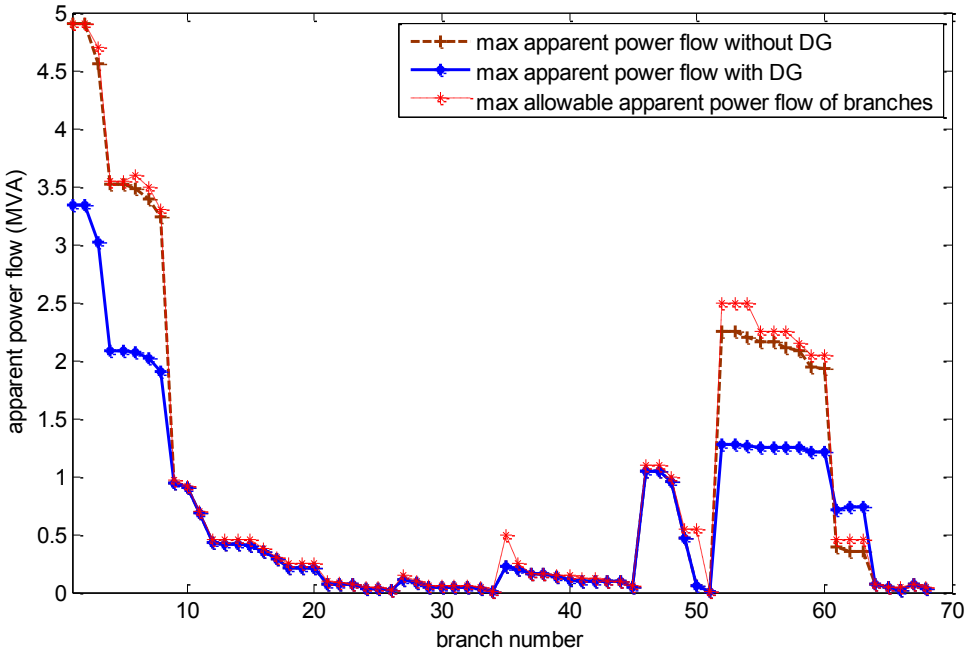

Figure 6.24: 69-bus branch apparent power flow/ line loading Scenario III (with short-circuit constraint), case II (two-DG); multi-objective optimisation

There is also a substantial reduction in the apparent power injected from the grid due to the connection of distributed generation as shown in Figures 6.26 and 6.27.

6.5.4 Scenario IV: considering line loading constraint only; multi-objective optimisation

The results of the MSPSO optimization process for this scenario are presented in Table 6.9. In Case I, the optimal size/location is obtained with one 3.0 MW generator consuming 1.509 Mvar located at bus number 59. A 46.42% power loss reduction is achieved compared with the base case. Moreover, the shunt capacitor (1.550Mvar) provides the entire reactive power demand of the generator at the optimal location locally. In Case II, the optimal size/location pair is obtained with two 2.0MW and 3.0MW generators consuming 0.9955 Mvar and 1.509Mvar located at bus number 61 and bus number 9, respectively. A 54.82% power loss reduction is achieved with the shunt capacitors (1.05Mvar and 1.550Mvar) providing the entire reactive power demands of the generators at their optimal locations locally.

Table 6.9: MSPSO RESULTS; 69-BUS NETWORK SCENARIO IV (WITH LINE LOADING CONST-RAINT), CASE I (SINGLE DG) AND CASE II (TWO-DG); MULTI-OBJECTIVE OPTIMISATION

	Single DG With line loading constraint Only; Case I	**Two DG With line loading constraint only; Case II**
Optimal bus location 1	59	61
DG 1 MWs generated	3.0 MW	2.0MW
DG 1 Mvars consumed	1.509 Mvar	0.9955 Mvar
Shunt capacitor var 1	1.550 Mvar	1.050 Mvar
Optimal bus location 2	-	9
DG 2 MWs generated	-	3.0 MW
DG 2 Mvars consumed	-	1.509 Mvar
Shunt capacitor var 2	-	1.50 Mvar
Σ MW loss	0.1205 MW	0.1016MW
Σ Mvar loss	0.0542 Mvar	0.0507Mvar
Min bus voltage	0.9750pu	0.9868pu
Max bus voltage	1.0150 pu	1.007pu
Mean voltage	0.9938pu	0.9985pu
Standard deviation	0.01031	0.006069
SSEV	0.009904	0.002651
Σ MW loss reduction	46.42%	54.82%
Σ Mvar loss reduction	46.86%	50.29%
Designed Isc (I_k)	11.4073kA	11.4073kA
Specified Isc (I_{spec})	-	
Isc with DGs (I_{fDG})	**12.2539kA**	**13.635kA**

The network voltage profiles are presented in Figure 6.25. An improvement in the network voltage profiles is obtained with the minimum bus voltage improved from 0.9092pu in the base case to 0.9750pu and 0.9868pu, for case I and II respectively. The best SSEV figure of 0.002651 is obtained in Case II. This is in agreement with the best of the mean voltage and the voltage standard deviation figures of 0.9985pu and 0.006069 respectively also obtained with Case II.

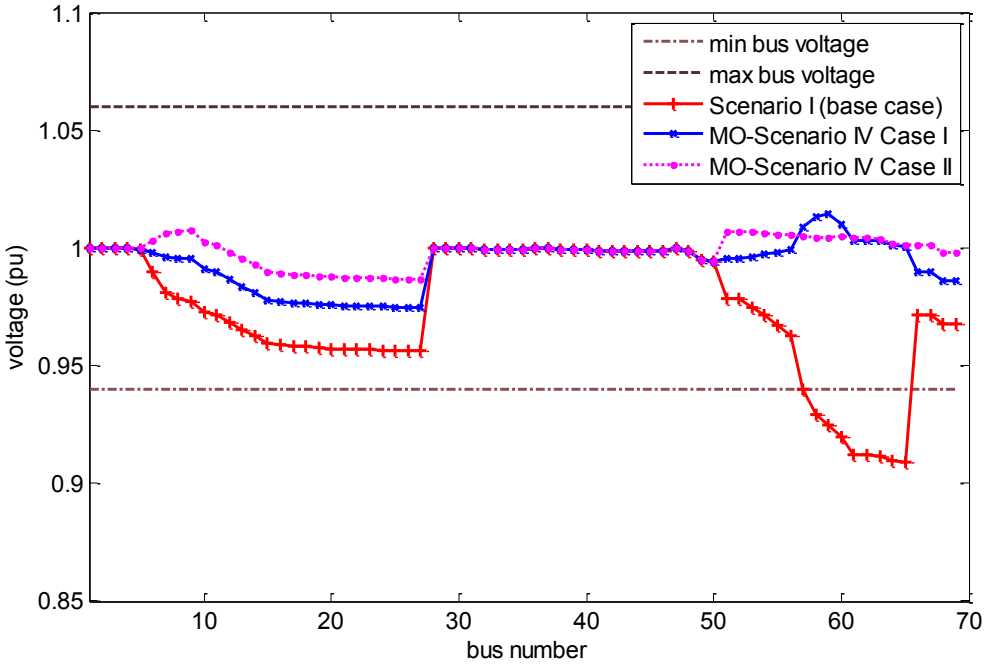

Figure 6.25: Voltage profile of the 69-bus radial distribution network Scenario IV (with line loading constraint): Case I (single generator) and Case II (two generators); multi-objective optimisation

The line loading constraint Equation (4.10) is implemented by giving an appropriate weighting coefficient to the line loading index of Equation (6.26). The real power loss is assigned a weighting of 90%, and the line loading index is assigned a 10% weighting. The apparent power (MVA) flows for all branches of the network are presented in Figures 6.26 and 6.27. The enforcement of line loading constraints ensured that the limitation imposed by the line capacity rating (Equation 4.10) is respected. It is evident from Figures 6.26 and 6.27 that the enforcement of the line loading constraints resulted in the removal of the overload noticed previously in Figures 6.23 and 6.24.

The results in Table 6.9 also show that the final values of short-circuit current of 12.2539kA and 13.635kA (for Case I and Case II, respectively) with the connection of the induction generators are higher than the specified value of the short-circuit current (11.90kA) limit for the network. The enforcement of line loading constraint only resulted in the increased in the short-circuit current of the network because of the relocation of the DG to a new optimal location. There is also a substantial reduction in the apparent power injected from the grid due to the connection of distributed generation as shown in Figures 6.26 and 6.27.

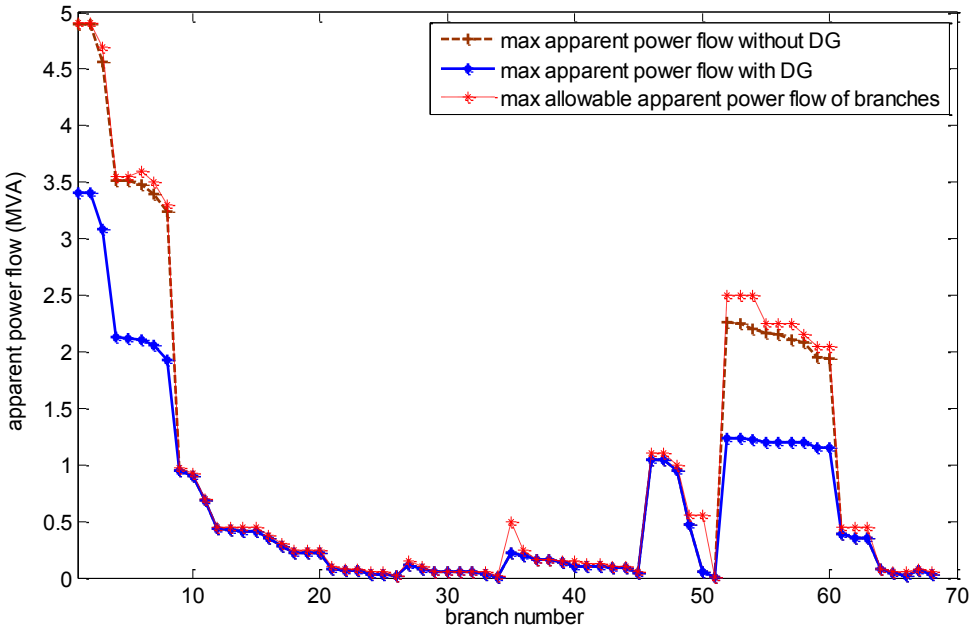

Figure 6.26: 69-bus branch apparent power flow/ line loading Scenario IV (with line loading constraint), Case I (single DG); multi-objective optimisation

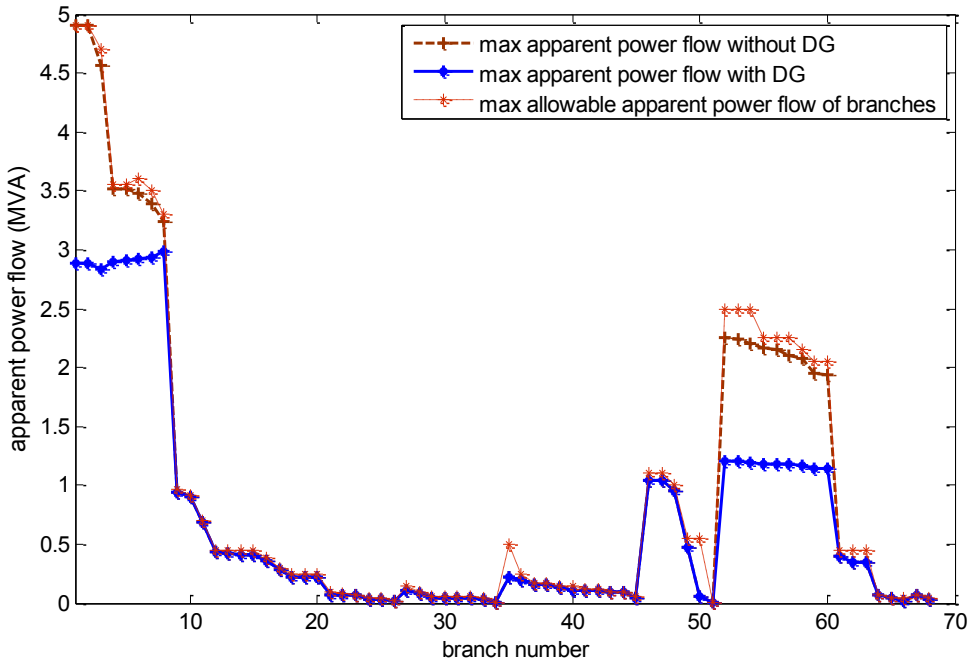

Figure 6.27: 69-bus branch apparent power flow/ line loading Scenario IV (with line loading constraint), Case II (two- DG); multi-objective optimisation

6.5.5 Scenario V: considering both constraints on short-circuit current and line loading; multi-objective optimisation

The results of the MSPSO optimization process for this scenario are presented in Table 6.10. In Case I, the optimal size/location is obtained with one 1.45MW generator consuming 0.9217 Mvar located at bus number 61. A 58.69% power loss reduction is achieved with the shunt capacitors providing the entire reactive power of the generators locally. In Case II, the optimal size/location pair is obtained with two optimally 1.0 MW generators, each consuming 0.6389 Mvar located at bus number 61 and bus number 60. A 61.85% power loss reduction is achieved in this case with the shunt capacitors providing the entire reactive power requirement of the generators locally.

Table 6.10: MSPSO RESULTS; 69-BUS NETWORK SCENARIO IV (WITH BOTH CONSTRAINTS), CASE I (SINGLE DG) AND CASE II (TWO-DG); MULTI-OBJECTIVE OPTIMISATION

	1DG With both short-circuit and line loading constraints: Case I	**2DG With both short-circuit and line loading constraints: Case II**
Optimal bus location 1	61	61
DG 1 MWs generated	1.45 MW	1.0MW
DG 1 Mvars consumed	0.9217 Mvar	0.6389 Mvar
Shunt capacitor var 1	0.950 Mvar	0.650 Mvar
Optimal bus location 2	-	60
DG 2 MWs generated	-	1.0 MW
DG 2 Mvars consumed	-	0.6389 Mvar
Shunt capacitor var 2	-	0.650 Mvar
Σ MW loss	0.0929 MW	0.0858MW
Σ Mvar loss	0.0452 Mvar	0.0414 Mvar
Min bus voltage	0.9636pu	0.9690pu
Max bus voltage	1.0000pu	1.0000pu
Mean voltage	0.9843pu	0.9879pu
Standard deviation	0.01399	0.01118
SSEV	0.030308	0.018524
Σ MW loss reduction	58.69%	61.85%
Σ Mvar loss reduction	55.68%	59.41%
Designed Isc (I_k)	11.4073kA	11.4073kA
Specified Isc (I_{spec})	**11.90kA**	
Isc with DGs (I_{fDG})	**11.8312kA**	**11.8273kA**

The network voltage profiles are shown in Figure 6.28. An improvement in the network voltage profiles is achieved with the minimum bus voltage improved from 0.9092pu in the base case to 0.9636pu and 0.9690pu for Case I and Case II, respectively. The best SSEV, mean voltage and standard deviation values of 0.018524, 0.9879pu and 0.01118, respectively, are obtained with Case II.

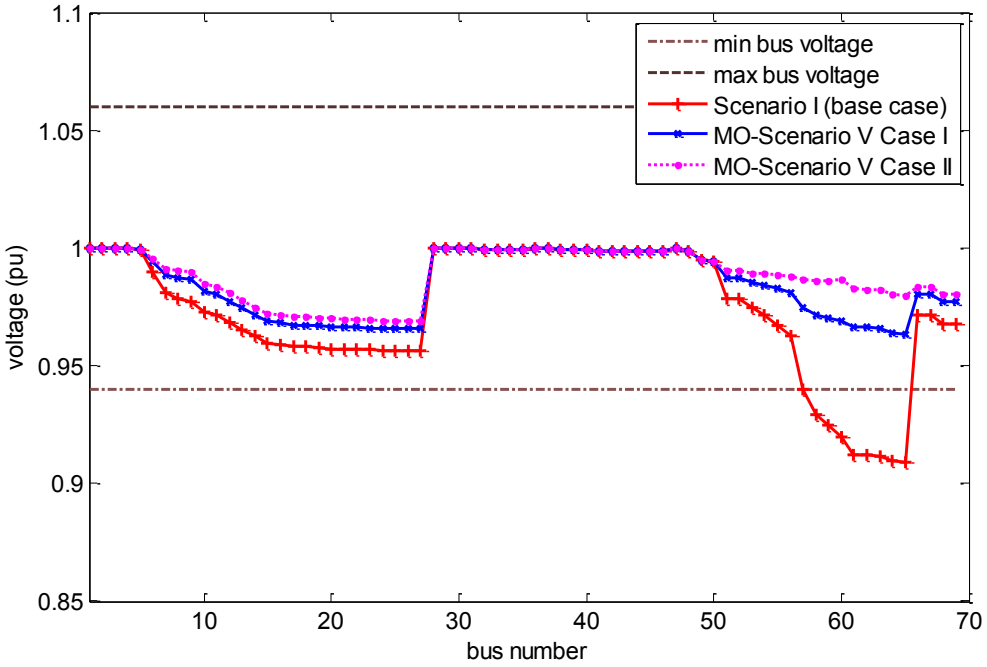

Figure 6.28: Voltage profile of the 69-bus radial distribution network Scenario V (with both constraints), Case I (single generator) and Case II (two generators); multi-objective optimisation

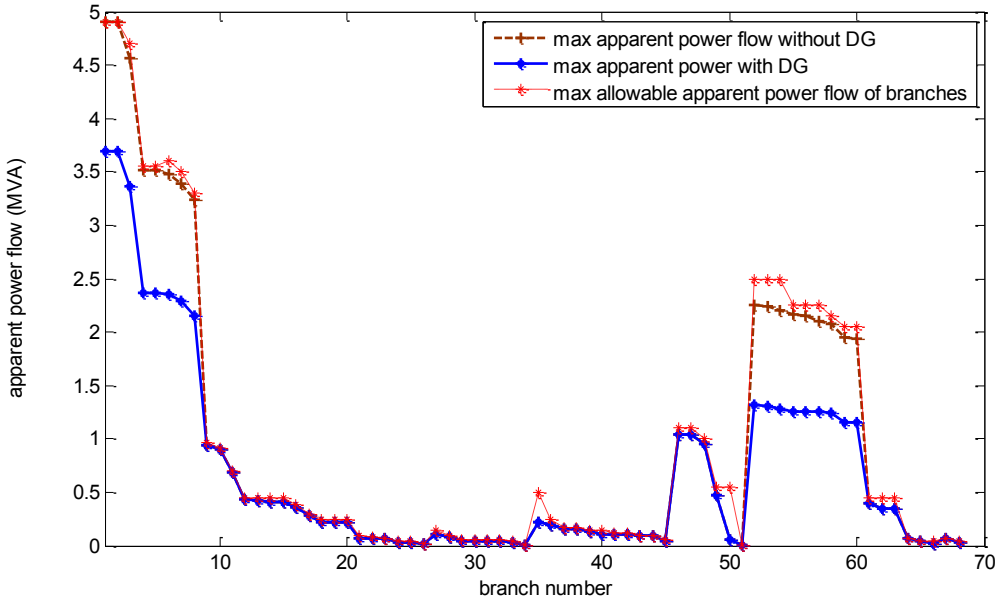

Figure 6.29: 69-bus branch apparent power flow/ line loading Scenario V (with both constraints), Case I (single DG); multi-objective optimisation

The results in Table 6.10 show that the final values of short-circuit current following the connection of DG are now lower than the specified value of the short-circuit current (11.90kA) limit for the network.

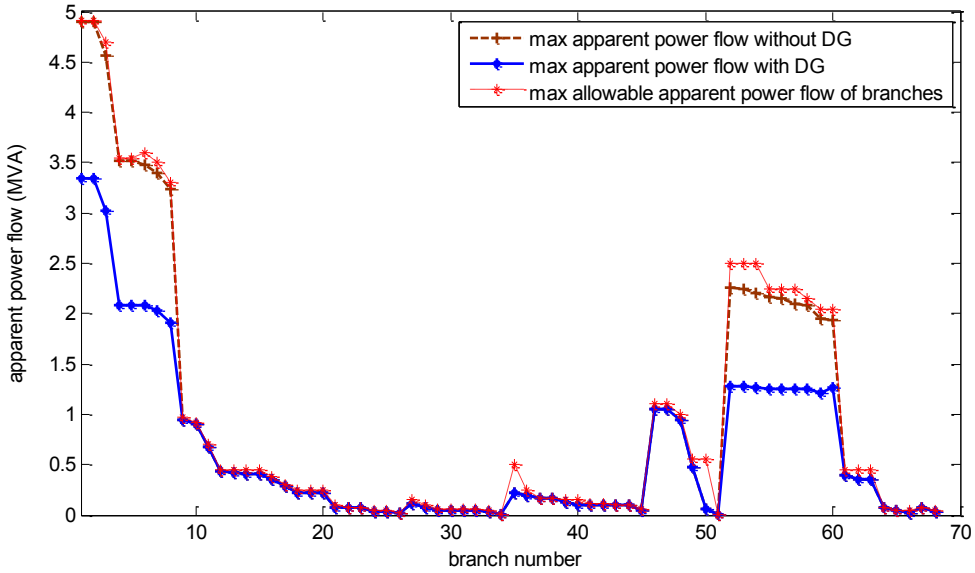

Figure 6.30: 69-bus branch apparent power flow/ line loading Scenario V (with both constraints), Case II (two- DG)

In addition, the enforcement of the constraint on line loading ensured that the apparent power flow in the branches remains within their allowable limits as shown in Figures 6.29 and 6.30. Some branches are still operating close to their maximum limits, but with no branch of the network overloaded. Case II resulted in a higher reduction in the apparent power injected from the grid, compared to the Case I, due to the connection of two DGs.

A summary of MSPSO results of the multi-objective optimization investigation is presented in Table 6.11 for all the studied scenarios. It is clear from these results that the capacity of the network to absorb new generations and the technical benefits of DG can be overestimated if the constraints imposed by switchgear rating and the line loading limit are neglected.

Finally, a comparison of the results of the single-objective and multi-objective optimisation studies is presented in Tables 6.12 and 6.13. It is evident from both tables that the multi-objective study resulted in a higher penetration level of the IG DG in almost all the scenarios of Case I and II compared to a single objective study. In scenario V of Case I, both single and multi-objective produced the same results while

scenario V of Case II also produced the same results for single and multi-objective optimisation.

Table 6.11: MSPSO SUMMARY RESULTS; 69-BUS NETWORK MULTI OBJECTIVE

			Optimal bus location(s)	Optimum DG size (s) (MW/Mvar)	Power loss reduction (%)	SSEV	Short-circuit current (kA)
Case I	Scenarios	I	-	-	-	0.0993	11.4073
		II	59	3/1.509	46.42	0.009904	12.2539
		III	65	2.0/0.9955	46.95	0.017415	11.8875
		IV	59	3/1.509	46.42	0.009904	12.2539
		V	61	1.45/0.9217	58.69	0.03038	11.8312
Case II	Scenarios	I	-	-	-	0.0993	11.4073
		II	63/18	2.0/0.9955;0.843/0.4001	61.12	0.001316	12.1348
		III	64/61	1.0/0.6389;1.0/0.6389	61.23	0.017537	11.8111
		IV	61/9	2/0.9955;3/1.509	54.82	0.002651	13.6350
		V	60/61	1/0.6389;1/0.6389	61.85	0.018524	11.8273

Table 6.12: MSPSO SUMMARY RESULTS; 69-BUS NETWORK SINGLE AND MULTI-OBJECTIVE OPTIMISATION CASE I

			Optimal bus location(s)	Optimum DG size (s) (MW/Mvar)	Power loss reduction (%)	SSEV	Short-circuit current
Case I SO	Scenarios	I	-	-	-	0.0993	11.4073
		II	61	1.85/0.9071	63.32	0.020344	11.9664
		III	63	1.65/0.7635	58.74	0.024907	11.894
		IV	61	1.85/0.9071	63.32	0.020344	11.9664
		V	61	1.45/0.9217	58.69	0.03038	11.8312
Case I MO	Scenarios	I	-	-	-	0.80993	11.4073
		II	59	3/1.509	46.42	0.009904	12.2539
		III	65	2.0/0.9955	46.95	0.017415	11.8875
		IV	59	3/1.509	46.42	0.009904	12.2539
		V	61	1.45/0.9217	58.69	0.03038	11.8312

Table 6.13: MSPSO SUMMARY RESULTS; 69-BUS NETWORK SINGLE AND MULTI-OBJECTIVE CASE II

			Optimal bus location(s)	Optimum DG size (s) (MW/Mvar)	Power loss reduction (%)	SSEV	Short-circuit current
Case II SO	Scenarios	I	-	-	-	0.0993	11.4073
		II	61/22	1.85/0.9071;0.33/0.2155	68.43	0.008387	11.9913
		III	64/60	0.843/0.4001;0.843/0.4001	63.36	0.023318	11.7285
		IV	61/9	1.85/0.9071;1.5/0.6589	65.41	0.008099	12.461
		V	60/61	1/0.6389;1/0.6389	61.85	0.018524	11.8273
Case II MO	Scenarios	I	-	-	-	0.0993	11.4073
		II	63/18	2.0/0.9955;0.843/0.4001	61.12	0.001316	12.1348
		III	64/61	1.0/0.6389;1.0/0.6389	61.23	0.017537	11.8111
		IV	61/9	2/0.9955;3/1.509	54.82	0.002651	13.6350
		V	60/61	1/0.6389;1/0.6389	61.85	0.018524	11.8273

6.6 Additional Test case for Comparative Study

This simple study is considered to allow direct comparisons of the results obtained from the MSPSO algorithm with previously published solutions obtained using analytical techniques [12, 59, 114] and PSO algorithm [59, 114]. The optimization studies in [12], [59] and [114] were limited to a single-objective function study minimising network losses (Equation 6.29). In all these studies, the reactive power requirement of the induction machine was calculated by an approximate empirical formula given by

$$Q_{DG} = -(0.5 + P_{DG}^2 \times 0.04) \quad (6.35).$$

Where, Q_{DG} and P_{DG} are the reactive power consumed and real power injected into the grid by the IG, respectively. Thus, given the generator output power, the reactive power requirement can be computed. Additionally, no shunt compensation capacitors were considered in these studies as part of the network optimization problem. Table 6.12 shows the optimal solutions (in terms of network loss reduction) achieved by all four studies.

Table 6.14: COMPARISON OF OPTIMAL DG SIZE AND LOCATION RESULTS TO THOSE OF PREVIOUS STUDIES

	69-bus network					
	Analytical Method [12]	Analytical Method [59]	Analytical Method [114]	PSO-W Algorithm [59]	PSO-W Algorithm [114]	Proposed MSPSO Algorithm
Optimum bus location	56	56	61	56	61	61
Optimum DG size (MW)	1.78	1.36	1.43	1.72	1.72	1. 50
Reactive power consumed (Mvar)	0.630	0.574	0.583	0.618	0.618	0.6589
% MW loss reduction	36.86%	25.33%	28.62%	24.73%	29.78%	24.68%

Comparisons of the results obtained by the three methods show that [12] and [59] give identical results in terms of the optimal location of the DG unit. While the proposed MSPSO algorithm and [114] produce a different optimal location of the DG unit. The three previous studies [12, 57 and 116] considered the induction generator size as a continuous variable and computed the reactive power requirement of the generator from the approximate empirical formula of Equation (6.35). This results in an underestimation of the reactive power required by the generators and an overestimation of the percentage power loss reduction figure. The proposed multi search PSO algorithm uses a pre-defined list of practical induction generator sizes to define the discrete DG size variable. The computation of the reactive power required by the generator is based on the per phase equivalent circuit of the machine using the generator's parameters. The result is a substantially more accurate estimated of the reactive power required by the induction generator when compared with the use of the approximate empirical formula.

In conclusion, it is worth mentioning that the model of the induction generator implemented in this study differs from those proposed in [115, 116]. In these previous studies, the models for each class of wind turbine generator units were developed to facilitate the computation of real and reactive power outputs for a specified wind speed and terminal voltage. This implies that both methods suppose prior knowledge of the WT features using the turbine's power curve, usually, supplied by the manufacturer. The model considered in this work, facilitates the computation of real and reactive power output for a specified generator rating (power output) and operating terminal

voltage. The slip is varied from zero at certain step intervals, and the corresponding output power is computed. The process is continued until the difference between the computed output power and the specified output power is within a specified error tolerance thus providing a simple and effective technique that can easily be incorporated into a network integration exercise involving induction generator based DG.

6.7 Summary

The integration of induction generator based DG in a power distribution network was investigated in this Chapter using the proposed MSPSO coupled with an algorithmic procedure that computes the reactive power requirement of the induction generator. The induction generator reactive power calculation procedure was interfaced with MATPOWER AC power flow software and the MSPSO to execute the optimization process. Unlike most previous studies, this investigation also considered the integration of shunt compensation capacitors as part of the optimization problem. The shunt compensation capacitors provided the reactive power requirement of the machine locally, resulting in a lower network reactive power flow and improved network losses.

The proposed algorithm was tested on the standard 69-bus benchmarking medium voltage radial distribution network used previously in Chapters 4 and 5. The investigation was conducted considering relevant network security constraints. Two studies were carried out: a single-objective study considering network loss reduction only and a multi-objective study considering network loss reduction and voltage profile improvement. Five scenarios were considered in each study, each with two Cases (Case I with one DG and Case II with two DGs). Shunt compensation capacitor is included as part of the optimization process so as to provide the entire reactive power required by the induction generator locally at the point of connection. The Results show that the best loss reduction and enhanced voltage profile is obtained when more than one optimally sized and located generators and shunt compensation capacitors are considered. The results of the study with enforcement of network constraints of short-circuit and line loading show that the capacity of the network to absorb new generations and the technical benefits of DG can be overestimated if these constraints are neglected.

In order to allow direct comparison of the MSPSO results with those of previously published studies, a mere single-objective study was also considered (minimising network real power loss). Results have shown that the consideration of the generator

size as a continuous variable and the use of an approximate empirical formula in those previous studies to compute the reactive power requirement of the generator lead to the underestimation/overestimation of the reactive power requirement of the machine and thus an overestimation/underestimation of the benefits of DG. In contrast, the proposed MSPSO was shown to be a useful optimization tool that can accurately handle this category of problem.

In the chapter that follows, the application of the proposed MSPSO to an actual distribution network in Nigeria is presented.

CHAPTER 7

Integration of DG in Nigerian Distribution Network

7.1 Background

The Nigerian Electricity Regulatory Commission (NERC) is Nigeria's independent regulatory agency for the Nigeria Electricity Supply Industry (NESI) established by the Electric Power Sector Reform Act (EPSRA) 2005. The Act provides the legal and regulatory framework for the electricity supply industry in Nigeria. It empowers NERC to regulate the NESI, comprising the Generation, Transmission and Distribution/Retail sectors[117]. The distribution system company (Disco) was unbundled into 11 independent companies which are free to procure additional (non-grid) power for their customers. A new procurement of power into a particular distribution network is governed by NERC's Embedded Generation (EG) regulation. The regulation covers issues such as distribution planning, connection requirements, technical and non-technical losses, commissioning procedure, commercial arrangement, and so forth.

In Nigeria DG is referred to as Embedded Generation (EG) simply, defined as a generator that is directly connected to the distribution network operated by a distribution licensee. Here, the generators are connected directly to or near the load centre on the distribution network, i.e., at 33kV, 11kVor 0.415kV[118]. The local industry definition of embedded generation is "The generation of electricity that is directly connected to and evacuated through a distribution system which is connected to the transmission network operated by a System Operations License"[119].

In Nigeria, there are currently 3 EG Licenses with a total licensed capacity of 374 MW but are yet to come into operation, and their current locations are depicted in Figure 7.1.

The part 3 section (1) (a) of the NERC regulations on EG, allows the connection of small size units having a nameplate rating greater than 1MW and not more than 6MW to be connected to 11kV medium distribution voltage. Moreover, large size units having a nameplate rating greater than 6MW and not more than 20MW is to be connected to 33kV medium distribution voltage.

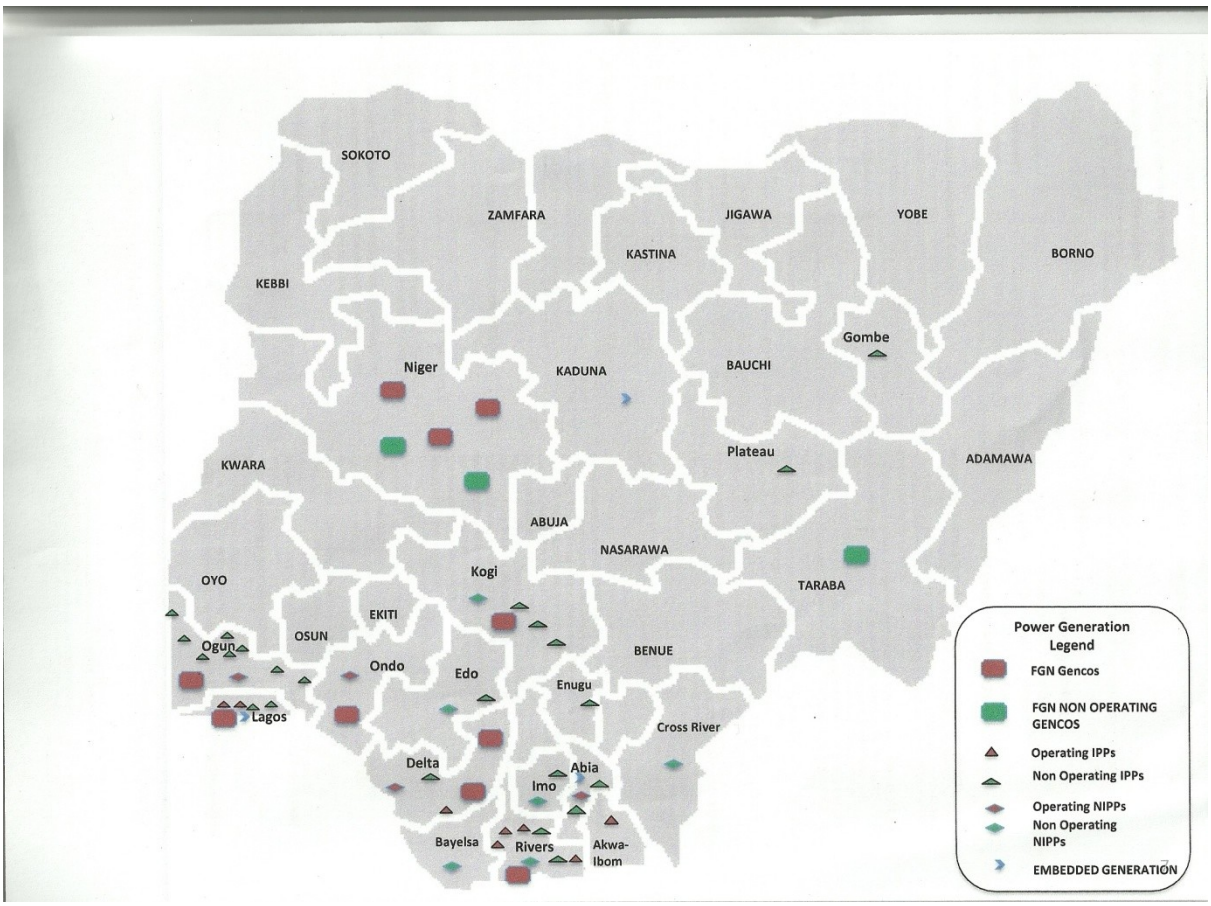

Figure 7.1: Nigeria Power Sector Outlooks – National [120]

7.2 Prospect for DG Integration in the Nigerian Network

In response to the problem of epileptic power supply besieging the country, the Nigerian government has set an aspiration power generation target of 40,000MW by the year 2020. The country currently relied on its bulk power generation from hydro and thermal stations with a total installed capacity of 6,504 MW and total licensed capacity of 10,552 MW. These bulk power stations are augmented with additional generations of the grid independent power producers (IPPs), National Integrated Power Projects (NIPPs), and Embedded Generation (EG). The On-Grid IPPs with total installed capacity of 1,899MW and total licensed capacity of 12,324 MW, the off-grid IPPs with total estimated installed capacity of 111.15MW and total licensed capacity of 274.5 MW. The NIPP projects with a total installed capacity of 750 MW and total licensed capacity of 4,180 MW. The EG licences have a total installed capacity of 374 MW but are yet to be in operation. Thus, the total estimated generating (operating and non-operating) capacity stood at 27,704.5 MW [120]. The daily peak delivery is estimated to be 4300 MW.

From the above analysis, EG constitutes only about 1.35% of the estimated total generation. The inabilities of the expected generations to be delivered are highly linked to some of the following hurdles;

- Access to gas, gas prices and gas supply framework
- Transmission network- losses and dilapidated infrastructure
- Maintenance turnaround of the existing national DISCOs
- Funding for the NIPP projects and
- Financing for the IPPs

The integration of DG (EG) in the existing networks will help the government achieve the national aspirations within a shorter time, reduce technical losses because of the proximity of DG to the network load, facilitating exchange of power between IPPs and DISCOs as excess power from the IPPs can be sold to DISCOs. In addition, there will be healthy competition in the market, resulting in the probable reduction of electricity prices with improved quality of services for the consumers.

In line with the advantages highlighted above, a fieldwork study was conducted on one of the existing Nigerian DISCOs MV distribution networks. Relevant network data were collated for the purpose of modelling and simulation of the network. The network was modelled and simulated with the proposed MSPSO algorithm and results validated with commercial power system analysis software 'ERACS'.

7.3 Modelling Lines Series impedance and Shunt admittance for Nigerian Network

The determination of the series and the shunt impedances of for overhead and underground lines are critical steps before the analysis of a distribution feeder can begin [104]. The available lines' data obtained from the fieldwork study are related to the conductor types and sizes. This section presents the mathematical formulations used in the computation of the lines (overhead and underground) impedance.

7.3.1 Series impedance for overhead and underground lines

The series impedance of the distribution line consists of the resistance of the conductors and the self- and mutual inductive reactance resulting from the magnetic fields surrounding the conductors [104]. The resistance component for the conductors is commonly obtained from a table of conductor data provided by the manufacturers of

such conductors. This data are also available from alternative literature sources[121] and[104] an example of which is provided in appendix C Table C.8.

7.3.1.1 Series impedance for overhead lines

The phase impedance of the overhead line can be computed using the Carson's equations [121] based on the general overhead construction configuration given in [121] as in appendix C Table C.8. Equation (7.1) gives the phase impedance matrix for a three-wire delta line determined by the application of Carson's equations

$$z_{abc} = \begin{bmatrix} z_{aa} & z_{ab} & z_{ac} \\ z_{bc} & z_{bb} & z_{bc} \\ z_{ca} & z_{cb} & z_{cc} \end{bmatrix} \Omega/\text{mile}. \quad (7.1)$$

The self- and mutual impedances for the phase impedance matrix of Equation (7.1) derived from the computation of inductive reactance [104] at an assumed frequency of 50Hz, and conductor length of 1 mile are given by the Equations (7.2) and (7.3) respectively.

$$\bar{z}_{ii} = r_i + j0.10111 \cdot \ln \frac{1}{GMR_i} \Omega / mile \quad (7.2)$$

$$\bar{z}_{ij} = j0.10111 \cdot \ln \frac{1}{D_{ij}} \Omega / mile \quad (7.3)$$

Where, r is the resistance in ohm/mile, and GMR_i is the Geometric Mean Radius of conductor *i* in foot obtained from a table of standard conductor data. D_{ij} is the distance between conductors' positions on the pole. It is also known as the Geometric Mean Distances (GMDs) between phases. The GMDs are used to form the distance matrix specifying the distant relationship between conductor *i* and *j* with each position on the pole in Cartesian coordinates using complex number notation. In the current study, the distribution line is assumed to be transposed. This assumption will require the modification of the phase impedance matrix of (7.1), by simulating the transposition. In a modification, the three diagonal terms of the Equation (7.1) are equal, and all of the off-diagonal terms are similar. This achieved by setting the three diagonal terms of the phase impedance matrix equal to the average of the diagonal terms of Equation (7.1) and the off-diagonal terms equal to the average of the off-diagonal terms of Equation (7.1) [104].

Thus, the self- and mutual impedances are defined respectively by the following Equations

$$z_s = \frac{1}{3} \cdot (z_{aa} + z_{bb} + z_{cc}) \ \Omega / mile \tag{7.4}$$

$$z_m = \frac{1}{3} \cdot (z_{ab} + z_{bc} + z_{ca}) \ \Omega / mile \tag{7.5}$$

The modified phase impedance matrix is then given as in Equation 7.6

$$Z_{abc} = \begin{bmatrix} z_s & z_m & z_m \\ z_m & z_s & z_m \\ z_m & z_m & z_s \end{bmatrix}, \Omega/\text{mile}. \tag{7.6}$$

The modified phase impedance matrix (transposed impedance matrix) is then used in the symmetrical component transformation of (7.7) resulting in the modified sequence impedance matrix

$$[Z_{012}] = [A_S]^{-1} \cdot [Z_{abc}] \cdot [A_S] \tag{7.7}$$

The (1,1) term of the resulting sequence impedance matrix is the zero sequence impedance, the (2,2) term is the positive sequence impedance while the (3,3) term is the negative sequence impedance. The off-diagonal terms are zero thus indicating that there is no mutual coupling between sequences due to symmetrical spacing between phases. The (2,2) and (3,3) terms are equal, thus, the value representing any of this term can be used as the impedance value for the transposed network in distribution feeder analysis.

7.3.1.2 Series impedance for underground lines

The phase impedance of the underground line can be computed using the Carson's equations [104] based on the general underground cable construction configuration given in [121]as shown in appendix C Table C.8. The cable considered is a three-wire delta line. The procedural steps are also based on the Equations (7.1) to (7.7).

7.3.2 Shunt admittance for overhead and underground lines

The shunt admittance of a line consists of the conductance and the capacitive susceptance. The conductance is small compared to the susceptance and thus, usually, ignored. The capacitance of a line is the result of the potential difference between conductors [104]. A charged conductor creates an electric field that emanates outward from the centre of the conductor.

7.3.2.1 Shunt admittance of overhead lines

The computation of shunt capacitance of overhead lines employed the method of conductors and their images [104]. Equation (7.8) gives the total voltage drop between conductor *i* and its image

$$V_{ii} = \frac{1}{2\pi\varepsilon}\left(2 \cdot q_i \ln \frac{S_{ii}}{RD_i} + 2 \cdot q_j \ln \frac{S_{ij}}{D_{ij}}\right) \tag{7.8}$$

where

S_{ii} is the distance from conductor *i* to its image *i'* (*ft*)

S_{ij} is the distance from conductor *i* to its image *j'* (*ft*)

D_{ij} is the distance from conductor *i* to conductor *j'* (*ft*)

RD_i is the radius of conductor *i* in (*ft*)

$\varepsilon = \varepsilon_o \varepsilon_r$ is the permittivity of the medium, ε_o is the permittivity of free space $\varepsilon_o = 8.85 \times 10^{-12}\ \mu F/m$, ε_r is the relative permittivity of the medium

q_i, q_j are the charge density on conductor *i* and *j,* respectively in cb/m

The voltage drop between conductor *i* and ground will be one-half of that given in Equation (7.8) as shown in Equation (7.9)

$$V_{ig} = \frac{1}{2\pi\varepsilon}\left(q_i \ln \frac{S_{ii}}{RD_i} + q_j \ln \frac{S_{ij}}{D_{ij}}\right) \tag{7.9}$$

Equation (7.9) can be written in general form as

$$V_{ig} = P_{ii} \cdot q_i + P_{ij} \cdot q_j \tag{7.10}$$

where P_{ii} and P_{ij} are the self- and mutual "potential coefficients."

Assuming a relative permittivity 1.0 for air in the case of overhead lines [104], the self- and mutual potential coefficients are redefined as in the Equations (7.11) and (7.12)

$$\hat{P}_{ii} = 11.17689 \cdot \ln \frac{S_{ii}}{RD_i}\ mile/\mu F \tag{7.11}$$

$$\hat{P}_{ij} = 11.17689 \cdot \ln \frac{S_{ij}}{D_{ij}}\ mile/\mu F \tag{7.12}$$

For an overhead line of *ncond* conductors, the Equations (7.11) and (7.12) are used to construct the "primitive potential coefficient matrix" $[\hat{P}_{primitive}]$. The Primitive Potential Coefficient Matrix (PPCM) will be an *ncond* × *ncond* matrix. The PPCM for a three-wire delta overhead lines is an *n-phase* × *n-phase* matrix with *n-phase=3*.

$$\left[\hat{P}_{primitive}\right] = \begin{bmatrix} \hat{P}_{aa} & \hat{P}_{ab} & \hat{P}_{ac} \\ \hat{P}_{bc} & \hat{P}_{bb} & \hat{P}_{bc} \\ \hat{P}_{ca} & \hat{P}_{cb} & \hat{P}_{cc} \end{bmatrix} \tag{7.13}$$

Because there is no neutral conductor, the PPCM is the same as *n-phase* × *n-phase* phase potential coefficient matrix $[P_{abc}]$:

$$[P_{abc}] = \left[\hat{P}_{primitive}\right] \tag{7.14}$$

The inverse of the potential coefficient matrix will give the *n-phase* × *n-phase* capacitance matrix $[C_{abc}]$:

$$[C_{abc}] = [P_{abc}]^{-1} \tag{7.15}$$

Neglecting the shunt conductance, the phase shunt admittance matrix is given by

$$[y_{abc}] = 0 + j \cdot \omega \cdot [C_{abc}]\ \mu S / mile \tag{7.16}$$

where

$\omega = 2 \cdot \pi \cdot f = 314.1593$, at $f = 50\ Hz$

The simulation of network transposition is carried out in a similar manner as in section 7.3.1.1 to obtain the modified phase admittance matrix $[Y_{abc}]$(transposed matrix) that is used in the symmetrical component transformation of Equation (7.17) resulting in the modified and symmetrical sequence admittance matrix.

$$[Y_{012}] = [A_s]^{-1} \cdot [Y_{abc}] \cdot [A_s] \tag{7.17}$$

The positive or negative sequence admittance value can be used as the per phase admittance value for the transposed network in distribution feeder analysis.

7.3.2.2 Shunt admittance of underground lines

Most underground distribution lines make use of concentric neutral or tape shield cables. The concentric neutral cable has one centre conductor as the phase conductor

and concentric neutral strands that are equally displaced around a circle of radius R_b (radius of a circle passing through the centres of the neutral strands). Tape-shield conductors can be seen as concentric neutral cables with an infinite number of strands [104]. The electric field of both concentric neutral and tape shield cables are confined to the insulation material. There are various types of insulation material in use, with each having a range of values for the relative permittivity. The neutral strands of concentric neutral conductors are all grounded. Therefore, the voltage drop between the phase conductor and the ground is given as in Equation (7.18).

$$V_{pg} = \frac{q_p}{2\pi\varepsilon}\left[\ln\frac{R_b}{RD_c} - \frac{1}{k}\left(\ln\frac{k\cdot RD_s}{R_b}\right)\right] \tag{7.18}$$

The capacitance from phase to ground for a concentric neutral cable is given by

$$C_{pg} = \frac{q_p}{V_{p1}} = \frac{2\pi\varepsilon}{\ln(R_b/RD_c) - (1/k)\ln(k\cdot RD_s/R_b)}\ \mu S/mile \tag{7.19}$$

Assuming a popular insulation of type Cross-linked polyethylene with a minimum relative permittivity of 2.3 [104], the shunt admittance matrix for the concentric neutral cable is given as

$$y_{ag} = 0 + j\frac{77.3619}{\ln(R_b/RD_c) - (1/k)\ln(k\cdot RD_s/R_b)}\ \mu S/mile \tag{7.20}$$

In the tape-shielded conductor, when k in (7.20) approaches infinity, the second term in the denominator of Equation (7.20) approaches zero. Thus, Equation 7.21 gives the shunt admittance of a tape –shielded conductor

$$y_{ag} = 0 + j\frac{77.3619}{\ln(R_b/RD_c)}\ \mu S/mile\ . \tag{7.21}$$

Where, $RD_c = d_c/2$ and $d_{c,\,is}$ the diameter of the phase conductor.

The *ncond* × *ncond* matrix of phase shunt admittance to ground can be computed using Equation (7.20) for concentric neutral cable and Equation (7.21) for tape-shield cable.

The simulation of network transposition to compute the per phase shunt admittance is carried out in a similar manner as in section 7.3.1.1. The positive or negative sequence shunts admittance value can be used as the per phase shunt admittance value for the transposed network in distribution feeder analysis.

7.4 Computation of Lines Series Impedance and Shunt Admittance for Nigerian Network

The computation of the lines (overhead and underground) parameters used in the analysis of the practical distribution feeder is based on the modelling equations of section 7.3. The available lines' data from a fieldwork study relating to the conductor or cable types and sizes used are shown in column 1 Table C.1, appendix C. The conductors and cables are made of aluminium (AL). The detail schematic layout of the network is shown in appendix C Figure C.1.

For the purpose of this study, the equivalent values in column 4 of Table C.1 are used. The resistance in ohms per mile, the Geometric Mean Radius (GMR) and the amperage capacity of the conductors and cables [104] are as presented in Table C.1 of appendix C. The series impedances for conductor and cable lines were computed using Equations (7.1) - (7.7) for conductors and cables. The results are presented in Tables C.2 and C.3, appendix C. From the modified sequence impedance matrix (transposed network impedance) of Tables C.2 and C.3, the (1,1) term of the resulting sequence impedance matrix is the zero sequence impedance, the (2,2) term is the positive sequence impedance while the (3,3) term is the negative sequence impedance. The off-diagonal terms are zero thus indicating that there is no mutual coupling between sequences due to symmetrical spacing between phases. The (2,2) and (3,3) terms are equal. Thus, the value representing any of this term can be used as the impedance value for the transposed network.

The shunt admittances for the line conductors and underground cables were computed using Equations (7.8) - (7.17) and Equations (7.18) to (7.21) respectively. The results are presented in Tables C.4 and C.5, appendix C. It is evident that the elements of the transposed phase admittances are very small and therefore were neglected in this study. Using the computed line parameters in appendix C, Tables C.2 and C.3, a complete network line parameters were computed, and the network data are as presented in appendix C, Table C.6.

The network load data are based on the quarterly meter reading of all substation loads for both utility and the dedicated consumers' substations. The peak annual load from each substation was adopted as the substation loads and used in the distribution feeder analysis. The details of load data are presented in appendix C, Table C.6. The loads are constant power load, modelled as a specified quantity of real and reactive power consumed at the bus.

7.5 The Test Network: Kaduna Distribution System Company (KADISCO) 33/11kV Injection Substation Network, Doka District

This proposed system is a practical Nigeria feeder network fed from one of the utility's 2x15MVA, 33/11kV injection substation feeder shown in Figure 7.2. The transformers TX1 and TX2 have percent impedance (Z) of 9.71% and 12.07% respectively.

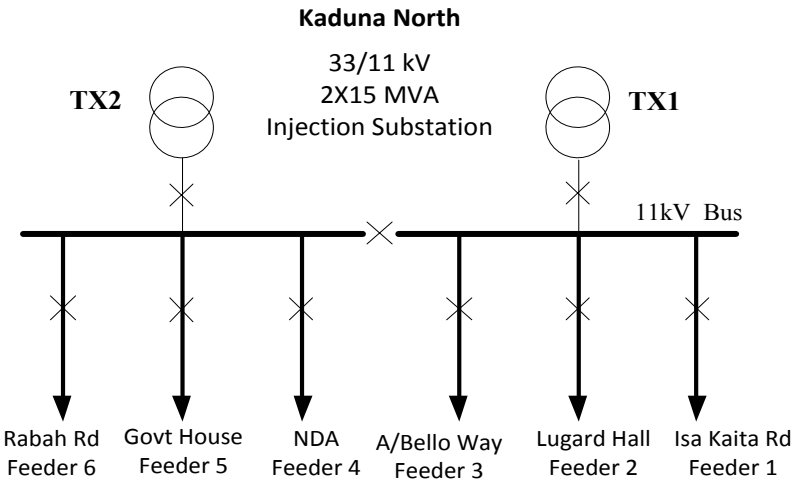

Figure 7.2: Single line diagram of 33/11kV injection substation

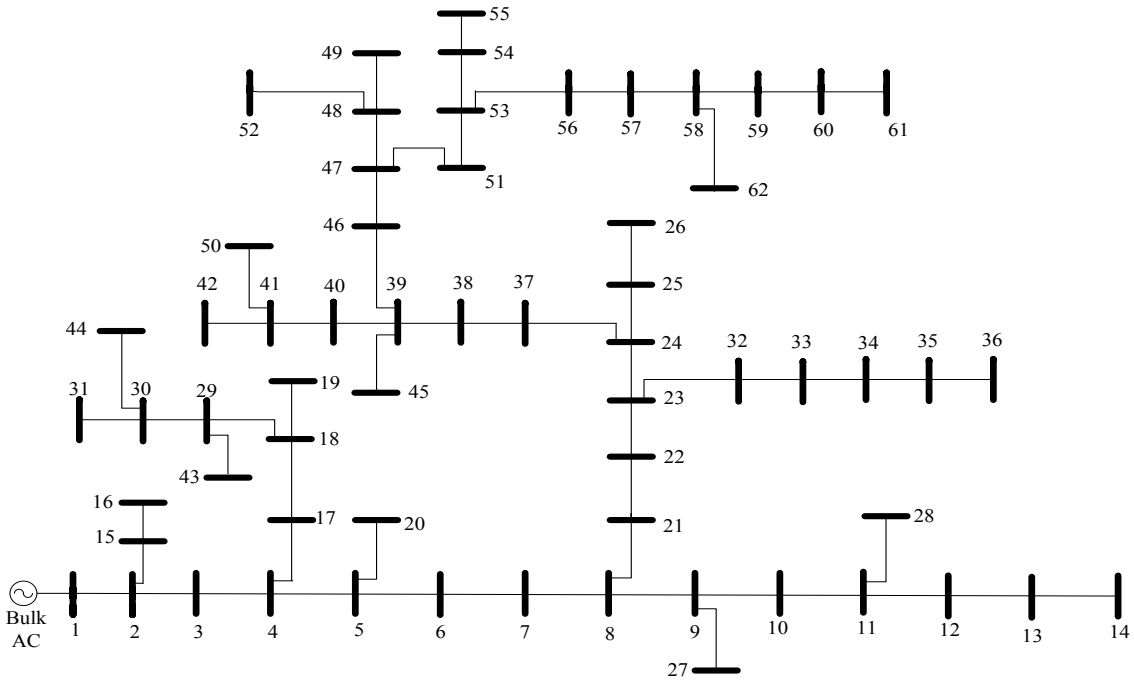

Figure 7.3: Single line diagram of 62 bus radial distribution network (Feeder 6)

The feeder considered for this study (feeder 6) is a 62-bus 11 kV radial primary distribution system [122]. The feeder has a short circuit current breaking capacity of 15.0 kA for 3seconds. A system base MVA of 10.0MVA is used for this study with system data as given in Table C.3, appendix C. The total substation loads is 7.25MW

and 3.12Mvar, the single line diagram of the network is shown in Figure 7.3. The base case real and reactive power loss in the system are 0.3146MW and 0.4952Mvar respectively.

The voltage profile of the base case system is lower than the nominal lower limit of 0.95 per unit for bandwidth of ±5% nominal voltage of 1.0 per unit assigned by the NERC Distribution code for 11kV operational voltage [118]. The mean voltage value of the network is 0.9467pu and a standard deviation of 0.01961 was computed. This implies that the network voltage profile is poor as shown in Figure 7.4.

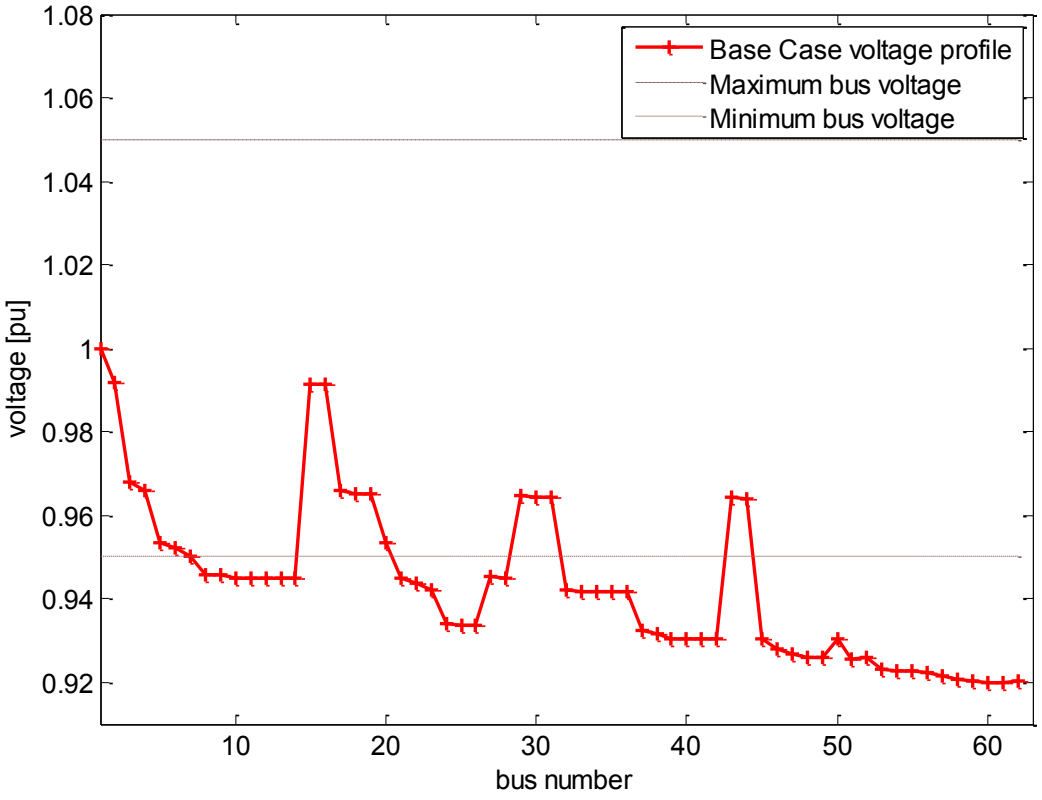

Figure 7.4: Voltage profile of 62 bus radial distribution network (Feeder 6) base case with no generation

The allocation of Distributed Generation operating with and without reactive power support is expected to improve the adequacy of power supply, reduce power loss and improve the voltage profile of the network. The proximity of the Distributed Generation will resultantly improve the quality of power supply and enhanced its reliability.

The country is adequately endowed with large quantities of renewable and nonrenewable sources of generation [123-125]. The power requirement of the country can only be met when these energy resources are strategically harnessed. DG aimed at full application of these natural resources to provide adequate power and sustain reasonable growth in the manufacturing, commercial, domestic and services sector of the economy.

7.5.1 Modification of the 62-bus Nigeria network for DG integration

The ERACS software available for validation of the results of the practical network is a 50- bus Version that only allows networks up to 50 bus bars to be simulated. Due to this licence limitation, the 62-bus practical network of Figure 7.3 is slightly modified to a 47-bus network using the following procedure steps;

Step 1: all laterals with only one bus (substation) are absorbed into the main lateral (ML) from where they emerged. Thus, bus 20, 27 and 28 are absorbed into bus 5, 9 and 11 respectively, with their load added to their sending end nodes.

Step 2: all minor laterals (ml) with only one bus (substation) are absorbed into their corresponding sublateral (sl) from where they emerged. Thus, bus 43, 44, 45, 50 and 52 are absorbed into bus 29, 30, 39, 41, and 48 respectively with their load added to their sending end nodes.

Step 3: some receiving end nodes at short distance from their sending end nodes were merged with their sending end nodes and their load absorbed into their respective sending end nodes. Thus, bus 51 absorbed in 47, bus 42 and 41 were absorbed into 40. Bus 55, 62, 26, and 61 are absorbed into bus 54, 58, 25 and 60 respectively.

The modified feeder is presented in Figure 7.5. So instead of the original 62-bus distribution system, having sixty-one (61) sections, it is reduced to 47 buses with forty-

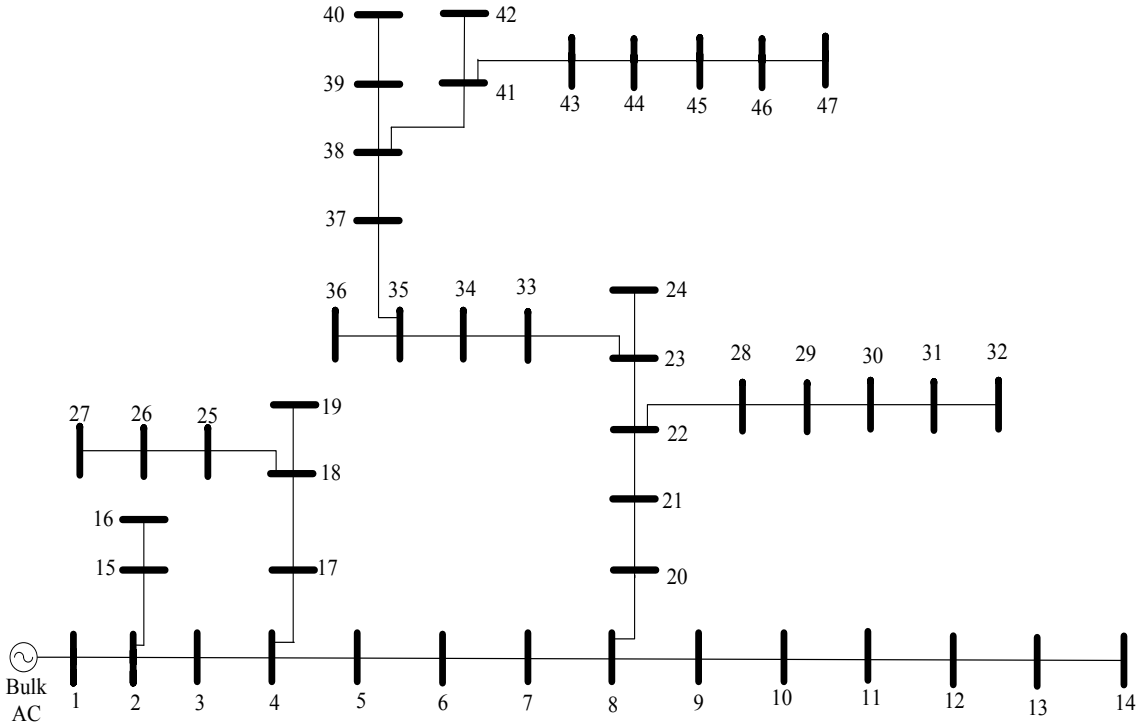

Figure 7.5: Single line diagram of 47 bus modified radial distribution network (Feeder 6)

six (46) sections. The loads are all three phase spot loads and the positive sequence impedance is used as the impedance of the feeder sections. After the modification, the total substation loads remained as 7.25MW and 3.12Mvar. The base case real and reactive power loss in the system is now 0.3046MW and 0.4876Mvar respectively.

7.6 Relationship between Generator Size and Fault currents

The short circuit current constraint is implemented as described in section 6.2, using Equations (6.15)-(6.17). The sub-transient reactance of generators is assumed to be about 15%–20% on the generator reactance base; the sub-transient reactance is then obtained by computing the percent reactance using the expression that evaluate the reactance of generator [20] given by Equation (7.22).

$$X^{g}_{p.u}(S^{g}) = X^{g}_{mim} + (X^{g}_{max} - X^{g}_{min})(1 - e^{-S^{g}/S^{smallGen}}) \tag{7.22}$$

$$\Rightarrow f(S^{g}) = 0.15 + 0.05\,.(1 - e^{-s^{g}/150})$$

In the above expression, X^{g}_{min}=15% and X^{g}_{max}=20% on the generator reactance base [20]. The function *f* computes the per unit sub-transient reactance of the generator with size S^{g}. Generators are considered to be small when their capacity is well below $S^{smallGen}$ =150MVA. Equation (7.22) can be translated into a graphical representation as shown in Figure 7.6. The pu reactance of the generator with respect to its capacity is obtained by dividing Equation (7.22) by the generator capacity (S^{g})

$$X_{p.u}(S^{g}) = \frac{0.15 + 0.05\,.(1 - e^{-s^{g}/150})}{S_{g}} \tag{7.23}$$

The sub-transient reactance of the generator on the system base MVA is computed as

$$X^{new}_{p.u}(S^{g}) = f(S^{g}).\frac{systembase\quad MVA}{S_{g}} \tag{7.24}$$

The DGs considered are in the commercially available sizes from 0kW to 5000kW as shown in appendix A, Table A.4.

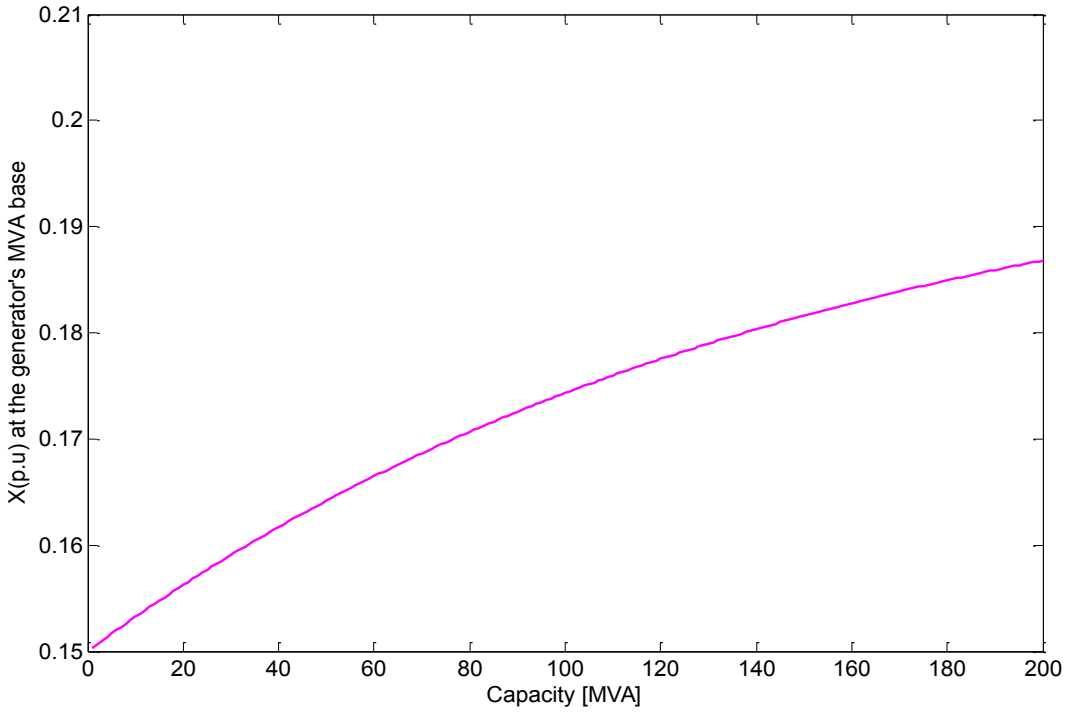

Figure 7.6: Per unit reactance of generators with respect to their MVA base

7.7 Integration of DG in Nigeria Network Using MSPSO; Objective Function Formulation

The study presented in this chapter and in common with previous chapters, is for the multi search PSO to find the optimal size and location of the DG unit (or units) in order to minimize the total real power loss in a network. Additionally, in common with previous chapters, the improvement in the voltage profile of the network is used in addition to the reduction in network power losses to solve the multi-objective optimization problems.

The network security constraints of short-circuit current rating of switchgear and line loading capacity are enforced where applicable. The constraint on switchgear rating is to ensure that with the penetration of DG, the consequence of upgrading the switchgear rating to accommodate new generation is evaded. Additionally, supplying power near to the loads may results in the diminishing of MVA flows in some sections of the network, realising more capacity, but in other sections the may also increase to levels beyond distribution line limits thus the need to consider line limits constraint [53]. The short circuit constraint is handled by a three-phase symmetrical fault algorithm prior to the optimization process. The fault algorithm operates on the swarm with the individuals swarm /solutions (DG sizes) violating the short circuit constraint rejected.

The objective function (f_{obj}) to be optimized is given in Equation (6.30) and repeated here in Equation (7.25) for convenience.

Minimise $f_{obj} = k_1 \cdot P_L + k_2 \cdot f(v) + k_3 \cdot f(IC)$ (7.25)

where: P_L is as given in Equation (6.31), *f(v)* is as given in Equation (6.32) and *f(IC)* is the quadratic index representing the objective of the line loading constraints to be minimised given in Equation (6.33) and repeated here in Equation (7.26) for convenience:

$$f(IC) = \sum_{l \varepsilon L} (S_l - S_l^{\max})^2 \tag{7.26}$$

S_l (S_{ij}) and S_l^{max} ($S_{ij}^{\max}$) define the apparent power (*MVAflowmax*) in a line section *l* and the maximum allowable apparent power flow (*MVAflowrated*) in section *l* respectively. In order to enforce the constraint of Equation (5.6), the index in (7.26) is computed, weighted and added to the objective function. The line overloads are computed as:

$$Overloads = \max [MVAflow \max - MVAflowrated] \tag{7.27}$$

where

$$MVAflow \max = \max_{l}^{L} \left[\left| \overline{S}_{ij} \right|, \left| \overline{S}_{ji} \right| \right] \tag{7.28}$$

MVAflowmax and *MVAflowrated* denote the $n_l \times 1$ vector of apparent power flow related to all sections (branches) of the network, with n_l the total number of sections of the distribution system under consideration. Implementation of the line loading constraint ensures that the location of DG is such that the MVA flow in network sections are within the maximum allowable rating of the sections/branches. The objectives of the study are therefore to minimize network power loss and voltage deviation to improve the voltage profile. Mathematically, the objective of both power loss and voltage optimization with the inclusion of line loading constraint can be expressed as:

Thus, to minimise

$$f_{obj} = k_1 \cdot \sum_{l \varepsilon L} (P_{i \to j}^{l} + P_{j \to i}^{l}) + k_2 \cdot \sum_{i=1}^{N_b} (V_i - V_{n,i})^2 + k_3 \cdot \sum_{l=1}^{L} (S_l - S_l^{\max})^2 \tag{7.29}$$

k_1, k_2 and k_3 defined the weighting factors that transformed the multi-objective problem to a single one: the different objective functions are weighted and added to form a single

objective function to be optimized as already discussed in section (6.3.2.1). In a single objective optimization, the first part of the equation (7.29) is used.

The MSPSO optimization results are recorded after 10 independent runs of the algorithm using a swarm population of 20 particles (with five informants) and a stopping criteria of 50 iterations where the objective function value remains within a margin of 10^{-9} or a maximum number of 1000 iterations. The social and the cognitive constants c1and c2 are set equals with both being assigned a value of 1.47 [77]. For the 69-bus network M = 70, maximum particle velocity (mv) = 1.5, α = 0.4 , w_{max}= 0.9 and w_{min} = 0.4 [87] are used.

7.8 Optimal Location and Sizing of One Generator in a 47 bus RDN Using MSPSO

NERC regulations on DG [119], allows the connection of small size units having name plate rating greater than 1MW and not more than 6MW to be connected to 11kV medium distribution voltage. The NERC Distribution code [118] allows generators connected to distribution system to provide ancillary services for reactive power and such generators should be capable of contributing to voltage control by continuous regulation of the reactive power supplied to the distribution system. The generators are allowed to operate and maintain a power factor of not less than 0.85 lagging. In line with the regulation, the study considered DG sizes in the range of 0kW to 5MW with a total installed capacity of less than 6MW.

This study involves the integration of one generator of optimal size at the optimal location, considering four scenarios (with two cases for scenarios III and IV). The study is based on 100% feeder load demand for the 47-bus RDN network of Figure 7.5. The first scenario is the base network with no DG connected. The second Scenario involves the integration of one DG with a single objective of power loss reduction and ignoring any network constraints. The third scenario also involves the connection of a single DG while the fourth scenario considers the connection of one DG unit operating at full rated power, but with a range of possible power factors of unity down to 0.85 lagging. For scenarios III and IV, a single objective function study that considered the enforcement of only short-circuit current constraint is used as Case I, while Case II is a multi-objective function that considered the enforcement of both short-circuit and line loading constraints.

7.8.1 Scenario I: base network with no generation

Table 7.1 shows a summary of the results for the base test network with no generation. The voltage profile of the original test network shown in Figure 7.4 clearly shows that nodal voltages are an issue under normal loading condition with an SSEV index 0.15105. The mean voltage value and the standard deviation for the base case network are 0.9467pu and 0.01961, respectively. The short circuit current of the base network is computed as 13.1223 kA and this value is typically used to select the standard rating of the switchgear required for the network. The switchgear rating for the feeder at the main substation is 15.0 kA. In order to demonstrate the importance of short-circuit current constraint in this study, it is assumed that the short-circuit current with the integration of DG should not exceed the rating of the switchgear (15.0 kA).

Table 7.1: SUMMARY OF RESULTS; 47-BUS SCENARIO I WITH NO GENERATION (BASE CASE)

Σ Load (MW)	Σ Load (Mvar)	Σ MW Loss	Σ Mvar Loss	Max. bus voltage (pu)	Min. bus voltage (pu)	Mean voltage (pu)	Std. Dev	SSEV	Short circuit-current (kA)
7.25	3.12	0.3046	0.4876	1.0000	0.9233	0.9467	0.01961	0.151051	13.1223

7.8.2 Scenario II: single generator neglecting short-circuit current and line loading constraints

The results of the optimization process using MSPSO for the optimum size / location of DG integrated into this network is presented in Table 7.2. The optimal size and location is obtained with one optimally sized 5.0MW and located generator at bus number 38. A 78.44% power loss reduction is achieved. The voltage profile of the network is presented in Figure 7.7. The mean voltage is computed as 0.9745pu with a standard deviation of 0.008334. The integration of 5.0MW generator resulted in the overall improvement of the voltage profile. The mean voltage and standard deviation are improved from 0.9467pu and 0.01961 respectively in the base case to 0.9745pu and 0.008334 respectively in scenario II.

The short-circuit current with the integration of one DG is computed as 15.7038 kA. The switchgear rating of the feeder at the main substation is 15.0kA. Thus, taking into consideration the practical constraint on short-circuit current capacity of the switchgear on feeder six at the substation bus (bus 1), implies that the location of 5MW at bus 38 will require the upgrading of the switchgear.

Table 7.2: MSPSO SUMMARY RESULTS; 47-BUS NETWORK SCENARIO II (NO CONSTRAINTS)

	One DG, single objective without short-circuit current and line loading Constraints
Optimal bus location	38
DG MWs generated	5 MW
Σ MW loss	0.0657 MW
Σ Mvar loss	0.1038 Mvar
Min bus voltage	0.9642 pu
Max bus voltage	1.000 pu
Mean voltage	0.9745 pu
Standard deviation	0.008334
Σ MW loss reduction	78.44%
Σ Mvar loss reduction	78.71.0%
Designed Isc (I_k)	13.1223 kA
Specified Isc (I_{spec})	**15.0 kA**
Isc with DGs (I_{fDG})	**15.7038 kA**

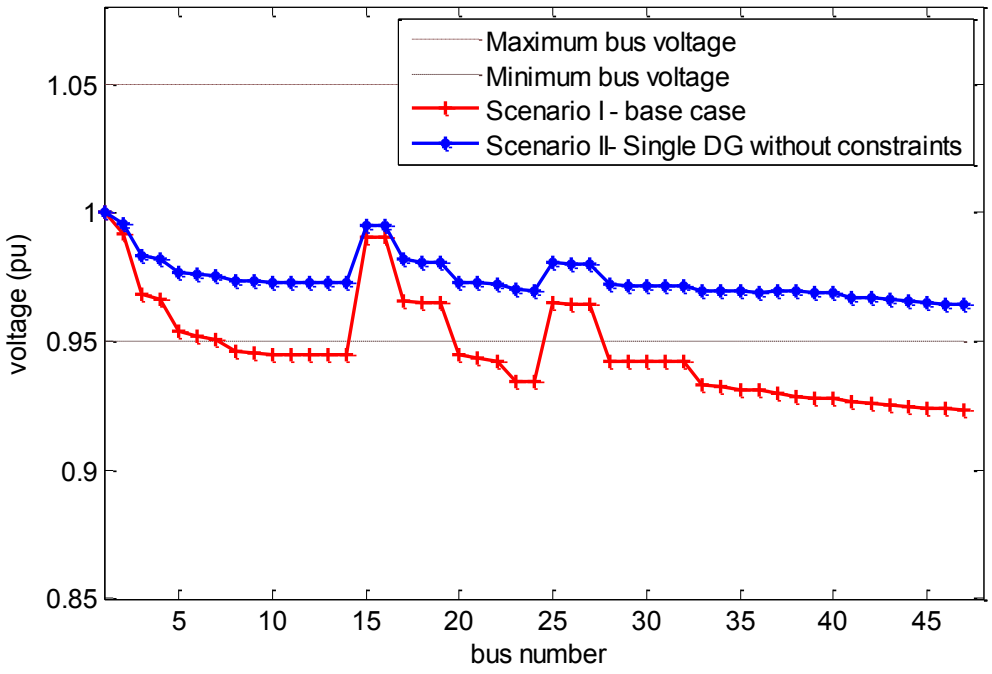

Figure 7.7: Voltage profile of the 47-bus radial distribution network (Feeder 6), Scenario II (single DG without constraints)

Figure 7.8 shows the apparent power (MVA) flows for all branches of the network for scenario II when all the network constraints are neglected. It is evident that the

connection of one DG drastically reduced the apparent power flow in some branches of the network. While some branches are found to be operating close to their maximum limits. It is obvious from Figure 7.8 that no branch of the network is shown to be overloaded following the inclusion of DG.

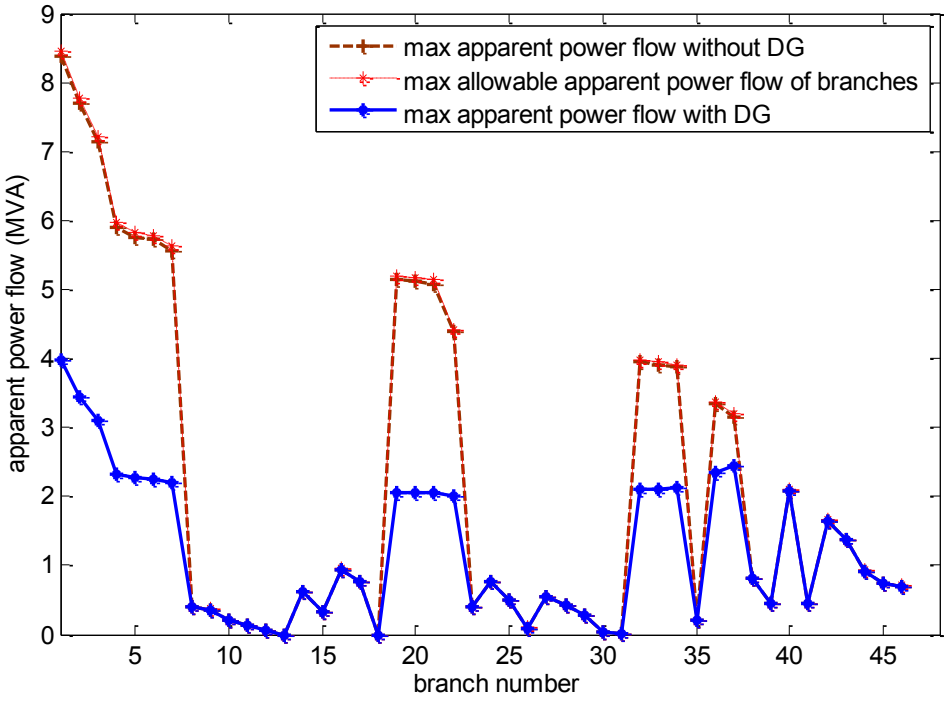

Figure 7.8: 47-bus branch apparent power flow/ line loading Scenario II (one DG, without constraints)

Additionally, the connection of DG resulted in a drastic reduction in the apparent power injected from the grid. Thus, the implementation of the optimal solution of scenario II will require only the upgrading of the switchgear rating of feeder six at the substation (bus 1).

7.8.3 Scenario III: I single generator, Case I and II (single and multi-objective)

The results of the MSPSO optimization process are presented in Table 7.3. In Case I, the optimal size generator is obtained as 3.4 MW located at optimal bus number 44, resulting in a 68.82% power loss reduction. For case II, the optimal size and location is obtained with one optimally sized 3.2 MW and located generator at bus number 41 producing a 67.24% power loss reduction.

The improvement obtained in the network voltage profiles with the integration of DG (Case I and II) are presented in Figure 7.9. The minimum bus voltage is improved from 0.9233pu in the base case to 0.9561pu and 0.95255pu for Case I and II, respectively.

Table 7.3: MSPSO SUMMARY RESULTS; 47-BUS NETWORK SCENARIO III, CASE I AND II (ONE DG, SINGLE AND MULTI-OBJECTIVE)

	One DG, a single objective with short-circuit current Constraint only **Case I**	**One DG, multi-objective with short-circuit current and line loading Constraints** **Case II**
Optimal bus location	44	41
DG MWs generated	3.40 MW	3.2 MW
Σ MW loss	0.095 MW	0.0998 MW
Σ Mvar loss	0.1491 Mvar	0.1556 Mvar
Min bus voltage	0.9561 pu	0.9525 pu
Max bus voltage	1.000 pu	1.000 pu
Mean voltage	0.9668 pu	0.9655 pu
Standard deviation	0.01115	0.01178
Σ MW loss reduction	68.82%	67.24%
Σ Mvar loss reduction	69.42.11%	67.88%
Designed Isc (I_k)	13.1223 kA	
Specified Isc (I_{spec})	**<15.0 kA**	
Isc with DGs (I_{fDG})	**14.9153 kA**	**14.8883 kA**

The mean voltage and the voltage standard deviation are improved from 0.9467pu and 0.01961 respectively in the base case to 0.9668pu and 0.01115 respectively in Case I and 0.9655pu and 0.01178 respectively in Case II. It is evident from Table 7.3 that the percent loss reduction in Case I (68.82%) is higher than the percent loss reduction obtained in Case II (67.24%). This is as a result of the enforcement of both short-circuit current and line loading constraints, resulting in a smaller DG size for Case II when compared with Case I.

Figures 7.10 and 7.11 show the apparent power (MVA) flow for all branches of the network for case I and II respectively. It is evident in both cases that the connection of DG drastically reduced the apparent power flow in some branches of the network. Additionally, in Case I some branches operate close to their maximum limits while branches 42 and 43 of the network are found to be overloaded. The enforcement of the network constraint of line loading in addition to short-circuit current constraint (case II) resulted in the removal of the overload experienced in branches 42 and 43 of Figure 7.10 as shown in Figure 7.11. However, this is obtained at the expense of smaller

optimal DG size (3.2 MW) at a new optimal bus location (bus number 41) compared with case I.

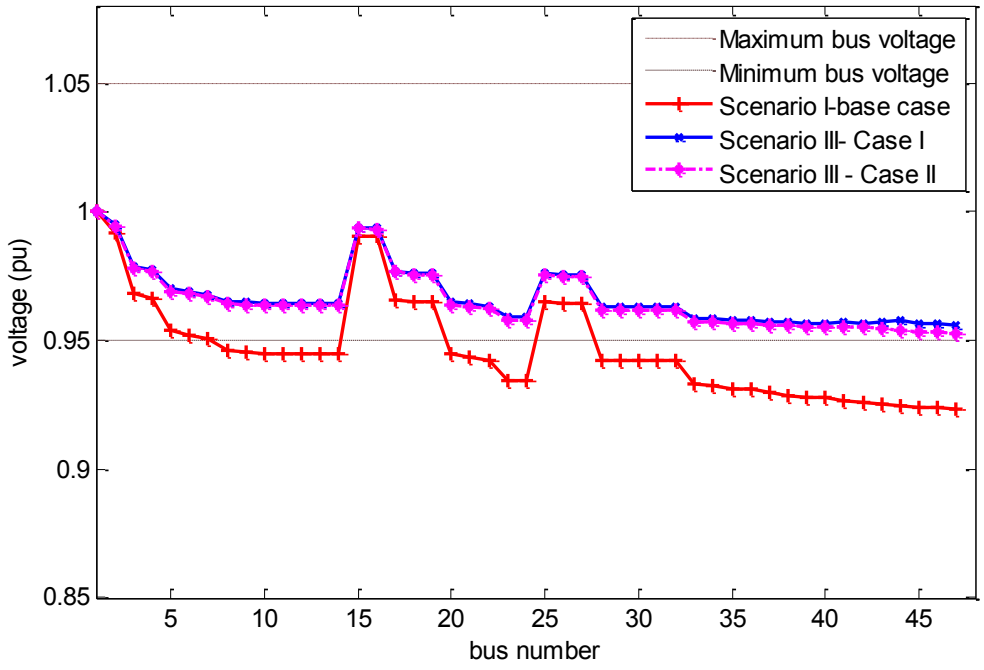

Figure 7.9: Voltage profile of the 47-bus radial distribution network (Feeder 6) Scenario III, Case I and II (single and multi-objective)

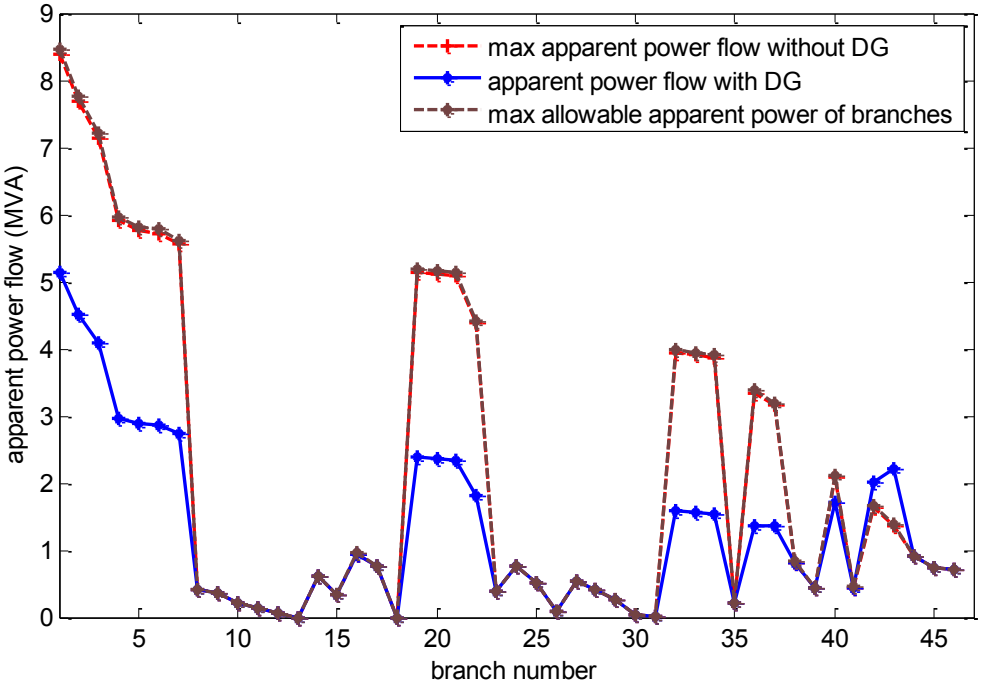

Figure 7.10: 47-bus branch apparent power flow/ line loading Scenario III, Case I (one DG, a single objective with short-circuit constraint)

The short circuit current (14.8883kA) computed at bus 1 for Case II, is still within the specified short-current rating of the switchgear (< 15.0 kA). However, this value of

short-circuit current (in Case II) is also lower than the value computed for Case I (14.9153 kA). Thus, the branch/ line loading is kept within their maximum allowable loading limits. It can be deduced that the realistic solution for the utility will be the implementation of all the relevant constraints.

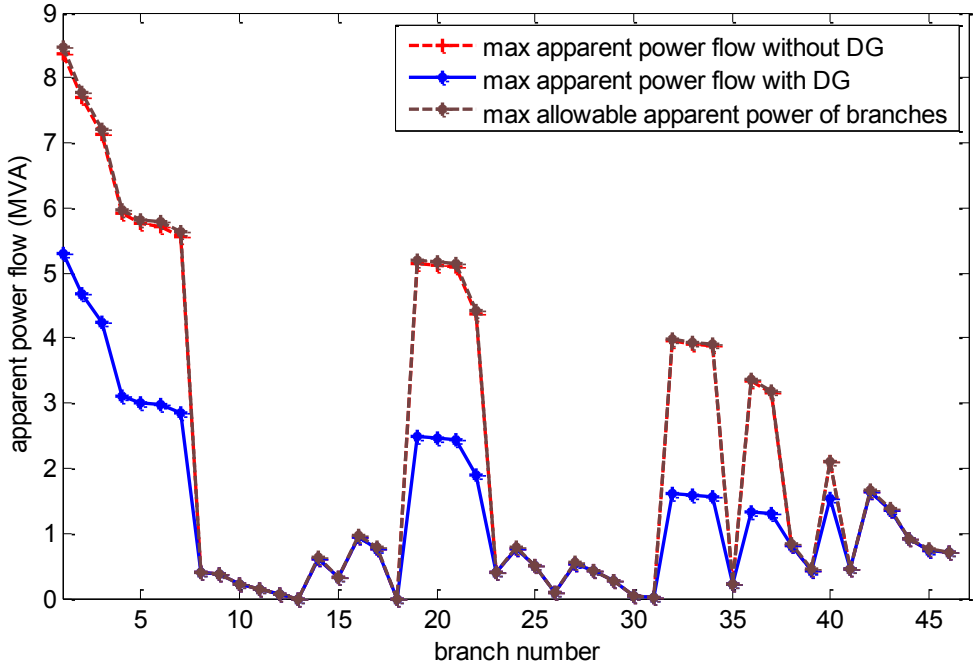

Figure 7.11: 47-bus branch apparent power flow/ line loading Scenario III Case II (one DG, multi-objective with short-circuit and line loading constraints)

7.8.4 Scenario IV: single generator operating at minimum PF of 0.85 lagging

This scenario involved finding the optimal location and size for a single generator operating with reactive power output capability (minimum operating power factor of 0.85 lagging). The results of the optimization process using MSPSO for the optimum size / location of the generator integrated into this network are presented in Table 7.4. The improvement in the network voltage profiles with the both cases is presented in Figure 7.12. The generator injects 3.075 MW/1.9057 Mvar at bus number 46 in Case I with a 77.45% power loss reduction. For Case II, 2.75 MW/1.7043 Mvar are injected in at bus number 41 producing a 75.38% reduction in power loss. It is apparent that in both cases the DG unit operates at the limit of its reactive power output. Significant improvements in terms of loss reduction and voltage profile (compared with previous scenarios III) are obtained because the generator is now producing both active and reactive power.

Table 7.4: MSPSO SUMMARY RESULTS; 47-BUS NETWORK SCENARIO IV, CASE I AND II (ONE DG AT 0.85 PF, SINGLE AND MULTI-OBJECTIVE)

	One DG, a single objective with short-circuit current Constraint operating at 0.85 PF: Case I	**One DG, multi-objective with short-circuit current and line loading Constraints operating at 0.85 PF: Case II**
Optimal bus location	46	41
DG MWs generated	3.075 MW	2.75 MW
DG Mvar generated	1.9057 Mvar	1.7043 MW
Σ MW loss	0.0687 MW	0.075 MW
Σ Mvar loss	0.1072 Mvar	0.1164 Mvar
Min bus voltage	0.9776 pu	0.9721 pu
Max bus voltage	1.000 pu	1.000 pu
Mean voltage	0.9816 pu	0.9777 pu
Standard deviation	0.005335	0.006546
Σ MW loss reduction	77.45%	75.38%
Σ Mvar loss reduction	78.01%	76.13%
Designed Isc (I_k)	13.1223 kA	
Specified Isc (I_{spec})	**< 15.0 kA**	
Isc with DGs (I_{fDG})	**14.9020 kA**	**14.9064 kA**

The improvement obtained in the network voltage profiles shows that the minimum bus voltage is improved from 0.9233pu in the base case to 0.9776pu and 0.9721pu for Case I and II respectively. The mean voltage and voltage standard deviation are improved from 0.9467pu and 0.01961 respectively in the base case to 0.9816pu and 0.005335 respectively in Case I and 0.9777pu and 0.006546 respectively in Case II.

It is evident from Table 7.4 that the percent loss reduction obtained for Case I (77.45%) is higher than the percent loss reduction obtained for case II (75.38%). Thus, the enforcement of both short-circuit current and line loading constraints in Case II, again resulted in a decrease in the capacity and the relocation of the optimal DG obtained in order to satisfy the constraints.

Figures 7.13 and 7.14 show the apparent power (MVA) flow for all branches of the network for Case I and II respectively. It is evident in both cases that the connection of DG drastically reduced the apparent power flow in some branches of the network. Moreover, some branches operate close to their maximum limits. Due to the enforcement of constraint on short-circuit current, the optimal size/location DG for Case

I resulted in the overloading of some branches of the network (branches 42-45) as shown in Figure (7.13).

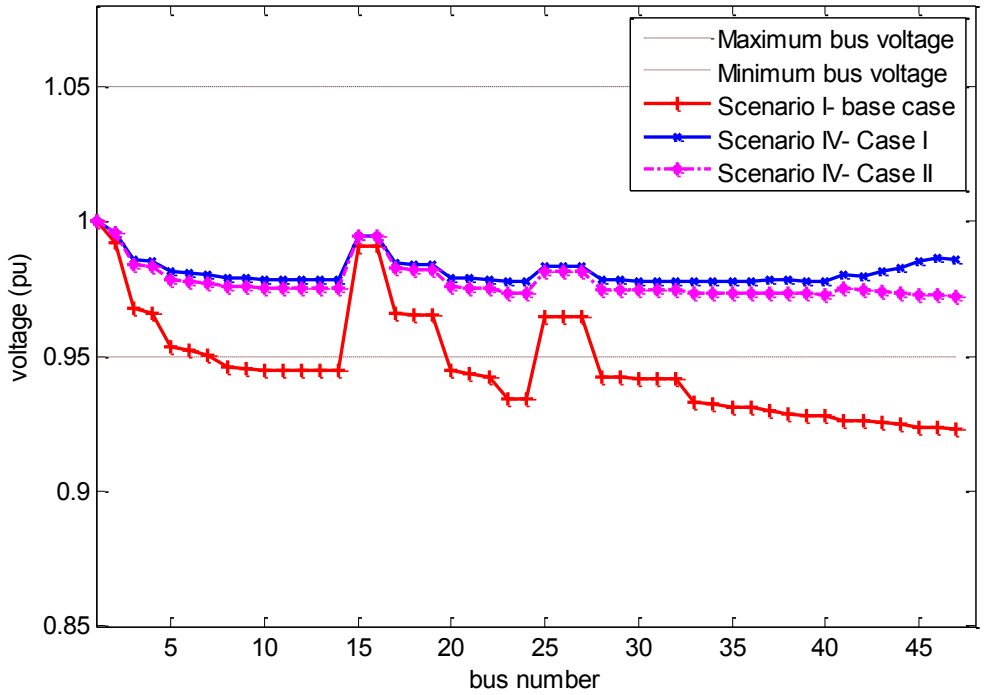

Figure 7.12: Voltage profile of 47 bus radial distribution network (Feeder 6) Scenario IV (one DG at 0.85 PF), case I and II (single and multi-objective)

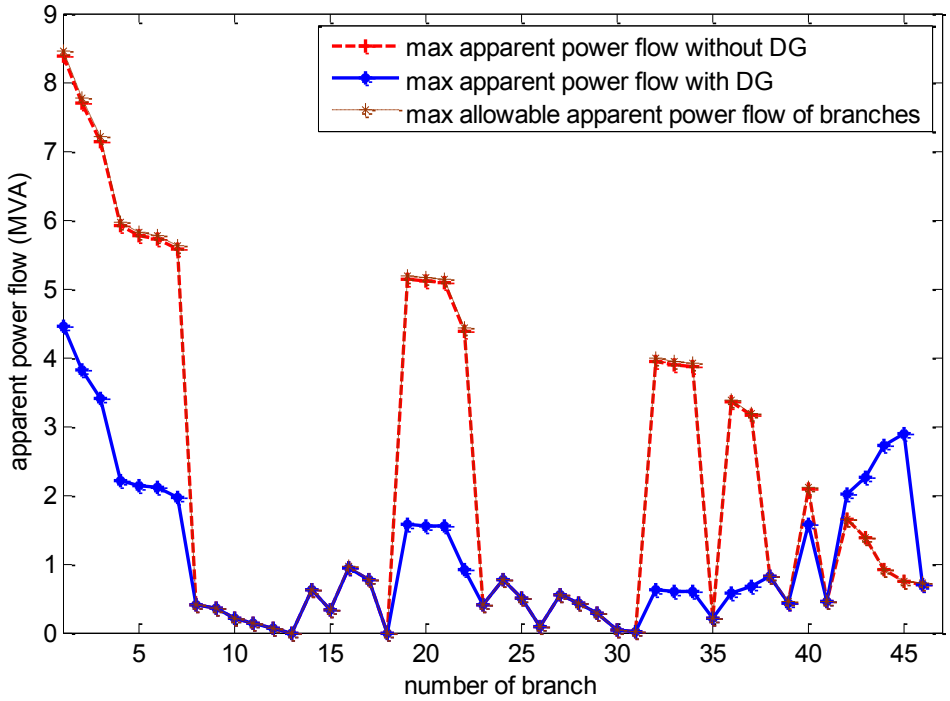

Figure 7.13: 47-bus branch apparent power flow/ line loading Scenario IV (one DG at 0.85 PF), Case I (single objective)

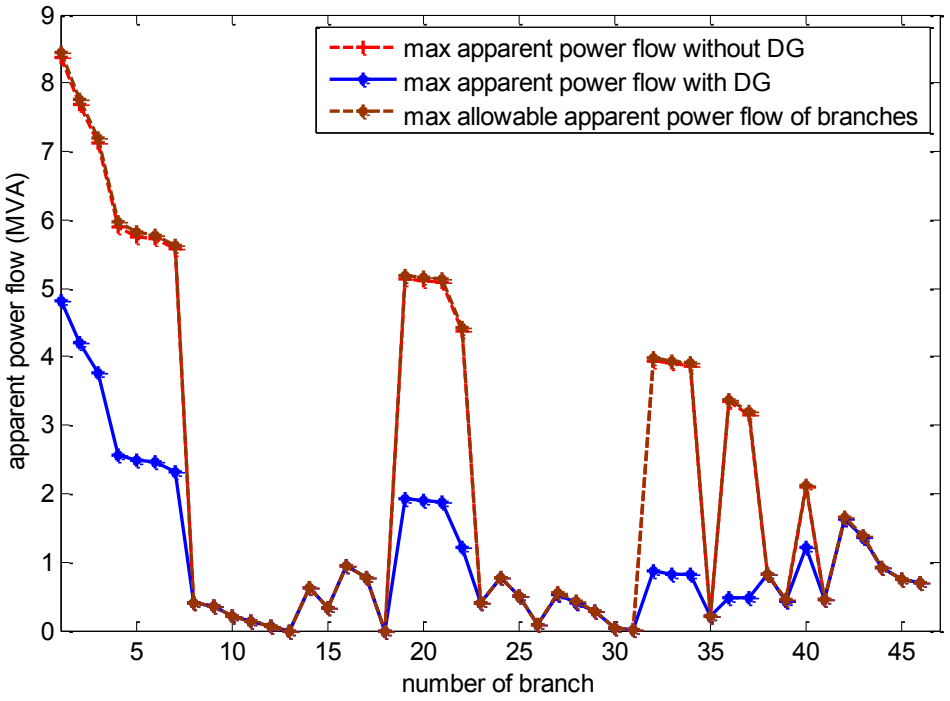

Figure 7.14: 47-bus branch apparent power flow/ line loading Scenario IV (one DG at 0.85 PF), Case II (multi- objective)

The enforcement of network constraint of line loading in addition to short-circuit current constraint in Case II resulted in the removal of the overload experienced in branches 42-45 as shown in Figure 7.14. However, this is obtained at the expense of smaller optimal DG size (2.75 MW) at a new optimal bus location (bus number 41) compared with Case I. The short circuit current (14.9064kA) computed at bus 1 is still within the specified short-current rating of the switchgear (< 15.0 kA). However, this value of short-circuit current (in Case II) is slightly higher than the value computed in Case I (14.9020 kA). However, the branch/line loading is kept within their maximum allowable loading limits.

7.9 Optimal Location and Sizing of Two Generator in a 47-bus RDN Using MSPSO

The problem of multiple DG deployment, considering the reliability of single large DG in contrast to multiple smaller DG units is considered in this section. Dispersing of smaller units of DG has a better advantage in terms of enhancing the reliability of the network, even though smaller capacity DG units may cost, higher than the larger capacity DG units. However, the failure of the large single DG unit in a network can be catastrophic if it is installed to meet the increased demand in growth of electricity consumption. In this section, three scenarios are considered based on 100% loading to demonstrate the capability of the MSPSO to solve the optimization problem. The first scenario is the base case network with no DG connected. The second Scenario involves the integration of two DG with a single objective of power loss reduction and ignoring any network constraints. The third scenario involves the connection of two DG considering two test cases. Case I involves a single objective function study with only short-circuit current constraint enforced. While Case II is a multi-objective function study with both short-circuit and line loading constraints enforced. For the operational constraints of voltage and line loading the weighting factors in Equation (7.29) are set to k_1=0.45, K_2=0.45 and k_3=0.10.Thus, significant priorities are given to the objectives of power loss reduction and voltage optimization compared to line loading objective.

7.9.1 Scenario I: base network with no generation

A summary of results for this scenario is presented in Table 7.1. The voltage profile of the original test network is the same as that shown in Figure 7.4. Similar to the study in 7.8.1, the specification of the switchgear rating is 15.0 kA.

7.9.2 Scenario II: two generator neglecting short-circuit current and line loading constraints

This scenario involved finding the optimal location and size for two generators operating at unity power factor with network constraints ignored. The results of the optimization process using MSPSO are presented in Table 7.5. The optimal size and location is obtained with two optimally sized 2.2683MW and 4.1MW generators located at bus number 5 and 38, respectively. An 81.94% power loss reduction is achieved in the process. The voltage profile of the network is presented in Figure 7.15. The integration of two optimal size generators resulted in the overall improvement of the voltage profile. The mean voltage and voltage standard deviation are improved from

0.9467pu and 0.01961 respectively in the base case to 0.9782pu and 0.007921 respectively in scenario II.

The short circuit current with the integration of two generators is computed as 16.4507 kA. This value (16.4507 kA) is higher than the allowable short-circuit current rating of the switchgear (15.0kA) set in section 7.9.1. It is also apparent from Table 7.5 that the total installed DG exceeded the 6MW allowed by the NERC regulations on DG for 11kV medium distribution voltage. Thus, taking into consideration the practical constraint on the short-circuit current capacity of the switchgear on feeder six at the substation bus (bus 1), the location of the 2.2683MW and 4.1MW generators at bus number 5 and 38, respectively, will require the upgrading of the switchgear rating.

Table 7.5: MSPSO SUMMARY RESULTS; 47-BUS NETWORK SCENARIO II (TWO DG, NO CONSTRAINTS)

	Two DG, a single objective without short-circuit current and line loading Constraints
Optimal bus location 1	5
DG1 MWs generated	2.2683 MW
Optimal bus location 2	38
DG1 MWs generated	4.1 MW
Σ MW loss	0.0550 MW
Σ Mvar loss	0.0877 Mvar
Min bus voltage	0.9669 pu
Max bus voltage	1.000 pu
Mean voltage	0.9782 pu
Standard deviation	0.007921
Σ MW loss reduction	81.94%
Σ Mvar loss reduction	82.01.0%
Designed Isc (I_k)	13.1223 kA
Specified Isc (I_{spec})	**< 15.0 kA**
Isc with DGs (I_{fDG})	**16.4507 kA**

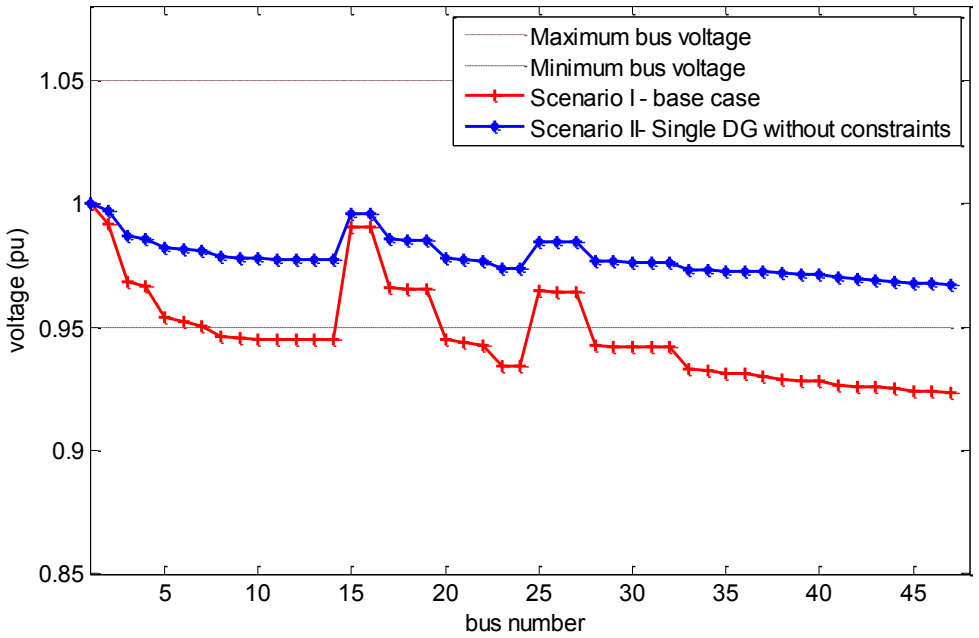

Figure 7.15: Voltage profile of 47-bus radial distribution network (Feeder 6), Scenario II (two DG without constraints)

Figure 7.16 shows the apparent power (MVA) flow for all branches of the network. The connection of DG drastically reduced the apparent power flow in some branches of the network with some branches operating close to their maximum limits. It is also obvious from Figure 7.15 that no branch of the network is overloaded following the location of two optimal DG.

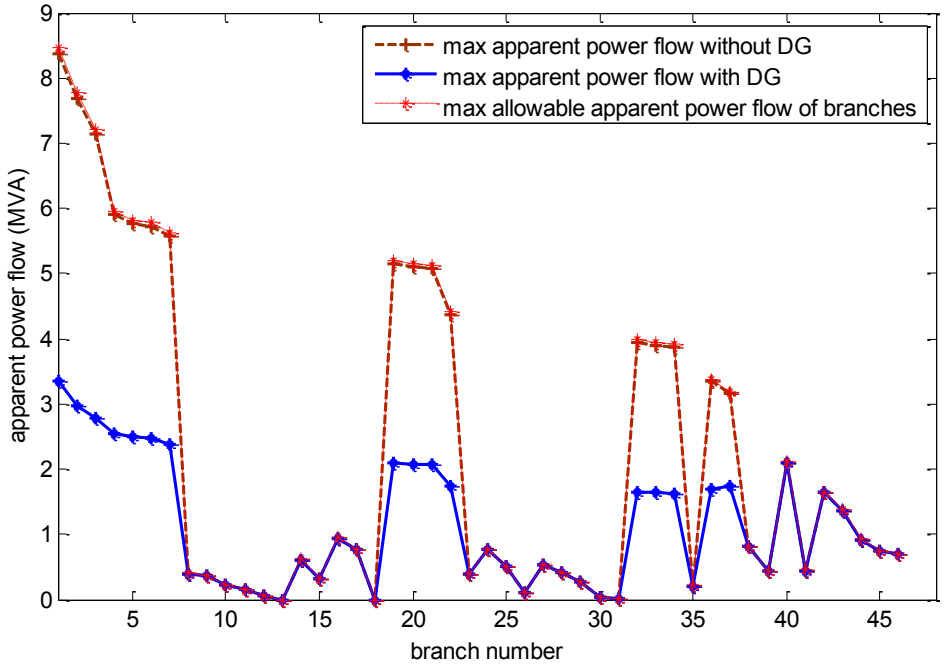

Figure 7.16: 47-bus branch apparent power flow/ line loading Scenario II (two DG without constraints)

Additionally, the connection of two DG resulted in a drastic reduction in the apparent power injected from the grid compared to integration of one DG (section 7.8.2, Figure 7.8). However, the optimal solution obtained for this scenario will require the upgrading of the switchgear rating at the substation to accommodate the 16.4507kA due to the location of two generators.

7.9.3 Scenario III: two generators Case I and II (single and multi-objective)

This scenario involved finding the optimal location and size for two generators operating at unity power factor, first with a single objective and considering only short-circuit current constraint (Case I) and with multi-objective where both short-circuit current and line loading constraints are considered (Case II). The results of the optimization process using MSPSO for this scenario are presented in Table 7.6.

Table 7.6: MSPSO SUMMARY RESULTS; 47-BUS NETWORK SCENARIO III (TWO GENERATORS), CASE I AND II (SINGLE AND MULTI-OBJECTIVE)

	Two DGs operating at unity PF, a single objective with short circuit Constraint only: Case I	**Two DGs operating at unity PF, multi-objective with short circuit, and line loading Constraints: Case II**
DG1 Optimal bus location	44	23
DG1 MWs generated	2.5 MW	1.42 MW
DG2 Optimal bus location	40	41
DG2 MWs generated	2.26 MW	2.75 MW
Σ MW loss	0.0657 MW	0.0728 MW
Σ Mvar loss	0.1034 Mvar	0.1139 Mvar
Min bus voltage	0.9655 pu	0.9572 pu
Max bus voltage	1.000 pu	1.000 pu
Mean voltage	0.9738 pu	0.9700 pu
Standard deviation	0.008384	0.0102
Σ MW loss reduction	78.43%	76.10%
Σ Mvar loss reduction	78.79%	76.64%
Designed Isc (I_k)	13.1223 kA	
Specified Isc (I_{spec})	15.0 kA	
Isc with DGs (I_{fDG})	**14.9992 kA**	**14.9074 kA**

The optimal size and location is obtained with two optimally sized 2.26 MW and 2.5 MW and located generator at bus number 40 and 44 respectively in Case I. A 78.43% power loss reduction is achieved. For case II, the optimal size and location is obtained with two optimally sized 1.42 MW and 2.75 MW and located generator at bus number 23 and 41 respectively. Moreover, a 76.10% power loss reduction is achieved.

The integration of two generators resulted in the overall improvement of the network voltage profiles as shown in Figure 7.17. The mean voltage and standard deviation are improved from 0.9467pu and 0.01961 respectively in the base case to 0.9738pu and 0.008334 respectively in Case I. While in Case II, the mean voltage and the voltage standard deviation are improved to 0.9700pu and 0.01020 respectively, when compared with the base case.

Figures 7.18 and 7.19 show the apparent power (MVA) flow for all branches of the network for case I and II respectively. It is evident in both cases that the connection of two DG as expected drastically reduced the apparent power flow in some branches and with others operating close to their maximum limits. It is apparent that, the enforcement of the constraint on short-circuit current only (Case I) resulted in the overloading of two branches of the network (branches 39 and 40) as shown in Figure 7.18. The enforcement of the network constraint of line loading constraint in addition to the constraint of short-circuit current (Case II) resulted in the removal of the overload experienced in branches 39 and 40 of Figure 7.18 as shown in Figure 7.19.

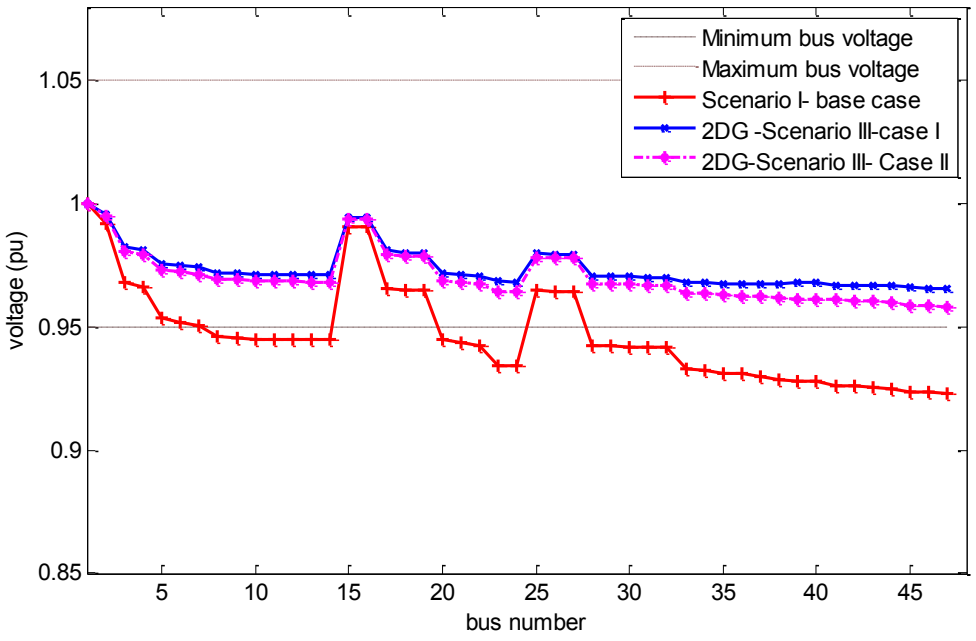

Figure 7.17: Voltage profile of 47 bus radial distribution network (Feeder 6) Scenario III (two generators), Case I and II (single and multi-objective)

However, this achievement is obtained at the expense of slightly lower penetration level of DG for Case II (57.5%) compared with Case I (65.7%). The short circuit current (14.9074kA) computed at bus 1 for Case II with the enforcement of both constraints is still within the specified short-current rating of the switchgear (< 15.0 kA). However, this value (in Case II) as expected is lower than the value computed for Case I (14.9992 kA).

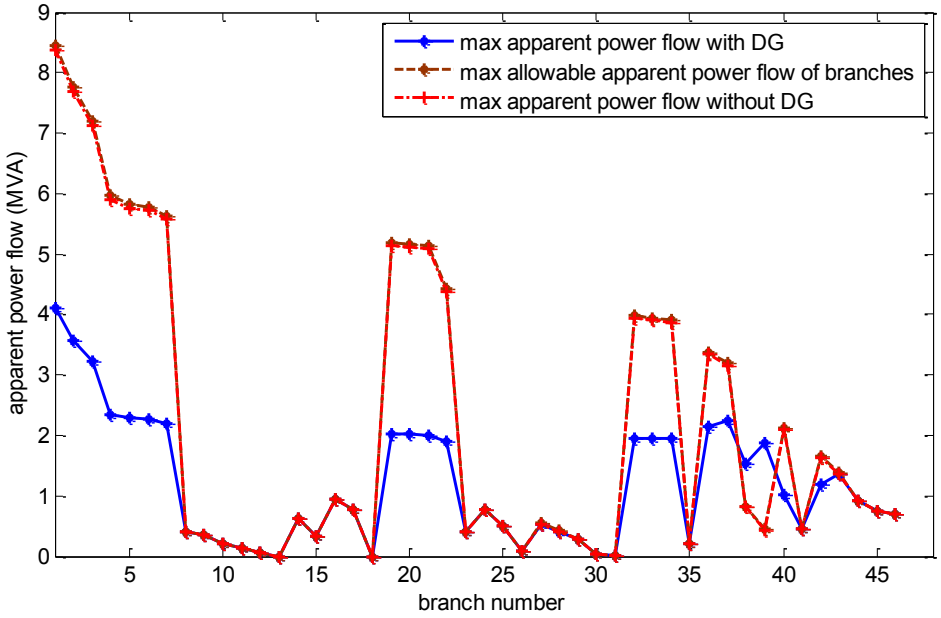

Figure 7.18: 47-bus branch apparent power flow/ line loading Scenario III (two DG), Case I (single objective with only short-circuit constraint)

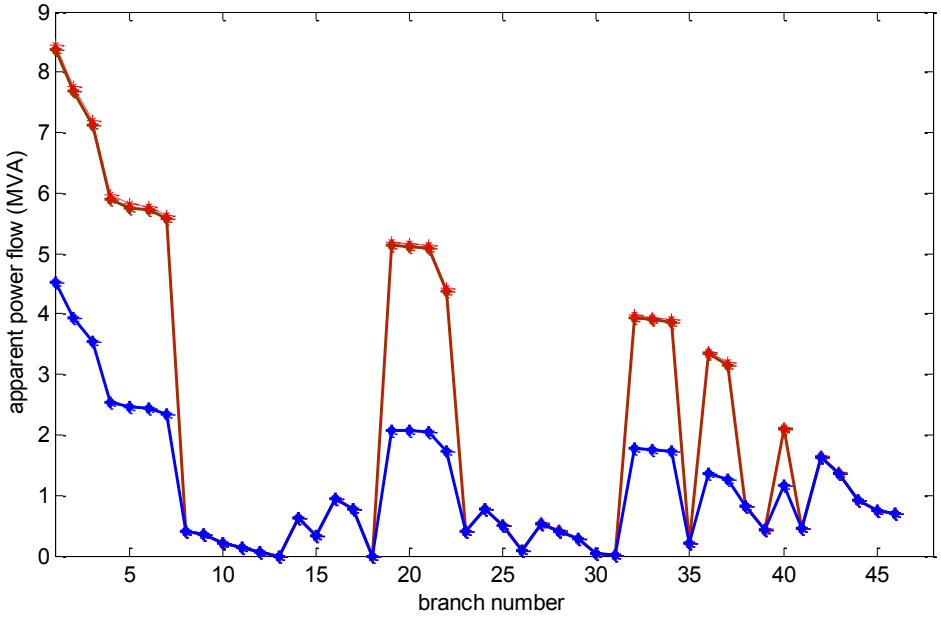

Figure 7.19: 47-bus branch apparent power flow/ line loading Scenario III (two DG), Case II (multi-objective with o short-circuit and line loading constraints)

Notwithstanding, the branch/line apparent power flows are kept within their maximum allowable loading limits with the enforcement of both constraints (Case II, Figure 7.19). The overall results of the studies show that magnificent results in terms of overall loss reduction and voltage profile improvement are obtained with the optimal size and location of two generators. There is also a drastic reduction in the apparent power injected from the grid due to the connection of two distributed generation. This reduction in apparent power flow is higher than the case of a single DG integration. The enforcement of short-circuit current ensures that the location of DG does not result from the flow of fault current above the breaking capacity of the switchgear at the substation during a fault. The enforcement of line loading constraint ensures the location of DG does not result in the overloading of the network branches. The advantages of which include, minimizing the needs for both upgrading of switchgear and reconductoring. Thus, an optimisation process that considers the constraints of switchgear and line loading can be useful to both the utilities and the network operators to plan deferment in switchgear upgrading and network reconductoring.

7.10 MSPSO Solution Validation by ERACS using 47-bus RDN

ERACS is an ERA Technology's suite of power system analysis software that allows modelling and simulation of electrical power system networks quickly and efficiently and judging their correct, safe and timely operation under user defined, and sometimes arduous situations [107]. The benefits associated with the use of ERACS software include reduced study times and improved technical capability for users. Thus, it meets the specific needs of engineers with practical problem to solve. The GUI forms the core of ERACS making it user-friendly with flexibility and up to 1500 bus bars can be simulated. The programs operational include some of the followings; load flow, short circuit, harmonics, transient stability and protection coordination. ERACS software has been used to solve power system problems [126-130] with an efficient solution.

7.10.1 Modelling and simulation of 47 bus radial distribution network using ERACS

This section presents the simulation results from ERACS software used for validating the solution of MSPSO on the 47 bus RDN. The first two scenarios and case I of third and fourth scenarios of section 7.8 from MSPSO simulation results based on a single DG integration are considered for validation. The first scenario was the base case with no generation. The second scenario was the integration of a single DG with the objective of power loss reduction and ignored any network constraints. The third scenario (with Case I) was based on the second scenario, considering only the constraint on short-circuit current. The fourth scenario (with Case I) was based on the third scenario with the generator allows to inject reactive power at a lagging power factor of 0.85.

7.10.2 Network modelling in ERACS

ERACS simulate a balanced and transposed 3phase network by using a per phase representation of the network. The balanced network Figure 7.5 is modelled as shown in Figure 7.20 with the following parameters;

The voltage source is modelled as External Grid (Grid Infeed) with the following parameters: Short Circuit (SC) MVA =250MVA for connection to 11kV and X/R=10 [107]. The upstream grid impedance (resistance and reactance) is computed using these parameters. A base apparent power (BaseMVA) of 10MVA is used with a base voltage of 11kV and a frequency of 50Hz. All loads connected to the busbars are spot load connected as 'shunt' element and are modelled as constant real and reactive power (PQ)

loads. All generators are modelled as fixed voltage behind source impedance (with their positive sequence impedance set equal to sub-transient value). The branches impedance of the network is represented by their per unit positive sequence impedance. ERACS allows representation of synchronous generator in different types such as Slack, PV, PQ and VA [107]. In this investigation, the generator can be modelled either as PV or PQ. In the PV model, the real power and the voltage magnitude of the generator are specified, and the load flow, calculates the reactive power and the voltage angle. In the PQ model, the real and the reactive power of the generator are specified, and the load flow calculates the voltage magnitude and angle.

.

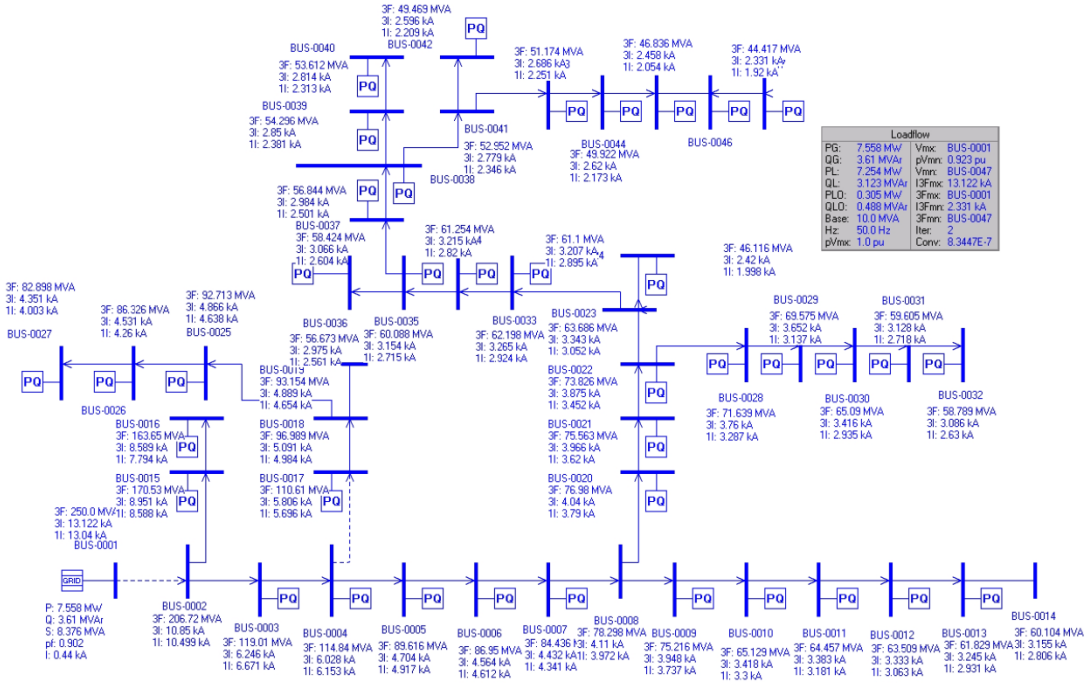

Figure 7.20: ERACS Model of 47 bus radial distribution network (Figure 7.5)

7.11 ERACS Load Flow and Fault Level Calculations

The purpose of the ERACS program load flow calculations used in this study is to determine the steady state voltage profile for the network and the associated branch and shunt flows under specified constraints. ERACS program by default after running the load flow will calculate both three-phase and single-phase to earth fault levels at every busbar in the network provided there is sufficient data for the network. Provided the positive sequence impedance has been specified for every synchronous machine the program will calculate three-phase fault levels. If, in addition to this, zero sequence impedance is specified for all lines, cables, transformers, and synchronous machines,

the program will also calculate the single phase to earth fault. In this investigation, only a balanced three-phase fault is considered.

In ERACS, the load flow three phase fault MVA, three phase fault current (kA), and X to R ratio at every busbar are calculated using the following equations [107]:

$$3I = \frac{v_{lf}}{Z_{1drv}}$$

$$3F = \sqrt{3} \cdot V_N \cdot 3I$$

$$3XR = \frac{X_{1drv}}{R_{1drv}} \tag{7.30}$$

where;

3I: is the three -phase fault current (kA).

3F: is the three-phase fault level (MVA).

3XR: is the three-phase X to R ratio.

$V_{N:}$ is the nominal voltage at the busbar.

$Z_{1drv:}$ is a positive sequence driving point impedance.

$R_{1drv:}$ is a positive sequence driving point resistance.

$X_{1drv:}$ is a positive sequence driving point reactance.

7.12 Simulation Results

The network of Figure 7.5 is modelled in ERACS as shown in Figure 7.20 based on the known parameters.

7.12.1 Comparison of Scenario I: base case network no generation

The summary of results (load flow and short circuit current level) using ERACS for the base case network compared with that of MSPSO is presented in Table 7.7.

The maximum short circuit current in the base case network (designed I_{SC}) evaluated with ERACS is 13.122 kA and occurs at bus 1 which is in agreement with the computed value using the MSPSO symmetrical fault algorithm as shown in Table 7.6. The short-circuit current computed for each bus using the MSPSO is compared with those from ERACS, and an average absolute error of 0.5% is recorded in the base case with no DG.

Table 7.7: SUMMARY OF RESULTS; SCENARIO I, WITH NO GENERATION (BASE NETWORK)

	47- Bus Network ERACS	47- Bus Network MSPSO
Σ MW loss	0.305 MW	0.3046 MW
Σ Mvar loss	0.448 Mvar	0.4876 Mvar
Min bus voltage	0.9233 pu	0.9233 pu
Max bus voltage	1.000 pu	1.000 pu
Σ Load MW	7.254 MW	7.25 MW
Σ Load Mvar	3.1230 Mvar	3.12 Mvar
Designed Isc (I_k)	**13.122 kA**	**13.1223 kA**

7.12.2 Comparison of results of Scenario II and III

These scenarios are validated with the following set of generators from ERACS reference Library having the following parameters;

1. A typical 11kV private generator with the key name G110; this is a 5MW, 5.88MVA 11kV 50Hz generator with a positive sequence impedance of $(0.00343 + j0.162)$ pu on rating
2. A G8ME, 5MW, 6.25MVA 3.3kV 50Hz generator with a positive sequence impedance value of $(0.0010 + j0.01)$ pu on rating and transformer rated 11/3.3kV, 5MVA, Yy0, 7.08%, ONAN with sequence impedance of $(0.25 + j3.53)$ % on rating
3. A GTRU, 3.4MW, 4.25MVA 11kV GAS Turbine generator with positive sequence impedance value of $(0.0064 + j0.11)$ pu on rating

These generators sizes correspond to the optimal DG sizes obtained using the MSPSO. The values of the positive sequence impedances giving above are the default values of ERACS library and therefore replaced with values computed by the optimization process using Equations (7.27) - (7.24). These values are $(0.0021 + j0.0303)$ pu on rating for 5MW generator and $(0.0031 + j0.0444)$ pu on rating for 3.4MW generator.

In scenario II, 5MW DG is located on bus 38. In scenario III, 3.4MW DG is placed in its optimal location (bus 44) as was determined by the MSPSO optimization process. The network is simulated, and the summaries of ERACS load flow results involving scenarios II and III are presented in Tables 7.8 and 7.9.

The maximum short circuit current obtained for the Scenario I using ERACS is 15.665kA while a value of 15.7038kA was computed at bus 1, using MSPSO. An absolute difference (error) of about 0.2% is obtained, showing that the two results are in agreement. In addition, result of total power loss after the integration of DG for ERACS (0.066MW) is in agreement with that obtained using MSPSO (0.0657MW).

Table 7.8: E ERACS LOAD FLOW STUDY 47-BUS; SCENARIO II (SINGLE DG WITH NO CONSTRAINTS) VS MSPSO

	47- Bus Network ERACS	47- Bus Network MSPSO
Σ MW loss	0.066 MW	0.0657 MW
Σ Mvar loss	0.104 Mvar	0.1038 Mvar
Min bus voltage	0.9640 pu	0.9640 pu
Max bus voltage	1.0000 pu	1.0000 pu
Σ Load MW	7.254 MW	7.25 MW
Σ Load Mvar	3.1230 Mvar	3.12 Mvar
Isc with DGs (I_{fDG})	**15.665 kA**	**15.7038 kA**

In a realistic situation, the DG output is limited by the current rating of the stator or rotor windings. Thus, the group assigned power of the DG is set at 4.995MW as against 5.0MW, resulting in a slight variation in the result of power loss computed with ERACS

The maximum short circuit current obtained with scenario III using ERACS is 14.896kA, while a value of 14.9153kA is computed using MSPSO. An absolute difference of 0.13% is recorded.

Table 7.9: ERACS LOAD FLOW STUDY 47-BUS; SCENARIO III (SINGLE DG), CASE I (WITH ONLY SHORT-CIRCUIT CONSTRAINT) VS MSPSO

	47- Bus Network ERACS	47- Bus Network MSPSO
Σ MW loss	0.095 MW	0.0948 MW
Σ Mvar loss	0.149 Mvar	0.1487 Mvar
Min bus voltage	0.9560 pu	0.9520 pu
Max bus voltage	1.0000 pu	1.0000 pu
Σ Load MW	7.254 MW	7.25 MW
Σ Load Mvar	3.1230 Mvar	3.12 Mvar
Isc with DGs (I_{fDG})	**14.896 kA**	**14.9153 kA**

The result of total power loss after the integration of DG with ERACS (0.095MW) for this scenario is in agreement with that obtained using MSPSO (0.095MW).

The connection of 5MW, 3.3kV generator through a transformer to the grid resulted in the reduction of the maximum short circuit current (13.998 kA) of the network (scenario III, with transformer) at the infeed bus 1. On the other hand, this resulted in an increase in power loss (0.108MW) compared to 0.095MW (scenario III, without transformer) as shown Table 7.10 due to the inclusion of transformer impedance.

Table 7.10: ERACS LOAD FLOW STUDY 47-BUS; SCENARIO III (WHEN DG IS CONNECTED TO GRID VIA TRANSFORMER)

	47- Bus Network ERACS with connection Transformer	47- Bus Network ERACS without connection Transformer
Σ MW loss	0.108 MW	0.095 MW
Σ Mvar loss	0.506 Mvar	0.149 Mvar
Min bus voltage	0.9590 pu	0.9560 pu
Max bus voltage	1.0000 pu	1.0000 pu
Σ Load MW	7.254 MW	7.254 MW
Σ Load Mvar	3.1230 Mvar	3.1230 Mvar
Isc with DGs (I_{fDG})	**13.998 kA**	**14.896 kA**

From the results in Table 7.10, it is evident that the presence of a transformer between the fault location and the contributing DG introduces high impedance in the network that reduced the fault level. However, this resulted in an increase in the network power loss due to increased network impedance and consequently impacted positively on the network voltage profile. The minimum voltage in Table 7.10 improved from 0.9560pu to 0.9590pu (without and with the connection transformer respectively).

7.12.3 Comparison of results of Scenario IV, Case I

This scenario was based a single generator operating at a minimum PF of 0.85 lagging, with constraint on short-circuit current only considered. In this validation, Scenario IV considered the optimal 3.075 MW DG located at its optimal location (bus 46) with the DG injecting reactive power to support the network. A 3.4 MW generator from ERACS library is used, and the group assigned real power (MW) output of the generator is set to 3.075 MW. The generator bus was modelled as PQ generator. The summary of results using ERACS simulation in this case is presented in Table 7.11. The group assigned

reactive power is set at 1.9057 Mvar. When DG is injecting var support of 1.9057Mvar to the network, the total real power loss after the integration of DG for ERACS reduces to 0.069MW, and the reactive power loss reduces to 0.107Mvar which is in agreement with the results obtained using MSPSO (0.0687MW and 0.1072Mvar).

Table 7.11: ERACS LOAD FLOW STUDY 47-BUS; SCENARIO IV (SINGLE DG OPERATING AT 0.85 PF LAGGING) CASE I (WITH ONLY SHORT-CIRCUIT CURRENT CONSTRAINT)

	47- Bus Network ERACS	47- Bus Network MSPSO
Σ MW loss	0.069 MW	0.0687 MW
Σ Mvar loss	0.107 Mvar	0.1072 Mvar
Min bus voltage	0.9780 pu	0.9776 pu
Max bus voltage	1.0000 pu	1.0000 pu
Σ Load MW	7.254 MW	7.25 MW
Σ Load Mvar	3.1230 Mvar	3.12 Mvar
Designed Isc (I_k)	**14.335 kA**	**14.9020 kA**

However, it is also possible to represent the 3.075MW optimal generator in ERACS using the value of the computed sub-transient reactance of the generator $(0.0029 + j0.418)$pu on rating from the MSPSO optimisation process. Thus, the group assigned power of the DG is set at 3.072MW as against 3.075MW (about 0.1% less than the actual generator rating) and the group assigned reactive power of the generator is set to 1.8 MW (about 94% of the generator reactive power capability). The total real power loss after the integration of DG using ERACS reduces to 0.069 MW, and the reactive power loss reduces to 0.108 Mvar confirming the accuracy of the previous result using 3.4MW generator.

The computed short circuit current and fault level MVA for all bus locations are presented in Figures 7.21 and 7.22 respectively. It is evident that in all the scenarios considered in this investigation, the results are in agreement with those from ERACS. The results of the validation exercise have so far shown that the developed MSPSO tool is a useful optimization tool for integration of DG into the power distribution system. Moreover, the proposed three-phase symmetrical fault algorithm (based on classical fault calculation method) implemented with the MSPSO can provide an acceptable solution to the problem of integration of DG within allowable fault level headroom.

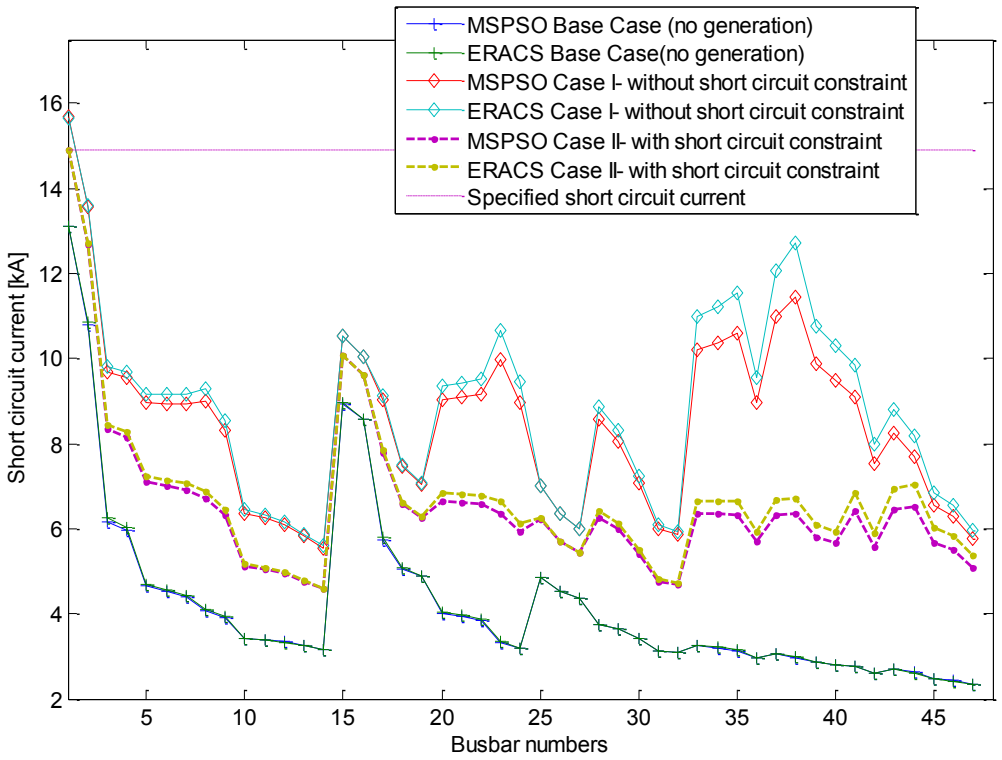

Figure 7.21: Short circuit current at different bus for cases I and II (MSPSO and ERACS)

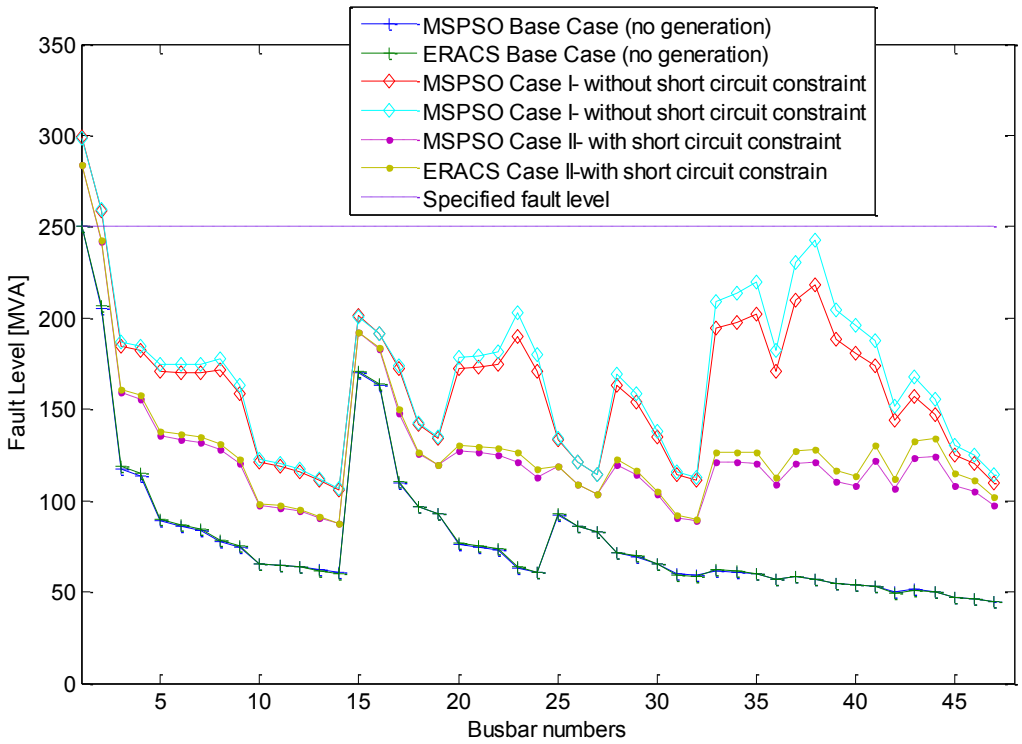

Figure 7.22: Fault level at different buses for cases I and II (MSPSO and ERACS)

The tool can be used to determine the optimal penetration level of DG in the distribution network that will minimize the need for upgrading of switchgear capacity/rating. In

addition, considering line loading constraints as part of the optimization process can defer the need for upgrading of network conductors.

7.13 Summary

In this chapter, MSPSO algorithm has been used to optimize the integration of distributed generation into a 47-bus Nigeria distribution system. The optimal size/location problem is solved taking into considerations pertinent, practical and network operational security constraints that could mitigate the development of the DG in power distribution networks. The study is carried out in three phases. The first phase considered the modelling of the network based on the data collated during the fieldwork study. The network is modelled with the assumption of a balanced and transposed system, paving ways for the determination of network parameters. The positive sequence impedance and admittance are adopted as the impedance and admittance parameters of the network, respectively.

In the second phase, MSPSO algorithm is used to study various network scenarios. The network scenarios are related to solving the optimal size and location problem based on a single and multi-objective formulation with one or two DG. The formulations considered a constraint on short circuit current of the protective switchgear at the infeed substation and the operational constraint of line loading capacity.

In the third phase, the validation of the MSPSO results with ERACS is carried out using the first four studied scenarios related to a single objective in the second phase. The results using ERACS are compared with those of the MSPSO and are found to be in agreement with each other. The slight difference in the results obtained with ERACS is because, in the real practical situation, the DG output is limited by the value of stator and rotor winding resistance. Thus, the group assigned power of the DG is, usually, set lower than the value used in the MSPSO simulation. The setting is to ensure that the current drawn from the generator does not exceed 100% of its rating.

The results of the studied scenarios revealed that considering the capacity of switchgear and line loading as part of the optimization process can defer the need for upgrading of network protective switchgear and reconductoring of the network lines while still achieving significant benefits in terms of reduce power loss and improve the voltage profile of the network.

The inclusion of the objective of voltage optimization into the objective power loss minimization to form a multi-objective has shown that DG can simultaneously

minimize network power loss and effectively provide voltage support for the network. However, as expected, the improvement in one objective results in the worsening of the other objective. The developed multi search PSO implemented with the three-phase symmetrical fault algorithm shows it is a useful optimization tool for DG integration within the acceptable fault level. Thus, allowing DG to be integrated within the allowable fault level headroom without the need for upgrading of switchgear capacity/rating.

In Chapter 8, the conclusions and recommendation for this research work are presented.

CHAPTER 8

Conclusions and Future Work

This chapter provides the conclusions of the work presented in this thesis and suggestions for further research related to the developed stochastic power system optimisation tool with applications to distributed generation integration in the power distribution network.

8.1 Conclusions

The ever increasing level of penetration of distributed generation in power distribution networks is not without its challenges for distribution system planning and operations engineers. Some of these challenges are in the areas of voltage regulation, increase of network fault levels and the disturbance to the network protection settings. One of the most-significant aspects of DG planning, however, is its optimal allocation. Thus, Distribution Network Operators (DNOs) will require an effective optimisation tool for network planning and integration of DG considering these challenges. DG can be beneficial to both electricity consumers and if the integration is properly engineered the energy utility. Hence, the demand for tools for their optimal placement cannot be over emphasised. Further, DG technologies are nowadays commercially available in compact and modular form with varying discrete sizes. The problem of DG sizing and arrangement is by its' very nature a multivariable search space (of integer, discrete and continuous variables) that calls for a multi search optimisation tool.

The aim of this thesis is to develop a power system tool based on the particle swarm optimisation algorithm (a stochastic search algorithm based on natural bird or bee swarm behaviour) with applications to planning and integration of distributed generation (both synchronous and induction machine based DG) in the power network. Furthermore, the proposed tool is to consider some pertinent and practical challenges (such as voltage, short circuit current level and line overloading constraints) that may impede the development of distributed generation in the power system distribution network. The developed optimisation tool (the multi-search particle swarm optimisation

or MSPSO) has been shown to be an effective and efficient method for DG planning and integration studies.

Considerable research has been carried out into the problem of distributed generation integration using several optimisation techniques where variables are continuous. These continuous-variables unnecessary increase the search space and hence the computational cost of the algorithm when finding the optimal or near-optimal solution of an optimisation problem. Previous studies will either round-up the continuous variable to define integer variable or used a fixed step size to represent discrete variable of the multi-search space problem. This will affect the accuracy of the optimisation results as the solutions are not likely to be the best-available practical choice as a consequence of missing out some generator sizes. A multi-search space problem of this nature will require an optimisation tool that will operate on the multi-control variables of the DG optimal integration problem.

A general overview of the proposed MSPSO tool (with the capability of handling multi-search space problem of both synchronous and induction machine based DG) was presented in Chapter 3. Appropriate handling techniques were developed for the different variables of the DG integration problem. These handling techniques include the multi-valued discrete PSO that handles the integer variable (bus location number) and the dichotomy algorithm that transform the continuous variable into a discrete variable used for generation and capacitor sizes. Further, to reduce the computational burden of the MSPSO, a few informants sub-routine algorithm was implemented. The concept is based on using few numbers of agents (particles) for fitness evaluations during the course of the optimisation process, thus, drastically reducing the number times the objective function needs to be evaluated.

The application of the developed multi-search particle swarm optimisation (with application to synchronous generator based DG integration problem) was presented in Chapters 4 and 5 using a standard compensated 69-bus radial distribution network as a benchmark test network. For the purposes of comparison, a study based on the particle swarm optimisation algorithm with inertia weight (PSO-W) was conducted first (Chapter 4). The problem was formulated both as a single-objective study to minimise network power loss and a multi-objective optimisation study to minimise power loss and provide voltage support for the network. Unlike in most-previous steady state optimisation studies in the literature, the objective functions were assessed with the DG node modelled as a PV node to inject reactive power into the network up to a given

minimum operating lagging power factor, thus allowing the DG reactive power control capability to be included in the analysis.

The investigation has shown that the best improvement in network loss reduction and voltage support (for a single objective study) are obtained when more than one generator are connected in the compensated network. Good results in terms of overall loss reduction and voltage profile improvement are obtained even when operating with the compensating capacitors disconnected since the generators are allowed to inject reactive power to provide network support. It is likewise demonstrated that the network power loss reduction is dependent on the operating power factor of the DG. Higher power loss reduction figures were obtained when operating at lagging power factors compared to unity operating power factor. The multi-objective optimisation study resulted in a conflict of interest with improvement in the voltage profile of the network resulting in a lower power loss reduction (compared with the single-objective study). The impact of voltage improvement was found to be most significant in the case of DG operating at unity power factor and when the network reactive power compensation devices were removed.

The application of the proposed multi-search particle swarm optimisation (MSPSO) algorithm to the same network scenarios and test cases is presented in Chapter 5. Unlike the PSO-W studies presented in Chapter 4 (where the DG sizes are treated as continuous variables), the MSPSO used a list of commercially available DG units to define the discrete size of DG units. Similar final results were obtained with small differences in optimum DG sizes and network loss reduction and voltage values because of the practical restriction imposed on the size of available DG units. Both algorithms found the same optimal locations for the DG units. The comparison showed that the conventional PSO-W algorithm results, in some instances, resulted in an overestimation (or underestimation) of the percentage power loss reduction and the SSEV (sum of the squared of error voltages) index used to quantify the network voltage profile improvement. This is a result of the rounding-off process of the DG sizes obtained with PSO-W and other optimisation methods affecting the accuracy of the obtained results. The multi-search PSO algorithm shows the advantage of fewer function evaluations as it uses few numbers of agents in the evaluation of the objective function compared to PSO-W. Other advantages of MSPSO include reduced search space with quicker results due to fewer iterations and the ability to explore discrete search space of DG control variables compared with the PSO-W for the same optimisation problem.

The benefit of the proposed MSPSO algorithm is further demonstrated by the comparison of its results with those obtained using other optimisation methods available in the literature that use either continuous variables or binary representation of the real variables. The MSPSO algorithm produced a better power loss reduction result compared with previous studies since it avoids the rounding up errors inherent in some methods. A slight improvement is also achieved when compared with other discrete algorithms that miss out some generator sizes because they only consider the DG sizes in even steps of 100kW.

The results have also shown that permitting voltage regulation by the distributed generation units will aid in realizing some of the theoretical or practical benefits of distributed generation. Such benefits include reduced voltage variation and relief from unnecessary reactive power flows resulting in a drastic reduction in network power loss and improved voltage profile.

In both chapter 4 and 5 it was found that, when the generator operates in a compensated network, the actual power factor is always higher than 0.95 lagging (compared with the minimum lagging possible operating power factors of 0.85 or 0.95). Thus, resulted in identical optimal results for both 0.85 and 0.95 minimum lagging operating PF, as there will be no need for the generators to go down to these power factors. Nevertheless, this situation was found to be different when the generator operates in an uncompensated network: the operating power factor will drop below 0.95 PF if necessary. Hence, there was a difference between the results for 0.85 and 0.95 minimum lagging PF.

The implementation of the proposed MSPSO algorithm for the integration of the induction generator based DG was demonstrated in Chapter 6, using the same standard 69-bus radial distribution network. Induction generators behave differently from the synchronous generator based DG units. An induction generator requires reactive power support from the network for its operation. In previously published studies, the reactive power requirement of this generator is commonly computed using an approximate empirical formula, resulting in the underestimation or overestimation of the reactive power requirement of the generator. In this work, an algorithm for computing the reactive power requirement of the induction generator is proposed based on the per phase equivalent circuit of the machine. The proposed MSPSO and the IG reactive power requirement calculation procedure are interfaced to perform the optimisation procedure. The outcomes have shown that the proposed technique can account for the reactive power requirement of the generator better than the approximate formula used in

the previous studies. The technique gives a more accurate estimation of the induction machine reactive power demand as a guaranteed leading to more accurate optimum solutions.

Unlike previous studies, the simultaneous integration of shunt compensation capacitors and induction generator DG units is considered. This reactive power requirement of the generator is usually supplied locally via var compensation capacitors and must be accounted for in the optimisation process. In this investigation, the shunt compensation capacitors are included as part of the optimisation problem, to compensate the reactive power drawn on the grid when the unit is delivering output at rated power. It is shown that this approach results in a lower reactive power flow in the network leading to improved network loss and improved voltage profile.

In previous steady state optimisation studies involving the integration of induction generator based distributed generation, the impact of the short circuit current rating of switchgear and line loading limits are not considered. In this research work, an algorithm procedure for computing a three-phase symmetrical fault current based on classical fault calculation method is implemented alongside the MSPSO algorithm. This fault algorithm is used to enforce the constraint on short-circuit rating of the switchgear, while the constraint on line loading capacity is enforced using a quadratic index. By considering the capacity of switchgear and line loading as part of the optimisation process, the need for upgrading of network protective switchgear and reconductoring of the network lines can be considered and avoided. The results show that when the constraints imposed by switchgear rating and the line loading limit are neglected, the capacity of the network to absorb new generation will be overestimated. This resulted in the overestimation of the technical benefits of DG.

In chapter 7, the effectiveness of the proposed MSPSO algorithm tested on a real 47-bus radial distribution network in Nigeria. Pertinent and practical network security constraints are considered in the optimisation process and the results checked and validated using the ERACS power system analysis software package.

In summary, the proposed stochastic multi-search particle swarm optimisation (MSPSO) algorithm has been shown to be an effective tool for power system optimisation studies involving the connection of distributed generation. The algorithm is capable of operating simultaneously with the integer, discrete and continuous variables that comprise the search space in the optimal DG sizing/location optimisation study, thus,

overcoming some of the limitations associated with the continuous optimisation algorithms used for solving this complex nonlinear optimisation problem. The search space and the computational cost of the algorithm are substantially reduced compared with other PSO methods used, without loss of quality in the attained optimal solution. The inclusion of the fault current calculation procedure alongside the MSPSO algorithm in conjunction with the enforcement of pertinent network security and operational constraints allows for a realistic optimisation solution.

8.2 Scope for future work

The techniques developed in this thesis are used to solve the problems of DG and shunt capacitor integration onto the radial distribution system. The concept can also be applied to meshed distribution network without any modification. Further, the algorithm can be extended to the problem of finding optimal substation location/size with a different mix of DG technologies for integration into a microgrid network as well as other power system optimisation problems such as the sizing and location of static reactive power compensation equipment and other FACTS devices.

In the current study, only operational, technical objectives and constraints were considered. It would be worthwhile in any future study to also consider economic considerations such as investment, revenues, income generation from ancillary services and operation and maintenance costs. Such an economic optimal strategy would naturally be non-generic because of the involvement of various stakeholders. For example, clients who want to improve self-sustainability, power producers, who desire to diversify their production peak, power system operators, who choose to plan grid investments and, last but not least, regulators and governments, who need to have a benchmark and a tool to assess the impact of support mechanisms [131]. Nevertheless, this is still a mixed integer, discrete and continuous problem that calls for the solution of complex optimisation functions and there is no reason why the proposed MSPSO algorithm cannot be extended to such a problem.

In chapter 6 and 7, a three-phase symmetrical fault calculation was implemented together with the MSPSO algorithm based on classical fault calculation methods. It would be worthwhile in the future subject to perform the fault calculation based on IEC 60909. A comparison can then be drawn between the two techniques (IEC 60909 is a standard established to give a general approach for the computation of short circuit current, providing conservative results, but with sufficient accuracy [106]).

In Chapters 6 and 7, the multi-objective formulation of the problem is effectively transformed into a single objective study by using the weighted aggregate method. The single objective function is constructed as the sum of objective functions multiplied by their weighting factors. In such cases, there is always the difficulty of determining the appropriate weights that can be assigned to different objectives when there is not enough information about the problem. It would be worthwhile in the future to compare the results of this study with an algorithm that can inherently handle multiple objective problems such as the newly developed modernized particle swarm optimisation 'Differential Search Algorithm' (DSA). DSA is a novel and efficient evolutionary algorithm for resolving real-valued numerical optimisation problems, inspired by the migration of super-organisms utilizing the concept of stable-motion [132].

REFERENCES

[1] N. Jenkins, J. B. Ekanayake, and G. Strbac, *Distributed Generation*. London: Institute of Engineering and Technology, 2010.

[2] S. Chowdhury, S. Chowdhury, and P. Crossley, *Microgrids and Active Distribution Networks*. London: Institute of Engineering and Technology, 2009.

[3] A. Thomas, A. Göran, and L. Söder, "Distributed generation: a definition," *Electric Power Systems Research,* vol. 57, pp. 195-204, 2001.

[4] A. M. Guseynov and B. S. Akhundov, "Defining Impact of Distributed Generation on Power System Stability," in *Proceedings of 5th International Conference, Asian Energy Cooperation (AEC)*, Yakutsu, Russia, 2006, pp. 122-125.

[5] N. Mithulananthan, O. Than, and P. Le Van, "Distributed Generator Placement in Power Distribution system Using Genetic Algorithm to Reduce Losses," *Thammasat International Journal of Science, Technology,* vol. 9, pp. 52-56, 2004.

[6] *The Future of the Electric Grid*: Massachusetts Institute of Technology, 2011.

[7] R. A. Walling and M. L. Reichard, "Short circuit behavior of wind turbine generators," in *Protective Relay Engineers, 2009 62nd Annual Conference for*, Austin, TX, 2009, pp. 492-502.

[8] I. Musa, B. Zahawi, and S. M. Gadoue, "Integration of induction generator based distributed generation and shunt compensation capacitors in power distribution networks," in *Power Engineering, Energy and Electrical Drives (POWERENG), 2013 Fourth International Conference on*, Istanbul, Turkey, 2012, pp. 1105-1109.

[9] H. Duong Quoc and N. Mithulananthan, "Multiple Distributed Generator Placement in Primary Distribution Networks for Loss Reduction," *Industrial Electronics, IEEE Transactions on,* vol. 60, pp. 1700-1708, 2013.

[10] N. Acharya, P. Mahat, and N. Mithulananthan, "An analytical approach for DG allocation in primary distribution network," *International Journal of Electrical Power & Energy Systems,* vol. 28, pp. 669-678, 2006.

[11] H. Duong Quoc, N. Mithulananthan, and R. C. Bansal, "Analytical Expressions for DG Allocation in Primary Distribution Networks," *Energy Conversion, IEEE Transactions on,* vol. 25, pp. 814-820, 2010.

[12] P. Mahat, W. Ongsakul, and N. Mithulananthan, "Optimal placement of wind turbine DG in primary distribution systems for real loss reduction," in *Energy for sustainable development: Prospects and Issues for Asia*, Phuket, Thailand, 2006, pp. 1-6.

[13] I. Musa, S. Gadoue, and B. Zahawi, "Integration of Distributed Generation in Power Networks Considering Constraints on Discrete Size of Distributed Generation Units," *Electric Power Components and Systems,* vol. 42, pp. 984-994, 2014/06/30 2014.

[14] A. Keane and M. O'Malley, "Optimal Allocation of Embedded Generation on Distribution Networks," *Power Systems, IEEE Transactions on,* vol. 20, pp. 1640-1646, 2005.

[15] A. F. Zobaa and C. Cecati, "A comprehensive review on distributed power generation," in *Power Electronics, Electrical Drives, Automation and Motion, 2006 (SPEEDAM 2006), International Symposium on*, Taormina, Italy, 2006, pp. 514-518.

[16] U. S. DOE, "The Potential Benefits of Distributed Generation and Rate-Related Issues That May Impede Its Expansion," U.S department of Energy 2007.

[17] *Distributed Generation Connection Guide: A guide for Connecting Generation to Distribution Network that falls under G59/2*: Energy Networks Associations, January 2013.

[18] H. M. Ayres, W. Freitas, M. C. de Almeida, and L. C. P. da Silva, "Method for determining the maximum allowable penetration level of distributed generation without steady-state voltage violations," *Generation, Transmission & Distribution, IET,* vol. 4, pp. 495-508, 2010.

[19] S. Boljevic and M. F. Conlon, "The contribution to distribution network short-circuit current level from the connection of distributed generation," in *Universities Power Engineering Conference, 2008 (UPEC 2008), 43rd International*, Padova, Italy 2008, pp. 1-6.

[20] P. N. Vovos and J. W. Bialek, "Direct incorporation of fault level constraints in optimal power flow as a tool for network capacity analysis," *Power Systems, IEEE Transactions on,* vol. 20, pp. 2125-2134, 2005.

[21] P. Chiradeja, "Benefit of Distributed Generation: A Line Loss Reduction Analysis," in *Transmission and Distribution Conference and Exhibition: Asia and Pacific, 2005 IEEE/PES*, Dalian, China, 2005, pp. 1-5.

[22] H. L. Willis, "Analytical methods and rules of thumb for modeling DG-distribution interaction," in *Power Engineering Society Summer Meeting, 2000. IEEE*, Seattle, WA, 2000, pp. 1643-1644

[23] F. Rothlauf, "Optimization Problems," in *Design of Modern Heuristics*: Springer Berlin Heidelberg, 2011, pp. 7-44.

[24] P. Paliwal, N. P. Patidar, and R. K. Nema, "A comprehensive survey of optimization techniques used for Distributed Generator siting and sizing," in *Southeastcon, 2012 Proceedings of IEEE*, Orlando, FL 2012, pp. 1-7.

[25] J. H. Holland, *Adaptation in Natural and Artificial Systems*. Ann Arbor, MI The University of Michigan Press, 1975.

[26] J. Kennedy and R. Eberhart, "Particle swarm optimization," in *Neural Networks, 1995. Proceedings., IEEE International Conference on*, Perth, WA 1995, pp. 1942-1948 vol.4.

[27] R. Eberhart and J. Kennedy, "A new optimizer using particle swarm theory," in *Micro Machine and Human Science, 1995. MHS '95., Proceedings of the Sixth International Symposium on*, 1995, pp. 39-43.

[28] D. Karaboga, "An idea based on honey bee swarm for numerical optimization," Computer Engineering Department, Erciyes University, Turkey,Technical Report TR06 2005.

[29] D. Karaboga, B. Gorkemli, C. Ozturk, and N. Karaboga, "A comprehensive survey: artificial bee colony (ABC) algorithm and applications," *Artificial Intelligence Review,* pp. 1-37, 2012.

[30] P. S. Georgilakis and N. D. Hatziargyriou, "Optimal Distributed Generation Placement in Power Distribution Networks: Models, Methods, and Future Research," *Power Systems, IEEE Transactions on,* vol. 28, pp. 3420-3428, 2013.

[31] S. Santoso, N. Saraf, and G. K. Venayagamoorthy, "Intelligent Techniques for Planning Distributed Generation Systems," in *Power Engineering Society General Meeting, 2007. IEEE*, Tampa, FL 2007, pp. 1-4.

[32] L. F. Ochoa, A. Padilha-Feltrin, and G. P. Harrison, "Evaluating Distributed Time-Varying Generation Through a Multiobjective Index," *Power Delivery, IEEE Transactions on,* vol. 23, pp. 1132-1138, 2008.

[33] L. F. Ochoa, A. Padilha-Feltrin, and G. P. Harrison, "Evaluating distributed generation impacts with a multiobjective index," *Power Delivery, IEEE Transactions on,* vol. 21, pp. 1452-1458, 2006.

[34] P. N. Vovos, G. P. Harrison, A. R. Wallace, and J. W. Bialek, "Optimal power flow as a tool for fault level-constrained network capacity analysis," *Power Systems, IEEE Transactions on,* vol. 20, pp. 734-741, 2005.

[35] A. Keane and M. O'Malley, "Optimal Utilization of Distribution Networks for Energy Harvesting," *Power Systems, IEEE Transactions on,* vol. 22, pp. 467-475, 2007.

[36] M. F. AlHajri, M. R. AlRashidi, and M. E. El-Hawary, "Improved Sequential Quadratic Programming Approach for Optimal Distribution Generation Deployments via Stability and Sensitivity Analyses," *Electric Power Components and Systems,* vol. 38, pp. 1595-1614, 2010.

[37] Y. M. Atwa, E. F. El-Saadany, M. M. A. Salama, and R. Seethapathy, "Optimal Renewable Resources Mix for Distribution System Energy Loss Minimization," *Power Systems, IEEE Transactions on,* vol. 25, pp. 360-370, 2010.

[38] Y. M. Atwa and E. F. El-Saadany, "Probabilistic approach for optimal allocation of wind-based distributed generation in distribution systems," *Renewable Power Generation, IET,* vol. 5, pp. 79-88, 2011.

[39] N. Khalesi, N. Rezaei, and M. R. Haghifam, "DG allocation with application of dynamic programming for loss reduction and reliability improvement," *International Journal of Electrical Power & Energy Systems,* vol. 33, pp. 288-295, 2011.

[40] R. A. Jabr and B. C. Pal, "Ordinal optimisation approach for locating and sizing of distributed generation," *Generation, Transmission & Distribution, IET,* vol. 3, pp. 713-723, 2009.

[41] B. A. de Souza and J. M. C. de Albuquerque, "Optimal Placement of Distributed Generators Networks Using Evolutionary Programming," in *Transmission & Distribution Conference and Exposition: Latin America, 2006. TDC '06. IEEE/PES*, Caracas, Venezuela. , 2006, pp. 1-6.

[42] H. Falaghi and M. Haghifam, "ACO Based Algorithm for Distributed Generation Sources Allocation and Sizing in Distribution Systems," in *Power Tech, 2007 IEEE Lausanne*, Lausanne, Switzerland 2007, pp. 555-560.

[43] M. F. Akorede, H. Hizam, I. Aris, and M. Z. A. Ab Kadir, "Effective method for optimal allocation of distributed generation units in meshed electric power systems," *Generation, Transmission & Distribution, IET,* vol. 5, pp. 276-287, 2011.

[44] S. Deependra, D. Singh, and K. S. Verma, "Multiobjective Optimization for DG Planning With Load Models," *Power Systems, IEEE Transactions on,* vol. 24, pp. 427-436, 2009.

[45] F. S. Abu-Mouti and M. E. El-Hawary, "Optimal Distributed Generation Allocation and Sizing in Distribution Systems via Artificial Bee Colony Algorithm," *Power Delivery, IEEE Transactions on,* vol. 26, pp. 2090-2101, 2011.

[46] G. P. Harrison, A. Piccolo, P. Siano, and A. R. Wallace, "Hybrid GA and OPF evaluation of network capacity for distributed generation connections," *Electric Power Systems Research,* vol. 78, pp. 392-398, 2008.

[47] Y. Del Valle, G. K. Venayagamoorthy, S. Mohagheghi, J. C. Hernandez, and R. G. Harley, "Particle Swarm Optimization: Basic Concepts, Variants and Applications in Power Systems," *Evolutionary Computation, IEEE Transactions on,* vol. 12, pp. 171-195, 2008.

[48] A. F. Zobaa and A. Lecci, "Particle swarm optimisation of resonant controller parameters for power converters," *Power Electronics, IET,* vol. 4, pp. 235-241, 2011.

[49] H. H. Zeineldin and A. F. Zobaa, "Particle Swarm Optimization of Passive Filters for Industrial Plants in Distribution Networks," *Electric Power Components and Systems,* vol. 39, pp. 1795-1808, 2014/01/27 2011.

[50] A. F. Zobaa and A. Lecci, "Power circuit design based on PSO optimization," in *Power Electronics and Motion Control Conference (EPE/PEMC), 2010 14th International*, pp. T6-121-T6-125.

[51] A. F. Zobaa and A. Lecci, "Power circuit design based on PSO optimization," in *Power Electronics and Motion Control Conference (EPE/PEMC), 2010 14th International*, Ohrid, Macedonia 2010, pp. T6-121-T6-125.

[52] A. Soroudi and M. Afrasiab, "Binary PSO-based dynamic multi-objective model for distributed generation planning under uncertainty," *Renewable Power Generation, IET,* vol. 6, pp. 67-78, 2012.

[53] A. M. El-Zonkoly, "Optimal placement of multi-distributed generation units including different load models using particle swarm optimisation," *Generation, Transmission & Distribution, IET,* vol. 5, pp. 760-771, 2011.

[54] M. Gomez-Gonzalez, A. Lopez, and F. Jurado, "Optimization of distributed generation systems using a new discrete PSO and OPF," *Electric Power Systems Research,* vol. 84, pp. 174-180, 2012.

[55] M. Gomez-Gonzalez, A. Lopez, and F. Jurado, "Hybrid discrete PSO and OPF approach for optimization of biomass fueled micro-scale energy system," *Energy Conversion and Management,* vol. 65, pp. 539-545, 2013.

[56] V. V. K. Satyakar, J. V. Rao, and S. Manikandan, "Analysis of Radial Distribution System by Optimal Placement of DG Using DPSO," *International Journal of Engineering,* vol. 1(10), 2012.

[57] M. Heydari, S. M. Hosseini, and S. A. Gholamian, "Optimal Placement and Sizing of Capacitor and Distributed Generation with Harmonic and Resonance Considerations Using Discrete Particle Swarm Optimization," *IJISA,* vol. 5(7), pp. 42-49, 2013.

[58] L. Refoufi, B. A. T. Al Zahawi, and A. G. Jack, "Analysis and modeling of the steady state behavior of the static Kramer induction generator," *Energy Conversion, IEEE Transactions on,* vol. 14, pp. 333-339, 1999.

[59] S. Kansal, B. B. R. Sai, B. Tyagi, and V. Kumar, "Optimal placement of wind-based generation in distribution networks," in *Renewable Power Generation (RPG 2011), IET Conference on*, Edinburgh, UK, 2011, pp. 1-6.

[60] W. Prommee and W. Ongsakul, "Optimal multi-distributed generation placement by adaptive weight particle swarm optimization," in *International Conference on Control, Automation and Systems*, Seoul, South Korea, 2008, pp. 1663-1668.

[61] K. Nigim, A. Zobaa, and I. El-Amin, "An introduction to reactive power compensation for wind farms," *International Journal of Energy Technology and Policy* vol. 3, pp. 185-195, 2005.

[62] K. V. Kumar and M. P. Selvan, "Planning and operation of Distributed Generations in distribution systems for improved voltage profile," in *Power Systems Conference and Exposition, 2009. PSCE '09. IEEE/PES*, Seattle, WA 2009, pp. 1-7.

[63] *Guidance Notes for Power Park Developers (2007), Grid Code Connection Conditions Compliance: Testing & Submission of Compliance Report– Issue 1.1*

[64] G. Pannell, B. Zahawi, D. J. Atkinson, and P. Missailidis, "Evaluation of the Performance of a DC-Link Brake Chopper as a DFIG Low-Voltage Fault-Ride-Through Device," *Energy Conversion, IEEE Transactions on,* vol. 28, pp. 535-542, 2013.

[65] A. Ekwue, O. Nanka-Bruce, J. Rao, and D. McCool, "Dynamic Stabilty Investigations of the Fault Ride-Through Capabilities of a Wind Farm" in *16th Power Systems Computation Conference (PSCC 2008 Glasgow)* Glasgow, Scotland, 2008.

[66] E. Muljadi, N. Samaan, V. Gevorgian, L. Jun, and S. Pasupulati, "Short circuit current contribution for different wind turbine generator types," in *Power and Energy Society General Meeting, 2010 IEEE*, Minneapolis, MN 2010, pp. 1-8.

[67] G. Pannell, D. J. Atkinson, and B. Zahawi, "Analytical Study of Grid-Fault Response of Wind Turbine Doubly Fed Induction Generator," *Energy Conversion, IEEE Transactions on,* vol. 25, pp. 1081-1091, 2010.

[68] R. Rabbani and A. Zobaa, "Dynamic performance of wind asynchronous generators using different types and locations of fault " *International Review on Modelling and Simulations* vol. 4 pp. 2795- 2801, 2011.

[69] *IEEE Standard for Interconnecting Distributed Resources with Electric Power systems*: IEEE Std. 1547-2003, 2003.

[70] Z. Kai, A. P. Agalgaonkar, K. M. Muttaqi, and S. Perera, "Voltage support by distributed generation units and shunt capacitors in distribution systems," in *Power & Energy Society General Meeting, 2009. PES '09. IEEE*, Calgary, AB Canada, 2009, pp. 1-8.

[71] A. D. T. Le, M. A. Kashem, M. Negnevitsky, and G. Ledwich, "Maximising Voltage Support in Distribution Systems by Distributed Generation," in *TENCON 2005 2005 IEEE Region 10*, 2005, pp. 1-6.

[72] V. H. M. Quezada, J. R. Abbad, Roma, x, and T. G. S. n, "Assessment of energy distribution losses for increasing penetration of distributed generation," *Power Systems, IEEE Transactions on,* vol. 21, pp. 533-540, 2006.

[73] K. Y. Lee and M. A. El-Sharkawi, "Moder Heuristic Optimization Techniques: Theory and Applications to Power Systems," London: John Wiley & Sons, Inc: The Institute of Electrical and Electronics2008.

[74] C. W. Reynolds, "Flocks, herds, and schools: A distributed behavioural model," *ACM Computer Graphics,* vol. 21(4), pp. 25-34, 1987.

[75] L. Grant, G. K. Venayagamoorthy, G. Krost, and G. A. Bakare, "Swarm intelligence and evolutionary approaches for reactive power and voltage control," in *Swarm Intelligence Symposium, 2008. SIS 2008. IEEE*, St. Louis, MO 2008, pp. 1-8.

[76] S. Yuhui and R. Eberhart, "A modified particle swarm optimizer," in *Evolutionary Computation Proceedings, 1998. IEEE World Congress on Computational Intelligence., The 1998 IEEE International Conference on*, Anchorage, AK 1998, pp. 69-73.

[77] M. Clerc, *Particle Swarm Optimization*. London: ISTE Ltd, 2006.

[78] R. C. Eberhart and S. Yuhui, "Particle swarm optimization: developments, applications and resources," in *Evolutionary Computation, 2001. Proceedings of the 2001 Congress on*, Seoul, SKorea, 2001, pp. 81-86 vol. 1.

[79] Y. Shi, "Particle Swarm Optimization," *IEEE Connections,Newsletter of the IEEE Neural Networks Society,* vol. 2, pp. 8–13, 2004.

[80] R. Poli, J. Kennedy, and T. Blackwell, "Particle Swarm Optimization: An overview," *Swarm Intelligence,* vol. 1, pp. 33-57, 2007.

[81] C. Wei-Neng, Z. Jun, H. S. H. Chung, Z. Wen-Liang, W. Wei-gang, and S. Yu-hui, "A Novel Set-Based Particle Swarm Optimization Method for Discrete Optimization Problems," *Evolutionary Computation, IEEE Transactions on,* vol. 14, pp. 278-300, 2010.

[82] J. Kennedy and R. C. Eberhart, "A discrete binary version of the particle swarm algorithm," in *Systems, Man, and Cybernetics, 1997. Computational Cybernetics and Simulation., 1997 IEEE International Conference on*, Orlando, Florida, 1997, pp. 4104-4108 vol.5.

[83] C.-L. Sun, J.-C. Zeng, and J.-S. Pan, "A Modified Particle Swarm Optimization with Feasibility-Based Rules for Mixed-Variable Optimization Problems," *International Journal of Innovative, Computing, Information and Control,* vol. 7(6), pp. 3081-3096, 2011.

[84] J. Kennedy and R. Eberhart, *Swarm intelligence*. San Mateo, CA Morgan Kaufmann, 2001.

[85] H. Yoshida, K. Kawata, Y. Fukuyama, S. Takayama, and Y. Nakanishi, "A particle swarm optimization for reactive power and voltage control considering voltage security assessment," *Power Systems, IEEE Transactions on,* vol. 15, pp. 1232-1239, 2000.

[86] J. Lampinen and I. Zelinka, "Mixed integer-discrete-continuous optimization by differential evolution, Part 1: The optimization method," in *proceedings 5th Int. Mendel Conf. Soft Computing*, Brno, Czech Republic, 1999, pp. 77–81.

[87] K. Veeramachaneni, L. Osadciw, and G. Karmath, "Probabilistically driven Particle Swarms for Optimization of Multi Valued Discrete Problems: Design and analysis," in *Proceedings of the 2007 IEEE Swarm intelligence Symposium*, Honolulu, HI USA, 2007, pp. 141-149.

[88] M. Zambrano-Bigiarini, M. Clerc, and R. Rojas, "Standard Particle Swarm Optimisation 2011at CEC-2013: A baseline for future PSO improvements," in *Evolutionary Computation (CEC), 2013 IEEE Congress on* Cancun, Mexico, 2013, pp. 2337-2344.

[89] J. Kennedy and R. Mendes, "Neighborhood topologies in fully informed and best-of-neighborhood particle swarms," *Systems, Man, and Cybernetics, Part C: Applications and Reviews, IEEE Transactions on,* vol. 36, pp. 515-519, 2006.

[90] E. M. N. Figueiredo and T. B. Ludermir, "Effect of the PSO Topologies on the Performance of the PSO-ELM," in *Neural Networks (SBRN), 2012 Brazilian Symposium on* Curitiba, Parana Brazil, 2012, pp. 178-183.

[91] T. K. Das, G. K. Venayagamoorthy, and U. O. Aliyu, "Bio-Inspired Algorithms for the Design of Multiple Optimal Power System Stabilizers: SPPSO and BFA," *Industry Applications, IEEE Transactions on,* vol. 44, pp. 1445-1457, 2008.

[92] T. K. Das and G. K. Venayagamoorthy, "Optimal design of power system stabilizers using a small population based PSO," in *Power Engineering Society General Meeting, 2006. IEEE*, Montreal, Que, 2006, p. 7 pp.

[93] G. A. Bakare, G. K. Venayagamoorthy, and U. O. Aliyu, "Reactive power and voltage control of the Nigerian grid system using micro-genetic algorithm," in *Power Engineering Society General Meeting, 2005. IEEE*, San Francisco, USA 2005, pp. 1916-1922 Vol. 2.

[94] Z. Jingrui, W. Jian, and Y. Chaoyuan, "Small Population-Based Particle Swarm Optimization for Short-Term Hydrothermal Scheduling," *Power Systems, IEEE Transactions on,* vol. 27, pp. 142-152, 2012.

[95] C. Wang, Y. Liu, and Y. Zhao, "Application of dynamic neighborhood small population particle swarm optimization for reconfiguration of shipboard power system," *Engineering Applications of Artificial Intelligence,* vol. 26, pp. 1255-1262, 2013.

[96] R. D. Zimmerman, C. E. Murillo-Sanchez, and R. J. Thomas, "MATPOWER: Steady-State Operations, Planning, and Analysis Tools for Power Systems

Research and Education," *Power Systems, IEEE Transactions on,* vol. 26, pp. 12-19, 2011.

[97] C. A. Coello Coello, "An updated survey of evolutionary multiobjective optimization techniques: state of the art and future trends," in *Evolutionary Computation, 1999. CEC 99. Proceedings of the 1999 Congress on*, Washington, DC 1999, p. 13 Vol. 1.

[98] Z. Kai, A. P. Agalgaonkar, K. M. Muttaqi, and S. Perera, "Multi-objective optimisation for distribution system planning with renewable energy resources," in *Energy Conference and Exhibition (EnergyCon), IEEE International*, Manama, Bahrain 2010, pp. 670-675.

[99] J. A. Momoh, *Electric Power Distribution, Automation, Protection, and Control*. London: CRC Press, 2008.

[100] I. Musa, B. Zahawi, S. M. Gadoue, and D. Giaouris, "Integration of Distributed Generation for network loss minimization and voltage support using Particle Swarm Optimization," in *Power Electronics, Machines and Drives (PEMD 2012), 6th IET International Conference on*, Bristol, UK, 2012, pp. 1-4.

[101] N. Mwakabuta and A. Sekar, "Comparative Study of the IEEE 34 Node Test Feeder under Practical Simplifications," in *Power Symposium, 2007. NAPS '07. 39th North American*, Las Cruces, NM 2007, pp. 484-491.

[102] M. E. Baran and F. F. Wu, "Network reconfiguration in distribution systems for loss reduction and load balancing," *Power Delivery, IEEE Transactions on,* vol. 4, pp. 1401-1407, 1989.

[103] T. N. Shukla, S. P. Singh, V. Srinivasarao, and K. B. Naik, "Optimal Sizing of Distributed Generation Placed on Radial Distribution Systems," *Electric Power Components and Systems,* vol. 38, pp. 260-274, 2013/11/08 2010.

[104] W. H. Kersting, *Distribution System Modelling and Analysis*. Boca Raton London New York Taylor & Francis Groups LLC:, 2012.

[105] H. Saadat, *Power System Analysis*: Tata McGraw-Hill Ltd, India, 2002.

[106] B. D. Metz-Noblat, F. Dumas, and C. Poulain, "Calculation of short-circuit currents," Schneider Electric,Cashier Technique no. 158, 2005.

[107] ERACS, *Technical Manual Electrical Power Systems Analysis Software*: ERA Technology Limited 1998-2009.

[108] IEEE, "IEEE Std. 551 IEEE Recommended Practice for Calculating Short-circuit Currents in Industrial and Commercial Power Systems," London: IEEE, 2006.

[109] "User's Guide Short Circuit Analysis Program ANSI/IEC/IEEE & Protective Device Evaluation, Ver. 6.60.00," Power Analytics Corporation, San Diego U.S.A 2011.

[110] B. Wu, Y. Lang, N. Zargari, and S. Kouro, *Power Conversion and Control of Wind Energy Systems*: John Wiley & Sons, Inc: The Institute of Electrical and Electronics 2011.

[111] N. Samaan, R. Zavadil, J. C. Smith, and J. Conto, "Modeling of wind power plants for short circuit analysis in the transmission network," in *Transmission and Distribution Conference and Exposition, 2008. T&D. IEEE/PES*, Chicago, IL 2008, pp. 1-7.

[112] L. Dusonchet, F. Massaro, and E. Telaretti, "Effects of electrical parameters of induction generator on the transient voltage stability of a fixed speed wind turbine," in *Universities Power Engineering Conference, 2008. UPEC 2008. 43rd International*, Padova, Italy, 2008, pp. 1-5.

[113] A. F. Rodriguez, "Improvement of a Fixed Speed Wind Turbnie Soft Starter based on a Sliding-Mode Controller," Seville: University of Seville, 2006, p. 49.

[114] M. Viswanadh and A. Sakher, "Minimization of power loss and improvement of voltage profile by optimal placement of wind generator in distribution network," *International Journal of Engineering Research and Applications,* vol. 2, pp. 987-993, 2012.

[115] K. C. Divya and P. S. N. Rao, "Models for wind turbine generating systems and their application in load flow studies," *Electric Power Systems Research,* vol. 76, pp. 844-856, 2006.

[116] A. E. Feijoo and J. Cidras, "Modeling of wind farms in the load flow analysis," *Power Systems, IEEE Transactions on,* vol. 15, pp. 110-115, 2000.

[117] NERC,"Nigerian Electricity Regulatory Commission," http://www.nercng.org/index.php/nerc-documents, 2012.

[118] NERC, "Distribution Code (D-Code)," http://www.nercng.org/index.php/nerc-documents/Codes-Standards-and-Manuals/, 2012.

[119] NERC, "Regulations on Embedded Generation," Abuja: http://www.nercng.org/index.php/document-library/func-startdown/4/, 2012.

[120] D. kukoyi, "The Concept of Embedded Generation: Prospect and Challenges " in *Workshop on the Embedded Generation Framework in the Nigerian Electricity Supply Industry* Victoria Island, Lagos 2012.

[121] W. H. Kersting, "Radial distribution test feeders," in *Power Engineering Society Winter Meeting, 2001. IEEE*, 2001, pp. 908-912 vol.2.

[122] PHCN, "Hourly Reading Log Book"," Power Holding Company of Nigeria (PHCN), Distribution Business Unit, Dispatch center, Kaduna January – February, 2007 and 2008 2008.

[123] A. Odubiyi and I. E. Davidson, "Distributed Generation in Nigeria's Electricity Industry Deregulation: Assessment and Integration," in *Proceedings IASTED International Conference, Power and Energy Systems*, Palm Springs, CA, USA, 2003.

[124] A. S. Sambo, "Renewable Energy for Rural Development: The Nigerian Perspective," *ISESCO Science and Technology Vision,* vol. 1, pp. 12-22, 2005.

[125] U. O. Aliyu and S. B. Elegba, "Prospect of small hydropower development for rural applications in Nigeria," *Nig. Journal of Renewable Energy,* vol. 1, pp. 74-86, 1990.

[126] M. S. Haruna and J. Katende, "System characterisation of the Nigerian electricity network," in *Reliability of Transmission and Distribution Networks (RTDN 2011), IET Conference on*, London, UK, 2011, pp. 1-8.

[127] K. N. Hasan, K. S. R. Rao, and Z. Mokhtar, "Analysis of load flow and short circuit studies of an offshore platform using ERACS software," in *Power and Energy Conference, 2008. PECon 2008. IEEE 2nd International*, Johor Bahru 2008, pp. 543-548.

[128] P. Nallagownden and F. A. Fauzi, "Modelling & simulation of an offshore platform (SUMANDAK Phase 2 - SUPG-B development project)," in *Intelligent and Advanced Systems, 2007. ICIAS 2007. International Conference on*, Kuala Lumpur 2007, pp. 845-850.

[129] P. Nallagownden, L. T. Thin, N. C. Guan, and C. M. H. Mahmud, "Application of Genetic Algorithm for the Reduction of Reactive Power Losses in Radial Distribution System," in *Power and Energy Conference, 2006. PECon '06. IEEE International*, Putra Jaya 2006, pp. 76-81.

[130] I. N. Perumal and Y. Chan Chee, "A proposed strategy of implementation for load shedding and load recovery with dynamic simulations," in *Power and Energy Conference, 2004. PECon 2004. Proceedings. National*, Kuala Lumpur, Malaysia 2004, pp. 185-189.

APPENDICES

Appendix A: Feeder Network Data for 69-bus RDN

Table A. 1: Line and load data for the 69-bus radial distribution network of Figure 4.1

Line numbers	Sending Bus	Receiving Bus	Resistance (Ω)	Reactance (Ω)	Load at Receiving End Bus	
					Real Load (KW)	Reactive Load (KVAr)
1	1	2	0.0005	0.0012	0	0
2	2	3	0.0005	0.0012	0	0
3	3	4	0.0015	0.0036	0	0
4	4	5	0.0251	0.0294	0	0
5	5	6	0.3660	0.1864	2.60	2.20
6	6	7	0.3811	0.1941	40.40	30.0
7	7	8	0.0922	0.0470	75.0	54
8	8	9	0.0493	0.0251	30.0	22.0
9	9	10	0.8190	0.2707	28.0	19
10	10	11	0.1872	0.0619	145.0	104.0
11	11	12	0.7114	0.2351	145.0	104.0
12	12	13	1.0300	0.3400	8.0	5.50;
13	13	14	1.0440	0.3450	8.0	5.50
14	14	15	1.0580	0.3496	0.0	0.0
15	15	16	0.1966	0.0650	45.50	30.0
16	16	17	0.3744	0.1238	60.0	35.0
17	17	18	0.0047	0.0016	60.0	35.0
18	18	19	0.3276	0.1083	0.0	0.0
19	19	20	0.2106	0.0696	1.0	0.60
20	20	21	0.3416	0.1129	114.0	81.0
21	21	22	0.01040	0.0046	5.3	3.50
22	22	23	0.1591	0.0526	0.0	0.0
23	23	24	0.3463	0.1145	28.0	20.0
24	24	25	0.7488	0.2475	0.0	0.0
25	25	26	0.3089	0.1021	14.0	10.0
26	26	27	0.1732	0.0572	14.0	10.0
27	3	28	0.00400	0.0108	26.0	18.60
28	28	29	0.0640	0.1565	26.0	18.60
29	29	30	0.3978	0.1315	0.0	0.0
30	30	31	0.0702	0.0232	0.0	0.0
31	31	32	0.3510	0.1160	0.0	0.0
32	32	33	0.8390	0.2816	14.0	10.0
33	33	34	1.7080	0.5646	19.50	14.0
34	34	35	1.4740	0.4873	6.0	4.0
35	3	36	0.0044	0.0108	26.0	18.55
36	36	37	0.0640	0.1565	26.0	18.55
37	37	38	0.1053	0.1230	0.0	0.0
38	38	39	0.0304	0.0355	24.0	17.0
39	39	40	0.0018	0.0021	24.0	17.0
40	40	41	0.7283	0.8509	1.20	1.0
41	41	42	0.3100	0.3623	0.0	0.0
42	42	43	0.0410	0.0478	6.0	4.30
43	43	44	0.0092	0.0116	0.0	0.0
44	44	45	0.1089	0.1373	39.22	26.30
45	45	46	0.0009	0.0012	39.22	26.30
46	4	47	0.0034	0.0084	0.0	0.0
47	47	48	0.0851	0.2083	79.0	56.40
48	48	49	0.2898	0.7091	384.70	274.5
49	49	50	0.822	0.2011	384.70	274.5
50	8	51	0.0928	0.0473	40.50	28.30

51	51	52	0.3319	0.1114	3.6	2.7
52	9	53	0.1740	0.0886	4.35	3.50
53	53	54	0.2030	0.1034	26.4	19.0
54	54	55	0.2842	0.1447	24.0	17.2
55	55	56	0.2813	0.1433	0.0	0.0
56	56	57	1.5900	0.5337	0.0	0.0
57	57	58	0.7837	0.2630	0.0	0.0
58	58	59	0.3042	0.1006	100.0	72.0
59	59	60	0.3861	0.1172	0.0	0.0
60	60	61	0.5075	0.2585	1244.0	888.0
61	61	62	0.0974	0.0496	32.0	23.0
62	62	63	0.1450	0.0738	0.0	0.0
63	63	64	0.7105	0.3619	227.0	162.0
64	64	65	1.0410	0.5302	59.0	42.0
65	11	66	0.2012	0.0611	18.0	13.0
66	66	67	0.0047	0.0014	18.0	13.0
67	12	68	0.7394	0.2444	28.0	20.0
68	68	69	0.0047	0.0016	28.0	20.0
69*	52	67	0.0047	0.0016	-	-
70*	15	69	0.0047	0.0016	-	-
71*	10	65	0.0047	0.0016	-	-
72*	46	50	0.0047	0.0016	-	-
73*	35	27	0.0047	0.0016	-	-
*Tie Lines, Substation Voltage =11.0 kV & Base MVA =10.0 MVA						

Table A. 2: Commercially available generator sizes used in the study

No.	**DG(MW)**	**No.**	**DG(MW)**	**No.**	**DG(MW)**	**No.**	**DG(MW)**	**No.**	**DG(MW)**	**No.**	**DG(MW)**
1	0	27	0.113	53	0.350	79	0.813	105	1.680	131	3.000
2	0.011	28	0.115	54	0.355	80	0.830	106	1.700	132	3.075
3	0.012	29	0.117	55	0.360	81	0.880	107	1.750	133	3.100
4	0.013	30	0.120	56	0.372	82	0.900	108	1.754	134	3.150
5	0.015	31	0.128	57	0.390	83	0.912	109	1.760	135	3.200
6	0.016	32	0.136	58	0.400	84	0.960	110	1.800	136	3.204
7	0.018	33	0.140	59	0.403	85	1.000	111	1.840	137	3.300
8	0.020	34	0.150	60	0.440	86	1.056	112	1.850	138	3.350
9	0.024	35	0.160	61	0.443	87	1.100	113	1.900	139	3.400
10	0.025	36	0.170	62	0.450	88	1.120	114	2.000	140	3.500
11	0.030	37	0.176	63	0.475	89	1.144	115	2.100	141	3.600
12	0.032	38	0.180	64	0.480	90	1.200	116	2.200	142	3.700
13	0.036	39	0.200	65	0.500	91	1.210	117	2.260	143	3.800
14	0.040	40	0.214	66	0.515	92	1.250	118	2.235	144	3.900
15	0.048	41	0.216	67	0.520	93	1.264	119	2.300	145	4.000
16	0.050	42	0.228	68	0.530	94	1.300	120	2.339	146	4.100
17	0.056	43	0.230	69	0.536	95	1.350	121	2.400	147	4.200

18	0.058	44	0.240	70	0.576	96	1.360	122	2.500	148	4.300
19	0.060	45	0.250	71	0.600	97	1.400	123	2.600	149	4.400
20	0.068	46	0.260	72	0.625	98	1.420	124	2.648	150	4.500
21	0.075	47	0.280	73	0.670	99	1.500	125	2.700	151	4.600
22	0.080	48	0.300	74	0.700	100	1.525	126	2.750	152	4.700
23	0.090	49	0.310	75	0.720	101	1.600	127	2.800	153	4.800
24	0.100	50	0.320	76	0.740	102	1.636	128	2.845	154	4.900
25	0.106	51	0.325	77	0.750	103	1.660	129	2.865	155	5.000
26	0.108	52	0.335	78	0.800	104	1.670	130	2.900		

Appendix B: Induction Generator Parameters

Table B. 1 Electrical Parameters of induction generators based distributed generation used in the study [110-113]

S. No	Induction Generator output power rating and Voltage	Rr (Ω)	Xr (Ω)	Rs(Ω)	Xs(Ω)	Xm(Ω)
1	0.33MW , 660V	0.010032	0.307428	0.009372	0.100584	4.553736
2	0.35MW , 690V	0.004444	0.04642	0.051736	0.083318	3.730561
3	0.50MW, 690V	0.009332	0.058941	0.003333	0.045134	1.405447
4	0.60MW, 690V	0.007221	0.10006	0.008094	0.083318	3.730561
5	0.843MW, 690V	0.004	0.066	0.00450	0.0513	2.2633
6	0.855MW, 575V	0.001547	0.069257	0.001856	0.04826	2.617931
7	1MW, 690V	0.002831	0.085929	0.002512	0.035169	1.340018
8	1.45MW, 575V	0.00139	0.01565	0.001354	0.03279	0.55605
9	1.5MW, 690V	0.000965	0.039453	0.001066	0.027569	1.492224
10	1.65MW, 690V	0.001635	0.021998	0.002031	0.018385	0.911052
11	1.85MW, 690V	0.00204	0.022898	0.00136	0.016323	0.775816
12	2MW, 690V	0.000238	0.002381	0.000238	0.002381	0.71415
13	2.3MW, 690V	0.001497	0.0204	0.001102	0.0204	0.67052
14	2.5MW, 575V	0.001542	0.0149	0.001447	0.023749	0.81645
15	3.0MW, 3300V	0.018152	0.2949	0.016623	0.2949	10.2421
16	4.0MW, 4000V	0.023152	0.532	0.022104	0.532	10.555

Appendix C: Feeder Network Data for 62-bus and 47 -bus Nigerian RDN

Table C. 1: DEFAULT LINE PARAMETERS [104]

Conductors/ Cables	Current(A)	Conversion	Std. Eqv. American size (cmils/AWG)	Resistance (ohms/mile)	GMR (ft)	Current (A)
150mm2 ACSR	470	269100	336400	0.306	0.0244	530
100mm2 ACSR	410	197400	266800	0.385	0.0217	460
70mm2 ACSR	290	138180	3,0	0.723	0.006	300
35mm2 ACSR	170	69090	#2	1.69	0.00418	180

Note: 1mm2=1974cmils

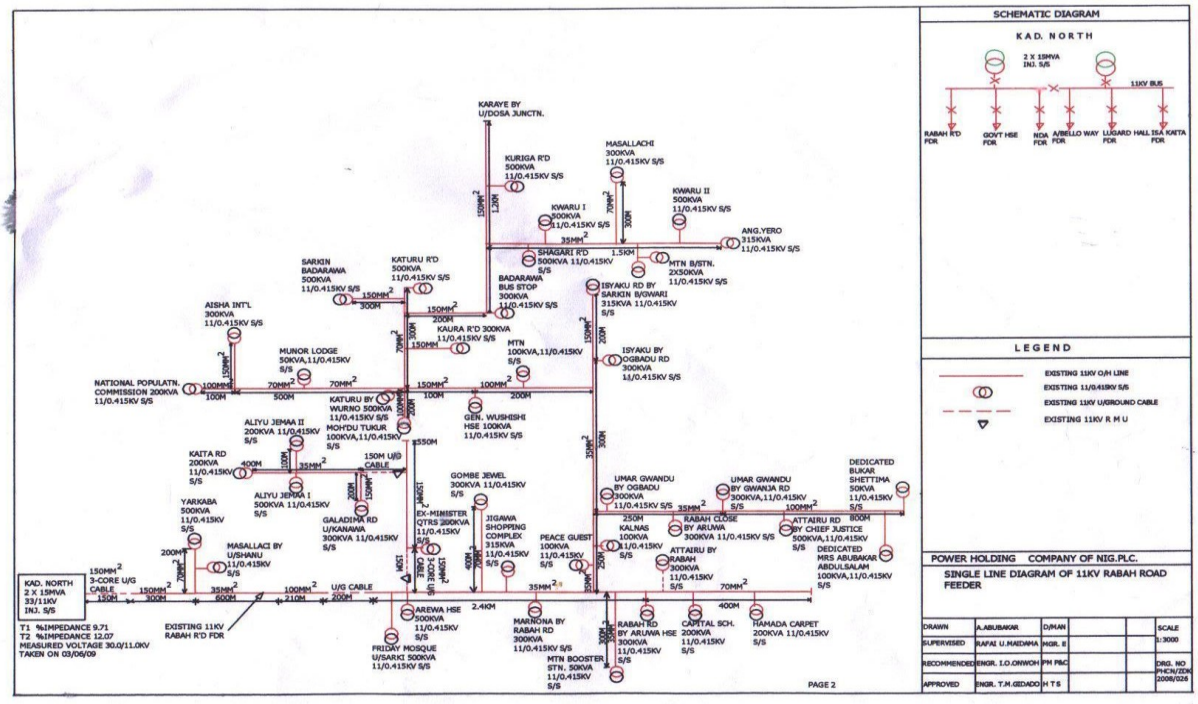

Figure C. 1: Single line diagram of 11kV Nigerian feeder

Table C. 2: Computed series impedance for different conductors

Conductors (cmils/AWG)	Series impedance Z(R+ j X) ohms/km
336400	0.1901 + 0.0504i -0.0000 + 0.0000i 0.0000 + 0.0000i -0.0000 + 0.0000i 0.1901 + 0.3247i -0.0000 - 0.0000i 0 0.0000 + 0.0000i 0.1901 + 0.3247i
266 800	0.2392 + 0.0578i -0.0000 + 0.0000i 0.0000 + 0.0000i -0.0000 + 0.0000i 0.2392 + 0.3321i -0.0000 - 0.0000i 0.0000 - 0.0000i 0.0000 + 0.0000i 0.2392 + 0.3321i
3,0	0.4493 + 0.1385i -0.0000 + 0.0000i 0.0000 - 0.0000i -0.0000 0.4493 + 0.4129i -0.0000 - 0.0000i 0 + 0.0000i 0.0000 - 0.0000i 0.4493 + 0.4129i

Note: 1 mile =1.609344km

Table C. 3: Computed series impedances for different cables

Cables	Series impedance Z(R+ j X) ohms/km
336400	0.3678 + 1.7868i -0.0000 - 0.0000i -0.0000 + 0.0000i -0.0000 - 0.0000i 0.1901 + 0.2043i 0.0000 - 0.0000i 0.0000 - 0.0000i -0.0000 - 0.0000i 0.1901 + 0.2043i
3,0	0.6269 + 1.8749i -0.0000 - 0.0000i -0.0000 + 0.0000i 0.0000 0.4493 + 0.2924i 0.0000 - 0.0000i 0.0000 - 0.0000i -0.0000 - 0.0000i 0.4493 + 0.2924i

Table C. 4: Computed hunt admittances for different conductors

Conductors (cmils/AWG)	Shunt admittance Y(0+ j B) μ Siemens/km
336400	1.0e-005 * 0 + 0.1370i -0.0000 - 0.0000i 0.0000 + 0.0000i 0 - 0.0000i 0.0000 + 0.3580i 0.0000 - 0.0000i -0.0000 - 0.0000i 0.0000 - 0.0000i -0.0000 + 0.3580i
266 800	1.0e-005 * 0 + 0.1358i -0.0000 - 0.0000i 0.0000 + 0.0000i 0 0.0000 + 0.3496i 0.0000 - 0.0000i 0 0 - 0.0000i -0.0000 + 0.3496i

3,0	1.0e-005 * 0 + 0.1332i -0.0000 + 0.0000i 0.0000 + 0.0000i 0 + 0.0000i 0.0000 + 0.3329i 0.0000 - 0.0000i 0 + 0.0000i 0.0000 + 0.0000i -0.0000 + 0.3329i

Table C. 5: Computed shunt admittances for different cables

Cables (cmils/AWG)	Shunt admittance Y(0+ j B) μ Siemens/km
336400	1.0e-003 * 0 + 0.1380i -0.0000 - 0.0000i 0.0000 + 0.0000i 0 0.0000 + 0.1380i 0.0000 - 0.0000i 0 + 0.0000i 0.0000 - 0.0000i -0.0000 + 0.1380i
3,0	1.0e-004 * 0 + 0.5211i -0.0000 - 0.0000i 0.0000 + 0.0000i 0 0.0000 + 0.5211i 0.0000 - 0.0000i 0.0000 + 0.0000i 0.0000 - 0.0000i -0.0000 + 0.5211i

Table C. 6: Line and load data for the 62-bus radial distribution network figure 8.2

Line number	Sending Bus	Receiving Bus	Distance (Km)	Resistance (Ω)	Reactance (Ω)	Load at Receiving End Bus		Installed Transformer (kVA)
						Real Load (KW)	Reactive Load (KVAr)	
1	1	2	0.45	0.0856	0.1461	0	0	
2	2	3	1.2	0.2282	0.3897	343.2	147.8	500
3	3	4	0.1	0.0190	0.0325	247.2	106.5	500
4	4	5	0.8	0.1521	0.2598	0.0	0.0	
5	5	6	0.11	0.0209	0.0357	23.2	10.0	315
6	6	7	0.11	0.0209	0.0357	132.8	57.2	300
7	7	8	0.3	0.0570	0.0974	0.0	0.0	
8	8	9	0.16	0.0304	0.0520	0.0	0.0	
9	9	10	0.63	0.1198	0.2046	132.8	57.2	300
10	10	11	0.05	0.0095	0.0162	0.0	0.0	
11	11	12	0.07	0.0133	0.0227	73.8	31.8	200
12	12	13	0.13	0.0247	0.0422	59.0	25.8	200
13	13	14	0.14	0.0266	0.0455	0.0	0.0	
14	2	15	0.12	0.0228	0.0390	265.7	114.4	500
15	15	16	0.08	0.0152	0.0260	298.9	128.7	500
16	4	17	0.15	0.0285	0.0487	163.8	70.5	200

17	17	18	0.4	0.0761	0.1299	0.0	0.0	
18	18	19	0.15	0.0285	0.0487	0.0	0.0	
19	5	20	0.4	0.0761	0.1299	66.4	28.6	300
20	8	21	0.07	0.0133	0.0227	20.7	8.9	100
21	21	22	0.08	0.0152	0.0260	22.1	9.5	100
22	22	23	0.1	0.0190	0.0325	143.9	62.0	300
23	23	24	0.69	0.1312	0.2241	0.0	0.0	
24	24	25	0.2	0.0380	0.0649	221.4	95.3	300
25	25	2	0.2	0.0380	0.0649	141.8	61.1	315
26	9	27	0.3	0.0570	0.0974	36.9	15.9	100
27	11	28	0.1	0.0190	0.0325	66.4	28.6	300
28	18	29	0.15	0.0285	0.0487	0.0	0.0	
29	29	30	0.25	0.0475	0.0812	203.7	87.7	500
30	30	31	0.15	0.0285	0.0487	88.6	38.1	200
31	23	32	0.125	0.0238	0.0406	110.7	47.7	300
32	32	33	0.125	0.0238	0.0406	132.8	57.2	300
33	33	34	0.3	0.0570	0.0974	221.4	95.3	500
34	34	35	0.43	0.0818	0.1396	18.5	7.9	100
35	35	36	0.07	0.0133	0.0227	9.2	4.0	50
36	24	37	0.12	0.0228	0.0390	36.9	15.9	100
37	37	38	0.08	0.0152	0.0260	22.1	9.5	100
38	38	39	0.1	0.0190	0.0325	262.0	112.8	500
39	39	40	0.3	0.0570	0.0974	12.9	5.6	50
40	40	41	0.2	0.0380	0.0649	0.0	0.0	
41	41	42	0.1	0.0761	0.1299	36.9	15.9	200
42	29	43	0.2	0.0380	0.0649	243.5	104.9	300
43	30	44	0.1	0.0190	0.0325	168.3	72.4	200
44	39	45	0.2	0.0380	0.0649	25.8	11.1	100
45	39	46	0.15	0.0285	0.0487	166.1	71.5	300
46	46	47	0.15	0.0285	0.0487	0.0	0.0	
47	47	48	0.25	0.0475	0.0812	0.0	0.0	
48	48	49	0.07	0.0133	0.0227	402.2	173.2	500
49	41	50	0.1	0.0190	0.0325	143.9	62.0	300
50	47	51	0.2	0.0380	0.0649	225.8	97.2	300
51	48	52	0.3	0.0570	0.0974	347.6	149.7	500
52	51	53	0.4	0.0761	0.1299	0.0	0.0	
53	53	54	0.4	0.0761	0.1299	409.6	176.4	500
54	54	55	0.4	0.0761	0.1299	0.0	0.0	
55	53	56	0.2	0.0380	0.0649	250.4	107.8	500
56	56	57	0.15	0.0285	0.0487	413.3	177.9	500
57	57	58	0.4	0.0761	0.1299	0.0	0.0	
58	58	59	0.1	0.0190	0.0325	36.9	15.9	100

59	59	60	0.25	0.0475	0.0812	428.8	184.6	500
60	60	61	0.3	0.0570	0.0974	214.3	92.3	315
61	58	62	0.3	0.0570	0.0974	159.4	68.6	300
Substation Voltage =11.0 kV & Base-MVA =10.0 MVA								

Table C. 7:Line and load data for the Modified 62-bus (47-bus) radial distribution network figure 7.2

Line numbers	Sending Bus	Receiving Bus	Distance (Km)	Resistance (Ω)	Reactance (Ω)	Load at Receiving End Bus	
						Real Load (KW)	Reactive Load (KVAr)
1	1	2	0.45	0.0856	0.1461		
2	2	3	1.2	0.2282	0.3897	0.344	0.147
3	3	4	0.1	0.0190	0.0325	0.247	0.106
4	4	5	0.8	0.1521	0.2598	0.066	0.028
5	5	6	0.11	0.0209	0.0357	0.023	0.01
6	6	7	0.11	0.0209	0.0357	0.133	0.058
7	7	8	0.3	0.0570	0.0974	0.0	0.0
8	8	9	0.16	0.0304	0.0520	0.037	0.016
9	9	10	0.63	0.1198	0.2046	0.133	0.058
10	10	11	0.05	0.0095	0.0162	0.066	0.028
11	11	12	0.07	0.0133	0.0227	0.074	0.032
12	12	13	0.13	0.0247	0.0422	0.059	0.025
13	13	14	0.14	0.0266	0.0455	0.0	0.0
14	2	15	0.12	0.0228	0.0390	0.266	0.114
15	15	16	0.08	0.0152	0.0260	0.299	0.129
16	4	17	0.15	0.0285	0.0487	0.164	0.070
17	17	18	0.4	0.0761	0.1299	0.0	0.0
18	18	19	0.15	0.0285	0.0487	0.0	0.0
19	8	20	0.07	0.0133	0.0227	0.021	0.009
20	20	21	0.08	0.0152	0.0260	0.022	0.010
21	21	22	0.1	0.0190	0.0325	0.144	0.062
22	22	23	0.69	0.1312	0.2241	0.0	0.0
23	23	24	0.2	0.0380	0.0649	0.363	0.156
24	18	25	0.15	0.0285	0.0487	0.244	0.104
25	25	26	0.25	0.0475	0.0812	0.371	0.160
26	26	27	0.15	0.0285	0.0487	0.089	0.038
27	22	28	0.125	0.0238	0.0406	0.111	0.048
28	28	29	0.125	0.0238	0.0406	0.133	0.058
29	29	30	0.3	0.0570	0.0974	0.221	0.095
30	30	31	0.43	0.0818	0.1396	0.019	0.008
31	31	32	0.07	0.0133	0.0227	0.009	0.004

32	23	33	0.12	0.0228	0.0390	0.037	0.016
33	33	34	0.08	0.0152	0.0260	0.022	0.010
34	34	35	0.1	0.0190	0.0325	0.289	0.124
35	35	36	0.3	0.0570	0.0974	0.194	0.083
36	35	37	0.15	0.0285	0.0487	0.166	0.071
37	37	38	0.15	0.0285	0.0487	0.226	0.097
38	38	39	0.25	0.0475	0.0812	0.348	0.150
39	39	40	0.07	0.0133	0.0227	0.403	0.173
40	38	41	0.4	0.0761	0.1299	0.0	0.0
41	41	42	0.4	0.0761	0.1299	0.410	0.177
42	41	43	0.2	0.0380	0.0649	0.250	0.108
43	43	44	0.15	0.0285	0.0487	0.413	0.178
44	44	45	0.4	0.0761	0.1299	0.159	0.069
45	45	46	0.1	0.0190	0.0325	0.037	0.016
46	46	47	0.25	0.0475	0.0812	0.643	0.277
Substation Voltage =11.0 kV & Base-MVA =10.0 MVA							

Table C. 8:Conductor and Cable Configuration for radial distribution network [121]

Overhead Spacing Models:
The spacing ID numbers and type for overhead lines are summarized in Table 2.

Table 2
Overhead Line Spacings

Spacing ID	Type
500	Three-Phase, 4 wire
505	Two-Phase, 3 wire
510	Single-Phase, 2 wire

Figure 1 shows the spacing distances between the phase conductors and the neutral conductor for Spacing ID numbers used for the overhead lines.

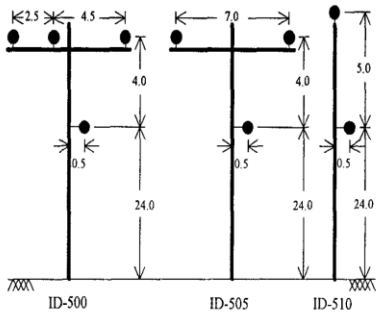

Figure 1 – Overhead Line Spacings

Conductor Data

Table 3 lists the characteristics of the various conductors that are used for the overhead configurations in the test feeders[2,3]. The columns correspond to:

1 – Conductor size in AWG or kcmil
2 – Type of conductor
AA = All Aluminum
ACSR = Aluminum Conductor Steel Reinforced
CU = Copper
3 – 60 Hz resistance at 50 degrees C (ohms/mile)
4 – Conductor outside diameter (inches)
5 – Geometric Mean Radius (ft.)
6 – Ampacity at 50 degrees C (amps)

Table 3
Conductor Data

1	2	3	4	5	6
1,000	AA	0.105	1.15	0.0368	698
556.5	ACSR	0.1859	0.927	0.0313	730
500	AA	0.206	0.813	0.026	483
336.4	ACSR	0.306	0.721	0.0244	530
250	AA	0.410	0.567	0.0171	329
# 4/0	ACSR	0.592	0.563	0.00814	340
# 2/0	AA	0.769	0.414	0.0125	230
# 1/0	ACSR	1.12	0.398	0.00446	230
# 1/0	AA	0.970	0.368	0.0111	310
# 2	AA	1.54	0.292	0.00883	156
# 2	ACSR	1.69	0.316	0.00418	180
# 4	ACSR	2.55	0.257	0.00452	140
# 10	CU	5.903	0.102	0.00331	80
# 12	CU	9.375	0.081	0.00262	75
# 14	CU	14.872	0.064	0.00208	20

Underground Spacing Models:

The spacing ID numbers and type for underground lines are summarized in Table 4.

Table 4
Underground Line Spacings

Spacing ID	Type
515	Three-Phase, 3 Cable
520	Single-Phase, 2 Cable

Figure 2 shows the spacing distances between cables for underground lines:

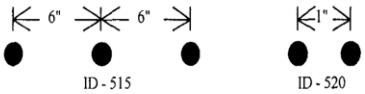

Figure 2 – Underground Line Spacings

Cable Data:

Table 5 lists the characteristics of the various concentric neutral cables [4] that are used in the test feeders. The column numbers correspond to:

1 – Conductor size in AWG or kcmil
2 – Diameter over insulation (inches)
3 – Diameter over screen (inches)
4 – Outside diameter (inches)
5 – Copper 1/3 neutral (No. x AWG)
6 – Ampacity in 4 inch duct

Table 5
Concentric Neutral 15 kV All Aluminum (AA) Cable

1	2	3	4	5	6
2(7x)	0.78	0.85	0.98	6 x 14	135
1/0(19x)	0.85	0.93	1.06	6 x 14	175
2/0(19x)	0.90	0.97	1.10	7 x 14	200
250(37x)	1.06	1.16	1.29	13 x 14	260
500(37x)	1.29	1.39	1.56	16 x 12	385
1000(61x)	1.64	1.77	1.98	20 x 10	550

Table 6 lists the characteristics of a tape shielded conductor used in the test feeders. The column numbers correspond to:

1 – Conductor size in AWG
2 – Diameter over insulation (inches)
3 – Diameter over the shield
4 – Jacket thickness (mils)

Appendix D: ERACS Feeder Network Data 47 -bus Nigerian RDN

Table D. 1: ERACS Study Parameters for Modified 62-bus (47-bus) radial distribution network figure 7.3

BUSBAR NAME	NOMINAL VOLTS (kV)	NOMINAL FREQ (Hz)	THREE PHASE FAULT MVA	SINGLE PHASE FAULT MVA
BUS-0001	11	50	250	250
BUS-0002	11	50	250	250
BUS-0003	11	50	250	250
BUS-0004	11	50	250	250
BUS-0005	11	50	250	250
BUS-0006	11	50	250	250
BUS-0007	11	50	250	250
BUS-0008	11	50	250	250
BUS-0009	11	50	250	250
BUS-0010	11	50	250	250
BUS-0011	11	50	250	250
BUS-0012	11	50	250	250
BUS-0013	11	50	250	250
BUS-0014	11	50	250	250
BUS-0015	11	50	250	250
BUS-0016	11	50	250	250
BUS-0017	11	50	250	250
BUS-0018	11	50	250	250
BUS-0019	11	50	250	250
BUS-0020	11	50	250	250
BUS-0021	11	50	250	250
BUS-0022	11	50	250	250
BUS-0023	11	50	250	250
BUS-0024	11	50	250	250
BUS-0025	11	50	250	250
BUS-0026	11	50	250	250
BUS-0027	11	50	250	250
BUS-0028	11	50	250	250
BUS-0029	11	50	250	250
BUS-0030	11	50	250	250
BUS-0031	11	50	250	250
BUS-0032	11	50	250	250
BUS-0033	11	50	250	250
BUS-0034	11	50	250	250
BUS-0035	11	50	250	250
BUS-0036	11	50	250	250
BUS-0037	11	50	250	250
BUS-0038	11	50	250	250
BUS-0039	11	50	250	250
BUS-0040	11	50	250	250
BUS-0041	11	50	250	250

BUS-0042	11	50	250	250
BUS-0043	11	50	250	250
BUS-0044	11	50	250	250
BUS-0045	11	50	250	250
BUS-0046	11	50	250	250
BUS-0047	11	50	250	250
BUS-0048	3.3	50	250	250

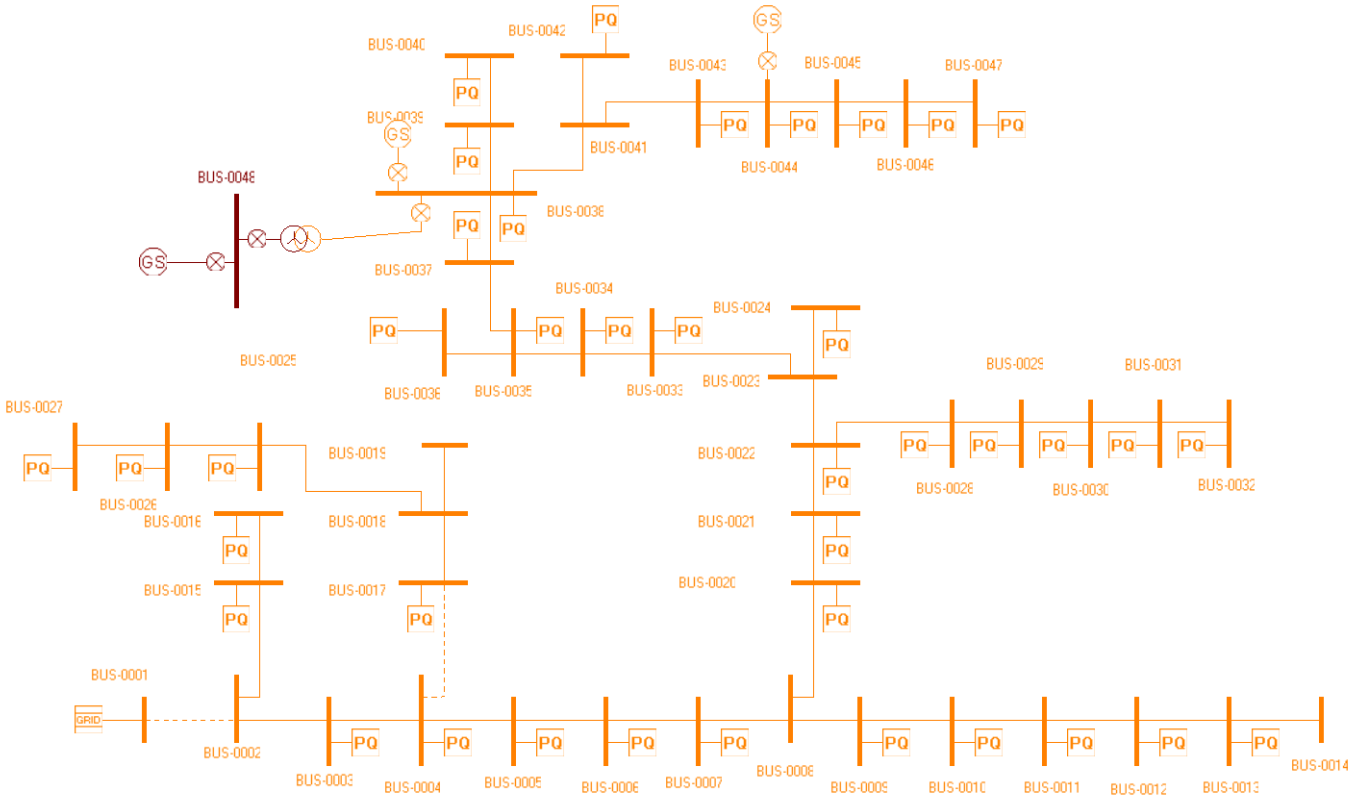

Figure D. 1: ERACs Model of 47-bus 11kV Nigerian feeder (Figure C.1)

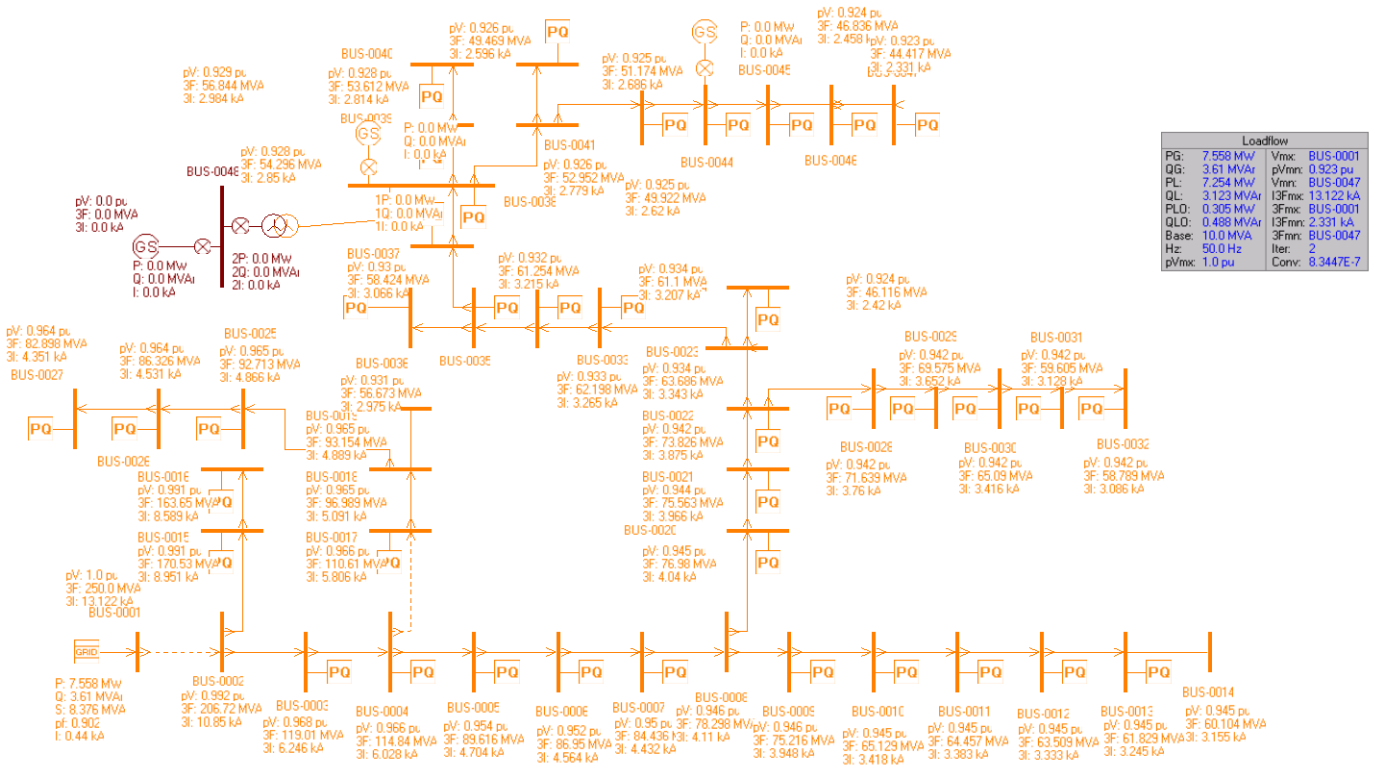

Figure D. 2: 47-bus 11kV Nigerian feeder ERACS Base case (Load flow with no Distributed Generation)

Table D. 2: ERACS Equipment and Grid Study Parameters for 47-bus RDN Test System

CABLE	FIRST	SECOND	No. OF	CABLE	LIBRARY	RATING	POS/NEG	POS/NEG	POS/NEG	ZERO	ZERO	ZERO						
ID	BUSBAR	BUSBAR	CIRCUITS	LENGTH	KEY	(kA)	R (pu)	X (pu)	B (pu)	R (pu)	X (pu)	B (pu)						
CAB-0001	BUS-0001	BUS-0002	1	1	UG_Cable	1	0.007	0.008	0	0.01	0.01	0						
CAB-0002	BUS-0004	BUS-0017	1	1	UG_Cable2	1	0.002	0.002	0	0.01	0.01	0						
TRANSFORMER	LIBRARY	WINDING	BUSBAR	RATED	WINDING	ANGLE	POS/NEG	POS/NEG	ZERO	ZERO	NEUTRAL	NEUTRAL	VOLTAGE	OFF-NOMINAL				
ID	KEY	NUMBER	NAME	MVA	TYPE	(DEG.)	R (pu)	X (pu)	R (pu)	X (pu)	R (pu)	X (pu)	RATIO	TAP (%)				
TX-0001	T039	1	BUS-0038	5	Y	0	0.005	0.0706	0.005	0.0706	0	0	1	0				
TX-0001	T039	2	BUS-0048	5	Y	0	0.005	0.0706	0.005	0.0706	0	0	1	0				
INFINITE GENERATOR	BUSBAR	RATED	RATED	RATED	ASSIGNED	POS. SEQ	POS. SEQ	NEG. SEQ	NEG. SEQ	ZERO SEQ	ZERO SEQ							
ID	NAME	S (MVA)	P (MW)	V (kV)	V (pu)	R (pu/r)	X (pu/r)	R (pu/r)	X (pu/r)	R (pu/r)	X (pu/r)							
GRID-0002	BUS-0001	250	24.8759	11	1	0.0995	0.995	0.0995	0.995	0.0995	0.995							
SYNCHRONOUS MACHINE	BUSBAR	TYPE	NO. OF	LIBRARY	RATED	RATED	RATED	ASSIGNED	ASSIGNED	ASSIGNED	NEUTRAL	NEUTRAL	POS. SEQ	POS. SEQ	NEG. SEQ	NEG. SEQ	ZERO SEQ	ZERO SEQ
ID	NAME		UNITS	KEY	S (MVA)	P (MW)	V (kV)	V (pu)	P (MW)	Q (MVAr)	R (pu/r)	X (pu/r)	R (pu/r)	X (pu/r)	R (pu/r)	X (pu/r)	R (pu/r)	X (pu/r)
GS-0001	BUS-0038	P.Q.	1	G011	5.88	5	11	0	4.995	0	0	0	0.0021	0.0303	0.0141	0.238	0.007	0.172
GS-0003	BUS-0044	P.Q.	1	GTRU	4.25	3.4	11	0	3.395	0	0	0	0.0064	0.11	0.0141	0.265	0.007	0.172
GS-0005	BUS-0048	P.Q.	1	G8ME2	6.25	5	3.3	0	4.995	0	0	0	0.005	0.17	0.003	0.22	0.005	0.05